PALLADIUM-CATALYZED SYNTHESIS OF N-HETEROCYCLES

FROM ALKOXY ALLENES AND SULFONYL YNAMINES

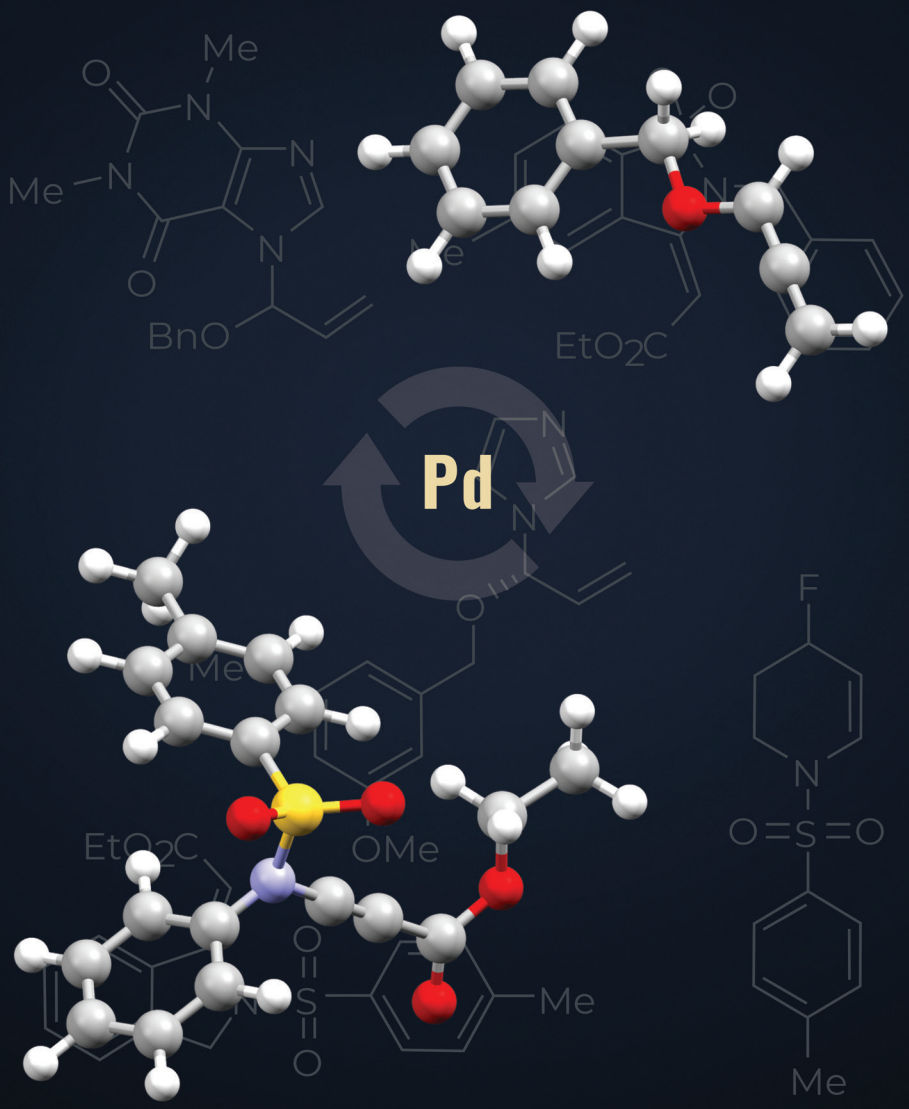

BY IVAN BERNAR

Palladium-Catalyzed Synthesis of *N*-Heterocycles from Alkoxy Allenes and Sulfonyl Ynamines

Ivan Bernar

This thesis has been supported by the Marie Skłodowska-Curie Actions of the European Commision under the FP7 "People" Programme via the Initial Training Network Expanding Capability in Heterocyclic Organic Synthesis (ITN-ECHONET)
MCITN-2012-316379

ISBN:
978-94-92896-83-4

Cover and lay-out design:
Maria Bernar
Monikabernar@gmail.com

Press:
Ipskamp, Enschede

Palladium-Catalyzed Synthesis of *N*-Heterocycles from Alkoxy Allenes and Sulfonyl Ynamines

Proefschrift

ter verkrijging van de graad van doctor

aan de Radboud Universiteit Nijmegen

op gezag van de rector magnificus prof. dr. J. H. J. M. van Krieken,

volgens besluit van het college van decanen

in het openbaar te verdedigen op donderdag 29 november 2018

om 10.30 uur precies

door

Ivan Bernar

geboren op 11 januari 1989

Khust (Oekraïne)

Promotor:

Prof. dr. Floris P. J. T. Rutjes

Copromotor:

Dr. Daniel Blanco Ania

Manuscriptcommissie:

Prof. dr. Binne Zwanenburg

Prof. dr. Jana Roithová

Prof. dr. Joseph P. A. Harrity (University of Sheffield, Verenigd Koninkrijk)

Paranimfen:

Dr. Alejandra Riesco Domínguez

María José Sánchez Fernández

Palladium-Catalyzed Synthesis of *N*-Heterocycles from Alkoxy Allenes and Sulfonyl Ynamines

Doctoral Thesis

to obtain the degree of doctor

from Radboud University Nijmegen

on the authority of the Rector Magnificus prof. dr. J. H. J. M. Van Krieken,

according to the decision of the Council of Deans

to be defended in public on Thursday, November 29, 2018

at 10.30 hours

by

Ivan Bernar

Born on January 11, 1989

Khust (Ukraine)

Supervisor:

Prof. dr. Floris P. J. T. Rutjes

Co-supervisor:

Dr. Daniel Blanco Ania

Doctoral Thesis Committee:

Prof. dr. Binne Zwanenburg

Prof. dr. Jana Roithová

Prof. dr. Joseph P. A. Harrity (University of Sheffield, United Kingdom)

Paranymphs:

Dr. Alejandra Riesco Domínguez

María José Sánchez Fernández

To my dad, mum, and sister

LIST OF ABBREVIATIONS AND SYMBOLS

Ac	acetyl
Ar	aryl
atm	atmosphere
B	base
Bn	benzyl
Bu	butyl
^{t}Bu	*tert*-butyl
cod	cyclooctadiene
Cy	cyclohexyl
dba	1,5-diphenylpenta-1,4-dien-3-one
DBU	1,8-diazabicyclo[5.4.0]undec-7-ene
DME	1,2-dimethoxyethane
DMSO	dimethyl sulfoxide
DFT	density functional theory
DIPEA	diisopropylethylamine
DMAP	*N*,*N*-dimethylpyridin-4-amine
DMF	*N*,*N*-dimethylformamide
dppp	1,3-bis(diphenylphosphanyl)propane
e^-	electron
ee	enantiomeric excess
e.g.	exempli gratia (for example)
equiv	equivalent
ESI	electrospray ionization
Et	ethyl
eV	electronvolt
FTIR	Fourier transform infrared spectroscopy
G	Gibbs energy
h	hour
Hex	hexyl
HOMO	highest occupied molecular orbital
HRMS	high-resolution mass spectroscopy
L	ligand
Me	methyl
Mes	2,4,6-trimethylphenyl
n.d.	not determined
NOE	nuclear Overhauser effect
n.r.	no reaction
Nu	nucleophile
Pe	pentyl
TBAI	tetrabutylammonium iodide
TBS	*tert*-butyl(dimethyl)silyl
Tf	trifluoromethanesulfonyl
TLC	thin-layer chromatography
TMP	2,2,6,6-tetramethylpiperidine
TMS	trimethylsilyl
o-Tol	*ortho*-tolyl
p-Tol	*para*-tolyl
Ts	4-methylbenzenesulfonyl
TS	transition state

TABLE OF CONTENTS

CHAPTER 1

Preface

Preparing a feast in 2018 is as easy as visiting the local supermarket or vegetable garden. However, things might change in about thirty years from now. By 2050, the world's population is expected to rise from the current 7.5 to over 10 billion people.[1] The world population's growth is putting increasing pressure on farmers and a growing demand for effective ways of farming. As a consequence, in the last few decades the use of agents for crop protection, such as *agrochemicals*, became a common practice in the farmers "toolbox". In fact, agrochemicals have been responsible for the beginning of the "Green Revolution", using the same surface of land to grow more nutritious fruits, vegetables, and grains the world population relies upon.

1.1 Impact of Agrochemicals: Their Benefits and Hazards

Agents for crop protection, or simply agrochemicals, provide farmers with a cost-effective way of improving the yield and quality of their crops. They also make harvesting more straightforward and maintain consistent yields from year to year. In most cases, agrochemicals refer to *pesticides*, substances that are meant to control pests (Figure 1.1). The main classes of pesticides are compounds that restrain insects (*insecticides*), weeds (*herbicides*), and fungi/mold (*fungicides*). Around 50% of the world's crops would die – entire crops might be lost – without their use. Potatoes and vines, which are very sensitive to fungal epidemics,[2] are examples of particularly high-risk crops. The loss of entire crops is of major concern, both to farmers, who lose income, and to consumers, who face rising prices of fruit and vegetables.

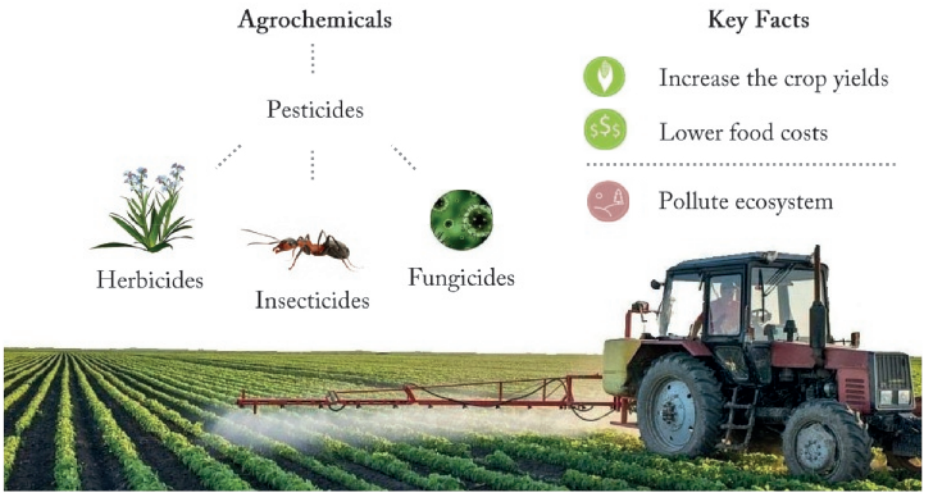

Figure 1.1 *Classification and Key Facts of Agrochemicals.*

The use of pesticides is often considered as a quick, easy and inexpensive solution to pest and weed control. However, the worldwide overuse of agrochemicals produces considerable damage to ecosystem. Uncontrolled agricultural practices can *pollute soil* with toxic agents and their degradation products. Thus, pesticides have an enormous negative impact on metabolism of soil microorganisms which leads to reduce in soil fertility.[3] Soil pollution affects not only its microorganisms, but also plants, animals and humans. The fate of pesticides in the soil should be permanently controlled to ensure the soil protection by measuring pesticide persistency parameters, which includes water solubility, soil-sorption constant, the octanol/water partition coefficient and half-life in soil.[4]

Several global companies focus on discovering, developing and selling new agrochemicals. However, it may take up to as much as 15 years to bring a new product to the market and to ensure that it meets the highest standards of safety to farmers, consumers and the environment.

1.2 *N*-Heterocycles as Key Structures of Agrochemicals

Roughly 70% of all agrochemicals that were introduced to the market within the last 20 years bear at least one heterocycle.[5] Although heterocycles may be inorganic, most of them are cyclic organic compounds containing at least one heteroatom. *Nitrogen heterocycles* of general structure **1** contain one or more nitrogen atoms in the ring and are of tremendous value for the agrochemical industry (Figure 1.2).

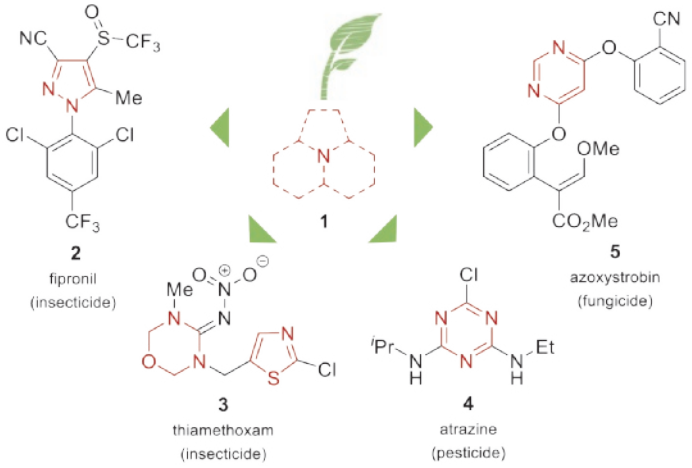

Figure 1.2 *Examples of Agrochemicals Containing N-Heterocycles.*

They are a key feature of the most potent and top selling agrochemicals, including the broad-spectrum insecticides fipronil **2** and thiamethoxan **3**, the most widely used herbicide in agriculture atrazine **4** and Syngenta's azoxystrobin **5** (best-selling crop protection product).[6]

N-Heterocycles present in crop protection agents often have a positive impact on their physicochemical properties, such as lipophilicity, solubility, and bioavailability. Because of this, they are often used in lead optimization strategies of agrochemicals (Scheme 1.1). For example, the replacement of a benzene by a pyridine in the herbicidal lead structure **6** considerably enhanced the partition coefficient of potential herbicide **7** and thus improved its ability to translocate into the plant tissue.[7] Another remarkable example is diphenoxy benzene **8**, a promising lead compound of the strobilurin class of fungicides, whose high lipophilicity showed low distribution within the plant. Replacing the central benzene ring by a more polar pyrimidine ring significantly increased its antifungal activity.[5] Nowadays, azoxystrobin **5** is a crop protection product with $1.24 thousand million sales in 2014.[8] Finally, several *N*-heterocycles perfectly act as bioisosteres of related carbocyclic rings and several functional groups. For example, 1*H*-tetrazole is frequently used to replace a carboxylic acid or ester group in drug design.[9] Thus, azimsulfuron **10** shows excellent herbicidal efficacy compared to its less active ethyl ester analog **9**.[6]

Scheme 1.1 *Fine-Tuning the Physicochemical Properties of Agrochemicals with N-Heterocycles.*

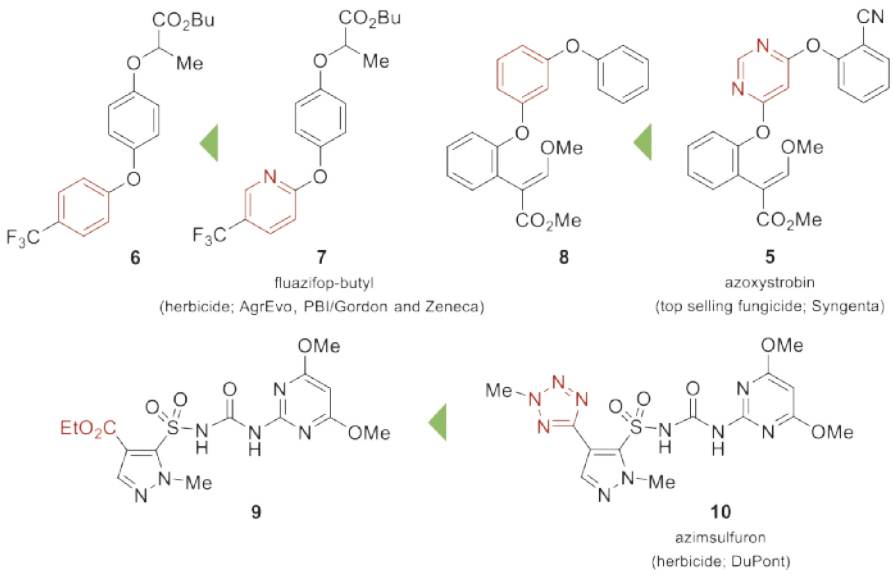

1.3 ECHONET ITN

Agrochemicals have greatly improved farming worldwide, but their benefit still remains limited because of the evolution of pesticide resistance of many pests. Like other living organisms, pests go through a similar evolution process as well. After being treated with a pesticide, the survived pests pass on the resistance as a genetic feature to their offspring, making all future species pest-resistant. As the pests evolve, the pesticide resistance increases, which exerts a tremendous toll on the agriculture. Thus, pesticide resistance costs $10 billion yearly for the agricultural sector and may even lead to loss of millions of lives because of insect-vectored diseases, e.g., malaria.[10] Therefore, research programs on agrochemicals are currently ongoing in various regions of the world to find a solution to this worldwide problem.

Developing new agrochemicals to combat pesticide resistance was a goal of the ECHONET program (abbreviation of Expanding Capability in Heterocyclic Organic Synthesis Network). This program offered novel synthetic concepts of preparation of small molecules and biologically active compounds that address current agrochemical challenges in food production. The program was created as a multi-partner Marie Curie Initial Training Network (ITN) consisting of both academic and industrial partners (Figure 1.3). The academic partners explored the syntheses and functionalization of lead heteroaromatic compounds, in particularly *N*-heterocyclic compounds. Concurrently, the industrial partners covered both technical and non-technical aspects of the research, e.g., use of equipment for large-scale synthesis, high throughput testing or industrial flow chemistry.[11]

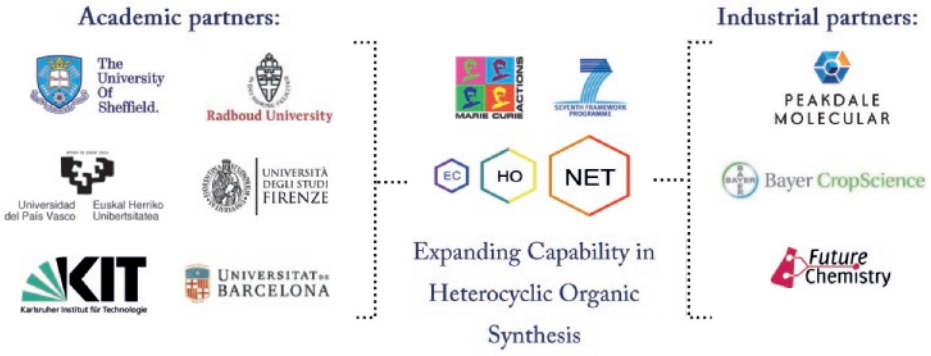

Figure 1.3 *Partners of the ECHONET ITN.*

1.4 Purpose and Outline of the Investigation

The research topics of this thesis are in line with the ECHONET concept. The presented work is focused on the design of synthetic methodologies for the preparation of chemical libraries with an ultimate goal to identify viable lead compounds for agrochemical research. In particular, this dissertation is focused on the use of palladium-catalyzed reactions of alkoxy allenes and sulfonyl ynamines for the preparation and functionalization of *N*-heterocycles.

The content of this thesis is divided in three parts:

- *The first part*, Chapter 2, presents a brief literature survey on the application of palladium-catalyzed reactions of alkoxy allenes and sulfonyl ynamines in the syntheses of *N*-heterocycles. It entails a brief introduction to palladium catalysis followed by various examples of palladium-catalyzed hydroamination of alkoxy allenes for the synthesis of nitrogen-containing natural products and heterocycles. Additionally, multiple examples of palladium-catalyzed cyclizations of sulfonyl ynamines are discussed.

- *The second part*, Chapters 3 and 4, follows up on the research of our group on palladium-catalyzed additions to alkoxy allenes. In particular, this part presents a comprehensive study of palladium-catalyzed hydroamination of alkoxy allenes with azoles as reacting nucleophiles. In Chapter 3, we explored the scope of the reaction for a series of azoles. This methodology yields fast and easy access to a broad range of chiral, heteroaromatic allylic *N,O*-acetals. Moreover, our computational studies for benzyloxyallene and imidazole suggest a new palladium(0)-driven mechanistic pathway that proceeds through a reactive carbene-like local minimum. Chapter 4 combines a collection of reactions for further functionalization of heteroaromatic allylic *N,O*-acetals and their incorporation into complex heterocyclic entities.

- *The third part*, Chapters 5 and 6, outlines a novel synthetic approach for the synthesis of 3-amino-1-benzothiophene-1,1-diones combining palladium-catalyzed cyclization of sulfonyl ynamines together with photoinduced 1/N→3/C-sulfonyl group migration. In Chapter 5 we studied the intramolecular hydroarylation of sulfonyl ynamines in the presence of a palladium catalyst. Our investigations reveal that the electron-withdrawing group on the triple bond of the sulfonyl ynamine is of utmost importance for the success of the reaction. This experimental observation was proven by computational studies suggesting an alkyne-directed 5-*exo*-*dig* cyclization pathway. The obtained products, 1,2-benzothiazole-1,1-diones, can further undergo

a photoinduced 1/N→3/C-sulfonyl group migration to form 3-amino-1-benzothiophene-1,1-diones (Chapter 6). These compounds are potentially bioactive molecules and hence valuable for medicinal and agrochemical research.

Several compounds prepared in this thesis will be tested at Bayer CropScience to evaluate their biological activity.[12]

Parts of this dissertation have been published or will be published soon.

1.5 References and Notes

[1] United Nations, Department of Economic and Social Affairs, Population Division *World Population Prospects: The 2015 Revision, Key Findings and Advance Tables*, United Nations New York, 2015.

[2] Oerke, E.-C. *J. Agricult. Sci.* **2006**, *144*, 31–43.

[3] (a) Jablonowski, N. D.; Linden, A.; Köppchen, S.; Thiele, B; Hofmann, D.; Mittelstaedt, W.; Pütz, T.; Burauel, P. *Environ. Pollut.* **2012**, *168*, 29– 36; (b) Joko, T.; Anggoro, S.; Sunoko, H. R.; Rachmawati, S. *Appl. Environ. Soil Sci.* **2017**, 1–7.

[4] Aktar, W.; Sengupta, D.; Chowdhury, A. *Interdisc. Toxicol.* **2009**, *2*, 1–12.

[5] *Bioactive Heterocyclic Compound Classes – Agrochemicals;* Lamberth, C., Dinges, J., Eds.; Wiley-VCH: Weinheim, Germany, 2012.

[6] *Modern Crop Protection Compounds;* Krämer, W., Schirmer, U., Eds.; Wiley-VCH: Weinheim, Germany, 2007; Vol. 3, pp 65–66.

[7] (a) Koyanagi, T.; Haga, T. *ACS Symp. Ser.* **1995**, *584*, 15–24; (b) Lamberth, C. *Pest Manag. Sci.* **2013**, *69*, 1106–1114.

[8] Front Research Home Page, http://www.frontresearch.com/news/the-top-ten-best-selling-agrochemical-products-of-syngenta (accessed June 29, 2018).

[9] Herr, R. J. *Bioorg. Med. Chem.* **2002**, *10*, 3379–3393.

[10] Gould, F.; Brown, Z. S.; Kuzma, J. *Science* **2018**, *360*, 728–732.

[11] ECHONET ITN Home Page, https://sites.google.com/a/sheffield.ac.uk/echonet-itn/ (accessed June 29, 2018, 2017).

[12] Due to the confidentiality agreement the results of the biological testing cannot be presented in the thesis.

CHAPTER 2

Palladium-Catalyzed Synthesis of *N*-Heterocycles from Alkoxy Allenes and Sulfonyl Ynamines

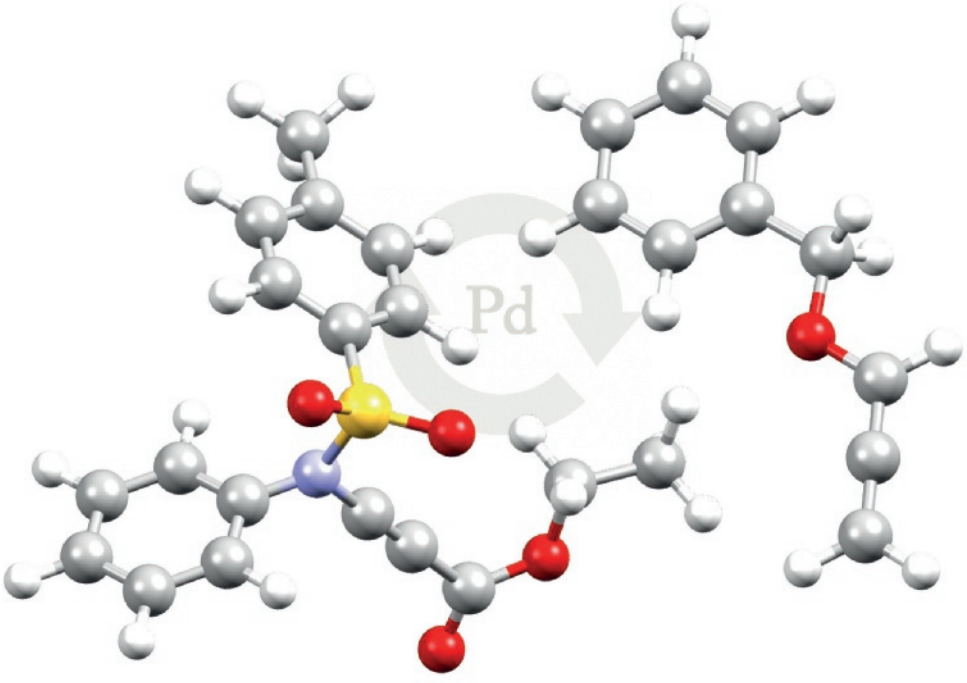

ABSTRACT

Palladium-catalyzed reactions are among the most attractive synthetic tools for the preparation of *N*-heterocycles. In this chapter we show the synthetic power of alkoxy allenes and sulfonyl ynamines for rapid assembly of complex *N*-heterocyclic structures using palladium catalysis. Multiple examples in this comprehensive and updated overview demonstrate that these transformations proceed in chemo-, regio- and stereoselective manner.

Part of this chapter will be published:
Bernar, I.; Ruliaman, R.; Blanco-Ania, D.; Rutjes, F. P. J. T. *Manuscript in preparation*.

Chapter cover: "Alkoxy Allene and Sulfonyl Ynamine Substrates in Palladium Catalysis"

2.1 Introduction

Palladium catalysis has revolutionized synthetic organic chemistry: it has made possible the construction of complex organic molecules in a highly efficient manner. Its discovery had a dramatic impact on heterocyclic chemistry and resulted in the emergence of new paradigms.[1] The significance of palladium catalysis is undisputed and underlined by the 2010 Nobel Prize for chemistry, which was awarded to R. Heck, A. Suzuki, and E. Negishi for their pioneering work in this field.[2]

Up to date, palladium-catalyzed reactions allow the preparation of advanced materials, pharmaceuticals and agrochemicals in fewer steps and with less waste than conventional non-catalyzed methods.[3] The synthesis of *N*-heterocyclic compounds is no exception to this fact. Several excellent reviews dealing with this topic have been published in the past decade. The vast amount of these studies were focused on a specific kind of transformation that enables the synthesis of *N*-heterocycles, e.g., palladium catalyzed cross-coupling reactions,[4] carbonylations,[5] hydrogenations,[6] oxidations,[7] C–H bond-activation processes,[8] and so forth. The shortcomings of these reviews are the restricted examples of the substrates involved, which are mainly limited to alkenes,[9] alkynes,[10] allenes,[11] saturated or unsaturated carbo- and heterocycles.[12]

In the light of recent advances in palladium catalysis, there is considerable interest in original and multipurpose substrates that may further expand the scope of reactions. In this context, alkoxy allenes **1**[13] and sulfonyl ynamines **2**[14] certainly represent two versatile substrate classes in organic synthesis (Figure 2.1). The electron-donating ability of the heteroatom present in their structures strongly polarizes the multiple CC bonds, allowing chemo-, regio- and stereoselective reactions to proceed with almost surgical precision. As a consequence, both substrates often emerge in palladium-catalyzed transformations in the synthesis of complex *N*-heterocycles, including natural products.

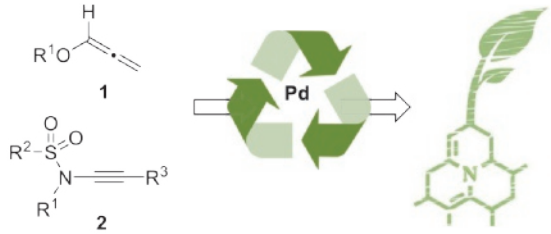

Figure 2.1 *Alkoxy Allenes 1 and Sulfonyl Ynamines 2 Are Versatile Substrates for the Palladium Catalysis.*

In this chapter, we aim to provide a comprehensive and updated overview of the synthesis of *N*-heterocycles based on palladium-catalyzed reactions of alkoxy allenes and sulfonyl ynamines. Particularly, we will review two transformations that constitute the backbone of this thesis. The first transformation presented in the first section of this chapter deals with palladium-catalyzed hydroamination of alkoxy allenes. This process allows fast and easy access to allylic *N,O*-acetals, precursors for iminium ion chemistry and metathesis reactions. The second transformation represents the use of sulfonyl ynamines in palladium-catalyzed cyclizations. These reactions are useful in the rapid synthesis of cyclic and polycyclic nitrogen heterocycles.

2.2 Allylic *N,O*-Acetals in the Synthesis of Bioactive Compounds and *N*-Heterocycles

2.2.1 Palladium-Catalyzed Hydroamination of Alkoxy Allenes

The palladium-catalyzed hydroamination of alkoxy allenes is a straightforward transformation for the synthesis of allylic *N,O*-acetals **4** (Scheme 2.1). The addition of nitrogen nucleophile **3** to alkoxy allene **1** proceeds under mild basic or acidic conditions and with complete regioselectivity.[15–19] Moreover, the reaction can be performed in a highly stereoselective manner delivering the stereodefined products **4** in excellent yields.[20–23]

Scheme 2.1 *Palladium-Catalyzed Hydroamination of Alkoxy Allenes.*

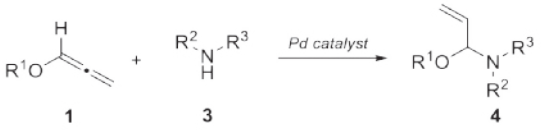

1 **3** **4**

The formation of product **4** can be explained through the reaction mechanism outlined in Scheme 2.2. This process is initiated by an oxidative addition of palladium into the N–H bond of amide **3** (e.g., $R^2 = SO_2Ph$) to form a hydridopalladium cationic complex L_2Pd^+–H (L = ligand) which undergoes addition to alkoxy allene **5** forming the η^3-allylpalladium species **7** (Scheme 2.2, route *a*).[24] Our recent studies show that under basic conditions alkoxy allene **1** prefers to form allene–palladium complex **6** which deprotonates amine **3** forming the same palladium species **7** (Scheme 2.2, route *b*).[25] Finally, the addition of the conjugate base of the pronucleophile or an external nucleophile leads to the branched product **8** with with the regeneration of the palladium(0) catalyst.

Scheme 2.2 *Mechanism of the Reaction.*

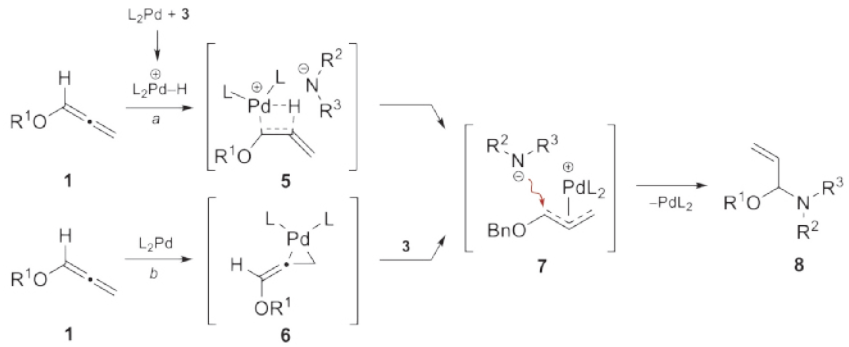

Allylic *N,O*-acetals have been frequently used as precursors in *N*-acyliminium ion chemistry to gain fast access to biologically active cyclic amino acids and quinolizidine alkaloids.[15–19] Besides, the vinyl group renders these acetals particularly attractive reaction partners for metathesis reactions (Scheme 2.3). Thus, ring-closing metathesis (RCM) of diolefins **10**, prepared through palladium-catalyzed addition of enamide **9** to alkoxy allenes **1**, constitutes a general protocol to access cyclic allylic *N,O*-acetals **11**. Compounds with this structure are considered useful building blocks for the synthesis of indolizidine alkaloids, azasugars, and a variety of *N*-heterocycles.[21–35]

Scheme 2.3 *General Strategy to Form Cyclic N,O-Acetals* ***11*** *with an Overview of Natural Products and N-Heterocycles Prepared from these Precursors.*

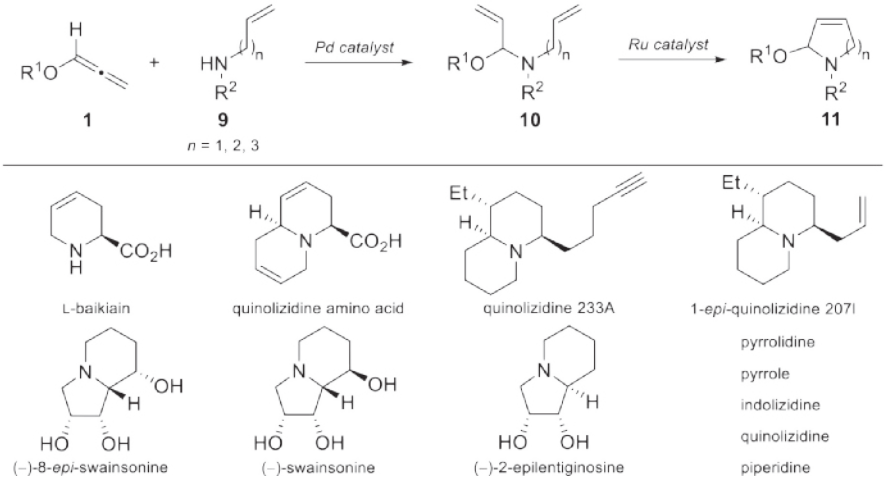

2.2.2 Transformations Involving *N*-Acyliminium Ions

The allylic *N,O*-acetals serve as suitable precursors for Lewis acid promoted additions and cyclizations to conjugated *N*-acyliminium ions. Our group used this approach for the stereoselective synthesis of a variety of unsaturated pipecolic and quinolizidine amino acids, including the natural product L-baikiain.[15] In our pioneering work, we used the palladium(II)-catalyzed addition of enantiopure nosyl-protected allylglycine methyl ester **12** to benzyloxyallene (**13**) and subsequent RCM to synthesize the cyclic, unsaturated *N,O*-acetal **14** in 80% overall yield as a 50:50 mixture of diastereoisomers (Scheme 2.4).

Scheme 2.4 *Crucial Steps in the Synthesis of Unsaturated Pipecolic Acids Employing Lewis Acid Promoted cis-Stereoselective Nucleophilic Addition as a Key Step.*

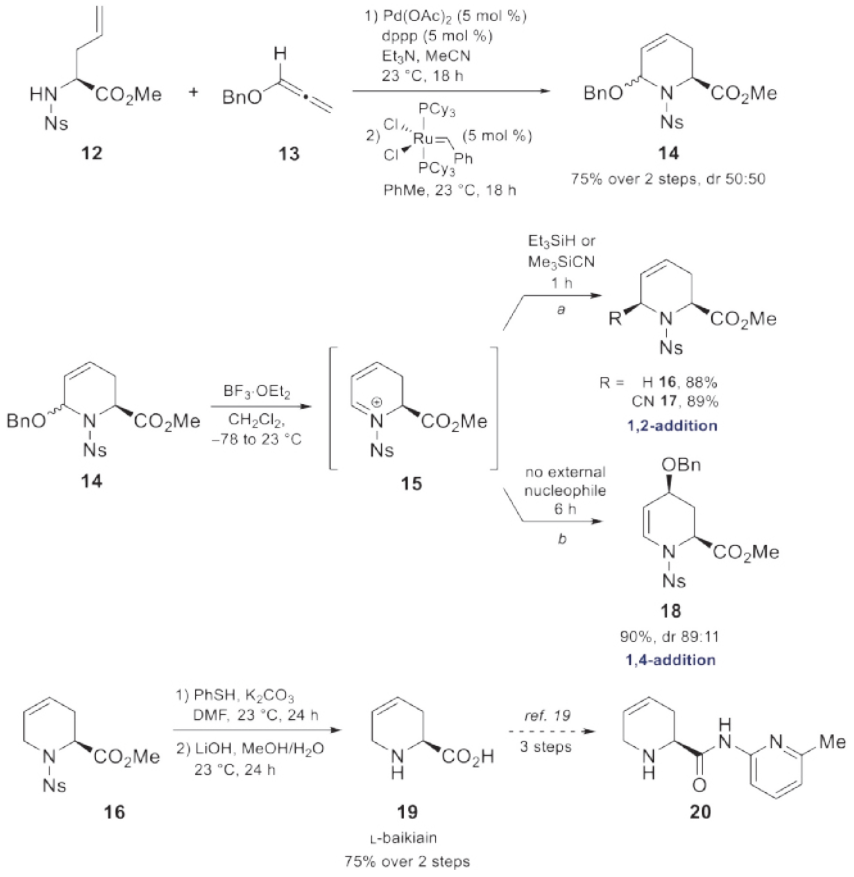

The key step toward the pipecolic acids consisted of a highly stereoselective nucleophilic addition to the *N*-sulfonyl iminium ion **15** generated from **14**. In all additions, only the *cis*-diastereoisomer was observed. Interestingly, whereas most of the nucleophiles led to a mixture of 1,2- and 1,4-adducts, triethylsilane and trimethylsilyl cyanide reacted exclusively at the 6-position, leading to the corresponding *cis*-2,6-disubstituted products (**16** and **17**) in very good yields (Scheme 2.4, route *a*). At the same time, in the absence of an external nucleophile, the *N,O*-acetal **14** underwent a diastereoselective rearrangement to *cis*-2,4-disubstituted compound **18** upon treatment with the Lewis acid (Scheme 2.4, route *b*). Finally, cleavage of the protecting group with benzenethiol and base in DMF followed by treatment with LiOH in an aqueous methanol solution converted the nosyl-protected cyclic product **16** into the natural occurring cyclic amino acid L-baikiain **19**[26] without epimerization of the stereocenter. This cyclic amino acid can be further transformed into the corresponding picolinamide **20**, a potential pharmacophore for treatment of immune and inflammatory disorders.[19]

Following this procedure, the enantiomerically pure unsaturated quinolizidine amino acid **22** was synthesized, nicely illustrating how the cyclic allylic *N,O*-acetals such as **14** can be used as building blocks for the synthesis of functionalized alkaloid systems (Scheme 2.5).[16,17] Precursor **21** was obtained as a single diastereoisomer with allyl(tributyl)stannane as the nucleophile; the nucleophilic attack proceeded smoothly via 1,2-addition. As in the example above, the selectivity was strongly influenced by the nature of the nucleophile [allyl(trimethyl)silane, instead of the more reactive allyl(tributyl)stannane, gave a 3:1 mixture of 1,2- and 1,4-regioisomers]. Starting from **21**, quinolizidine amino acid **22** was further prepared in four steps in a highly stereocontrolled manner. This compound not only represents a new amino acid, it may also be used as a starting point for new asymmetric ligands in organocatalysis, or directly applied as a building block in alkaloid synthesis.

Scheme 2.5 *Synthesis of Quinolizidine Amino Acid 22.*

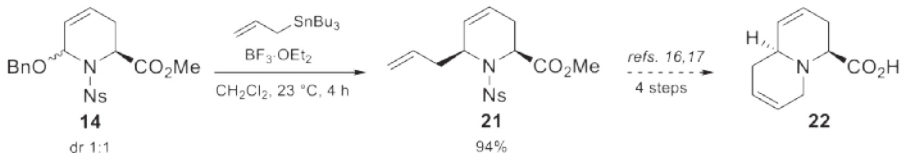

Our group was among the first to apply the cyclization onto the *N*-sulfonyl iminium ion derived from allylic *N,O*-acetals for the synthesis of 1-ethyl substituted quinolizidines (Scheme 2.6).[18] The quinolizidine skeleton was constructed from the enantiopure nosyl-protected amine **23** that incorporated an allylsilane substructure. Palladium(II)-catalyzed hydroamination of benzyloxyallene **13** with **23** afforded *N,O*-acetal **24** in very good yield as a mixture of diastereomers. This acyclic product was then further used in an allylsilane-directed cyclization via a *N*-sulfonyl iminium ion. It is worth to pay attention to the $Sn(OTf)_2$ catalyzed cyclization that proceeded through a chairlike transition state (**25**), in which the vinyl group and the ester are *cis*-oriented, occupying a pseudo axial orientation in order to minimize the steric interaction between the vinyl and the sulfonyl groups. Overall, the cyclization provided the energetically favored product **26** in 82% yield.[17] Next, the enantiomerically pure amino alcohol **27** was synthesized in four steps starting from sulfonamide **26** in an overall yield of 60%. The key synthon **27** was subsequently used in the synthesis of 1-*epi*-quinolizidine 207I (**28**) and quinolizidine 233A (**29**).[27] The natural products bearing this skeleton belong to an alkaloid class that is present in minor quantities in the skin of the poisonous frogs of the genus *Dendrobates* and the Madagascan frog of the genus *Mantella*.[28]

Scheme 2.6 *Formal Syntheses of 1-Ethylquinolizidine Alkaloids.*

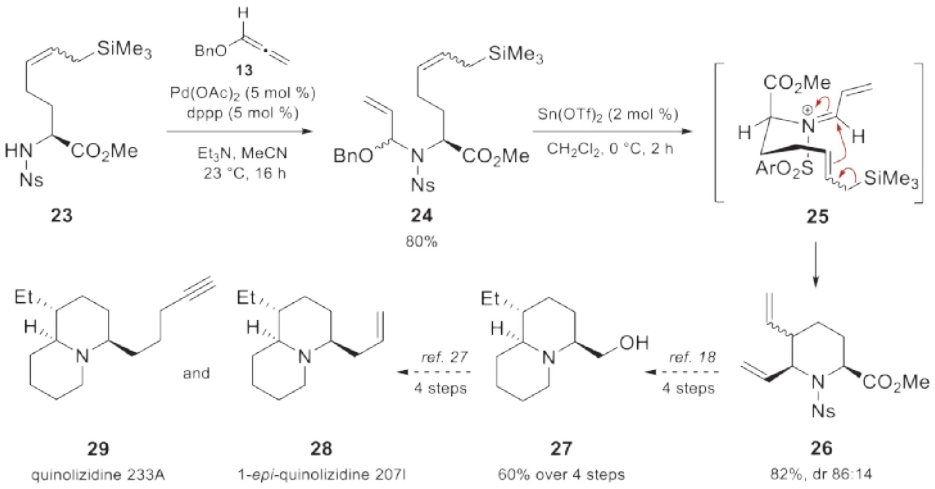

Following these results, Rhee's research group reported several successful examples of chiral ligand-directed asymmetric hydroaminations. Kim et al. showed that the synthesis of the *N,O*-

acetals **32** could be accomplished in a highly stereocontrolled *anti*- or *syn*-manner depending on the stereochemistry of the phosphine ligand (Scheme 2.7).[20] Furthermore, this group combined a palladium-catalyzed asymmetric hydroamination with a gold-catalyzed cycloisomerization to prepare piperidines **35** with excellent stereochemical induction. The authors claimed that in this case the stereoinduction arose from the corresponding iminium ions **33** and **34** as the reactive intermediates. Moreover, the stereochemical transfer in the reaction strongly suggested the conservation of the iminium ion geometry with a very slow isomerization of both configurations. Thus, this work represents a rare example where the geometry of the iminium ion can be successfully controlled.

Scheme 2.7 *Synthesis of Stereodefined N,O-Acetals and Their Subsequent Cycloisomerization.*

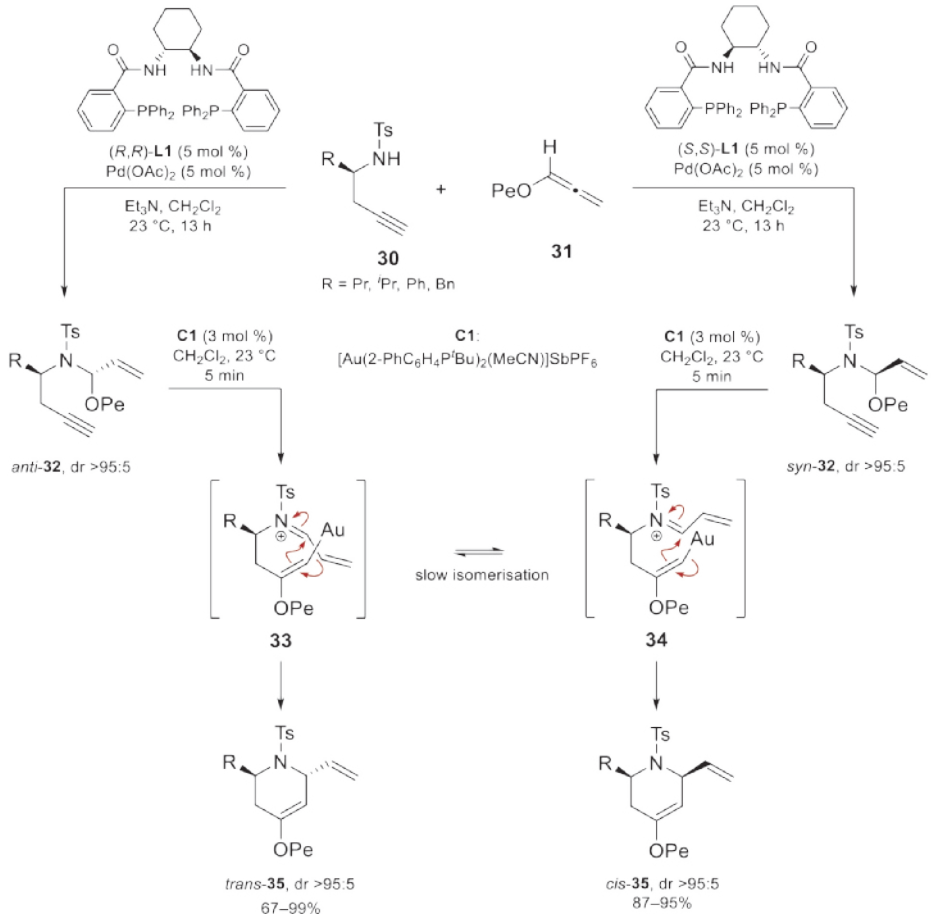

Kim et al. have established a general two-step protocol to access stereodefined cyclic *N,O*-acetals **38** by combination of palladium-catalyzed enantioselective hydroamination of alkoxy allene **31** with sulfonamide **36** and ring-closing metathesis of the obtained diolefins **37** (scheme 2.8).[21]

Scheme 2.8 *Two-Step Strategy for the Enantioselective Synthesis of Cyclic Allylic N,O-Acetals 38.*

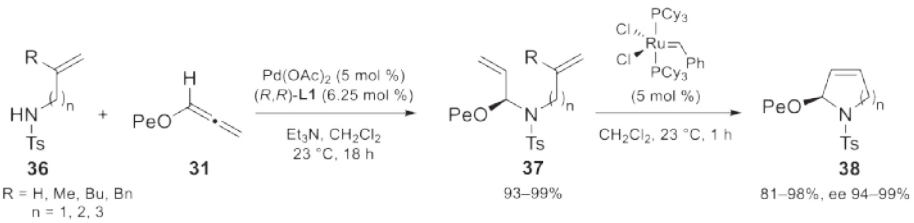

These acetals are often seen as *"diversity-generating elements"* because the endocyclic double bond can readily undergo diastereoselective transformations, such as dihydroxylation or epoxidation reactions (Scheme 2.9).[21]

Scheme 2.9 *Examples of the Use of Cyclic N,O-Acetal 39 as a Diversity-Generating Element.*

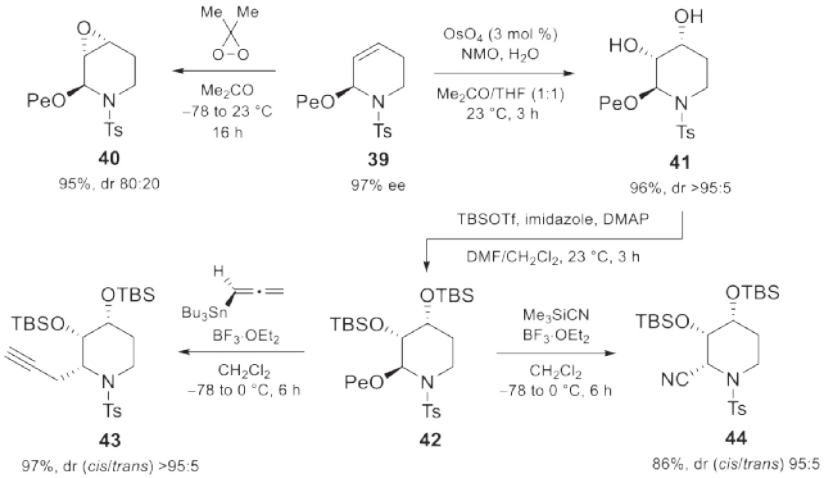

Thus, the reaction of **39** with dimethyldioxirane (DMDO) gave epoxide **40** in high yield with 80:20 selectivity. Another example of a stereocontrolled transformation included the dihydroxylation of **39** using catalytic OsO_4 (3 mol %). Here, diol product **41** was obtained in 95% yield with a ratio of >95:5 and with no drop of the ee value. Having proven the role of the *N,O*-acetal moiety as the stereocontrol element, the authors further investigated the late-stage

installation of various substituents via iminium ion-mediated CC bond formation. These experiments were conducted on bis(TBS ether) **42** upon treatment with $BF_3{\cdot}OEt_2$ and allenyl(tributyl)stannane or trimethylsilyl cyanide. In both cases the corresponding products **43** and **44** were obtained in high yield and high diastereoselectivity.

Furthermore, the choice of protecting groups on the vicinal diols played a key role in the stereochemistry of the Lewis acid mediated substitution (Scheme 2.10).[22] Thus, bis(TBS ether) **45a** was converted into product **46** with an excellent *cis*-selectivity, where the attack was performed through an inside addition of the carbon nucleophile controlled by the stereoelectronic effect of the cyclic iminium ion intermediate (Scheme 2.10, route *a*).[29] Conversely, the reaction of diprotected substrate **45b** was completed within 2 min and gave product **47** in 97% yield with excellent *trans*-selectivity. The almost complete formation of **47** can be explained by the attack of the carbon nucleophile onto the iminium ion from the less-hindered convex face in the bicyclic intermediate (Scheme 2.10, route *b*).

Scheme 2.10 *Protecting Group-Dependent Stereoselective Alkylation of Cyclic N,O-Acetal 45.*

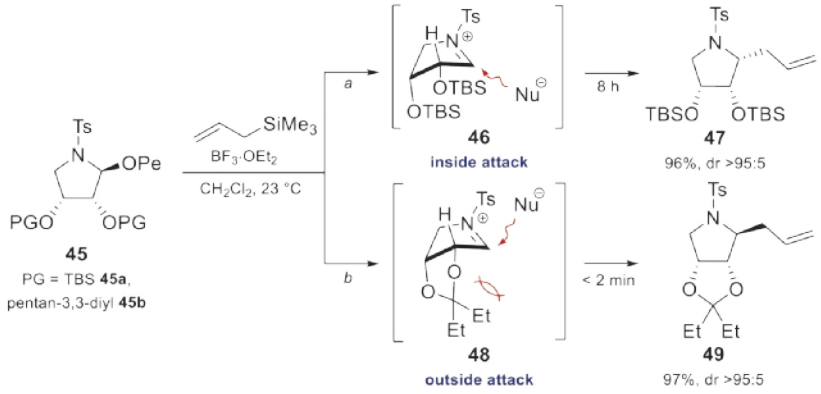

From a synthetic viewpoint, this stereocontrolled strategy establishes an efficient access to pyrrolidine-3,4-diols, important motifs in the synthesis of various bioactive natural products such as azasugars and polyhydroxylated alkaloids. Thus, Kang et al. applied *trans*-selective alkylation of **45b** to obtain **49**, a key component in the synthesis of the naturally occurring indolizidine alkaloid (–)-2-epilentiginosine (**53**)[30] (Scheme 2.11).[22] This synthesis was accomplished in five steps, including the incorporation of a second allyl group (compound **51**) and the construction

of the six-membered ring via RCM (compound **52**). Olefin reduction and deprotection of the diol completed the synthesis in 32% overall yield.

Scheme 2.11 *Synthesis of (–)-2-Epilentiginosine (53).*

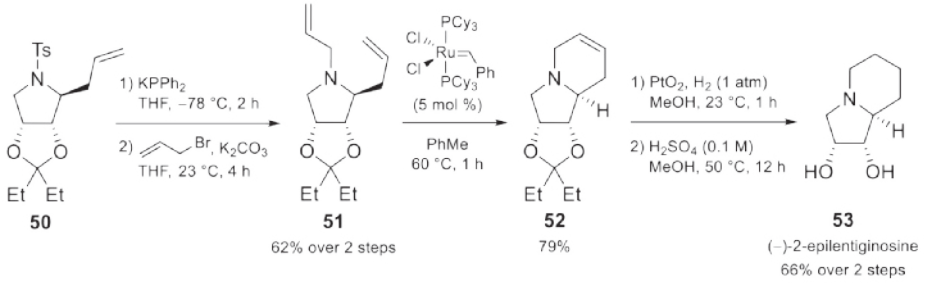

In addition to this example, Lim et al. successfully accomplished a concise formal synthesis of some indolizidine alkaloids where the key step featured the synthesis of *cis*-2,3-pyrrolidine intermediate **56** (Scheme 2.12).[23]

Scheme 2.12 *Synthesis of Polyhydroxylated Alkaloids* ***61*** *and* ***62*** *Employing Stereoselective Dihydroxylation and cis-Selective Cyanation of Cyclic N,O-Acetal* ***54*** *to Generate the Stereodiversity.*

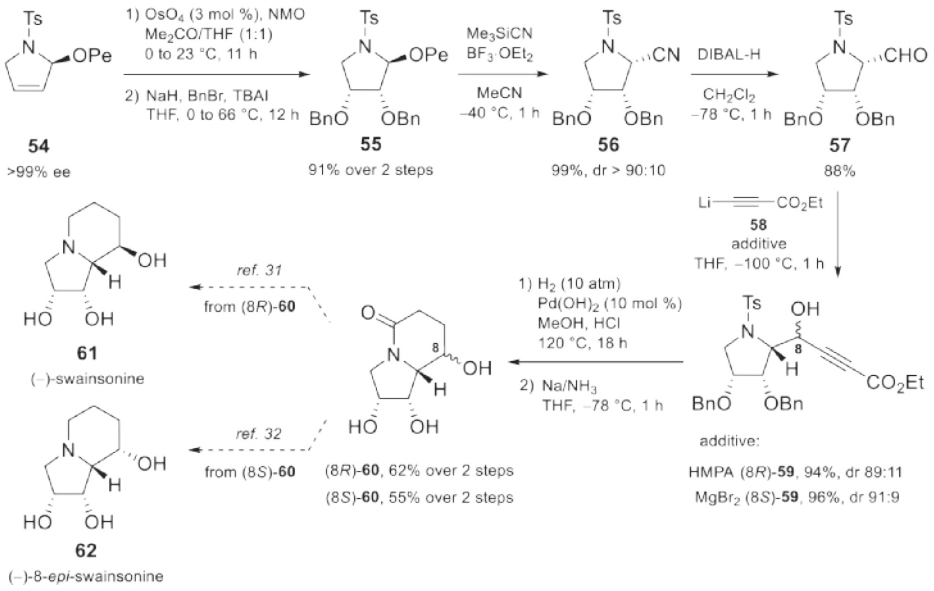

This precursor was prepared on multigram scale via an osmium-catalyzed diastereoselective dihydroxylation and alcohol protection of cyclic allylic *N,O*-acetal **54** yielding **55** in 91% yield. The subsequent Lewis acid mediated addition of trimethylsilyl cyanide proceeded in a highly stereocontrolled *cis*-manner, similar to that of **47**, and in near quantitative yield. The obtained cyanide **56** was then reacted with diisobutylaluminum hydride (DIBAL-H) and the resulting imine–aluminum complex was further treated with 1 N aqueous HCl to yield aldehyde **57** in 88% yield. Compound **57** was immediately converted into either of both isomers of propargyl alcohol **59** with comparable synthetic efficiency using hexamethylphosphoramide (HMPA) or $MgBr_2$ as additives. The inversion of the stereoselectivity was explained by the authors by the chelation-controlled addition of lithium alkynide **58** when using $MgBr_2$, which led to change in diastereoselectivity from 91:9 for (8*R*)-**59** to 89:11 for (8*S*)-**59**.[23] Debenzylation of (8*R*)-**59** and (8*S*)-**59** with concomitant alkyne hydrogenation proceeded well with palladium hydroxide on carbon (Pearlman's catalyst) under a H_2 atmosphere (10 atm) in the presence of HCl. Finally, the removal of the *p*-toluenesulfonyl group followed by lactam formation proceeded smoothly using dissolving-metal conditions (Na/NH_3) yielding alcohols (8*R*)-**59** and (8*S*)-**59** in 62 and 55% overall yields, respectively. Both compounds were further successfully used for the total synthesis of (–)-swainsonine **58** and its isomer (–)-8-*epi*-swainsonine **59**.[31,32]

2.2.3 Transformations Involving RCM Followed by Elimination of a Leaving Group

As shown above, allylic *N,O*-acetals are valuable precursors for a variety of regio- and stereoselective additions via Lewis acid catalysis. Nonetheless their application is not limited to only iminium ion chemistry. In the last decade, allylic *N,O*-acetals have been widely used in the synthesis of aromatic heterocycles, e.g., pyrroles. This approach for the preparation of aromatic compounds after a RCM reaction requires the subsequent elimination of a leaving group under mild acidic conditions. Our group was among the first to describe the formation of *N*-tosylpyrrole as a result of decomposition of intermediate **65** on silica gel (Scheme 2.13).[16]

Scheme 2.13 *Formation of N-Tosylpyrrole* **66** *as a Result of Decompostion of* **65** *on Silica Gel.*

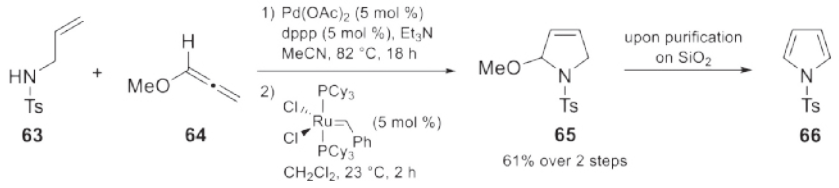

Donohoe et al. further extended this reaction to a palladium coupling/RCM/elimination protocol for the synthesis of C-3 functionalized pyrroles (Scheme 2.14).[33] This procedure allowed an additional derivatization at the central carbon of the allene without adding any extra steps in the preparation of the precursor of the metathesis reaction. The reaction mechanism involves oxidative addition of palladium(0) to the aryl halide to form palladium(II) species **70,** followed by carbopalladation of methoxyallene (**64**) to form the π-allyl species **71**.[34] Addition of the anion of the sulfonamide **67** to the most electron deficient end of this intermediate forms *N,O*-acetal **68** with regeneration of the palladium(0) catalyst. Subsequent RCM of diolefin **68** and exposure to TFA resulted in the elimination of MeOH to afford pyrrole **69** in fair to good yields over two steps.

Scheme 2.14 *Palladium Coupling/RCM/Elimination Route to 2,4-Disubstituted Pyrroles.*

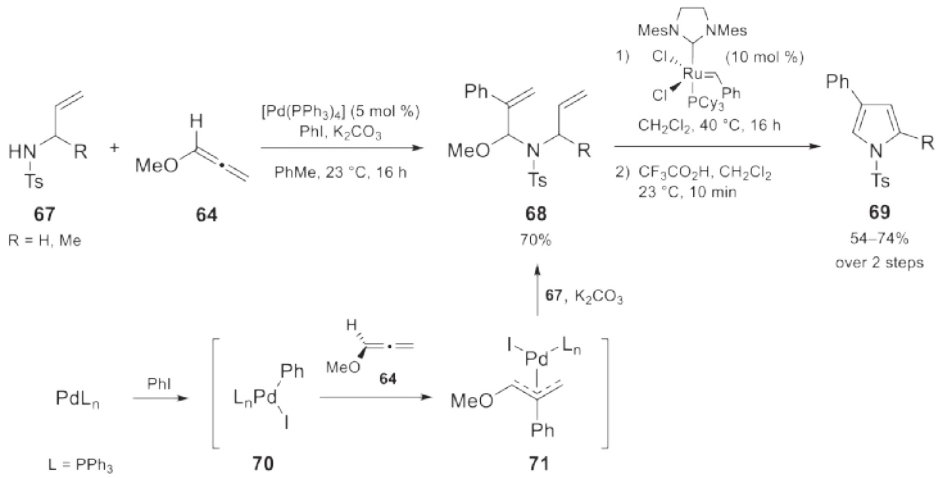

This procedure is not only limited to the preparation of simple *N*-heterocyclic frameworks. We have reported the construction of 3-(trifluoromethyl)pyrrole **74** via the same three-step sequence involving the palladium-catalyzed addition of allyl sulfonamide **72** to alkoxy allene **13** followed by RCM of the formed diolefin **73** (Scheme 2.15).[35] Such an approach offers many opportunities for the rapid construction of trifluoromethylated nitrogen heterocycles.

Scheme 2.15 *Synthesis of Trifluoromethyl-Substituted Pyrrole* **74**.

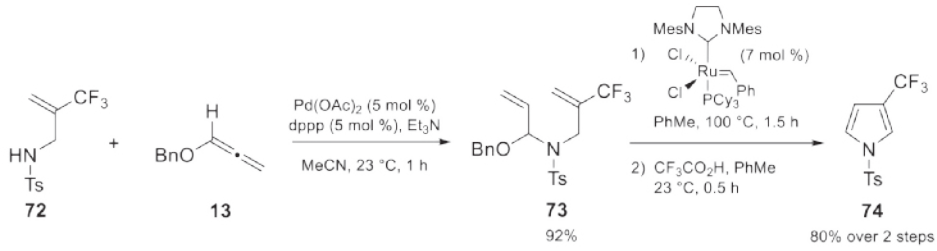

Encouraged by the numerous examples of applications of allylic *N,O*-acetals in synthetic chemistry, we decided to expand this research to azole heterocycles. The scope of the palladium-catalyzed hydroamination of alkoxy allenes with azoles as well as the mechanism of the transformation are presented in Chapter 3. This methodology could open up straightforward excess to functionalized *N*-heterocycles: key synthons for a variety of heterocyclic scaffolds valuable for the ECHONET program. Our initial studies to this topic are described in Chapter 4.

2.3 Sulfonyl Ynamines in the Synthesis of *N*-Heterocycles Using Palladium Catalysis

2.3.1 Introduction to Sulfonyl Ynamines

Ynamines are among the fastest growing and most versatile building blocks in organic synthesis that have been reported during the last decade.[14] Compared to classical alkynes, ynamines are more reactive towards both electrophiles and nucleophiles, which is caused by the electron-donating ability of the nitrogen atom present in their structure (Scheme 2.16). Thus, *N*-allenyl resonance structure **76** represents the dual reactivity of ynamines: the terminal carbon is nucleophilic and the central one electrophilic.

Scheme 2.16 *Ynamine Resonance Structures.*

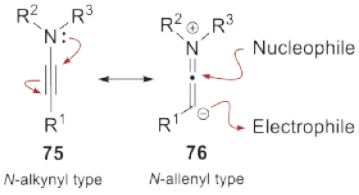

One of the drawbacks of ynamines is their high reactivity, which complicates their preparation, storage, and application. Introduction of an electron withdrawing group (EWG) on the nitrogen atom tempers the reactivity of its lone pair, and thus leads to less reactive compounds. These types of ynamines are commonly named ynamides (e.g., R^3 = EWG in **75**) and are very convenient to handle because of their well-balanced reactivity and thermal stability.[14a] Up to date, there are four main groups of ynamides, in which the nitrogen atom forms part of lactams, carbamates, ureas, and sulfonamides. Among them, sulfonyl ynamines **2** have been extensively used in a broad spectrum of palladium-catalyzed transformations (Scheme 2.17).

Scheme 2.17 *Overview of Products of Palladium-Catalyzed Cyclizations of Sulfonyl Ynamines* **2**.

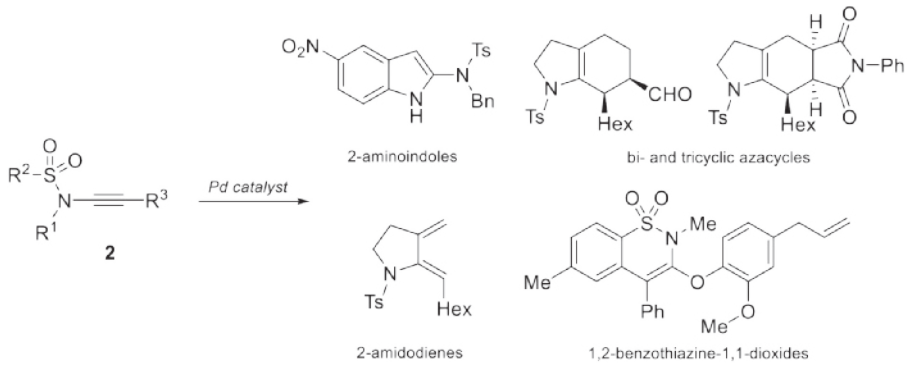

In particular, palladium-catalyzed cyclizations of sulfonyl ynamines are immensely useful for the inclusion of nitrogen-based functionalities into complex organic molecules. In addition to their synthetic utility, such reactions are mechanistically interesting. Finally, the obtained *N*-heterocyclic products are often key elements of biologically active compounds.

2.3.2 Palladium-Catalyzed Cyclizations of Sulfonyl Ynamines

Over the past decade there have been significant advances in the area of palladium-catalyzed cyclizations of sulfonyl ynamines. The main reason for this success was the development of fast and simple methods for their preparation. In 2003 Witulski et al. introduced *N*-alkynyl-2-iodoanilines **80** into this field (Scheme 2.18).[36] These substrates were easily prepared from readily available 2-iodoanilines **77** by *N*-tosylation (**78**) followed by an *N*-ethynylation reaction with alkynyl iodonium salts **79** to form *N*-alkynyl-2-iodoanilines **80** in 80–90% yields.

Scheme 2.18 *Synthesis of N-Alkynyl-2-iodoanilines* ***80****.*

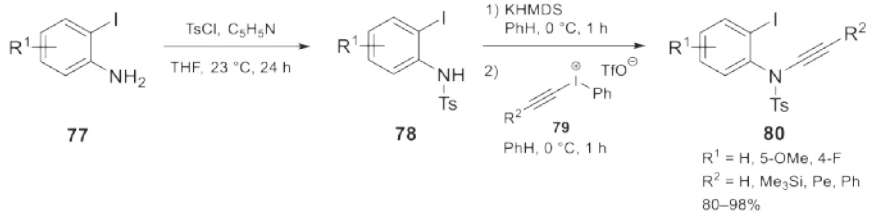

Consequently, *N*-alkynyl-2-iodoanilines **80** were reacted with several amines **81** in the presence of a palladium catalyst to afford 2-aminoindoles **82** in good to excellent yields (Scheme 2.19). The reaction was initiated by oxidative addition of palladium(0) into the aryl–iodine bond of **80** resulting in palladium(II) complex **83**. This intermediate further underwent amino-palladation (**84**) followed by deprotonation with a base (**85**) and reductive elimination to yield final products **82**. This amination-cyclization protocol tolerated primary and secondary amines and afforded a wide range of 2-aminoindole products (e.g., **82a–c**) in good to excellent yields.

Scheme 2.19 *Palladium-Catalyzed Amination-Cyclization of N-Alkynyl-2-iodoanilines* ***80****.*

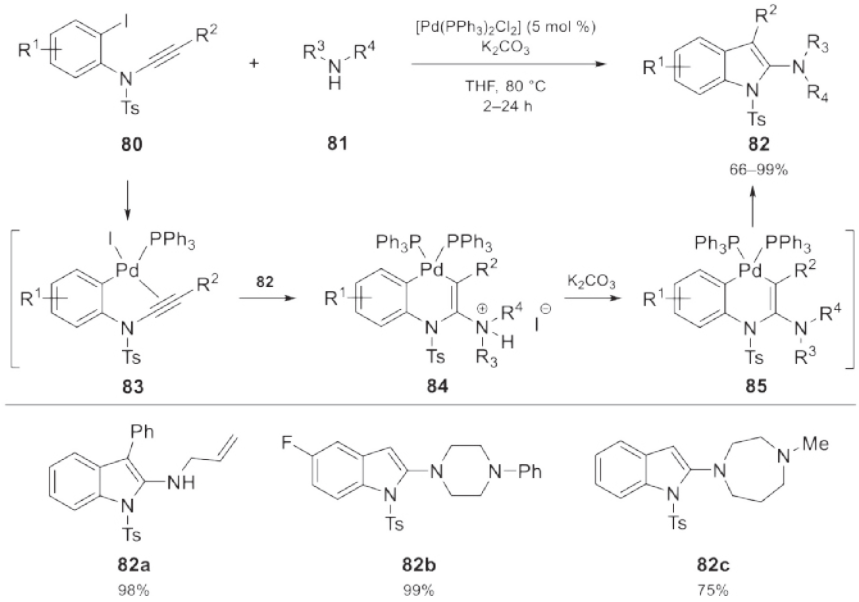

A few years later, Dooleweerdt et al. developed a very interesting variation of this indole synthesis (Scheme 2.20).[37] The transformation involved a palladium-catalyzed coupling of sulfonyl ynamine **86** with *o*-iodoaniline derivatives **87**. The authors proposed that this reaction proceeded via a Sonogashira coupling of **86** with **87** followed by an intramolecular hydroamination of the triple bond. Although the yields of the final products **89** varied from poor to fair, the reaction proceeded under mild basic conditions and in the absence of a copper salt.

Scheme 2.20 *Synthesis of 2-Sulfonamidoindoles from Sulfonyl Ynamine **86** and o-Iodoanilines **87**.*

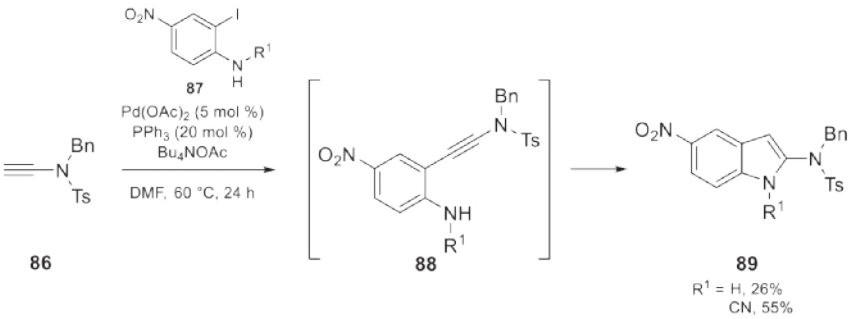

Anderson's research group was among the first that utilized sulfonyl bromoenynamines **92** for a palladium-catalyzed cascade reaction (Scheme 2.21).[38] These ynamines were prepared from sulfonamide **90** and bromoalkenes **91** using Hsungs's[39] method (catalytic $CuSO_4$/1,10-phenanthroline, K_3PO_4, toluene, 80 °C). In all cases, the corresponding sulfonyl ynamines **92** were obtained in fair to excellent yields, including the alkyl- or heteroaryl substituted ynamines (**92a** and **92b**), and more complex examples featuring additional stereogenic centers (e.g., **92c**).

Scheme 2.21 *Synthesis of Sulfonyl Bromoenynamines **92**.*

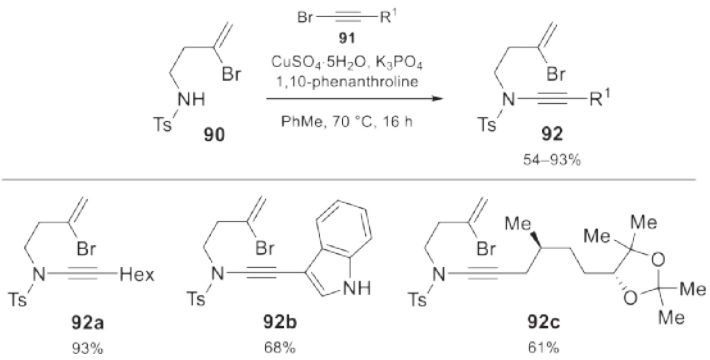

With a range of sulfonyl bromoenynamines in hand, Greenaway et al. then established a cascade sequence to form aminodienes **94** in very good yields (Scheme 2.22).[40] Their sequence consisted of a palladium-catalyzed cyclization and cross-coupling of bromoenynamine **92a** followed by 6π-electron electrocyclization of the formed triene intermediate **93**.

Scheme 2.22 *Palladium-Catalyzed Cascade Reaction of Sulfonyl Bromoenynamine* ***92a****.*

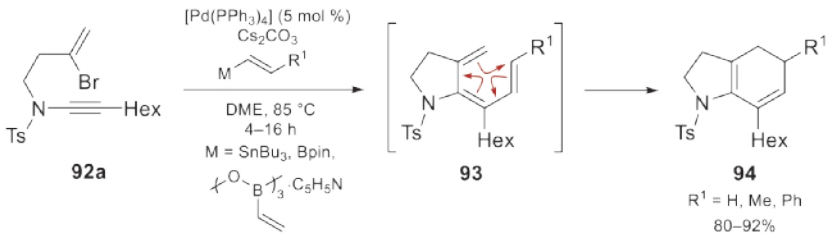

Subsequently, Greenaway et al. reported a similar cyclization of bromoenynamide **92a** and its analogs to afford cyclic 2-sulfonamidodienes such as **96** (Scheme 2.23).[41] This process required the use of an alcohol as a hydride source to terminate the *cis*-carbopalladation step (**95**). The obtained cyclic 2-sulfonamidodiene **96** was further used in Diels–Alder reactions with electron-deficient alkenes and alkynes and, as such, represented a straightforward route to bi- and tricyclic azacycles (e.g., **97a–c**).

Scheme 2.23 *Palladium-Catalyzed Reductive Cyclization of Sulfonyl Bromoenynamine* ***92a****.*

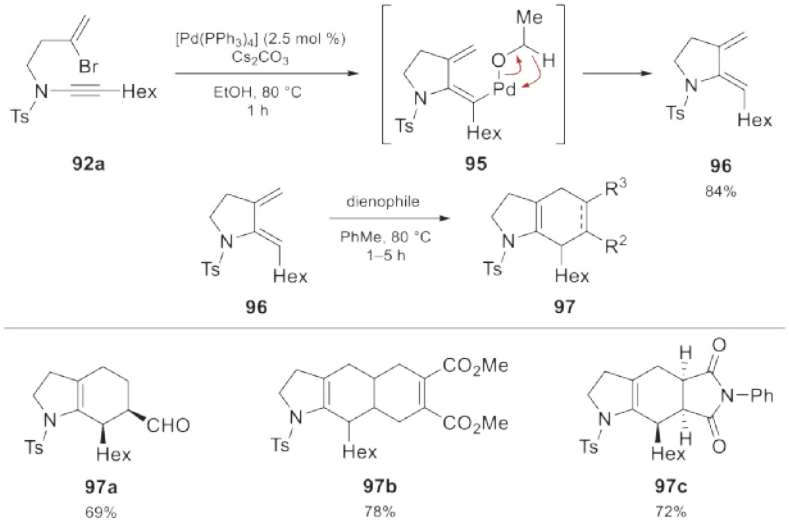

Walker et al. improved the atom economy of the synthesis of 2-sulfonamidodienes through palladium-catalyzed cycloisomerization of sulfonyl enynamines **98** and **100** (Scheme 2.24).[42] Alkyl-, silyl-, and aryl-substituted sulfonyl enynamines **98** delivered pyrrolidine products **99** with $Pd(OAc)_2$ and *N,N'*-di(benzylidene)ethylenediamine (bbeda) as the catalytic system in a highly stereoselective manner (*Z*/*E*-ratio up to 97:3). Additionally, cycloisomerization of enynamides **100** featuring 1,2-disubstituted alkenes resulted in mixtures of 1,3- and 1,4-dienes in most of the cases (products **101** and **102**, respectively). Overall, the reaction tolerated a range of substituents on both the ynamine and alkene, underlining their potential utility as an atom-economical source of azacycles. Interestingly, the styrenyl sulfonyl ynamines afforded exclusively 1,3-dienes (e.g., **101a**) because of the hydrogen atoms required for 1,4-diene formation. In contrast, cyclization of cycloalkenyl ynamides gave the 1,4-dienes (e.g., spirocyclic 1,4-diene **102a**) with minor amounts of the 1,5-dienes arising from palladium-catalyzed alkene isomerization.

Scheme 2.24 *Palladium-Catalyzed Cycloisomerization of Sulfonyl Enynamines **98** and **100**.*

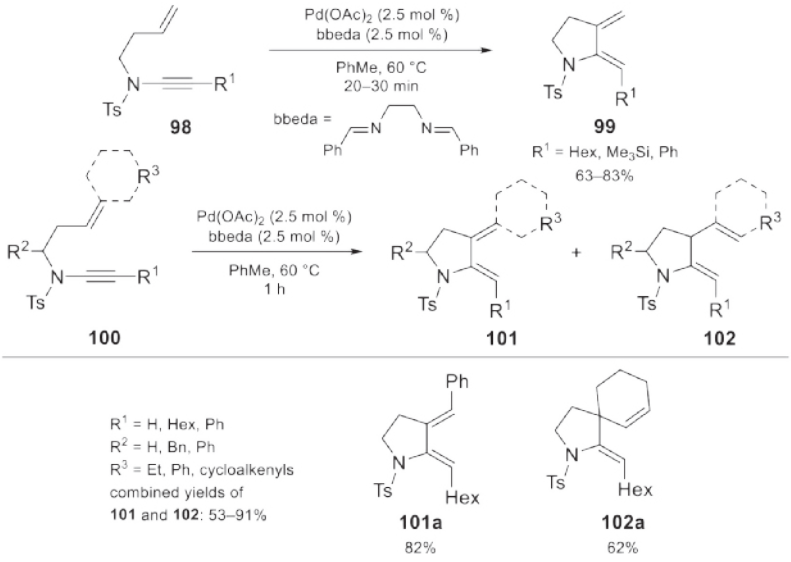

Mekareeya et al. disclosed the mechanistic pathway by which this reaction proceeded (Scheme 2.25).[43] Extensive ^1H NMR spectroscopic studies and isotope effects supported a palladium(II) hydride-catalyzed pathway and revealed crucial roles of bbeda and water in the origin of the catalyst formation. Thus, partial hydrolysis of initial complex **103** in a wet solvent liberates benzaldehyde and amine complex **104**, which further undergoes β-hydride elimination to form the

palladium(II) hydride complex **105**. This species is in equilibrium with palladium(0)-complex **106** required for coordination to the substrate (**107**) followed by hydropalladation (**108**) and carbopalladation to form the relatively stable alkylpalladium(II) species **109**. Further coordination of palladium to the bridgehead hydrogen atom in **110** triggers the β-hydride elimination leading to palladium(II) hydride complex **111**. Finally, isomerization to palladium(0) complex **112** and decoordination of the active catalyst delivers the 2-sulfonamidodiene product **99** and restarts the catalytic cycle.

Scheme 2.25 *Mechanism of Palladium-Catalyzed Cycloisomerization of Sulfonyl Enynamines* ***98****.*

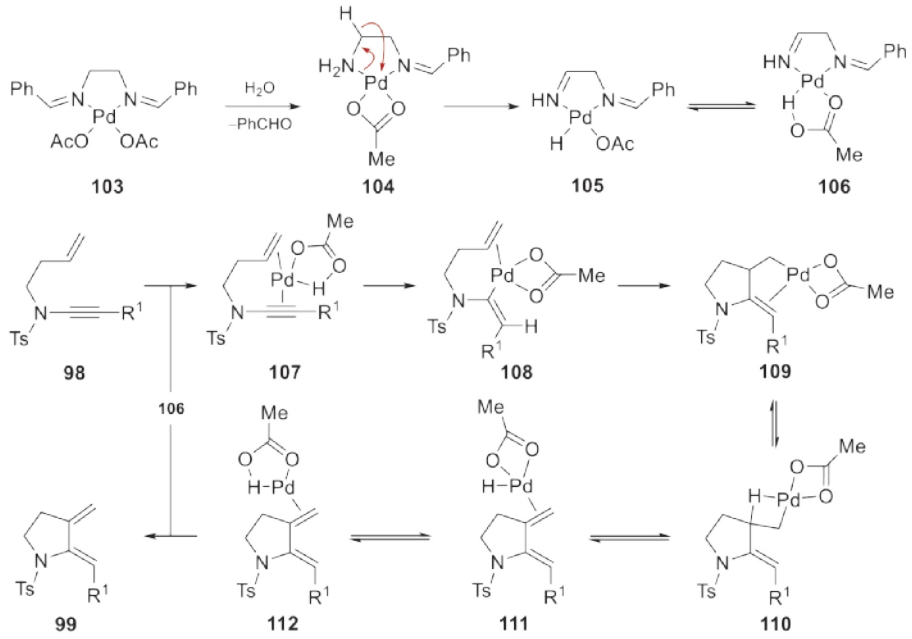

Fujino et al. published an interesting example of catalyst-dependent 5-*exo*/6-*endo* regioselective arylative cyclization of sulfonyl ynamines containing alkynol **113** (Scheme 2.26).[44] The regioselectivity was accurately dictated by the choice of the ligand of the palladium catalyst. The bulky monodentate phosphine ligand XPhos directed a 5-*exo*-dig cyclization to form tetrahydrofuran derivatives **114** in very good yields and excellent regioselectivities. In contrast, cyclization of **113** in the presence of oxygen-linked bidentate ligand Xantphos proceeded in a 6-*endo*-dig fashion affording dihydropyrans **115** in a highly regiocontrolled manner. A proposed reaction mechanism highlighted the intermediate **116** as the divergence point in the formation of

two distinct scaffolds **114** and **115** (Scheme 2.27). When XPhos ligand was used, initial palladium complex **116** (Scheme 2.27, route *a*, L = XPhos) had a preferential affinity for a hydroxy group forming complex **117**. Further insertion of the alkyne into the oxygen–palladium bond (**118**) followed by a reductive elimination afforded product **114**. Conversely, the arylpalladium–Xantphos catalyst **116** (Scheme 2.27, route *b*, L = Xantphos) activated the ynamide under Lewis acid catalysis (**119**) allowing the nucleophilic addition of the hydroxy group through a 6-*endo*-dig pathway. Formed in this manner, intermediate **120** underwent reductive elimination to form product **115**.

Scheme 2.26 *Ligand-Controlled Palladium-Catalyzed Arylative Cyclization of Sulfonyl Ynamines **113**.*

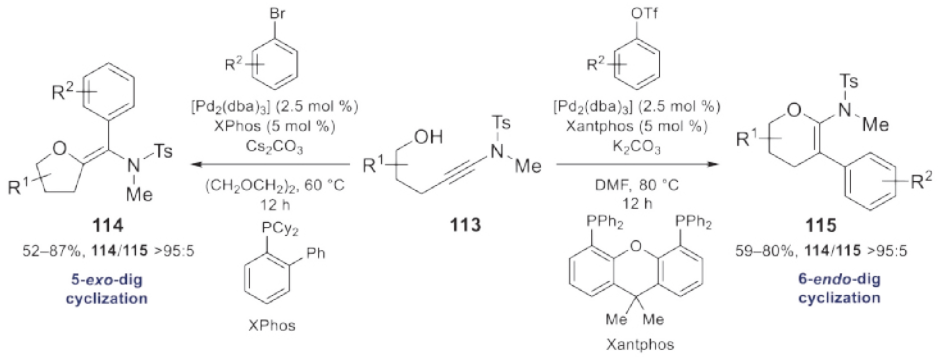

Scheme 2.27 *Plausible Mechanism of the Cyclization.*

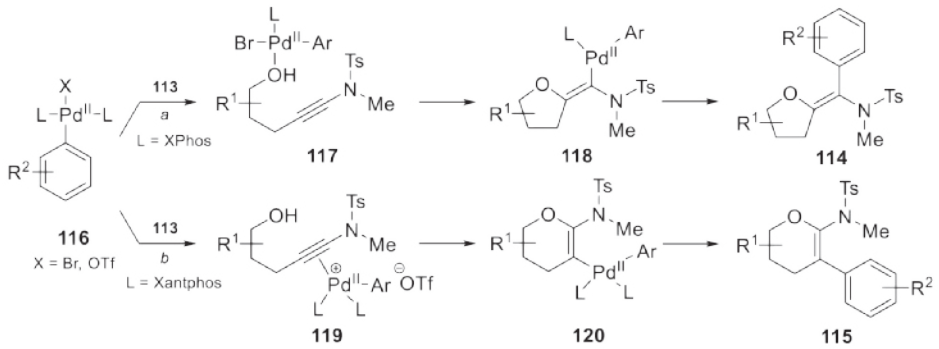

The research group of Swamy et al. has developed a palladium-catalyzed tandem cyclization of 2-iodobenzenesulfonyl ynamines **121** to afford a wide range of 1,2-benzothiazine-1,1-dioxides **122** (Scheme 2.28).[45] Similar to the examples above, this transformation proceeded through nucleophilic attack onto functionalized ynamines through palladium(0)-catalysis (e.g., Scheme

2.19). The scope of the nucleophiles included amines, amides, and phenols leading to the corresponding products **122** in good to excellent yields. Additionally, medicinally useful compounds like nortriptyline and eugenol were used as nucleophiles (products **122a** and **122b**, respectively). This method represented an attractive route for the pharmaceutically attractive 1,2-benzothiazine-1,1-dioxide derivatives **123** that are widely used in medicinal chemistry.[46]

Scheme 2.28 *Synthesis of 1,2-Benzothiazine-1,1-dioxides 122.*

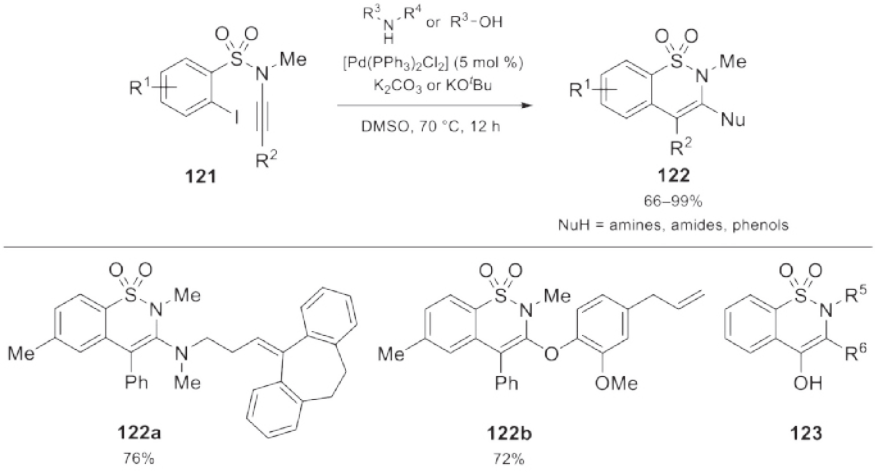

These examples show that palladium-catalyzed cyclizations of sulfonyl ynamines have the potential to contribute to the ECHONET network with the synthesis of complex *N*-heterocyclic systems and especially in the lead search of potentially bioactive molecules for the agrochemical industry. A novel palladium-catalyzed intramolecular cyclization of sulfonyl ynamines is discussed in Chapter 6, as well as its application to the synthesis of libraries of heteroaromatic compounds of potential value as crop protection agents (Chapter 7).

2.4 Conclusion

Palladium catalysis has revolutionized the field of heterocyclic chemistry by facilitating the construction of complex organic molecules in a highly efficient manner. The present overview highlights the use of alkoxy allenes and sulfonyl ynamines as versatile substrates for palladium-catalyzed transformations. In particular, we showcased palladium-catalyzed hydroaminations of alkoxy allenes as a straightforward process for the preparation of allylic *N,O*-acetals, precursors of various bioactive compounds and *N*-heterocycles. Moreover, the use of sulfonyl ynamines in a

wide range of palladium-mediated cyclizations is presented. We hope that this comprehensive overview helps to promote the continued interest in palladium catalysis in combination with the chemistry of alkoxy allenes and sulfonyl ynamines.

2.5 References and Notes

[1] (a) Tsuji, J. *Palladium Reagents and Catalysts: New Perspectives for the 21st Century,* 2nd ed.; Wiley-Blackwell: Hoboken, NJ, 2004; (b) *Palladium in Heterocyclic Chemistry,* 2nd ed.; Li, J. J., Gribble, G., Eds.; Elsevier, Oxford, U.K., 2007; (c) *Palladium-Catalyzed Coupling Reactions: Practical Aspects and Future Developments;* Molnár, Á., Ed.; Wiley-VCH: Weinheim, Germany, 2013; (d) *New Trends in Cross-Coupling – Theory and Applications;* Colacot, T. J., Ed.; RSC Publishing: Cambridge, U.K., 2015; (e) *Strategies for Palladium-Catalyzed Non-Directed and Directed C–H Bond Functionalization,* 1st ed.; Kapdi, A.; Maiti, D., Eds.; Elsevier, Amsterdam, 2017.

[2] (a) Wu, X.-F.; Anbarasan, P.; Neumann, H.; Beller, M. *Angew. Chem. Int. Ed.* **2010**, *49*, 9047–9050; (b) Negishi, E. *Angew. Chem. Int. Ed.* **2011**, *50*, 6738–6764; (c) Suzuki, A. *Angew. Chem. Int. Ed.* **2011**, 50, 6722–6737; (d) The Official Web Site of the Nobel Prize, https://www.nobelprize.org/nobel_prizes/chemistry/laureates/2010/popular-chemistryprize2010.pdf (accessed April 10, 2018).

[3] Torborgaand, C.; Beller, M. *Adv. Synth. Catal.* **2009**, *351*, 3027–3043.

[4] (a) Lundgren, R. J.; Stradiotto, M. *Chem. Eur. J.* **2012**, *18*, 9758–9769; (b) Johansson Seechurn, C. C. C.; Kitching, M. O.; Colacot, T. J.; Snieckus, V. *Angew. Chem. Int. Ed.* **2012**, *51*, 5062–5085; (c) Ruiz-Castillo, P.; Buchwald, S. L. *Chem. Rev.* **2016**, *116*, 12564–12649; (d) Royaand, D.; Uozumi, Y. *Adv. Synth. Catal.* **2018**, *360*, 602–625.

[5] (a) Barnard, C. F. J. *Organometallics* **2008**, *27*, 5402–5422; (b) Brennführer, A.; Neumann, H.; Beller, M. *Angew. Chem. Int. Ed.* **2009**, *48*, 4114–4133; (c) Grigg, R.; Mutton, S. P. *Tetrahedron* **2010**, *66*, 5515–5548; (d) Wu, X. F.; Neumann, H.; Beller, M. *Chem. Soc. Rev.* **2011**, *40*, 4986–5009; (e) Wu, X. F.; Neumann, H.; Beller, M. *Chem. Rev.* **2013**, *113*, 1–35; (f) Gadgea, S. T.; Bhanage, B. M. *RSC Adv.* **2014**, *4*, 10367–10389.

[6] (a) *The Handbook of Homogeneous Hydrogenation;* de Vries, J. G., Elsevier, C. J., Eds.; WILEY-VCH: Weinheim, Germany, 2008; (b) Chen, Q.-A.; Ye, Z.-S.; Duana, Y.; Zhou, Y.-G. *Chem. Soc. Rev.* **2013**, *42*, 497–511; (c) Wang, D.; Astruc, D. *Chem. Rev.* **2015**, *115*, 6621–6686 and references therein.

[7] (a) Wu, W.; Jiang, H. *Acc. Chem. Res.* **2012**, *45*, 1736–1748; (b) Obora, Y.; Ishii, Y. *Catalysts* **2013**, *3*, 794–810; (c) Dong, J. J.; Browne, W. R.; Feringa, B. L. *Angew. Chem. Int. Ed.* **2015**, *54*, 734–744; (d) Wang, D.; Weinstein, A. B; White, P. B.; Stahl, S. S. *Chem. Rev.* **2018**, *118*, 2636–2679.

[8] (a) Chen, X.; Engle, K. M.; Wang, D.-H.; Yu, J.-Q. *Angew. Chem. Int. Ed.* **2009**, *48*, 5094–5115; (b) Lyons, T. W.; Sanford, M. S. *Chem. Rev.* **2010**, *110*, 1147–1169; (c) Jiao, K.-J.; Zhao, C.-Q.; Fang, P.; Mei, T.-S. *Tetrahedron Lett.* **2017**, *58*, 797–802.

[9] (a) McDonald, R. I.; Liu, G.; Stahl, S. S. *Chem. Rev.* **2011**, *111*, 2981–3019; (b) Schultz, D. M.; Wolfe, J. P. *Synthesis* **2012**, 351–361; (c) Dong, Z.; Ren, Z.; Thompson, S. J.; Xu, Y.; Dong, G. *Chem. Rev.* **2017**, *117*, 9333–9403 and reference 4.

[10] (a) Chinchilla, R.; Nájera, C. *Chem. Rev.* **2014**, *114*, 1783–1826; (b) Trost, B. M.; Masters, J. T. *Chem. Soc. Rev.* **2016**, *45*, 2212–1238; (c) Ansell, M. B.; Navarro, O.; Spencer, J. *Coord. Chem. Rev.* **2017**, *336*, 54–77 and reference 4.

[11] (a) Ye, J.; Ma, S. *Acc. Chem. Res.* **2014**, *47*, 989–1000; (b) Le Brasa, J.; Muzart, J. *Chem. Soc. Rev.* **2014**, *43*, 3003–3040; (c) Lledó, A.; Pla-Quintana, A.; Roglans, A. *Chem. Soc. Rev.* **2016**, *45*, 2010–2023.

[12] (a) Broggini, G.; Beccalli, E. M.; Fasana, A.; Gazzola, S. *Beilstein J. Org. Chem.* **2012**, *8*, 1730–1746; (b) Majumdar, K. C.; Samanta, S.; Sinha, B. *Synthesis* **2012**, *44*, 817–847; (c) Ferraccioli, R. *Synthesis* **2013**, *45*, 581–591.

[13] Masterful review on alkoxy allenes: Zimmer, R.; Reissig, H.-U. *Chem. Soc. Rev.* **2014**, *43*, 2888–2903.

[14] Recent reviews on sulfonyl ynamines and ynamines in general: (a) Dekorver, K. A.; Li, H.; Lohse, A. G.; Hayashi, R.; Lu, Z.; Zhang, Y.; Hsung, R. P. *Chem. Rev.* **2010**, *110*, 5064–5106; (b) Evano, G.; Coste, A.; Jouvin, K. *Angew. Chem. Int. Ed.* **2010**, *49*, 2840–2859; (c) Lu, T.; Hsung, R. P. *ARKIVOC* **2014**, *i*, 127–141; (d) Wang, X.-N.; Yeom, H.-S.; Fang, L.-C.; He, S.; Ma, Z.-X.; Kedrowski, B. L.; Hsung, R. P. *Acc. Chem. Res.* **2014**, *47*, 560–578; (e) Cook, A. M.; Wolf, C. *Tetrahedron Lett.* **2015**, *56*, 2377–2392.

[15] Tjen, K. C. M. F.; Kinderman, S. S.; Schoemaker, H. E.; Hiemstra, H.; Rutjes, F. P. J. T. *Chem. Commun.* **2000**, 699–700.

[16] Kinderman, S. S.; Doodeman, R.; van Beijma, J. W.; Russcher, J. C.; Tjen, K. C. M. F.; Kooistra, T. M.; Mohaselzadeh, H.; van Maarseveen, J. H.; Hiemstra, H.; Schoemaker, H. E.; Rutjes, F. P. J. T. *Adv. Synth. Catal.* **2002**, *344*, 736–748.

[17] Kinderman, S. S. Transition Metal Catalyzed Formation and Transformations of Allylic *N,O*-Acetals with a Focus on Olefinic α-Amino Acids. Ph.D. Thesis, University of Amsterdam, the Netherlands, 2003.

[18] Kinderman, S. S.; de Gelder, R.; van Maarseveen, J. H.; Schoemaker, H. E.; Hiemstra, H.; Rutjes, F. P. J. T. *J. Am. Chem. Soc.* **2004**, *126*, 4100–4101.

[19] Wiles, J. A.; Phadke, A. S; Agarwal, A.; Chen, D.; Gadhachanda, V. R.; Hashimoto, A.; Pais, G.; Wang, Q.; Chen, D.; Wang, X.; Greenlee, W. Ether Compounds for Treatment of Immune and Inflammatory Disorders. WO 2017035411, March 2, 2017.

[20] (a) Kim, H.; Rhee, Y. H. *J. Am. Chem. Soc.* **2012**, *134*, 4011–4014; (b) Kim, H.; Rhee, Y. H. *Synlett* **2012**, *23*, 2875–2879.

[21] Kim, H.; Lim, W.; Im, D.; Kim, D.; Rhee, Y. H. *Angew. Chem. Int. Ed.* **2012**, *51*, 12055–12058.

[22] Kang, S.; Kim, D.; Rhee, Y. H. *Chem. Eur. J.* **2014**, *20*, 16391–16396.

[23] Lim, W.; Rhee, Y. H. *Tetrahedron* **2015**, *71*, 5939–5945.

[24] Hydridopalladium complexes as key intermediates in the process: (a) Leoni, P.; Sommovigo, M.; Pasqall, M.; Midollini, S.; Braga, D.; Sabatino, P. *Organometallics* **1991**, *10*, 1038–1044; (b) Grushin, V. V. *Chem. Rev.* **1996**, *96*, 2011–2034; (c) Trost, B. M. *Chem. Eur. J.* **1998**, *4*, 2405–2412; (d) Amatore, C.; Jutand, A.; Meyer, G.; Carelli, I.; Chiarotto, I. *Eur. J. Inorg. Chem.* **2000**, 1855–1859; (e) Trost, B. M.; Xie, J.; Sieber, D. *J. Am. Chem. Soc.* **2011**, *133*, 20611–20622 and references therein.

[25] Bernar, I.; Fiser, B.; Blanco-Ania, D.; Gómez-Bengoa, E.; Rutjes, F. P. J. T. *Org. Lett.* **2017**, *19*, 4211–4214.

[26] (a) Ginesta, X.; Pericas, M. A.; Riera, A. *Tetrahedron Lett.* **2002**, *43*, 779–782; (b) Guillena, G.; Najera, C. *J. Org. Chem.* **2000**, 65, 7310–7322; (c) Mazon, A.; Najera, C. *Tetrahedron: Asymmetry* **1997**, *11*, 1855–1858.

[27] Michel, P.; Rassat, A.; Daly, J. W.; Spande, T. F. *J. Org. Chem.* **2000**, *65*, 8908–8918.

[28] (a) Garraffo, H. M.; Spande, T. F.; Daly, J. W.; Baldessari, A.; Gros, E. G. *J. Nat. Prod.* **1993**, *56*, 357–373; (b) Jain, P.; Garraffo, H. M.; Yeh, H. J. C.; Spande, T. F.; Daly, J. W.; Andriamaharavo, N. R.; Andriantsiferana, M. *J. Nat. Prod.* **1996**, *59*, 1174–1178.

[29] (a) Larsen, C. H.; Ridgway, B. H.; Shaw, J. T.; Woerpel, K. A. *J. Am. Chem. Soc.* **1999**, *121*, 12208–12209; (b) Shenoy, S. R.; Smith, D. M.; Woerpel, K. A. *J. Am. Chem. Soc.* **2006**, *128*, 8671–8677 and references therein.

[30] (a) Rajender, A.; Rao, J. P.; Rao, B. V. *Eur. J. Org. Chem.* **2013**, 1749–1757; (b) Zhuang, J.-J.; Ye, J.-L.; Zhang, H.-K.; Huang, P.-Q. *Tetrahedron* **2012**, *68*, 1750–1755; (c) Muramatsu, T.; Yamashita, S.; Nakamura, Y.; Suzuki, M.; Mase, N.; Yoda, H.; Takabe, K. *Tetrahedron Lett.* **2007**, *48*, 8956–8959.

[31] Shi, G.-F.; Li, J.-Q.; Jiang, X.-P.; Cheng, Y. *Tetrahedron* **2008**, *64*, 5005–5012.

[32] Fleet, G. W. J.; Peach, J. M.; Smith, P. W.; Austin, G. N.; Baird, P. D.; Watkin, D. J. *Tetrahedron* **1987**, *43*, 3095–3108.

[33] (a) Donohoe, T. J.; Orr, A. J.; Gosby, K.; Bingham, M. *Eur. J. Org. Chem.* **2005**, 1969–1971; (b) Donohoe, T. J.; Orr, A. J.; Bingham, M. *Angew. Chem. Int. Ed.* **2006**, *45*, 2664–2670; (c) Donohoe, T. J.; Fishlock, L. P.; Procopiou, P. A. *Chem. Eur. J.* **2008**, *14*, 5716–5726; (d) Donohoe, T. J.; Kershaw, N. M.; Orr, A. J.; Wheelhouse, K. M. P.; Fishlock, L. P.; Lacy, A. R.; Bingham, M.; Procopiou, P. A. *Tetrahedron* **2008**, *64*, 809–820.

[34] (a) Trost, B. M.; Simas, A. B. C.; Plietker, B.; Jakel, C.; Xie, J. *Chem. Eur. J.* **2005**, *11*, 7075–7082; (b) Trost, B. M.; Xie, J.; Sieber, J. D. *J. Am. Chem. Soc.* **2011**, *133*, 20611–20622.

[35] De Matteis, V.; Dufay, O.; Waalboer, D. C. J.; van Delft, F. L.; Tiebes, J.; Rutjes, F. P. J. T. *Eur. J. Org. Chem.* **2007**, 2667–2675.

[36] Witulski, B.; Alayrac, C.; Tevzadze-Saeftel, L. *Angew. Chem. Int. Ed.* **2003**, *42*, 4257–4260.

[37] Dooleweerdt, K.; Ruhland, T.; Skrydstrup, T. *Org. Lett.* **2009**, *11*, 221–224.

[38] Campbell, C. D.; Greenaway, R. L.; Holton, O. T.; Walker, P. R.; Chapman, H. A.; Russell, C. A.; Carr, G.; Thomson, A. L.; Anderson, E. A. *Chem. Eur. J.* **2015**, *21*, 12627–12639.

[39] Zhang, X.; Zhang, Y.; Huang, J.; Hsung, R. P.; Kurtz, K. C. M.; Oppenheimer, J.; Petersen, M. E.; Sagamanova, I. K.; Shen, L.; Tracey, M. R. *J. Org. Chem.* **2006**, *71*, 4170–4177.

[40] Greenaway, R. L.; Campbell, C. D.; Holton, O. T.; Russell, C. A.; Anderson, E. A. *Chem. Eur. J.* **2011**, *17*, 14366–14370.

[41] Greenaway, R. L.; Campbell, C. D.; Chapman, H. A.; Anderson, E. A. *Adv. Synth. Catal.* **2012**, *354*, 3187–3194.

[42] Walker, P. R.; Campbell, C. D.; Suleman, A.; Carr, G.; Anderson, E. A. *Angew. Chem. Int. Ed.* **2013**, *52*, 9139–9143.

[43] Mekareeya, A.; Walker, P. R.; Couce-Rios, A.; Campbell, C. D.; Steven, A.; Paton, R. S.; Anderson, E. A. *J. Am. Chem. Soc.* **2017**, *139*, 10104–10114.

[44] Fujino, D.; Yorimitsu, H.; Osuka, A. *J. Am. Chem. Soc.* **2014**, *136*, 6255–6258.

[45] Siva Reddy, A.; Leela Siva Kumari, A.; Saha, S.; Kumara Swamya, K. C. *Adv. Synth. Catal.* **2016**, *358*, 1625–1638.

[46] For an overview on the synthesis and application of 1,2-benzothiazine-1,1-dioxides, see: Majumdar, K. C.; Mondal, S. *Chem. Rev.* **2011**, *111*, 7749–7773.

CHAPTER 3

Palladium-Catalyzed Hydroamination of Alkoxy Allenes with Azoles

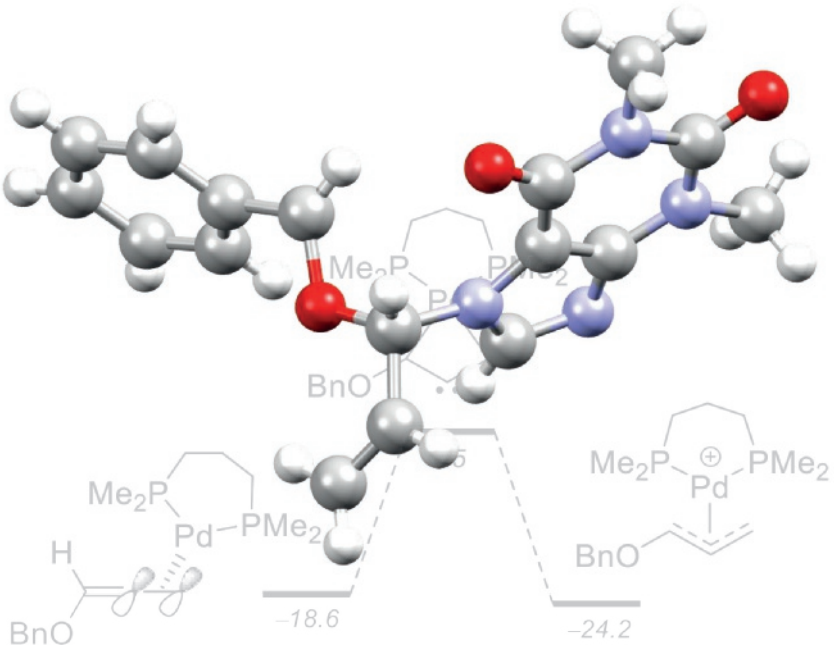

ABSTRACT

Allylic *N,O*-acetals have been frequently used as key intermediates in the synthesis of biologically active heterocycles and natural products. This chapter describes a strategy for the preparation of heteroaromatic allylic *N,O*-acetals in a highly efficient and enantioselective manner (yields up to 95% and ee's up to 94%). Additionally, our computational studies of the reaction for alkoxy allenes and nonacidic nucleophiles suggest a new palladium(0)-driven mechanistic pathway that proceeds through a reactive, carbene-like local minimum.

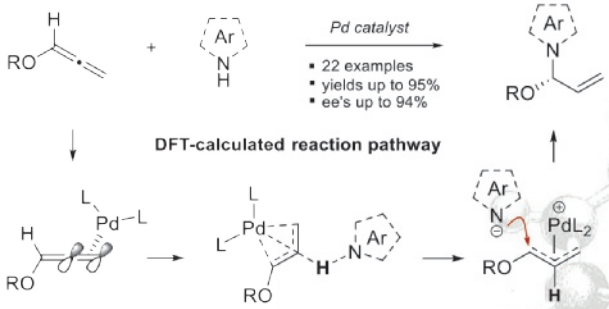

Part of this chapter was published in:

Bernar, I.; Fiser, B.; Blanco-Ania, D.; Gómez-Bengoa, E.; Rutjes, F. P. J. T. *Org. Lett.* **2017**, *19*, 4211–4214, DOI: 10.1021/acs.orglett.7b01826.

Chapter cover: "Crystal structure of allylic *N,O*-acetal (*S*)-**8q**"

3.1 Introduction

Allylic *N,O*-acetals **1** are key intermediates for many useful synthetic transformations (Scheme 3.1). Such acetals are especially well-suited for Lewis acid promoted generation of conjugated iminium ions, such as **2** or **3**. Furthermore, they are widely applied for construction of complex *N*-heterocylic molecules by olefin metathesis processes. These reactive structures have been widely used as key intermediates in the synthesis of biologically active heterocycles and natural products (Chapter 2). Examples from our group include the stereoselective synthesis of the natural product L-baikiain (**4**) and a formal total synthesis of the alkaloid quinolizidine 233A (**5**).[1]

Scheme 3.1 *Applications of Allylic N,O-Acetals 1.*

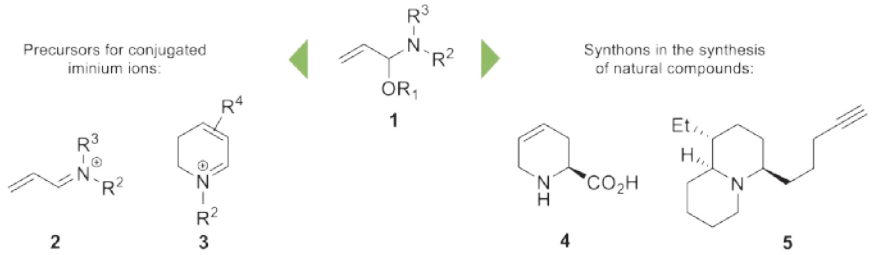

Only few synthetic routes to allylic *N,O*-acetals have been reported to date. These unique structures can be generally constructed by palladium-catalyzed hydroamination of alkoxy allenes **6** developed by us and others (Scheme 3.2).[1,2] These examples cover the addition of a broad variety of nitrogen nucleophiles to alkoxy allenes, such as amines, amides and lactams. To follow up on these results, we envisioned that also azoles **7** would be of particular interest as reactants in such hydroaminations.

Scheme 3.2 *General Approach for the Synthesis of Heteroaromatic Allylic N,O-Acetals 8.*

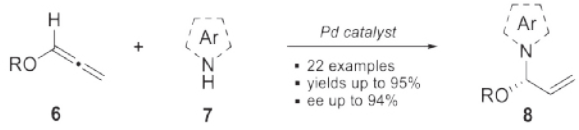

Thus, in this chapter we explored the potential of catalytic and enantioselective reactions at the azole nitrogen that allow fast and easy access to a broad range of chiral, heteroaromatic allylic *N,O*-acetals **8**.

3.2 Results and Discussion

3.2.1 Synthesis of the Alkoxy Allenes

Most of the alkoxy allenes used in this study were synthetized using a two-step procedure previously developed by Brandsma et al. (Scheme 3.3).[3] First, propargylic ethers **11a–e** were prepared by a Williamson ether synthesis. Thus, **11a**, **11c** and **11d** were obtained by alkylation of propargylic alcohol (**9**) with the corresponding benzyl bromide. Alternatively, **11b** and **11e** were prepared starting from phenol (**10b**) or 1-naphthol (**10e**) and propargyl bromide. In a next step, the obtained ethers **11a–e** were converted into the corresponding alkoxy allenes **6a–e** by a base-promoted isomerization. Here, we used a catalytic amount of KO^{t}Bu to generate the propargyl anion **12**. This anion is stabilized by resonance by its allenyl form **13**, which upon protonation leads to alkoxy allene **6**. Alkoxy allenes are special enol ethers, which implies that isomerization of terminal alkynes is favored thermodynamically because of the electron-donating effect of the alkoxy group.[4] Additionally, KO^{t}Bu is not strong enough to deprotonate the allene and thus the reaction stops at this stage. Following this procedure alkoxy allenes **6a–e** were obtained in good yields over two steps and further used for the palladium-catalyzed hydroamination with azoles.

Scheme 3.3 *Synthesis of Alkoxy Allenes* ***6a–e****: Mechanism and Scope of the Reaction.*

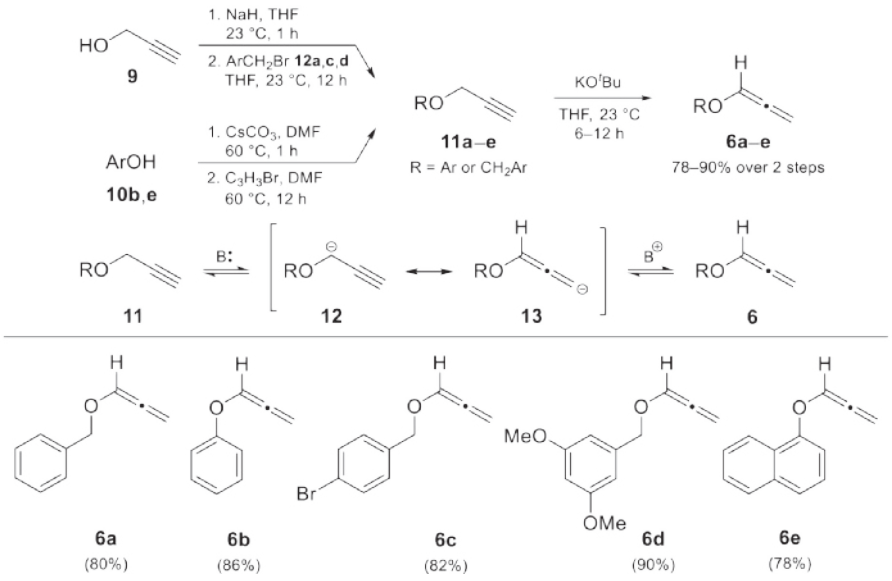

3.2.2 Palladium-Catalyzed Addition of Azoles to Benzyloxyallene

Initial studies to synthesize heteroaromatic allylic *N,O*-acetals were guided by previous work from our group on metal-catalyzed additions of nitrogen nucleophiles to alkoxy allenes. Although this reaction can be catalyzed by a variety of transition metals, e.g., gold[5] or rhodium,[6] palladium was the most efficient leading in most cases to exclusively branched product **8a**.[1a] Imidazole (**7a**) and benzyloxyallene (**6a**) were used for optimizing the reaction conditions (Table 3.1). Gratifyingly, the presence of DBU (1.5 equiv) and a catalytic amount of $Pd(OAc)_2$/dppp in THF at 60 °C provided the desired product **8a** in 82% yield as a single regioisomer (entry 1). Similar results were obtained by changing the catalyst, temperature and solvent (entries 2–5). Unexpectedly, in the absence of additional base and under the optimal reaction conditions {$[Pd_2(dba)_3]$ (2.5 mol %), dppp (5.0 mol %) in THF} the reaction went to completion in 4 h at 60 °C, yielding the desired *N,O*-acetal **8a** in 93% yield (entry 6).

Table 3.1 *Optimization of the Reaction.*

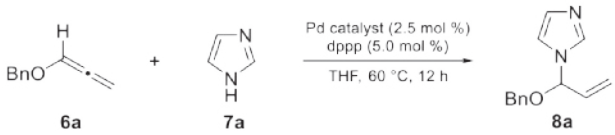

6a **7a** **8a**

Entry	Base	Catalyst	Yield (%)[a]
1	DBU	$Pd(OAc)_2$/dppp	82
2	DBU	$[Pd_2(dba)_3]$/dppp	87
3	DBU	$[Pd(PPh_3)_4]$	85
4[b]	DBU	$[Pd_2(dba)_3]$/dppp	62
5[c]	DBU	$[Pd_2(dba)_3]$/dppp	78
6	–	$[Pd_2(dba)_3]$/dppp	93

[a]Isolated yield. [b]23 °C. [c]MeCN was used as a solvent.

Along with these results, different heterocyclic systems containing the azole framework were subjected to the optimized reaction conditions (Scheme 3.4). Generally, the anticipated *N,O*-acetals **8b–r** were obtained in fair to excellent yields (54–92%). Imidazole-2-carbaldehyde and imidazole-4,5-dicarbonitrile gave a fast and clean conversion to the *N,O*-acetals in excellent yields after purification by column chromatography (**8b** and **8c**, respectively). Benzimidazole, 1,3-dimethylpyrazole, ethyl indole-2-carboxylate, and 1,2,4-triazole also showed good reactivity

in the intermolecular palladium-catalyzed addition and the corresponding *N,O*-acetals **8d–8g** were obtained in good yields. In the case of asymmetrically substituted imidazoles, mixtures of the 4- and 5-substituted isomers **8h–k** were obtained. Thus, 4-nitroimidazole and imidazole-4-carbaldehyde were converted into C-4 allylic *N,O*-acetals **8h** and **8i** in good yields with nearly complete regioselectivity. In contrast, 4-methylimidazole and 4-iodoimidazole showed almost no regioselectivity, yielding a close to 1:1 mixture of the 4- and 5-substituted isomers **8j** and **8k**, respectively.

Scheme 3.4 *Scope of the Azoles.*

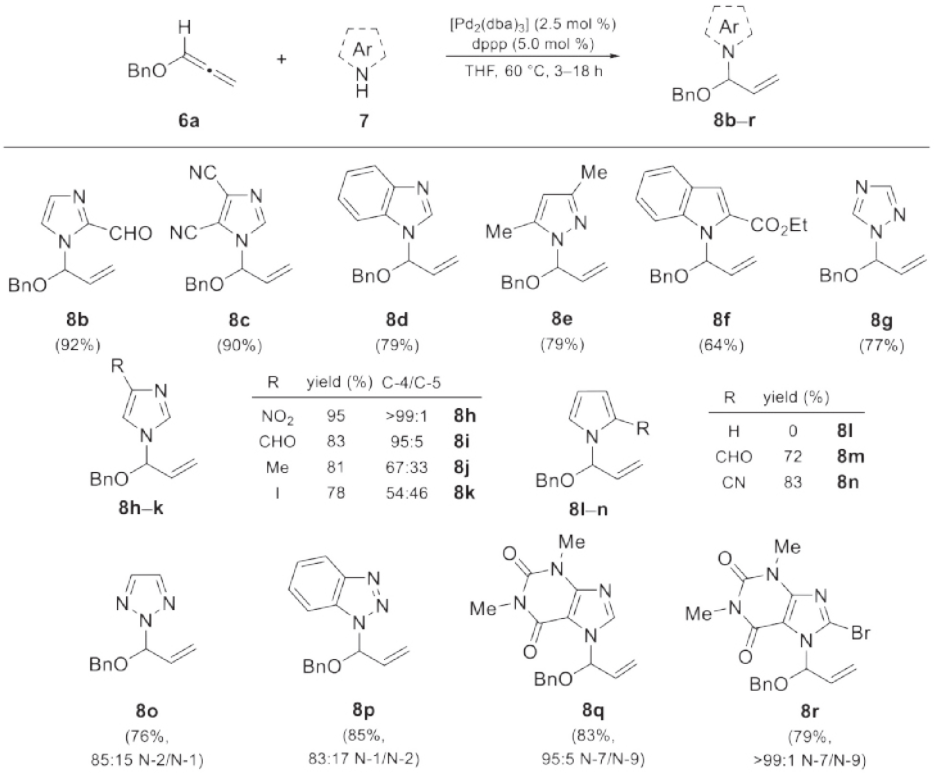

Remarkably, in the case of pyrrole, only degradation of allene **6a** was observed.[7] Changing the reaction conditions (temperature, palladium catalysts, addition of base) did not lead to product **8l** either. In contrast, pyrroles substituted with electron-withdrawing groups, in particular pyrrole-2-carbaldehyde and pyrrole-2-carbonitrile, showed nearly the same reaction rates as imidazole and gave the desired products in good yields (72 and 83% for **8m** and **8n**, respectively).

Azoles with multiple *N*-nucleophilic centers also showed good reactivity in the intermolecular addition to benzyloxyallene (**6a**). To our delight, the corresponding triazole-containing *N,O*-acetals **8o–p** were obtained in good to excellent yields and excellent regioselectivities. Likewise, when bulky substrates such as theophylline and 8-bromotheophylline were used the corresponding *N,O*-acetals **8q** and **8r** were formed with good regioselectivity.

3.2.3 Screening of Reaction Conditions for Enantioselective Hydroamination

Next, we examined the asymmetric version of palladium-catalyzed hydroamination of alkoxy allenes. Our strategy was based on the work concerning palladium- and rhodium-catalyzed asymmetric additions to allenes.[2,6] In analogy to this work, we evaluated several commercially available chiral bisphosphine ligands, solvents, and additives. We commenced our study with imidazole (**7a**) and benzyloxyallene (**6a**) in the presence of $[Pd_2(dba)_3]$ and several chiral bisphosphine ligands in THF at 60 °C (Table 3.2 and Figure 3.1).

Table 3.2 *Catalyst Screening.*

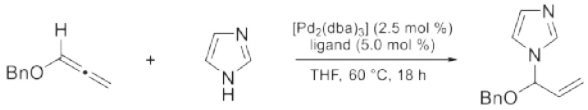

6a **7a** **8a**

Entry	Ligands	Yield (%)[a]	ee (%)[b]
1	**L1**	56	–
2	**L2**	72	11
3	**L3**	32	33
4	**L4**	n.r.	–
5	**L5**	82	–
6	**L6**	85	–
7	**L7**	42	–
8	**L8**	14	–
9	(*R*,*R*)-**L9**	74	77
10	(*R*,*R*)-**L10**	61	83

[a]Isolated yield. [b]Enantiomeric excess was determined by HPLC.

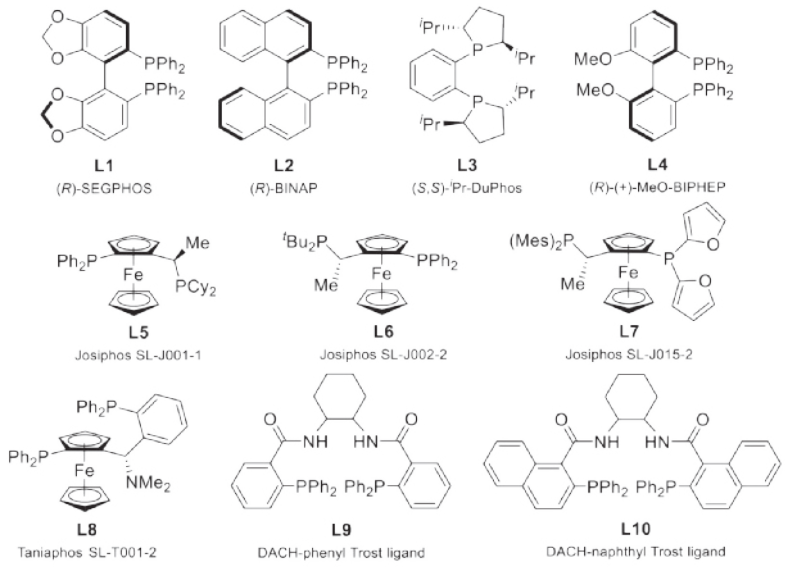

Figure 3.1 *Chiral Ligands Used in the Study.*

The reaction showed no enantioselectivity with (*R*)-SEGPHOS **L1** as the chiral ligand, even though the yield was satisfactory (entry 1). (*R*)-BINAP **L2** and (*S*,*S*)-^{i}Pr-DuPhos **L3** showed good reactivity, but poor enantioselectivity (entries 2 and 3). No reaction occurred when using (*R*)-MeO-BIPHEP **L4** as ligand (entry 4). Josiphos type (**L5–L7**) and Taniaphos type (**L8**) ligands led to variable yields (from poor to very good) of the product, albeit no stereoinduction was observed (entries 5–8). To our delight, promising enantioselectivities were obtained employing ligands (*R*,*R*)-**L9** and (*R*,*R*)-**L10** (entries 9 and 10, respectively), which were previously proven to be optimal for the coupling of *N*-nucleophiles with alkoxy allenes.[2,8] Thus, in the presence of ligand (*R*,*R*)-**L10** the reaction proceeded in a fair yield (61%) and fairly good enantioselectivity (82% ee).

Next, we aimed to investigate all the parameters of the reaction when using ligand **L10** (Table 3.3). 1,2-Dichloroethane (DCE) showed the highest enantioselectivity for the hydroamination reaction among all the solvents (entries 1–3): the product was isolated in 59% yield and 92% ee. Further screenings revealed that performing the reaction at lower temperatures had a negative effect on both product yield and enantiomeric excess (entries 4–5) and prolongation of the reaction time led to partial racemization (entry 6). The use of additives such as DBU (1.5 equiv) caused a slight drop in the stereoselectivity (entry 7).

Table 3.3 *Screening of the Reaction Conditions.*

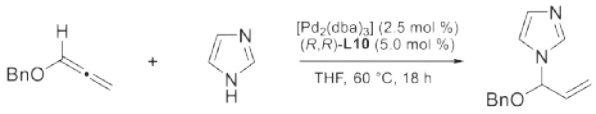

6a **7a** **8a**

Entry	Solvent	*t* (°C)	Time (h)	Yield (%)[a]	ee (%)[b]
1	MeCN	60	18	55	87
2	1,4-Dioxane	60	18	63	82
3	DCE	60	18	59	92
4	DCE	23	18	21	87
5	DCE	40	18	44	82
6	DCE	60	30	70	78
7[c]	DCE	60	18	74	82

[a]Isolated yield. [b]Enantiomeric excess was determined by HPLC. [c]DBU was used.

3.2.4 Enantioselective Palladium-Catalyzed Addition of Imidazole to Alkoxy Allenes

With the optimized conditions in hand {[$Pd_2(dba)_3$] (2.5 mol %), **L10** (5 mol %) in DCE, 60 °C}, we investigated the scope of different allenes for the enantioselective palladium-catalyzed addition of imidazole (Scheme 3.5).

Scheme 3.5 *Scope of the Alkoxy Allenes for Enantioselective Palladium-Catalyzed Addition of Imidazole.*

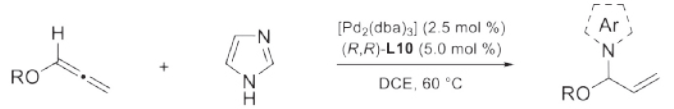

6 **7a** **8a,s–w**

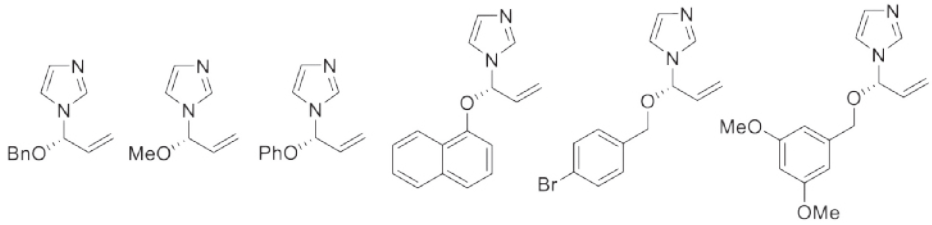

(*S*)-**8a** (89%, 92% ee) (*S*)-**8s** (54%, 83% ee) (*S*)-**8t** (72%, 90% ee) (*S*)-**8u** (67%, 94% ee) (*S*)-**8v** (89%, 93% ee) (*S*)-**8w** (90%, 94% ee)

We were pleased to observe that a number of alkoxy allenes reacted well with imidazole giving rise to products (*S*)-**8a** and (*S*)-**8s–w**, not only in good yields, but in most cases also with high enantioselectivities (up to 94% ee). In general, sterically hindered substrates were obtained with slightly better enantioselectivities [(*S*)-**8a,t–w**] than the product of hydroamination to methoxyallene (compound (*S*)-**8s**).

To determine the absolute configuration of the obtained products, we performed the reaction with theophylline and benzyloxyallene (Scheme 3.6). Similar to the result described for the racemic synthesis of **8q** (see Section 3.2.2), in the enantioselective version the desired product **8q** was again obtained with excellent N^7-selectivity. Furthermore, the reaction in the presence of (*R,R*)-**L10** proceeded with 74% yield and 92% ee. The crystal structure of the major enantiomer of product **8q** was then elucidated and the absolute configuration was assigned to be *S*. Moreover, the reaction was performed with (*S,S*)- **L10** leading to enantiomer (*R*)-**8q** in 71% yield and 90% ee.

Scheme 3.6 *Enantioselective Synthesis of Allylic N,O-Acetals (S)- and (R)-8q.*

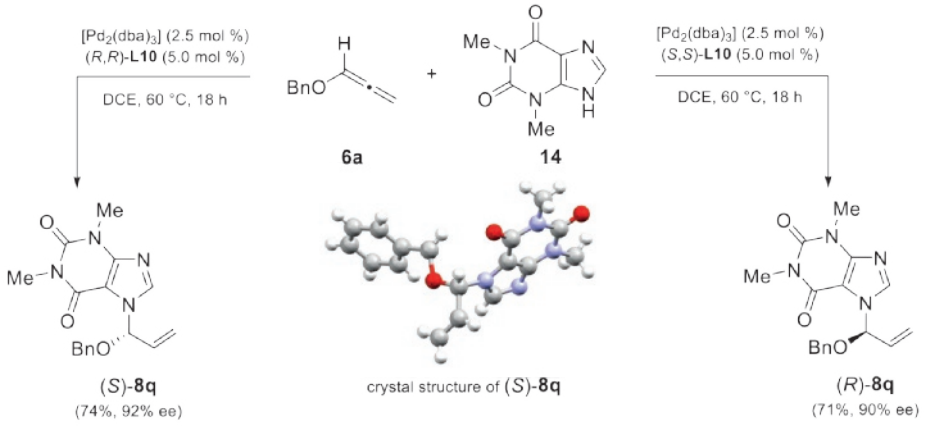

The assignment of the absolute configuration of the other products was accomplished with the help of circular dichroism (CD) spectroscopy.[9] The CD spectra of (*S*)-**8q** (92% ee) and (*R*)-**8q** (90% ee) were recorded and the Cotton effect at around 210 nm was observed. Thus, a positive Cotton effect in the CD spectra at this area would indicate that allylic *N,O*-acetals **8a** and **8s–w** belong to series of (*S*)-enantiomers and vice versa. All of the studied compounds showed a positive Cotton effect and were assigned to be *S*, which is in correspondence with the expected stereochemistry.[10]

3.2.5 DFT Studies of the Reaction Mechanism

The mechanism of the palladium-catalyzed additions of pronucleophiles with relatively acidic protons to allenes has been thoroughly investigated by the research group of Trost[8] and others.[11] These experimental studies showed that this process is initiated by oxidative addition of a 14-e⁻ palladium complex into the acidic X–H bond (e.g., X = CF_3CO_2) to form a cationic palladium–hydride species (**15**; Scheme 3.7). This intermediate can readily react with the allene thereby generating the η^3-allylpalladium species **16**. The alkoxy allenes are special enol ethers which implies that hydride transfer occurs at the central carbon of the allene moiety because of the electron-donating effect of the alkoxy group.[12] Addition of the conjugate base of the pronucleophile or an external nucleophile to this intermediate through trajectories *a* or *b* then leads to the products **17** and **18** with regeneration of the palladium(0) catalyst.

Scheme 3.7 *Accepted Mechanism of the Hydroamination of Allenes. Free Energies (298 K) with Respect to the Starting Materials Are Shown in kcal/mol.*

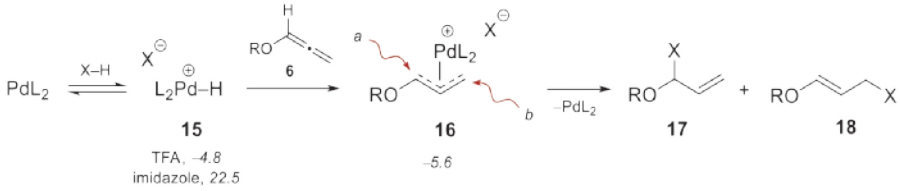

We turned to DFT calculations to shed light on a plausible mechanism for our alkoxy allene/imidazole reaction since no studies have been reported on the oxidative addition of low-valent palladium to X–H bond of weak acids (e.g., imidazole, **7a**). Therefore we considered initially a similar pathway to that outlined in Scheme 3.7. We used M06/6-311+G**(SDD) level of theory to conduct our calculations in all cases, and for verification purposes, other theoretical levels were applied when necessary. Indeed, our preliminary calculations showed that **15** (X^- = imidazolide, L_2 = 1,3-bis(dimethylphosphanyl)propane, dmpp) is a reasonable intermediate of the reaction. Its computed free energy value was 5.6 kcal/mol lower than the sum of the initial substrates (PdL_2 + allene **6a** [R = Bn] + imidazole **7a**; Scheme 3.7), and also, its reaction with the imidazolide nucleophile preferentially occurs through the *a* trajectory (8.0 kcal/mol lower than *b*) to form the *N,O*-acetal product **17**, in agreement with the experimental findings. However, some critical inconsistencies were observed around the participation of intermediate **15** in the mechanism (Scheme 3.7), because its existence was incompatible with the following data:

a) A determining preference of 18.9 kcal/mol for the coordination of Pd(dmpp) to allene **6a** over imidazole was found (**23** vs **19**, Figure 3.2), severely compromising any further participation of palladium species **15** in the mechanism of the reaction.

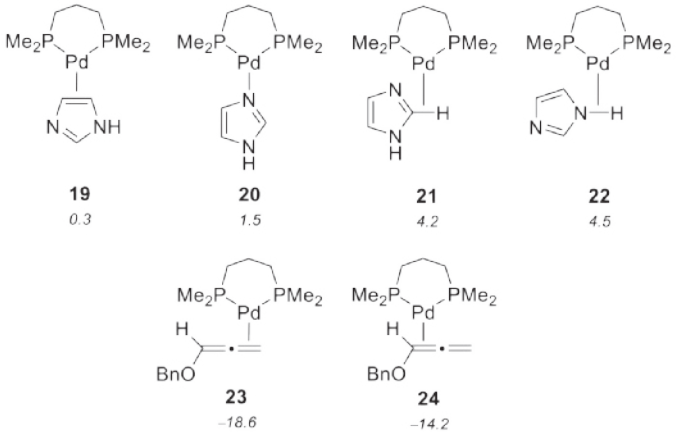

Figure 3.2 *Coordination Complexes of Pd(dmpp) with Imidazole (Top) and Benzyloxyallene (Bottom). Free Energies (298 K) with Respect to Starting Materials Are Shown in kcal/mol.*

b) The formation of $[L_2Pd^{+}–H]\ X^{-}$ species of type **15** has been exclusively described for strong X–H acids, and the hydride has not been observed when weaker acids were used.[11] In agreement with these experimental facts, the computed equilibrium between palladium(0) and trifluoroacetic acid is shifted towards the formation of cationic $[L_2Pd^{+}–H]\ X^{-}$ species **15** by 4.8 kcal/mol (Scheme 3.7), whilst using imidazole as a proton source, the formation of the hydride complex is disfavored by more than 22.5 kcal/mol.

c) The combination of factors a) and b) affords an unrealistic energy of 41.1 kcal/mol for hydride **15** over **23**, which is unreachable by any means. We can safely state that under these conditions, $[L_2Pd^{+}–H]\ X^{-}$ species **15** would never form.

Therefore, the intriguing findings that intermediates **23** and **16** plausibly participate in the transformation, but are at the same time not connected through the cationic $[L_2Pd^{+}–H]\ X^{-}$ species **15**, led us to search for a pathway to connect both intermediates.

3.2.6 Complex Formation and Binding Energies

First, we studied the possible coordination complexes of Pd(dmpp) with either imidazole or benzyloxyallene (Figure 3.2). The calculations indicate that four coordination types for imidazole were higher in energy than the sum of those of the starting species. Among them, the most stable complex is the result of coordination of Pd(dmpp) to the CC double bond at positions 4 and 5 (**19**, G = 0.3 kcal/mol). In contrast, the coordination of benzyloxyallene is highly favorable, presenting large binding energies with either CC double bond. Thus, it is clear that palladium coordinates with the allene fragment through its less hindered, terminal double bond (**23**). This difference between **19** and **23** was rather large, 18.9 kcal/mol.

3.2.7 Mechanism A. Hydropalladation of Benzyloxyallene

Next, we undertook computational investigations of a mechanistic scenario, involving oxidative addition of palladium into the imidazole N–H bond, formation of hydridopalladium cationic complex **15** and its addition to allene **6a** (Figure 3.3).

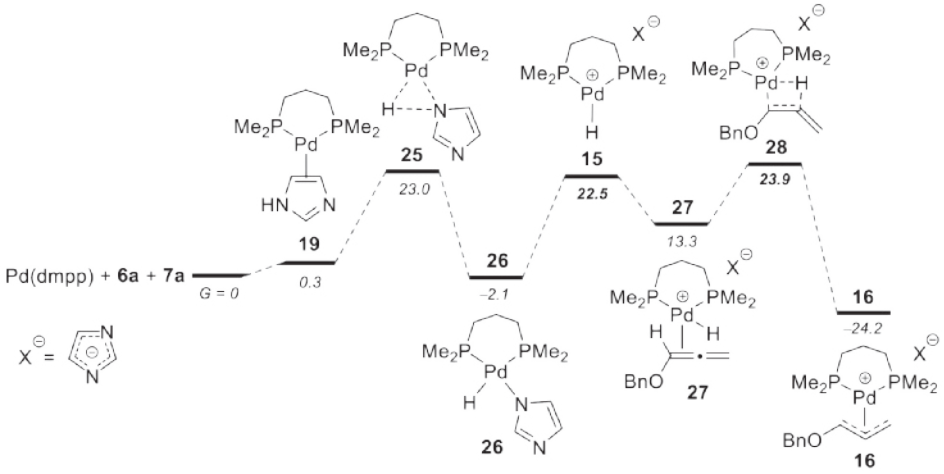

Figure 3.3 *Reaction Sequence Involving N–H Oxidative Addition to Form* ***15*** *Followed by Addition to Allene (****28****). Free Energies (298 K) with Respect to Starting Materials Are Shown in kcal/mol.*

After applying DFT calculations with both M06 and B3LYP levels of theory, the calculations indicate that the key intermediates **15** and **28** are too unstable to exist. Thus, intermediate **15** is too high in energy (22.5 kcal/mol), as this type of cationic complex has only been described for

strong acids (like TFA, *vide supra*), whereas imidazole is only slightly acidic. Futhermore, complex **15** is a coordinatively unsaturated (14-e$^-$) cationic palladium(II) species, which together with the high basicity of the imidazole counteranion turns it into the bottleneck of this mechanism. Upon coordination to the allene in **27**, the energy seems to relax by *ca.* 10 kcal/mol, confirming that the instability of **15** is partially due to its high coordinative unsaturation. The following hydropallation transition step (**28**) raises again the energy to 23.9 kcal/mol, for a total barrier height value of 26.0 kcal/mol (from –2.1 kcal/mol in **26** to 23.9 kcal/mol in **28**), which is at or beyond the limit of the present experimental conditions (25 °C). Overall, the main weakness of this proposal consists of the decoordination of the imidazole from the stable intermediate **26** to the extremely unstable intermediate **15** (24.6 kcal/mol increase). In addition, formation of different [L_2Pd^+–H] X^- species can be stabilized by a polar solvent.[11a] Indeed, the inclusion of a molecule of acetonitrile induces a computed stabilization of 8.3 kcal/mol in **15**, from 22.5 kcal/mol to 14.2 kcal/mol. However, the key hydridopalladium cationic complex is still too unstable and we can tentatively discard the participation of **15** in the mechanism.

Another alternative approximation to form **16** would be the initial coordination of palladium(0) to benzyloxyallene **6a**, subsequent oxidative addition of the formed complex **23** to N–H bond of imidazole via **27** and final addition to allene, as in **28**, forming η^3-allylpalladium species (Figure 3.4).

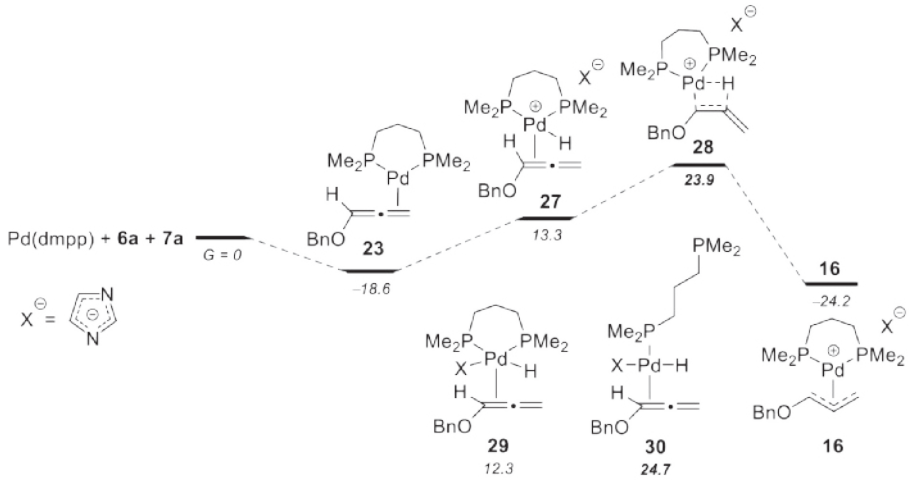

Figure 3.4 *Reaction Sequence Involving Initial Coordination of Pd(dmpp) to Allene (**23**), Oxidative Addition to N–H bond of Imidazole Foming **27**, Followed by Addition to Allene (**28**). Free Energies (298 K) with Respect to Starting Materials Are Shown in kcal/mol.*

However, the transformation of **23** to **27** involves an exceedingly high-energy increase (31.9 kcal/mol), regardless of the nature of the mechanism proposed for this transformation. The coordination of imidazole to palladium at that point, forming the pentacoordinated species **29** does not seem to ease the situation, for similar reasons (G = 12.3 kcal/mol). On the other hand, the option of decoordination of one of the phosphines from palladium to form a monodentate dmpp ligand is not energetically feasible. As an example, intermediate **30** presents an energy of 24.7 kcal/mol, and in general, the monocoordinated dppp complexes present *ca.* 10 kcal/mol higher energies than their more stable dicoordinated counterparts in all studied cases. It is interesting to note that in **27**, **29**, and **30**, the electrophilic palladium(II) coordinates preferentially to the internal, more electron-rich double bond of the allene, in contrast to the preferential coordination of palladium(0) to the terminal double bond in **23**.

3.2.8 Mechanism B. Palladium(0)–Allene Complex as Active Species

As was already shown before, the coordination of the allene to Pd(dmpp) leads to the highly exergonic formation of **23**, –18.6 kcal/mol lower than the initial mixture of starting materials. Thus, an alternative reaction sequence considered in the DFT calculations implies the direct protonation of this palladium complex with imidazole (Figure 3.5).

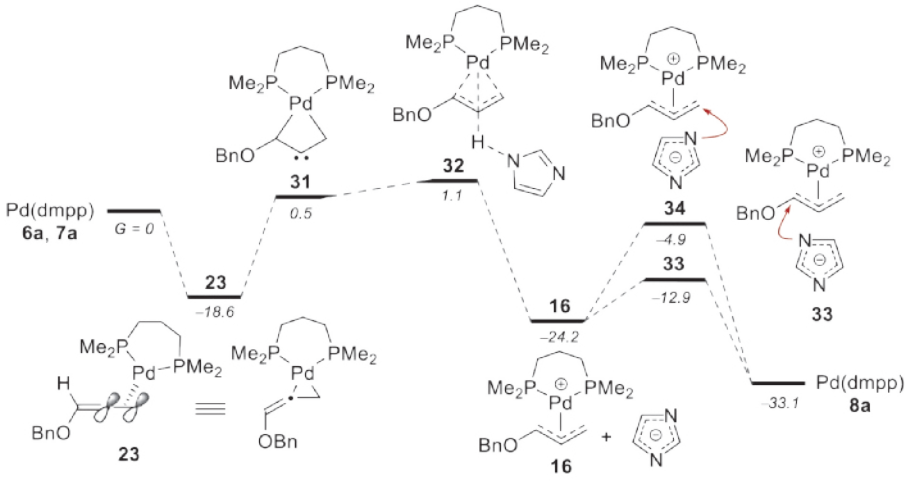

Figure 3.5 *Reaction Sequence Involving Initial Coordination of Pd(dmpp) to Allene (**23**), Bending of a π-Allyl-Type System Forming **31**, Followed by Protonation by Imidazole (**32**). Free Energies (298 K) with Respect to Starting Materials Are Shown in kcal/mol.*

After additional computational studies, a new transition state **32** was located for both M06 and B3LYP functionals with an energy of G = 1.1 kcal/mol over the starting materials and a moderate activation barrier of 19.7 kcal/mol (from **23** to **32**).[13] This energy value is surprisingly low, and above all, much lower than any of the previous examined structures **15**, **27**, and **29**. From the computational point of view, protonation step **32** forming η^3-allylpalladium complex **16** happens already at room temperature. Finally, the attack of imidazolide to **16** was found to occur through pathway *a*, as in Scheme 3.7 (**33**, Figure 3.5), with an activation free energy of 11.3 kcal/mol (from **16** to **33**). This result is in line with our experimental observations where branched isomer **8a** was formed almost exclusively.

3.2.9 Formation of 32 and the Nature of Complex 31

The structure of transition state **32** is new and therefore highly interesting and implies that the allene, after coordination to palladium(0) in **23**, becomes sufficiently basic at the central carbon atom to deprotonate imidazole. Indeed, a very high-energy local minimum structure (**31**, 19.1 kcal/mol higher than **23**) was located during the intrinsic reaction coordinate (IRC) of the transition state **32**, corresponding to a bidentate coordination mode of allene to Pd(dmpp) (Scheme 3.8).

Scheme 3.8 *Structural Comparison and Equilibrium between Intermediates **23** and **31**. Free Energies (298 K) with Respect to the Starting Materials Are Shown in kcal/mol.*

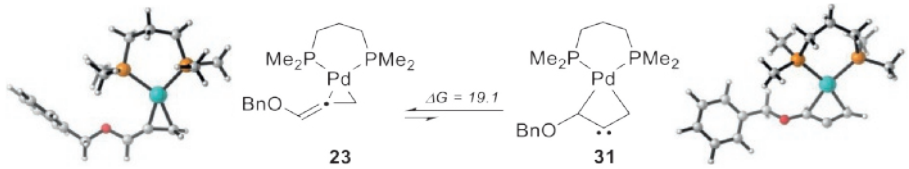

This new palladium species is the precursor of the protonation step, bearing a bent π-allyl-type structure wherein the metal is bound to the two terminal carbon atoms of the allene with high nucleophilic carbene character on the central carbon atom. The carbene-like species **31** is so close in energy ($\Delta\Delta G^{\ddagger}$ = 0.6 kcal/mol) to the transition state **32** that it could not be considered a stable reaction intermediate, but rather as a very unstable and reactive isomer of the allene–palladium complex **23**. Its participation would be almost negligible in a hypothetical equilibrium between the different allene complexes, but its significance stems from the computational fact that its protonation with a weak acid like imidazole occurs almost without an energy barrier.

These data seem to indicate that **31** is a transient intermediate, which develops a significant negative charge at the central carbon atom and in the presence of acids gets very easily protonated to form the stable complex **16**.[14] The structure and energy of **31** are closer to a transition state than to a minimum (although it is in fact a local minimum in the potential energy surface), and it becomes significant only when protonated acidic species participate in the reaction.

Next, the geometry of **31** can be further rationalized by inspection of electrophilicity/nucleophilicity indexes and HOMO energies of the free allene **6a**, and allene–palladium complexes **23** and **31**. The computed Fukui nucleophilicity indexes at the central allene C_b atom indicate that it presents a medium/low nucleophilicity (+0.25 e^-) in the free allene, that becomes insignificant (−0.04 e^-) when coordinated to the palladium atom in **23** (Figure 3.6). However, the formation of the carbene-like structure in **31** induces a severe increase in its nucleophilicity to reach a maximum of −0.58 e^-, confirming that the central carbon becomes very nucleophilic and reactive in this high-energy complex. Noteworthy, the Fukui electrophilicity indexes at that specific carbon do not show any change between the three species. It is also noticeable that the total electrophilicity indexes w (defined as the division between the electron chemical potential and chemical hardness) of the three species show the expected behavior, with the highest index for the free allene (2.52 eV), 2.46 eV for **23**, and the lowest for **31** (2.39 eV). In other words, the allene becomes more nucleophilic (less electrophilic) with the coordination to palladium, and even more so after the isomerization to its bent form, although it must be noted that the difference between the three values is not really large.

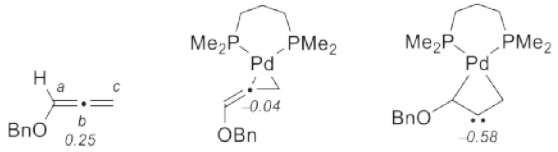

6a **23** **31**

Figure 3.6 *Fukui Nucleophilicity Indexes of the Carbon C_b. Computed Data Are Shown in Electron Units.*

The most significant data are related to the energies and atomic contributions of the HOMO (Figure 3.7), which is the reacting orbital during the protonation. First, its energies in the different compounds show a clear trend, increasing from the free allene (−6.8 eV) to **23** (−5.6 eV), and even more in **31** (−5.2 eV). Of note, the $HOMO_{allene}$ is centered in the oxygen lone pair and in the π-system of the CC double bond next to the oxygen, similar to that of an enol ether.

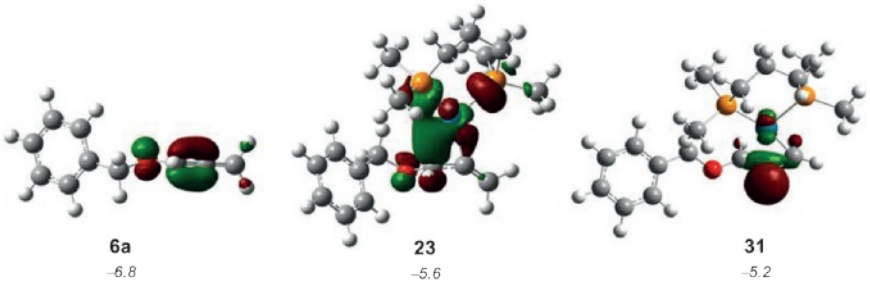

Figure 3.7 *3D Representation of the HOMOs and Their Energies in eV for the Free Allene* ***6a*** *and Complexes* ***23*** *and* ***31****.*

In **23**, the major contribution of the HOMO comes from one of the d-orbitals in palladium, probably the one involved in binding the C_a atom of the allene. Finally, the HOMO in **31** corresponds to an electron lone pair, located in a sp^2 orbital of the C_b atom, coplanar to the other two carbons (C_a and C_c). This is a clear confirmation of the carbene nature of the central carbon atom in **31**.

3.2.10 Trapping of Carbene 31 with 1-(Trimethylsilyl)imidazole

Inspired by our computational findings, we tried to trap the reactive carbene-like species **31** with electrophiles different from H^+, e.g., Me_3Si^+ derived from 1-(trimethylsilyl)imidazole **35** (Scheme 3.9).

Scheme 3.9 *Envisioned Trapping of Carbene* ***21*** *with 1-(Trimethylsilyl)Imidazole* ***35*** *(Top) and a Control Experiment (Bottom).*

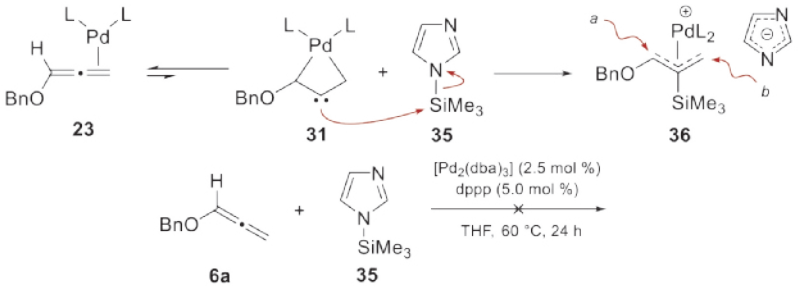

The rationale was that the allene complex **23** formed under the reaction conditions would isomerize to reactive carbene **31**, which would then be immediately trapped with 1-(trimethylsilyl)-imidazole forming the silylated η^3-allylpalladium intermediate **36**. Finally, the addition of imidazolide to this intermediate would lead to branched (trajectory *a*) and linear (trajectory *b*)

products. Pioneering experiments were conducted with allene **6a**, 1-(trimethylsilyl)imidazole **35** and a catalytic amount of $[Pd_2(dba)_3]$ under the standard reaction conditions. However, no desired reaction occurred and only the starting materials were recovered. Noteworthy, if the reaction was conducted for a period longer than 24 h, partial hydrolysis of 1-(trimethylsilyl)imidazole **35** to imidazole was observed, followed by its reaction with alkoxy allene to form **8a**. We realized that experimentally proving the participation of allene–palladium complex **31** in the hydroamination reaction would require a whole different type of carbene trapping. Therefore this line of research was left for future investigations.

3.3 Conclusion

In conclusion, we have developed highly effective palladium-catalyzed protocols for the addition of a wide scope of azoles to alkoxy allenes providing a unique way to synthesize aromatic allylic *N,O*-acetals in high yields (up to 95%) and enantiomeric excesses (up to 94%). All these products represent the privileged synthons with a possibility for further functionalization to gain excess to a variety of *N*-heterocycles (their application can be found in Chapter 4). A non-conventional palladium(0)-driven mechanistic pathway was proposed based on the DFT calculations of the studied process. This should be considered as an alternative pathway for non-acidic nucleophiles, where highly favorable coordination of allene to the palladium catalyst followed by the protonation with a week acid forms η^3-allylpalladium species. Such a process involves a reactive, carbene-like local minimum, which is a crucial link that connects both intermediates. At the same time, acidic nucleophiles, as well as acid/base additives would rather prefer to form the η^3-allylpalladium complex through cationic palladium–hydride species.

3.4 Acknowledgments

This research work was conducted with support from Dr. B. Fiser (University of Miskolc, Hungary) and Prof. dr. E. Gómez-Bengoa (University of the Basque Country, Spain). Prof. dr. B. de Bruin and Dr. J. C. Slootweg (University of Amsterdam) are kindly acknowledged for useful suggestions. Dr. P. T. Tinnemans (Radboud University) is gratefully acknowledged for the crystal structure determination of compound (*S*)-**8q**. I would also like to thank Dr. Dennis W. P. M. Löwik (Radboud University) for providing the practical knowledge necessary for the recording of CD spectra.

3.5 Experimental Section

Experimental studies: reagents were obtained from commercial suppliers and were used without purification. Methoxyallene (**6f**) was directly purchased from Sigma-Aldrich. Standard syringe techniques were applied for the transfer of dry solvents and air- or moisture-sensitive reagents. All inert reactions were carried out under a nitrogen atmosphere using flame-dried flasks. ^{1}H and ^{13}C NMR spectra were recorded at 298 K on a Varian Inova 400 MHz or Bruker 500 MHz spectrometer in the solvent indicated. Chemical shifts are given in parts per million (ppm) with respect to tetramethylsilane (0.00 ppm) as internal standard for ^{1}H NMR; and $CDCl_3$ (77.16 ppm) as internal standard for ^{13}C NMR. Coupling constants are reported as *J* values in hertz (Hz). ^{1}H NMR data are reported as follows: chemical shift (ppm), multiplicity (s = singlet, d = doublet, t = triplet, quint = quintet and combination of them), coupling constants (Hz) and integration. All NMR signals were assigned on the basis of ^{1}H NMR, ^{13}C NMR, gCOSY, gHSQC, gHMBS and NOESY experiments. Mass spectra were recorded on a JEOL AccuTOF CS JMST100CS (ESI) mass spectrometer. IR spectra were recorded on a Bruker Tensor 27 FTIR spectrometer. CD and HV spectra were recorded on Jasco J-815 CD spectrometer. The chiral HPLC measurements were performed on a Shimadzu LC2010C Analytical HPLC system equipped with a Diacel Chiralpak OD-H or Phenomenex Lux 3u Cellulose-1 column using the stated eluents. Melting points were analyzed with a Büchi melting point B-545. Automatic flash column chromatography was performed using Biotage Isolera Spektra One, using SNAP cartridges (Biotage, 30–100 μm, 60 Å), 10–50 g. TLC-analysis was conducted on Silicagel F254 (Merck KGaA) with detection by UV-vis absorption (254 nm) where applicable, and by dipping into a solution of $KMnO_4$/Na_2CO_3/NaOH in water followed by charring at *ca.* 150 °C.

Computational studies: the structures were optimized by using density functional theory (DFT) at the M06/6-311+G** (SDD for Pd) level of theory[15] as implemented in Gaussian 09. The stationary points were characterized by frequency calculations in order to verify that they have the right number of imaginary frequencies. The calculation of the reaction species involves a correction to the free energy, that takes into account the change in degrees of freedom, e.g., association/dissociation steps. Solvent effects were taken into account at the same levels of theory by applying the conductor-like polarizable continuum model (CPCM, Solvent = MeCN).[16,17] For verification purposes the following theoretical levels were also applied in special cases: M06/def2TZVPP,[18,19] and B3LYP-D3/6-31G** (LANL2DZ for palladium).[20,21] Cartesian coordinates of the structures involved in the computational study can be found here.[10]

Synthesis of Propargyl Ethers 11 a–e

General procedure A:[22] Propargyl alcohol (1.0 g, 17.8 mmol, 1.0 equiv) was added dropwise at 0 °C to a suspension of sodium hydride (60% dispersion in mineral oil; 780 mg, 19.6 mmol, 1.1 equiv) in THF (40 mL) and the reaction mixture was allowed to warm up to room temperature in 1 h. Tetrabutylammonium iodide (330 mg, 0.9 mmol, 0.05 equiv) and the corresponding benzyl bromide (19.6 mmol, 1.1 equiv) were added to the mixture successively. After completion of the reaction (TLC), the mixture was filtered over a diatomaceous-earth pad and concentrated. The obtained crude product was used directly in the next step without further purification.

General procedure B:[23] Mixture of the corresponding phenol (17.8 mmol, 1.0 equiv) and anhydrous Cs_2CO_3 (6.9 g, 21.4 mmol, 1.2 equiv) in DMF (40 mL) was heated to 60 °C for 30 min under a nitrogen atmosphere. The reaction mixture was then cooled to 23 °C and propargyl bromide (80 wt % solution in toluene; 3.4 g, 23.1 mmol, 1.3 equiv) was added slowly. After completion of the reaction (TLC), the mixture was diluted with ether (40 mL) and washed with brine (3 × 50 mL). The obtained crude product, after solvent evaporation, was used directly in the next step without further purification.

{[(Prop-2-yn-1-yl)oxy]methyl}benzene 11a.

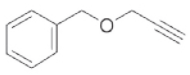

11a

Following the general procedure A, propargyl ether **11a** was obtained as a light yellow oil (2.3 g, 90%). **^{1}H NMR** [400 MHz, δ (ppm), $CDCl_3$]: 2.47 (t, J = 2.4 Hz, 1 H), 4.17 (d, J = 2.4 Hz, 2 H), 4.61 (s, 2 H), 7.27–7.39 (m, 5 H). **^{13}C NMR** [101 MHz, δ (ppm), $CDCl_3$]: 57.1, 71.4, 74.5, 79.4, 127.5, 128.1, 128.3, 137.2. These data were in accordance to those reported in the literature.[24]

[(Prop-2-yn-1-yl)oxy]benzene 11b.

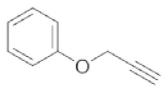

11b

Following the general procedure B, propargyl ether **11b** was obtained as a light yellow oil (1.8 g, 78%). **^{1}H NMR** [400 MHz, δ (ppm), $CDCl_3$]: 2.52 (t, J = 2.4 Hz, 1 H), 4.70 (d, J = 2.4 Hz, 2 H), 6.96–7.03 (m, 3 H), 7.28–7.31 (m, 2 H). **^{13}C NMR** [101 MHz, δ (ppm), $CDCl_3$]: 55.6, 75.4, 78.6, 114.8, 121.5, 129.4, 157.4. These data were in accordance to those reported in the literature.[23]

1-Bromo-4-{[(prop-2-yn-1-yl)oxy]methyl}benzene 11c.

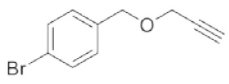

11c

Following the general procedure A, crude propargyl ether **11c** was obtained as a light yellow oil. The residue was then purified by column chromatography on silica gel (heptane/AcOEt 20:1→10:1) to afford product **11c** as a yellow oil (3.2 g, 81%). **^{1}H NMR** [400 MHz, δ (ppm), $CDCl_3$]: 2.47 (t, *J* = 2.4 Hz, 1 H), 4.17 (d, *J* = 2.3 Hz, 2 H), 4.56 (s, 2 H), 7.21–7.25 (m, 2 H), 7.45–7.50 (m, 2 H). **^{13}C NMR** [101 MHz, δ (ppm), $CDCl_3$]: 57.2, 70.7, 74.8, 79.3, 121.8, 129.6, 131.5, 136.3. **FTIR** [$\bar{\nu}$ (cm^{-1})]: 482, 630, 801, 1011, 1070, 1488, 2172, 2852, 2922, 3287. **HRMS** (ESI$^+$) calcd. for $(C_{10}H_9BrO + Na)^+$ 246.9729, found 246.9725.

1,3-Dimethoxy-5-{[(prop-2-yn-1-yl)oxy]methyl}benzene 11d.

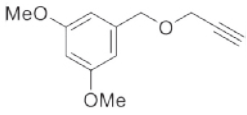

11d

Following the general procedure A, propargyl ether **11d** was obtained as a light yellow oil (3.5 g, 94%). **^{1}H NMR** [400 MHz, δ (ppm), $CDCl_3$]: 2.47 (t, *J* = 2.4 Hz, 1 H), 3.79 (s, 6 H), 4.17 (d, *J* = 2.4 Hz, 2 H), 4.56 (s, 2 H), 6.40 (t, *J* = 2.3 Hz, 1 H), 6.52 (d, *J* = 2.3 Hz, 2 H). **^{13}C NMR** [101 MHz, δ (ppm), $CDCl_3$]: 55.3, 57.0, 71.5, 74.6, 79.6, 100.0, 105.7, 139.6, 160.9. These data were in accordance to those reported in the literature.[25]

1-[(Prop-2-yn-1-yl)oxy]naphthalene 11e.

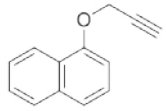

11e

Following the general procedure B, propargyl ether **11e** was obtained as a light yellow oil (2.7 g, 84%). **^{1}H NMR** [400 MHz, δ (ppm), $CDCl_3$]: 2.54 (t, *J* = 2.4 Hz, 1 H), 4.89 (d, *J* = 2.4 Hz, 2 H), 6.94 (d, *J* = 7.6 Hz, 1 H), 7.38 (t, *J* = 8.0 Hz, 1 H), 7.45–7.52 (m, 3 H), 7.78–7.82 (m, 1 H), 8.24–8.30 (m, 1 H). **^{13}C NMR** [101 MHz, δ (ppm), $CDCl_3$]: 56.1, 75.5, 78.6, 105.5, 121.2, 122.0, 125.4, 125.5, 125.6, 126.5, 127.4, 134.5, 153.3. These data were in accordance to those reported in the literature.[23]

Synthesis of Allenyl Ethers 6a–e

General procedure:[26] KO^{t}Bu (3.0 mmol, 0.3 equiv) was added at 23 °C to a solution of propargyl ether **11** (10 mmol, 1 equiv) in THF (25 mL). The suspension was stirred at 23 °C for the appropriate time (6–12 h, TLC), then filtered through a diatomaceous-earth pad and washed with heptane. The solvent mixture was removed in vacuo and the crude residue was purified by column chromatography as indicated.

{[(Propa-1,2-dien-1-yl)oxy]methyl}benzene 6a.

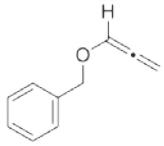

6a

Column chromatography (heptane/AcOEt 20:1→10:1; silica gel was washed with 1% Et_3N before being used for column chromatography) afforded product **6a** as a light yellow oil (1.2 g, 80%). **^{1}H NMR** [400 MHz, δ (ppm), $CDCl_3$]: 4.61 (s, 2 H), 5.48 (d, J = 6.0 Hz, 2 H), 6.84 (t, J = 5.9 Hz, 1 H), 7.28–7.38 (m, 5 H). **^{13}C NMR** [101 MHz, δ (ppm), $CDCl_3$]: 70.6, 91.1, 121.6, 127.7, 127.8, 128.3, 137.3, 201.3. These data were in accordance to those reported in the literature.[26]

[(Propa-1,2-dien-1-yl)oxy]benzene 6b.

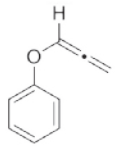

6b

Column chromatography (heptane/AcOEt 40:1→20:1; silica gel was washed with 1% Et_3N before being used for column chromatography) afforded product **6b** as a light yellow oil (1.1 g, 86%). **^{1}H NMR** [400 MHz, δ (ppm), $CDCl_3$]: 5.45 (d, J = 5.9 Hz, 2 H), 6.85 (t, J = 5.9 Hz, 1 H), 7.03–7.10 (m, 2 H), 7.28–7.35 (m, 3 H). **^{13}C NMR** [101 MHz, δ (ppm), $CDCl_3$]: 89.5, 116.7, 122.7, 129.5, 202.8. These data were in accordance to those reported in the literature.[27]

1-Bromo-4-{[(propa-1,2-dien-1-yl)oxy]methyl}benzene 6c.

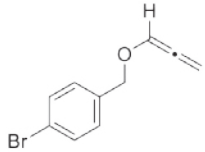

6c

Column chromatography (heptane/AcOEt 20:1; silica gel was washed with 1% Et_3N before being used for column chromatography) afforded product **6c** as a light yellow oil (1.8 g, 82%). **^{1}H NMR** [400 MHz, δ (ppm), $CDCl_3$]: 4.56 (s, 2 H), 5.47 (d, J = 5.7 Hz, 2 H), 6.81 (t, J = 6.0 Hz, 1 H), 7.20–7.25 (m, 2 H), 7.44–7.51 (m, 2 H). **^{13}C NMR** [101 MHz, δ (ppm), $CDCl_3$]: 69.6, 91.7, 121.5, 121.9, 129.3, 131.4, 136.6, 201.2. These data were in accordance to those reported in the literature.[28]

1,3-Dimethoxy-5-{[(propa-1,2-dien-1-yl)oxy]methyl}benzene 6d.

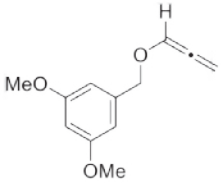

6d

Column chromatography (heptane/AcOEt 40:1→20:1; silica gel was washed with 1% Et_3N before being used for column chromatography) afforded product **6d** as a light yellow oil (1.9 g, 90%). **^{1}H NMR** [400 MHz, δ (ppm), $CDCl_3$]: 3.79 (s, 6 H), 4.55 (s, 2 H), 5.48 (d, J = 6.0 Hz, 2 H), 6.40 (t, J = 2.3 Hz, 1 H), 6.51 (t, J = 5.9 Hz, 2 H), 6.83 (t, J = 5.9 Hz, 1 H). **^{13}C NMR** [101 MHz, δ (ppm), $CDCl_3$]: 55.3, 70.5,

91.2, 100.0, 105.4, 121.5, 139.6, 160.8, 201.2. **FTIR** [$\tilde{\nu}$ (cm^{-1})]: 832, 1153, 1205, 1461, 1598, 2838, 2936. **HRMS** (ESI$^+$) calcd. for $(C_{12}H_{14}O_3 + Na)^+$ 229.0835, found 229.0833.

1-[(Propa-1,2-dien-1-yl)oxy]naphthalene 6e.

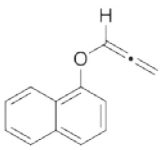

6e

Column chromatography (heptane/AcOEt 40:1→20:1; silica gel was washed with 1% Et_3N before being used for column chromatography) afforded product **6e** as a light yellow oil (1.4 g, 78%). **^{1}H NMR** [400 MHz, δ (ppm), $CDCl_3$]: 5.48 (d, J = 5.9 Hz, 2 H), 7.00 (t, J = 5.8 Hz, 1 H), 7.09 (d, J = 7.5 Hz, 1 H), 7.34–7.57 (m, 4 H), 7.76–7.85 (m, 1 H), 8.21–8.31 (m, 1 H). **^{13}C NMR** [101 MHz, δ (ppm), $CDCl_3$]: 89.6, 109.5, 118.1, 121.9, 122.5, 125.5, 125.7, 126.5, 127.5, 134.6, 153.1, 203.0. These data were in accordance to those reported in the literature.[29]

Palladium-Catalyzed Addition of Azoles to Benzyloxyallene (6a)

General procedure: The reaction was performed in a 5.0 mL Schlenk tube under an nitrogen atmosphere. $[Pd_2(dba)_3]$ (6.9 mg, 0.0075 mmol, 0.025 equiv) and 1,3-bis(diphenylphosphino)-propane (6.2 mg, 0.015 mmol, 0.05 equiv) were disolved in dry THF (3.0 mL). Azole (0.36 mmol, 1.2 equiv) and benzyloxyallene **6a** (44.0 mg, 0.3 mmol, 1.0 equiv) were added and the flask was sealed. The reaction mixture was stirred at 60 °C for the appropriate time (3–18 h). After cooling to 23 °C, the solvent was removed in vacuo and the crude residue was purified by column chromatography as indicated.

1-[1-(Benzyloxy)allyl]-1*H*-imidazole 8a.

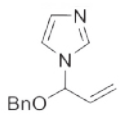

8a

Imidazole (24.5 mg, 0.36 mmol) was treated with benzyloxyallene (**6a**) according to the general procedure and the reaction mixture was stirred and heated for 3 h. The solvent was removed in vacuo and the crude residue was filtered over a diatomaceous-earth pad with heptane to afford product **8a** as a light yellow oil (60.0 mg, 93%). R_F (silica gel, heptane): 0.43 (UV, $KMnO_4$ solution). **^{1}H NMR** [400 MHz, δ (ppm), $CDCl_3$]: 4.34 (d, J = 11.9 Hz, 1 H), 4.53 (d, J = 11.9 Hz, 1 H), 5.39 (ddd, J = 10.5, 1.5, 0.9 Hz, 1 H), 5.41 (ddd, J = 17.2, 1.6, 0.9 Hz, 1 H), 5.90 (dt, J = 4.3, 1.5 Hz, 1 H), 6.04 (ddd, J = 17.2, 10.5, 4.3 Hz, 1 H), 7.06 (t, J = 1.3 Hz, 1 H), 7.14 (t, J = 0.9 Hz, 1 H), 7.27–7.40 (m, 5 H), 7.63 (t, J = 1.0 Hz, 1 H). **^{13}C NMR** [101 MHz, δ (ppm), $CDCl_3$]: 69.7, 84.3, 110.0, 116.9, 119.0, 127.9, 128.2, 128.6, 130.0, 134.1, 136.3. **FTIR** [$\tilde{\nu}$

(cm^{-1})]: 700, 741, 811, 1062, 1218, 1496, 2873, 3031. **HRMS** (ESI$^+$) calcd. for ($C_{13}H_{14}N_2O$ + H)$^+$ 215.1184, found 215.1179.

1-[1-(Benzyloxy)allyl]-1*H*-imidazole-2-carbaldehyde 8b.

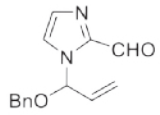

8b

Imidazole-2-carbaldehyde (115.0 mg, 1.2 mmol) was treated with benzyloxyallene (**6a**) according to the general procedure and the reaction mixture was stirred and heated for 4 h. Column chromatography (heptane/AcOEt 20:1→4:1) afforded product **8b** as a light yellow oil (223.0 mg, 92%). R_F (silica gel, heptane/AcOEt 1:1): 0.69 (UV, $KMnO_4$ solution). **^{1}H NMR** [400 MHz, δ (ppm), $CDCl_3$]: 4.49 (d, J = 11.5 Hz, 1 H), 4.54 (d, J = 11.5 Hz, 1 H), 5.35 (ddd, J = 10.5, 1.4, 0.9 Hz, 1 H), 5.40 (ddd, J = 17.2, 1.5, 0.9 Hz, 1 H), 5.98 (ddd, J = 17.2, 10.5, 4.5 Hz, 1 H), 6.98 (dt, J = 4.6, 1.4 Hz, 1 H), 7.24–7.28 (m, 2 H), 7.30–7.36 (m, 4 H), 7.47 (t, J = 1.0 Hz, 1 H), 9.83 (d, J = 1.0 Hz, 1 H). **^{13}C NMR** [101 MHz, δ (ppm), $CDCl_3$]: 71.1, 84.8, 119.0, 122.7, 127.9, 128.2, 128.5, 132.4, 134.1, 136.2, 143.5, 182.5. **FTIR** [$\tilde{\nu}$ (cm^{-1})]: 700, 754, 831, 1069, 1406, 1688, 2844, 3032. **HRMS** (ESI$^+$) calcd. for ($C_{14}H_{14}N_2O_2$ + H)$^+$ 243.1134, found 243.1128.

1-[1-(Benzyloxy)allyl]-1*H*-imidazole-4,5-dicarbonitrile 8c.

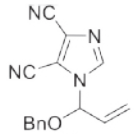

8c

Imidazole-4,5-dicarbonitrile (42.5 mg, 0.36 mmol) was treated with benzyloxyallene (**6a**) according to the general procedure and the reaction mixture was stirred and heated for 4 h. Column chromatography (heptane/AcOEt 20:1→4:1) afforded product **8c** as a light yellow oil (71.4 mg, 90%). R_F (silica gel, heptane/AcOEt 2:1): 0.44 (UV, $KMnO_4$ solution). **^{1}H NMR** [400 MHz, δ (ppm), $CDCl_3$]: 4.60 (d, J = 11.9 Hz, 1 H), 4.68 (d, J = 11.9 Hz, 1 H), 5.59 (dd, J = 10.3, 1.3 Hz, 1 H), 5.60 (dd, J = 17.2, 1.3 Hz, 1 H), 5.88 (dt, J = 4.9, 1.3 Hz, 1 H), 6.02 (ddd, J = 17.1, 10.4, 4.9 Hz, 1 H), 7.28–7.38 (m, 5 H), 7.80 (s, 1 H). **^{13}C NMR** [101 MHz, δ (ppm), $CDCl_3$]: 72.0, 86.8, 107.6, 110.7, 111.3, 122.1, 123.8, 128.1, 128.9, 130.0, 131.6, 134.6, 139.7. **FTIR** [$\tilde{\nu}$ (cm^{-1})]: 699, 738, 803, 1023, 1343, 1454, 1655, 2241, 2922, 3032. **HRMS** (ESI$^+$) calcd. for ($C_{15}H_{12}N_4O$ + H)$^+$ 265.1089, found 265.1082.

1-[1-(Benzyloxy)allyl]-1*H*-benzimidazole 8d.

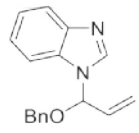

8d

Benzimidazole (42.5 mg, 0.36 mmol) was treated with benzyloxyallene (**6a**) according to the general procedure and the reaction mixture was stirred and heated for 4 h. Column chromatography (heptane/AcOEt 10:1→1:1) afforded product **8d** as a light yellow oil (62.6 mg, 79%). R_F (silica gel, heptane/AcOEt 1:1): 0.27 (UV, $KMnO_4$ solution). **^{1}H NMR** [400 MHz, δ (ppm), $CDCl_3$]: 4.36 (d, J = 11.9 Hz, 1 H), 4.55 (d, J = 11.9 Hz, 1 H), 5.42 (d, J = 10.7 Hz, 1 H), 5.47 (d, J = 17.3 Hz, 1 H), 5.95–5.99 (m, 1 H), 6.15 (ddd, J = 17.0, 10.5, 4.1 Hz, 1 H), 7.24–7.27 (m, 2 H), 7.28–7.40 (m, 5 H), 7.48–7.53 (m, 1 H), 7.80–7.87 (m, 1 H), 8.00 (s, 1 H). **^{13}C NMR** [101 MHz, δ (ppm), $CDCl_3$]: 69.9, 83.9, 111.5, 119.3, 120.5, 122.7, 123.3, 128.0, 128.3, 128.6, 132.4, 133.6, 136.1, 141.9, 144.3. **FTIR** [$\bar{\nu}$ (cm^{-1})]: 699, 723, 809, 1061, 1223, 2884, 3032. **HRMS** (ESI$^+$) calcd. for $(C_{17}H_{16}N_2O + H)^+$ 265.1341, found 265.1328.

1-[1-(Benzyloxy)allyl]-3,5-dimethyl-1*H*-pyrazole 8e.

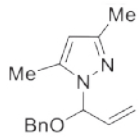

8e

3,5-Dimethylpyrazole (34.6 mg, 0.36 mmol) was treated with benzyloxyallene (**6a**) according to the general procedure and the reaction mixture was stirred and heated for 4 h. Column chromatography (heptane/AcOEt 10:1→1:1) afforded product **8e** as a light yellow oil (57.4 mg, 79%). R_F (silica gel, heptane/AcOEt 10:1): 0.22 (UV, $KMnO_4$ solution). **^{1}H NMR** [400 MHz, δ (ppm), $CDCl_3$]: 2.22 (s, 3 H), 2.24 (s, 3 H), 4.42 (d, J = 11.9 Hz, 1 H), 4.46 (d, J = 12.0 Hz, 1 H), 5.34 (ddd, J = 10.5, 1.7, 1.2 Hz, 1 H), 5.36 (ddd, J = 17.3, 1.7, 1.2 Hz, 1 H), 5.86 (s, 1 H), 5.90 (dt, J = 4.3, 1.7 Hz, 1 H), 6.15 (ddd, J = 17.3, 10.6, 4.4 Hz, 1 H), 7.25–7.35 (m, 5 H). **^{13}C NMR** [101 MHz, δ (ppm), $CDCl_3$]: 11.4, 13.5, 69.5, 88.2, 107.1, 118.2, 127.8, 127.9, 128.4, 134.3, 137.1, 139.6, 147.9. **FTIR** [$\bar{\nu}$ (cm^{-1})]: 699, 737, 824, 1066, 1314, 1456, 1559, 2843, 3032. **HRMS** (ESI$^+$) calcd. for $(C_{15}H_{18}N_2O + H)^+$ 243.1497, found 243.1493.

Ethyl 1-[1-(benzyloxy)allyl]-1*H*-indole-2-carboxylate 8f.

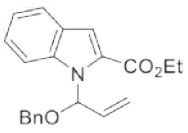

8f

Ethyl indole-2-carboxylate (68.1 mg, 0.36 mmol) was treated with benzyloxyallene (**6a**) according to the general procedure and the reaction mixture was stirred and heated for 18 h. Column chromatography (heptane/AcOEt 20:1→1:1) afforded product **8f** as a light yellow oil (64.4 mg, 64%). R_F (silica gel, heptane/AcOEt 10:1): 0.39 (UV, $KMnO_4$ solution). **^{1}H NMR** [400 MHz, δ (ppm), $CDCl_3$]: 1.37 (t, J = 7.1 Hz, 3 H), 4.31 (dq, J = 10.8, 7.1 Hz, 1 H),

4.34 (dq, *J* = 10.8, 7.1 Hz, 1 H), 4.39 (d, *J* = 11.7 Hz, 1 H), 4.42 (d, *J* = 11.7 Hz, 1 H), 5.26 (dd, *J* = 10.6, 1.4 Hz, 1 H), 5.34 (dd, *J* = 17.3, 1.4 Hz, 1 H), 6.21 (ddd, *J* = 17.2, 10.6, 4.1 Hz, 1 H), 7.15 (ddd, *J* = 8.0, 7.0, 0.9 Hz, 1 H), 7.19–7.30 (m, 7 H), 7.36 (d, *J* = 0.8 Hz, 1 H), 7.66 (dd, *J* = 8.0, 0.8 Hz, 1 H), 7.84 (ddd, *J* = 8.3, 1.6, 0.7 Hz, 1 H). **^{13}C NMR** [101 MHz, δ (ppm), $CDCl_3$]: 14.4, 60.8, 70.0, 85.0, 112.3, 115.1, 117.9, 121.2, 122.5, 125.0, 126.9, 127.8, 128.0, 128.1, 128.3, 134.9, 137.3, 138.0, 162.2. **FTIR** [$\tilde{\nu}$ (cm^{-1})]: 698, 750, 813, 1065, 1198, 1703, 2869, 3031. **HRMS** (ESI^+) calcd. for $(C_{21}H_{21}NO_3 + H)^+$ 336.1600, found 336.1617.

1-[1-(Benzyloxy)allyl]-1*H*-1,2,4-triazole 8g.

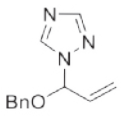

8g

1,2,4-Triazole (24.9 mg, 0.36 mmol) was treated with benzyloxyallene **(6a)** according to the general procedure and the reaction mixture was stirred and heated for 4 h. Column chromatography (heptane/AcOEt 20:1→4:1) afforded product **8g** as a light yellow oil (71.4 mg, 90%). R_F (silica gel, heptane/AcOEt 2:1): 0.44 (UV, $KMnO_4$ solution). **^{1}H NMR** [400 MHz, δ (ppm), $CDCl_3$]: 4.53 (d, *J* = 11.9 Hz, 1 H), 4.62 (d, *J* = 11.9 Hz, 1 H), 5.47 (ddd, *J* = 10.3, 1.4, 0.9 Hz, 1 H), 5.55 (ddd, *J* = 17.2, 1.5, 0.9 Hz, 1 H), 5.98 (dt, *J* = 4.6, 1.4 Hz, 1 H), 6.10 (ddd, *J* = 17.1, 10.5, 4.6 Hz, 1 H), 7.28–7.39 (m, 5 H), 8.00 (s, 1 H), 8.26 (s, 1 H). **^{13}C NMR** [101 MHz, δ (ppm), $CDCl_3$]: 70.9, 87.1, 110.0, 120.0, 127.9, 128.3, 128.6, 132.7, 137.4, 151.9. **FTIR** [$\tilde{\nu}$ (cm^{-1})]: 678, 699, 740, 808, 1073, 1273, 1500, 2874, 3032. **HRMS** (ESI^+) calcd. for $(C_{12}H_{13}N_3O + H)^+$ 216.1137, found 216.1129.

1-[1-(Benzyloxy)allyl]-4-nitro-1*H*-imidazole 8ha.

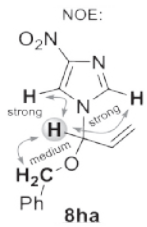

8ha

4-Nitroimidazole (40.7 mg, 0.36 mmol) was treated with benzyloxyallene **(6a)** according to the general procedure and the reaction mixture was stirred and heated for 4 h. Ratio C-4/C-5 > 99:1 was determined by ^{1}H NMR spectroscopy. Crude product was filtered through a diatomaceous-earth pad and washed with CH_2Cl_2 affording product **8ha** as a light yellow oil (73.9 mg, 95%). R_F (silica gel, heptane/AcOEt 1:1): 0.42 (UV, $KMnO_4$ solution). **^{1}H NMR** [400 MHz, δ (ppm), $CDCl_3$]: 4.48 (d, *J* = 12.0 Hz, 1 H), 4.64 (d, *J* = 12.0 Hz, 1 H), 5.53 (ddd, *J* = 10.9, 1.5, 0.8, 1 H), 5.56 (ddd, *J* = 17.2, 1.5, 0.9 Hz, 1 H), 5.69 (dt, *J* = 4.6, 1.4 Hz, 1 H), 6.00 (ddd, *J* = 17.2, 10.5, 4.6 Hz, 1 H), 7.27–7.32 (m, 2 H), 7.35–7.42 (m, 3 H), 7.55 (d, *J* = 1.6 Hz, 1 H), 7.84 (d, *J* = 1.6 Hz, 1 H). **^{13}C NMR** [101 MHz, δ (ppm), $CDCl_3$]: 70.8, 85.8, 116.7, 117.2, 120.8, 128.0, 128.8, 128.9, 132.7, 134.6, 142.3. **FTIR** [$\tilde{\nu}$ (cm^{-1})]: 700, 752,

824, 1070, 1276, 1340, 1491, 2856, 3029. **HRMS** (ESI$^+$) calcd. for $(C_{13}H_{13}N_3O_3 + H)^+$ 260.1035, found 260.1039.

1-[1-(Benzyloxy)allyl]-1*H*-imidazole-4-carbaldehyde 8ia.

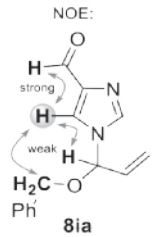

8ia

Imidazole-4-carbaldehyde (34.6 mg, 0.36 mmol) was treated with benzyloxyallene (**6a**) according to the general procedure and the reaction mixture was stirred and heated for 3 h. Ratio C-4/C-5 = 95:5 was determined by ^{1}H NMR spectroscopy. Column chromatography (heptane/AcOEt 10:1→1:2) afforded product **8ia** as a light yellow oil (50.9 mg, 70%). R_F (silica gel, heptane/AcOEt 1:1): 0.16 (UV, $KMnO_4$ solution). **^{1}H NMR** [400 MHz, δ (ppm), $CDCl_3$]: 4.42 (d, J = 11.9 Hz, 1 H), 4.59 (d, J = 11.9 Hz, 1 H), 5.47 (ddd, J = 10.7, 1.5, 0.7 Hz, 1 H), 5.49 (ddd, J = 17.2, 1.5, 0.6 Hz, 1 H), 5.70 (dt, J = 4.5, 1.5 Hz, 1 H), 6.02 (ddd, J = 17.2, 10.4, 4.5 Hz, 1 H), 7.26–7.42 (m, 5 H), 7.70 (d, J = 1.2 Hz, 1 H), 7.74 (d, J = 1.2 Hz, 1 H), 9.91 (s, 1 H). **^{13}C NMR** [101 MHz, δ (ppm), $CDCl_3$]: 70.4, 85.2, 120.1, 122.5, 127.9, 128.6, 128.8, 133.2, 135.5, 137.5, 142.6, 186.2. **FTIR** [$\bar{\nu}$ (cm^{-1})]: 700, 774, 807, 1070, 1534, 1685, 2841, 3033. **HRMS** (ESI$^+$) calcd. for $(C_{14}H_{14}N_2O_2 + H)^+$ 243.1134, found 243.1136.

1-[1-(Benzyloxy)allyl]-4-methyl-1*H*-imidazole 8ja and 1-[1-(benzyloxy)allyl]-5-methyl-1*H*-imidazole 8jb.

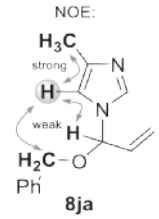

8ja

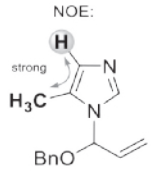

8jb

4-Methylimidazole (30.0 mg, 0.36 mmol) was treated with benzyloxyallene (**6a**) according to the general procedure and the reaction mixture was stirred and heated for 3 h. Ratio C-4/C-5 = 67:33 was determined by ^{1}H NMR spectroscopy. Column chromatography (heptane/AcOEt 10:1→1:2) afforded the product as a non-separable mixture of both regioisomers **8ja** and **8jb** (55.5 mg, 81%) as a light yellow oil. R_F (silica gel, heptane/AcOEt 1:2): 0.06–0.29 (UV, $KMnO_4$ solution). The signals of main isomer are indicated with an asterisk (*). **^{1}H NMR** [400 MHz, δ (ppm), $CDCl_3$]: 2.18 (d, J = 1.0 Hz, 3 H)*, 2.25 (d, J = 1.0 Hz, 3 H), 4.34 (d, J = 11.9 Hz, 1 H)*, 4.35 (d, J = 11.8 Hz, 1 H), 4.52 (d, J = 11.9 Hz, 1 H)*, 4.55 (d, J = 11.8 Hz, 1 H), 5.29 (ddd, J = 17.2, 1.7, 0.9 Hz, 1 H), 5.37 (ddd, J = 10.5, 1.5, 0.9 Hz, 1 H)*, 5.37 (ddd, J = 10.6, 1.5, 0.6 Hz, 1 H), 5.41 (ddd, J = 17.2, 1.6, 1.0 Hz, 1 H)*, 5.57 (dt, J = 4.3, 1.5 Hz, 1 H)*, 5.65 (dt, J = 4.1, 1.7 Hz, 1 H), 6.01 (ddd, J = 17.2, 10.5, 4.4 Hz, 1 H)*, 6.04 (ddd, J = 17.2, 10.3, 4.2 Hz, 1 H), 6.76 (d, J = 1.3 Hz, 1 H)*, 6.83 (d, J = 1.3 Hz, 1

H), 7.27–7.39 (m, 10 H)*, 7.55 (d, *J* = 1.3 Hz, 1 H)*, 7.57 (d, *J* = 1.3 Hz, 1 H). **^{13}C NMR** [101 MHz, δ (ppm), $CDCl_3$]: 9.9, 13.7*, 69.5*, 69.6, 83.7, 84.3*, 113.2, 118.78, 118.82*, 127.7, 127.86*, 127.92, 128.15*, 128.21, 128.58*, 128.61, 134.2*, 134.3, 135.5*, 136.2, 136.3*, 139.0*. **FTIR** [$\tilde{\nu}$ (cm^{-1})]: 669, 739, 814, 1065, 1494, 2871, 3032. **HRMS** (ESI$^+$) calcd. for ($C_{14}H_{16}N_2O$ + H)$^+$ 229.1341, found 229.1348.

1-[1-(Benzyloxy)allyl]-4-iodo-1*H*-imidazole 8ka and 1-[1-(benzyloxy)allyl]-5-iodo-1*H*-imidazole 8kb.

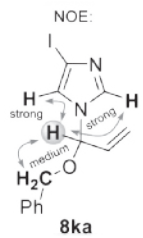

8ka

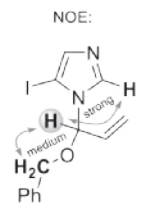

8kb

4-Iodoimidazole (100.0 mg, 0.52 mmol) was treated with benzyloxyallene **(6a)** (85 mg, 0.57 mmol) according to the general procedure and the reaction mixture was stirred and heated for 3 h. C-4/C-5 > 54:46 was determined by ^{1}H NMR spectroscopy. Column chromatography (heptane/AcOEt 10:1→1:2) afforded product **8ka** (70.0 mg, 36%) and product **8kb** (81.0 mg, 42%) as light yellow oils. Compound **8ka**: R_F (silica gel, heptane/ AcOEt 1:1): 0.69 (UV, $KMnO_4$ solution). **^{1}H NMR** [400 MHz, δ (ppm), $CDCl_3$]: 4.37 (d, *J* = 12.0 Hz, 1 H), 4.56 (d, *J* = 12.0 Hz, 1 H), 5.41 (ddd, *J* = 10.5, 1.5, 0.8 Hz, 1 H), 5.44 (ddd, *J* = 17.2, 1.5, 0.8 Hz, 1 H), 5.61 (dt, *J* = 4.3, 1.5 Hz, 1 H), 5.98 (ddd, *J* = 17.2, 10.5, 4.3 Hz, 1 H), 7.14 (d, *J* = 1.4 Hz, 1 H), 7.27–7.41 (m, 5 H), 7.51 (d, *J* = 1.4 Hz, 1 H). **^{13}C NMR** [101 MHz, δ (ppm), $CDCl_3$]: 70.0, 82.6, 84.6, 119.6, 122.6, 127.9, 128.4, 128.7, 133.6, 135.9, 137.7. **FTIR** [$\tilde{\nu}$ (cm^{-1})]: 462, 698, 738, 803, 1072, 1209, 1454, 2873, 3027. **HRMS** (ESI$^+$) calcd. for ($C_{13}H_{13}IN_2O$ + H)$^+$ 341.0151, found 341.0159. **Compound 8kb**: R_F (silica gel, heptane/AcOEt = 1:1): 0.59 (UV, $KMnO_4$ solution). **^{1}H NMR** [400 MHz, δ (ppm), $CDCl_3$]: 4.45 (d, *J* = 11.7 Hz, 1 H), 4.59 (d, *J* = 11.7 Hz, 1 H), 5.39 (ddd, *J* = 17.1, 1.5, 0.7 Hz, 1 H), 5.42 (ddd, *J* = 10.6, 1.5, 0.7 Hz, 1 H), 5.76 (dt, *J* = 4.5, 1.5 Hz, 1 H), 5.98 (ddd, *J* = 17.1, 10.6, 4.4 Hz, 1 H), 7.28–7.40 (m, 6 H), 7.77 (s, 1 H). **^{13}C NMR** [101 MHz, δ (ppm), $CDCl_3$]: 70.7, 87.8, 119.8, 128.08, 128.12, 128.4, 128.7, 133.4, 135.7, 140.4. **FTIR** [$\tilde{\nu}$ (cm^{-1})]: 432, 682, 804, 1062, 1254, 2871, 3033. **HRMS** (ESI$^+$) calcd. for ($C_{13}H_{13}IN_2O$ + H)$^+$ 341.0151, found 341.0160.

1-[1-(Benzyloxy)allyl]-1*H*-pyrrole 8l and 3,3-bis(benzyloxy)prop-1-ene 35.

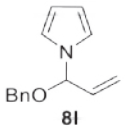

8l

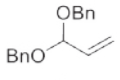

35

Pyrrole (24.2 mg, 0.36 mmol) was treated with benzyloxyallene (**6a**) according to the general procedure and the reaction mixture was stirred and heated for 6 h. Column chromatography (heptane/CH_2Cl_2 40:1→10:1) afforded product **8l** (<1 mg, trace) and product **35** (28.2 mg, 37%) as light yellow oils. Compound **35**: R_F (silica gel, heptane/CH_2Cl_2 2:1): 0.11 (UV, $KMnO_4$ solution). **^{1}H NMR** [400 MHz, δ (ppm), $CDCl_3$]: 4.58 (d, J = 11.8 Hz, 2 H), 4.67 (d, J = 11.8 Hz, 2 H), 5.14 (dt, J = 4.7, 1.2 Hz, 1 H), 5.39 (ddd, J = 10.6, 1.3, 0.9 Hz, 1 H), 5.51 (ddd, J = 17.4, 1.3, 0.9 Hz, 1 H), 5.95 (ddd, J = 17.4, 10.6, 4.7 Hz, 1 H), 7.26–7.38 (m, 10 H). **^{13}C NMR** [101 MHz, δ (ppm), $CDCl_3$]: 67.1, 100.3, 119.0, 127.6, 127.8, 128.4, 134.9, 138.0. These data were in accordance to those reported in the literature.[30]

1-[1-(Benzyloxy)allyl]-1*H*-pyrrole-2-carbaldehyde 8m.

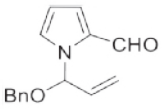

8m

1*H*-Pyrrole-2-carbaldehyde (34.2 mg, 0.36 mmol) was treated with benzyloxyallene (**6a**) according to the general procedure and the reaction mixture was stirred and heated for 6 h. Column chromatography (heptane/AcOEt 20:1→4:1) afforded product **8m** as a light yellow oil (52.1 mg, 72%). R_F (silica gel, heptane/AcOEt 1:1): 0.74 (UV, $KMnO_4$ solution). **^{1}H NMR** [400 MHz, δ (ppm), $CDCl_3$]: 4.47 (d, J = 11.5 Hz, 1 H), 4.53 (d, J = 11.5 Hz, 1 H), 5.28 (ddd, J = 10.5, 1.3, 0.8 Hz, 1 H), 5.33 (ddd, J = 17.1, 1.3, 0.8 Hz, 1 H), 6.01 (ddd, J = 17.1, 10.5, 4.4 Hz, 1 H), 6.33 (dd, J = 3.9, 2.7 Hz, 1 H), 6.97–7.01 (m, 2 H), 7.26–7.35 (m, 6 H), 9.58 (d, J = 1.0 Hz, 1 H). **^{13}C NMR** [101 MHz, δ (ppm), $CDCl_3$]: 70.6, 85.1, 111.0, 118.1, 125.4, 127.86, 127.92, 128.1, 128.4, 131.9, 135.2, 137.0, 179.8. **FTIR** [$\tilde{\nu}$ (cm^{-1})]: 700, 747, 803, 1064, 1242, 1468, 1681, 2853, 3032. **HRMS** (ESI^+) calcd. for $(C_{15}H_{15}NO_2 + H)^+$ 242.1181, found 242.1163.

1-[1-(Benzyloxy)allyl]-1*H*-pyrrole-2-carbonitrile 8n.

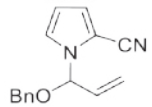

8n

1*H*-Pyrrole-2-carbonitrile (33.2 mg, 0.36 mmol) was treated with benzyloxyallene (**6a**) according to the general procedure and the reaction mixture was stirred and heated for 6 h. Column chromatography (heptane/AcOEt 20:1→4:1) afforded product **8n** as a light yellow oil (59.3 mg, 83%). R_F (silica gel, heptane/AcOEt 10:1): 0.42 (UV, $KMnO_4$ solution). **^{1}H NMR** [400 MHz, δ (ppm), $CDCl_3$]: 4.45 (d, J = 11.6 Hz, 1 H), 4.51 (d, J = 11.6 Hz, 1 H), 5.39 (ddd, J = 10.5, 1.4, 0.8 Hz, 1 H), 5.41 (ddd, J = 17.1, 1.5, 0.8 Hz, 1 H), 5.86 (dt, J = 4.4, 1.5 Hz, 1 H), 6.04 (ddd, J

= 17.2, 10.5, 4.5 Hz, 1 H), 6.27 (dd, *J* = 3.8, 2.9 Hz, 1 H), 6.86 (dd, *J* = 3.9, 1.6 Hz, 1 H), 7.04 (dd, *J* = 2.8, 1.6 Hz, 1 H), 7.28–7.39 (m, 5 H). **^{13}C NMR** [101 MHz, δ (ppm), $CDCl_3$]: 70.5, 86.2, 103.1, 110.6, 113.4, 119.3, 120.8, 124.2, 128.0, 128.2, 128.6, 133.9, 136.1. **FTIR** [$\bar{\nu}$ (cm^{-1})]: 699, 740, 809, 1063, 1268, 1452, 2218, 2917, 3031. **HRMS** (ESI^+) calcd. for ($C_{15}H_{14}N_2O$ + H)$^+$ 239.1184, found 239.1177.

2-[1-(Benzyloxy)allyl]-2*H*-1,2,3-triazole 8oa and 1-[1-(benzyloxy)allyl]-1*H*-1,2,3-triazole 8ob.

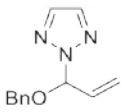

8oa

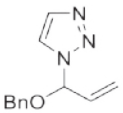

8ob

1H-1,2,3-Triazole (24.9 mg, 0.36 mmol) was treated with benzyloxyallene (**6a**) according to the general procedure and the reaction mixture was stirred and heated for 6 h. Ratio N-2/N-1 = 85:15 was determined by ^{1}H NMR spectroscopy. Column chromatography (heptane/AcOEt 10:1→2:1) afforded product **8oa** (50.0 mg, 76%) and product **8ob** (8 mg, 12%) as light yellow oils. Compound **8oa**: R_F (silica gel, heptane/AcOEt 1:1): 0.69 (UV, $KMnO_4$ solution). **^{1}H NMR** [400 MHz, δ (ppm), $CDCl_3$]: 4.47 (d, *J* = 12.1 Hz, 1 H), 4.53 (d, *J* = 12.1 Hz, 1 H), 5.44 (dt, *J* = 10.5, 1.1 Hz, 1 H), 5.56 (dt, *J* = 17.2, 1.1 Hz, 1 H), 6.16 (dt, *J* = 5.4, 1.2 Hz, 1 H), 6.27 (ddd, *J* = 17.1, 10.5, 5.3 Hz, 1 H), 7.26–7.38 (m, 5 H), 7.71 (s, 2 H). **^{13}C NMR** [101 MHz, δ (ppm), $CDCl_3$]: 70.4, 90.7, 119.6, 127.97, 127.99, 128.4, 132.7, 135.0, 136.4. **FTIR** [$\bar{\nu}$ (cm^{-1})]: 699, 738, 820, 1064, 1314, 2874, 3032. **HRMS** (ESI^+) calcd. for ($C_{12}H_{13}N_3O$ + H)$^+$ 216.1137, found 216.1133. Compound **8ob**: R_F (silica gel, heptane/AcOEt 1:1): 0.46 (UV, $KMnO_4$ solution). **^{1}H NMR** [400 MHz, δ (ppm), $CDCl_3$]: 4.50 (s, 2 H), 5.45 (ddd, *J* = 10.6, 1.6, 0.9 Hz, 1 H), 5.57 (ddd, *J* = 17.2, 1.6, 0.9 Hz, 1 H), 6.06 (ddd, *J* = 17.2, 10.6, 4.2 Hz, 1 H), 6.35 (dt, *J* = 4.2, 1.6 Hz, 1 H), 7.27–7.39 (m, 5 H), 7.72 (d, *J* = 1.1 Hz, 1 H), 7.78 (d, *J* = 1.2 Hz, 1 H). **^{13}C NMR** [101 MHz, δ (ppm), $CDCl_3$]: 69.6, 86.1, 118.9, 120.1, 127.0, 127.2, 127.6, 131.7, 133.6, 135.0. **FTIR** [$\bar{\nu}$ (cm^{-1})]: 672, 816, 1064, 1086, 1250, 2902, 3030. **HRMS** (ESI^+) calcd. for ($C_{12}H_{13}N_3O$ + H)$^+$ 216.1137, found 216.1130.

1-[1-(benzyloxy)-allyl]-1*H*-benzotriazole 8pa and 2-[1-(Benzyloxy)allyl]-2*H*-benzotriazole 8pb.

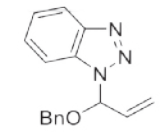

8pa

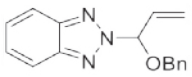

8pb

Benztriazole (42.9 mg, 0.36 mmol) was treated with benzyloxyallene (**6a**) according to the general procedure and the reaction mixture was stirred and heated for 6 h. Ratio N-1/N-2 = 87:13 was determined by ^{1}H NMR spectroscopy. Column chromatography (heptane/AcOEt 20:1→10:1) afforded product product **8pa** (68.0 mg, 85%) and **8pb** (5.1 mg, 6%) as light yellow oils. Compound **8pa**: R_F (silica gel, heptane/AcOEt 10:1): 0.23 (UV, $KMnO_4$ solution). **^{1}H NMR** [400 MHz, δ (ppm), $CDCl_3$]: 4.43 (d, J = 11.9 Hz, 1 H), 4.47 (d, J = 11.9 Hz, 1 H), 5.48 (ddd, J = 10.6, 1.8, 0.9 Hz, 1 H), 5.60 (ddd, J = 17.2, 1.7, 0.9 Hz, 1 H), 6.20 (ddd, J = 17.2, 10.6, 3.9 Hz, 1 H), 6.67 (dt, J = 3.7, 1.8 Hz, 1 H), 7.24–7.35 (m, 5 H), 7.39 (ddd, J = 8.1, 7.0, 1.1 Hz, 1 H), 7.46 (ddd, J = 8.2, 7.0, 1.1 Hz, 1 H), 7.71 (dt, J = 8.3, 1.0 Hz, 1 H), 8.09 (dt, J = 8.2, 1.0 Hz, 1 H). **^{13}C NMR** [101 MHz, δ (ppm), $CDCl_3$]: 70.4, 87.7, 109.8, 111.7, 119.8, 120.0, 124.3, 127.5, 128.1, 128.2, 128.5, 132.5, 136.1. **FTIR** [$\bar{\nu}$ (cm^{-1})]: 699, 747, 815, 927, 1077, 1237, 1450, 2916, 3030. **HRMS** (ESI$^+$) calcd. for $(C_{16}H_{15}N_3O + H)^+$ 266.1293, found 266.1285. Compound **8pb**: R_F (silica gel, heptane/AcOEt 10:1): 0.35 (UV, $KMnO_4$ solution). **^{1}H NMR** [400 MHz, δ (ppm), $CDCl_3$]: 4.53 (d, J = 12.0 Hz, 1 H), 4.06 (d, J = 12.0 Hz, 1 H), 5.47–5.51 (m, 1 H), 5.61–5.68 (m, 1 H), 6.38 (ddd, J = 17.4, 10.5, 5.4 Hz, 1 H), 6.40–6.44 (m, 1 H), 7.26–7.37 (m, 5 H), 7.40–7.45 (m, 2 H), 7.90–7.95 (m, 2 H). **^{13}C NMR** [101 MHz, δ (ppm), $CDCl_3$]: 70.9, 92.7, 118.6, 120.1, 126.9, 128.05, 128.09, 128.4, 132.7, 144.4. **FTIR** [$\bar{\nu}$ (cm^{-1})]: 698, 747, 816, 849, 1082, 1251, 2918, 3030. **HRMS** (ESI$^+$) calcd. for $(C_{16}H_{15}N_3O + H)^+$ 266.1293, found 266.1282.

7-[1-(Benzyloxy)allyl]-1,3-dimethyl-1*H*-purine-2,6(3*H*,7*H*)-dione 8q.

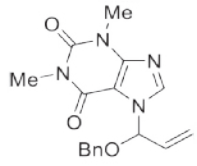

8q

Theophylline (64.9 mg, 0.36 mmol) was treated with benzyloxyallene (**6a**) according to the general procedure and the reaction mixture was stirred and heated for 6 h. Ratio N-7/N-9 > 95:5 was determined by ^{1}H NMR spectroscopy. Column chromatography (heptane/AcOEt 10:1→1:1) afforded product **8q** as a white powder (81.3 mg, 83%). R_F (silica gel, heptane/AcOEt 1:1): 0.38 (UV, $KMnO_4$ solution). M_P: 84–88 °C. **^{1}H NMR** [400 MHz, δ (ppm), $CDCl_3$]: 3.43 (s, 3 H), 3.60 (s, 3 H), 4.62 (d, J = 11.5 Hz, 1 H), 4.71 (d, J = 11.6 Hz, 1 H), 5.43 (ddd, J = 10.7, 1.3, 0.9 Hz, 1 H), 5.55 (ddd, J = 17.3, 1.4, 4.1 Hz, 1 H), 6.07 (ddd, J = 17.1, 10.5, 4.8 Hz, 1 H), 6.70 (dt, J = 4.7, 1.4 Hz, 1 H), 7.25–7.35 (m, 5 H), 7.82 (s, 1 H).

^{13}C NMR [101 MHz, δ (ppm), $CDCl_3$]: 28.1, 29.8, 71.6, 85.2, 106.7, 119.7, 127.8, 128.2, 128.5, 133.6, 136.4, 139.4, 148.6, 151.5, 155.2. **FTIR** [$\tilde{\nu}$ (cm^{-1})]: 699, 747, 1064, 1540, 1659, 1702, 2918, 3112. **HRMS** (ESI$^+$) calcd. for $(C_{17}H_{18}N_4O_3 + H)^+$ 327.1457, found 327.1450.

7-[1-(Benzyloxy)allyl]-8-bromo-1,3-dimethyl-1*H*-purine-2,6(3*H*,7*H*)-dione 8r.

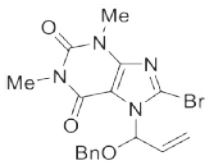
8r

8-Bromotheophylline (93.2 mg, 0.36 mmol) was treated with benzyloxyallene (**6a**) according to the general procedure and the reaction mixture was stirred and heated for 6 h. Ratio N-7/N-9 > 99:1 was determined by ^{1}H NMR spectroscopy. Column chromatography (heptane/AcOEt 10:1→1:1) afforded product **8r** as yellow solid (96.0 mg, 79%). R_F (silica gel, heptane/AcOEt 1:1): 0.23 (UV, $KMnO_4$ solution). M_P: 92–94 °C. **^{1}H NMR** [400 MHz, δ (ppm), $CDCl_3$]: 3.41 (s, 3 H), 3.54 (s, 3 H), 4.56 (d, J = 11.9 Hz, 1 H), 4.67 (d, J = 11.9 Hz, 1 H), 5.38–5.50 (m, 2 H), 6.36 (ddd, J = 16.1, 10.2, 5.2 Hz, 1 H), 6.85 (bs, 1 H), 7.27–7.30 (m, 5 H). **^{13}C NMR** [101 MHz, δ (ppm), $CDCl_3$]: 28.2, 30.0, 71.8, 85.4, 106.8, 119.8, 128.0, 128.3, 128.6, 133.8, 136.4, 139.6, 148.8, 151.6, 155.4. **FTIR** [$\tilde{\nu}$ (cm^{-1})]: 513, 700, 747, 977, 1087, 1361, 1532, 1658, 1702, 2923. **HRMS** (ESI$^+$) calcd. for $(C_{17}H_{17}BrN_4O_3 + H)^+$ 405.0562, found 405.0553.

Enantioselective Palladium-Catalyzed Hydroamination Reactions

General procedure: The reaction was performed in a 5.0 mL Schlenk tube under a nitrogen atmosphere. $[Pd_2(dba)_3]$ (6.9 mg, 0.0075 mmol, 0.025 equiv) and (*R*,*R*)-**L10** (6.2 mg, 0.015 mmol, 0.05 equiv) were dissolved in dry DCE (3.0 mL). The resulting catalyst solution was stirred for 30 min. Imidazole (24.5 mg, 0.36 mmol, 1.2 equiv) and alkoxy allene (0.3 mmol, 1.0 equiv) were added and the flask was sealed. The reaction mixture was stirred at 60 °C for 18 h. After cooling to 23 °C, the solvent was removed in vacuo and the crude residue was purified by column chromatography as indicated.

(*S*)-1-(1-Methoxyallyl)-1*H*-imidazole (*S*)-8s.

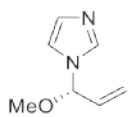
(*S*)-**8s**

Imidazole was treated with allene **6f** (21.0 mg, 0.3 mmol) according to the general procedure. Column chromatography (heptane/AcOEt 40:1→20:1) afforded product (*S*)-**8s** as a light yellow oil (22.4 mg, 54%). R_F (silica gel, heptane/AcOEt 20:1): 0.58 (UV, $KMnO_4$ solution). **^{1}H NMR** [400 MHz, δ (ppm), $CDCl_3$]: 3.28 (s, 3 H), 5.39 (ddd, J = 10.6, 1.5, 0.9 Hz, 1 H), 5.40 (ddd, J = 17.2, 1.5, 0.9 Hz, 1 H), 5.52 (dt, J = 4.2, 1.3 Hz, 1 H), 6.01 (ddd, J = 17.2, 10.5, 4.4

Hz, 1 H), 7.03 (s, 1 H), 7.12 (s, 1 H), 7.66 (s, 1 H). **^{13}C NMR** [101 MHz, δ (ppm), $CDCl_3$]: 55.7, 87.3, 116.8, 119.0, 129.7, 133.9, 136.2. **FTIR** [$\bar{\nu}$ (cm^{-1})]: 1067, 1218, 1411, 1491, 2939, 3112. **HRMS** (ESI$^+$) calcd. for $(C_7H_{10}N_2O + H)^+$ 139.0871, found 139.0862. **HPLC**: 83% ee, Chiralpak OD-H (250 × 4.6 mm), flow: 1.0 mL/min, heptane/ethanol 98:2, retention times: (*R*)-**8s** 24.201 min, (*S*)-**8s** 26.823 min. **$[\alpha]_D^{22}$**: +0.9 (*c* 0.3, $CHCl_3$).

(*S*)-1-(1-Phenoxyallyl)-1*H*-imidazole (*S*)-8t.

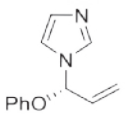
(*S*)-**8t**

Imidazole was treated with allene **6b** (39.7 mg, 0.3 mmol) according to the general procedure. Column chromatography (heptane/AcOEt 40:1→20:1) afforded product (*S*)-**8t** as a light yellow oil (43.2 mg, 72%). R_F (silica gel, heptane/AcOEt 10:1): 0.28 (UV, $KMnO_4$ solution). **^{1}H NMR** [400 MHz, δ (ppm), $CDCl_3$]: 5.52 (ddd, *J* = 10.5, 1.4, 0.6 Hz, 1 H), 5.57 (ddd, *J* = 17.1, 1.5, 0.6 Hz, 1 H), 6.18 (ddd, *J* = 17.1, 10.5, 4.3 Hz, 1 H), 6.30 (dt, *J* = 4.3, 1.5 Hz, 1 H), 6.84–6.89 (m, 2 H), 7.03–7.11 (m, 3 H), 7.23–7.31 (m, 2 H), 7.61 (s, 1 H). **^{13}C NMR** [101 MHz, δ (ppm), $CDCl_3$]: 85.2, 116.9, 117.7, 119.9, 123.6, 129.8, 129.9, 133.3, 136.0, 155.9. **FTIR** [$\bar{\nu}$ (cm^{-1})]: 692, 755, 796, 1071, 1210, 1489, 1589, 2916, 3109. **HRMS** (ESI$^+$) calcd. for $(C_{12}H_{12}N_2O + H)^+$ 201.1028, found 201.1018. **HPLC**: 90% ee, Chiralpak OD-H (250 × 4.6 mm), flow: 1.0 mL/min, heptane/ethanol 97:3, retention times: (*R*)-**8t** 20.989 min, (*S*)-**8t** 27.478 min. **$[\alpha]_D^{22}$**: +0.7 (*c* 0.25, $CHCl_3$).

(*S*)-1-[1-(Naphthalen-1-yloxy)allyl]-1*H*-imidazole (*S*)-8u.

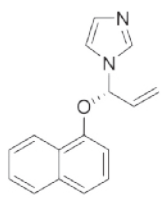
(*S*)-**8u**

Imidazole was treated with allene **6e** (54.7 mg, 0.3 mmol) according to the general procedure. Column chromatography (heptane/AcOEt 20:1→4:1) afforded product (*S*)-**8u** as a light yellow oil (50.3 mg, 67%). R_F (silica gel, heptane/AcOEt 1:2): 0.36 (UV, $KMnO_4$ solution). **^{1}H NMR** [400 MHz, δ (ppm), $CDCl_3$]: 5.60 (dd, *J* = 10.5, 0.9 Hz, 1 H), 5.71 (dd, *J* = 17.1, 1.0 Hz, 1 H), 6.30 (ddd, *J* = 17.1, 10.5, 4.3 Hz, 1 H), 6.45 (dt, *J* = 4.3, 1.4 Hz, 1 H), 6.74 (d, *J* = 7.5 Hz, 1 H), 7.30 (t, *J* = 8.0 Hz, 1 H), 7.46–7.53 (m, 2 H), 7.55 (d, *J* = 8.3 Hz, 1 H), 7.78–7.85 (m, 1 H), 8.09–8.15 (m, 1 H). **^{13}C NMR** [101 MHz, δ (ppm), $CDCl_3$]: 85.4, 110.7, 117.2, 120.3, 121.6, 123.5, 125.7, 126.2, 126.5, 126.8, 127.9, 130.2, 133.3, 134.9, 136.3, 151.9. **FTIR** [$\bar{\nu}$ (cm^{-1})]: 662, 773, 794, 1069, 1262, 1393, 1579, 2919, 3054. **HRMS** (ESI$^+$) calcd. for $(C_{16}H_{14}N_2O + H)^+$ 251.1184, found 251.1172. **HPLC**: 94% ee, Chiralpak OD-H (250 × 4.6 mm), flow: 1.0 mL/min, heptane/ethanol 97:3, retention times: (*R*)-**8u** 23.367 min, (*S*)-**8u** 28.622 min. **$[\alpha]_D^{22}$**: +1.3 (*c* 0.3, $CHCl_3$).

(*S*)-1-[1-(Benzyloxy)allyl]-1*H*-imidazole (*S*)-8a.

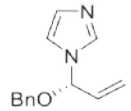

(*S*)-**8a**

Imidazole was treated with allene **6a** (43.9 mg, 0.3 mmol) according to the general procedure. The solvent was removed in vacuo and the crude residue was filtered over a diatomaceous-earth pad with heptane to afford product (*S*)-**8a** as a light yellow oil (57.0 mg, 89%). All analytical data are identical to those reported previously. **HPLC**: 92% ee, Chiralpak OD-H (250 × 4.6 mm), flow: 1.0 mL/min, heptane/ethanol 97:3, retention times: (*R*)-**8a** 19.953 min, (*S*)-**8a** 22.876 min. **[α]**$_D^{22}$: +0.5 (*c* 0.2, $CHCl_3$).

(*S*)-1-{1-[(4-Bromobenzyl)oxy]allyl}-1*H*-imidazole (*S*)-8v.

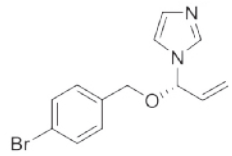

(*S*)-**8v**

Imidazole was treated with allene **6c** (67.5 mg, 0.3 mmol) according to the general procedure. Column chromatography (heptane/AcOEt 20:1→10:1) afforded product (*S*)-**8v** as a light yellow oil (78.0 mg, 89%). R_F (silica gel, heptane/AcOEt 10:1): 0.17 (UV, $KMnO_4$ solution). **^{1}H NMR** [400 MHz, δ (ppm), $CDCl_3$]: 4.31 (d, *J* = 12.0 Hz, 1 H), 4.43 (d, *J* = 12.0 Hz, 1 H), 5.40 (ddd, *J* = 10.5, 1.5, 0.9 Hz, 1 H), 5.41 (ddd, *J* = 17.2, 1.5, 0.9 Hz, 1 H), 5.65 (dt, *J* = 4.3, 1.5 Hz, 1 H), 6.04 (ddd, *J* = 17.2, 10.5, 4.3 Hz, 1 H), 7.05 (s, 1 H), 7.11–7.18 (m, 3 H), 7.45–7.51 (m, 2 H), 7.64 (s, 1 H). **^{13}C NMR** [101 MHz, δ (ppm), $CDCl_3$]: 69.1, 84.7, 117.0, 119.3, 122.3, 129.6, 130.3, 131.9, 134.0, 135.4, 136.3. **FTIR** [$\tilde{\nu}$ (cm^{-1})]: 479, 663, 805, 1011, 1068, 1216, 1488, 2873, 3109. **HRMS** (ESI^+) calcd. for $(C_{13}H_{13}BrN_2O + Na)^+$ 315.0103, found 315.0111. **HPLC**: 93% ee, Chiralpak OD-H (250 × 4.6 mm), flow: 1.0 mL/min, heptane/ethanol 97:3, retention times: (*R*)-**8v** 22.208 min, (*S*)-**8v** 27.493 min. **[α]**$_D^{22}$: +0.8 (*c* 0.3, $CHCl_3$).

(*S*)-1-{1-[(3,5-Dimethoxybenzyl)oxy]allyl}-1*H*-imidazole (*S*)-8w.

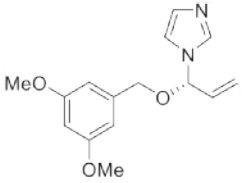

(*S*)-**8w**

Imidazole was treated with allene **6d** (61.9 mg, 0.3 mmol) according to the general procedure. Column chromatography (heptane/AcOEt 1:1) afforded product (*S*)-**8w** as a light yellow oil (74.0 mg, 90%). R_F (silica gel, heptane/AcOEt 1:1): 0.43 (UV, $KMnO_4$ solution). **^{1}H NMR** [400 MHz, δ (ppm), $CDCl_3$]: 3.78 (s, 6 H), 4.27 (d, *J* = 12.2 Hz, 1 H), 4.48 (d, *J* = 12.2 Hz, 1 H), 5.39 (ddd, *J* = 10.5, 1.4, 0.8 Hz, 1 H), 5.42 (ddd, *J* = 17.2, 1.5, 0.8 Hz, 1 H), 5.67 (dt, *J* = 4.3, 1.3 Hz, 1 H), 6.04 (ddd, *J* = 17.2, 10.5, 4.3 Hz, 1 H), 6.41 (t, *J* = 2.1 Hz, 1 H), 6.43 (d, *J* = 2.0 Hz, 2 H), 7.06 (s, 1 H), 7.14 (s, 1 H), 7.64 (s, 1 H). **^{13}C NMR** [101 MHz, δ (ppm), $CDCl_3$]: 55.3, 69.6, 84.3, 100.1, 105.6, 116.9,

119.0, 130.0, 134.1, 136.3, 138.5, 161.0. **FTIR** [$\bar{\nu}$ (cm^{-1})]: 664, 833, 1060, 1064, 1153, 1205, 1462, 1597, 2931, 3110. **HRMS** (ESI$^+$) calcd. for $(C_{15}H_{18}N_2O_3 + H)^+$ 275.1396, found 275.1384. **HPLC**: 94% ee, Chiralpak OD-H (250 × 4.6 mm), flow: 1.0 mL/min, heptane/ethanol 97:3, retention times: (*R*)-**8w** 30.201 min, (*S*)-**8w** 35.069 min. $[\alpha]_D^{22}$: +1.0 (*c* 0.3, $CHCl_3$).

(*S*)-7-[1-(Benzyloxy)allyl]-1,3-dimethyl-1*H*-purine-2,6(3*H*,7*H*)-dione (*S*)-8q.

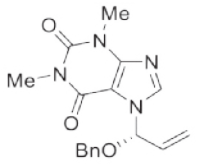

(*S*)-**8q**

Theophylline (64.9 mg, 0.36 mmol) was treated with allene **6a** (43.9 mg, 0.3 mmol) according to the general procedure. Column chromatography (heptane/AcOEt 10:1→1:1) afforded product (*S*)-**8q** as a white powder (72.0 mg, 74%). All analytical data are identical to those reported previously. **HPLC**: 92% ee, Phenomenex Lux 3u Cellulose-1, flow: 0.5 mL/min, heptane/propan-2-ol 70:30, retention times: (*R*)-**8q** 15.832 min, (*S*)-**8q** 16.518 min. $[\alpha]_D^{22}$: +0.4 (*c* 0.2, $CHCl_3$).

Determination of the Absolute Configuration

General procedure: High quality single crystal of (*S*)-**8q** was obtained by slow solvent evaporation: a saturated solution of **8q** in toluene was prepared and filtered over an Acrodisc HPLC syringe filter to ensure the absence of crystallites. The resulting filtrate was transferred to a scintillation flask that was sealed and equipped with a hollow needle to allow slow evaporation of the solvent. The acquired single crystal was subjected to single X-ray diffraction and was subsequently analyzed with chiral HPLC to unambiguously link the absolute configuration with the retention time of one of the enantiomers of **8q**.

3.6 References and Notes

[1] (a) Tjen, K. C. M. F.; Kinderman, S. S.; Schoemaker, H. E.; Hiemstra, H.; Rutjes, F. P. J. T. *Chem. Commun.* **2000**, 699–700; (b) Kinderman, S. S.; Doodeman, R.; van Beijma, J. W.; Russcher, J. C.; Tjen, K. C. M. F.; Kooistra, T. M.; Mohaselzadeh, H.; van Maarseveen, J. H.; Hiemstra, H.; Schoemaker, H. E.; Rutjes, F. P. J. T. *Adv. Synth. Catal.* **2002**, *344*, 736–748; (c) Kinderman, S. S. Transition Metal Catalyzed Formation and Transformations of Allylic *N,O*-Acetals with a Focus on Olefinic α-Amino Acids. Ph.D. Dissertation, University of Amsterdam, the Netherlands, 2003; (d) Kinderman, S. S.; de Gelder, R.; van Maarseveen, J. H.; Schoemaker, H. E.; Hiemstra, H.; Rutjes, F. P. J. T. *J. Am. Chem. Soc.* **2004**, *126*, 4100–4101.

[2] (a) Kim, H.; Rhee, Y. H. *J. Am. Chem. Soc.* **2012**, *134*, 4011–4014; (b) Kim, H.; Rhee, Y. H. *Synlett* **2012**, *23*, 2875–2879; (b) Kim, H.; Lim, W.; Im, D.; Kim, D.; Rhee, Y. H. *Angew. Chem. Int. Ed.* **2012**, *51*, 12055–12058; (c) Kang, S.; Kim, D.; Rhee, Y. H. *Chem. Eur. J.* **2014**, *20*, 16391–16396; (d) Lim, W.; Rhee, Y. H. *Tetrahedron* **2015**, *71*, 5939–5945. For more examples see Chapter 2 and references therein.

[3] (a) Hoff, S.; Brandsma, L.; Arens, J. F. *Rec. Trav. Chim. Pays-Bas* **1968**, *87*, 916–924; (b) Brandsma, L.; Verkruijsse, H. D. *Synthesis of Acetylenes, Allenes and Cumulenes: a Laboratory Manual*; Elsevier: Amsterdam, 1981; Vol. 8.

[4] Krause, N.; Hashmi, A. S. K. *Modern Allene Chemistry*; Wiley-VCH: Weinheim, Germany, 2004; Vol. 1 and 2.

[5] The reaction was also carried out in the presence of [(Ph_3P)AuCl] and $AuBr_3$. In the course of the reaction, both the gold(I) and gold(III) catalysts showed catalytic activity towards addition of imidazole (**7a**) to benzyloxyallene (**6a**), however significantly lower yields were obtained and longer reaction times (up to 48 h) were needed. Furthermore, allylic *N,O*-acetal **8a** was the only product found in the presence of [(Ph_3P)AuCl]. In contrast, in case of $AuBr_3$, the nucleophilic addition to benzyloxyallene (**6a**) led to a 65:35 mixture of C-3 and C-1 addition products.

[6] Selected examples of rhodium-catalyzed asymmetric additions to allenes: (a) Koschker, P.; Breit, B. *Acc. Chem. Res.* **2016**, *49*, 1524–1536; (b) Thieme, N.; Breit, B. *Angew. Chem. Int. Ed.* **2017**, *56*, 1520–1524 and references therein.

[7] 3,3-Bis(benzyloxy)prop-1-ene **35** was formed as the major product. This side product is presumably formed after partial degradation of benzyloxyallene (**6a**) followed by addition of released BnOH to **6a**. For similar results see reference 8b.

[8] Selected examples of palladium-catalyzed asymmetric additions onto allenes: (a) Trost, B. M.; Jäkel, C.; Plietker, B. *J. Am. Chem. Soc.* **2003**, *125*, 4438–4439; (b) Trost B. M.; Simas, A. B. C.; Plietker, B.; Jäkel, C.; Xie, J. *Chem. Eur. J.* **2005**, *11*, 7075–7082; (c) Trost, B. M.; Xie, J.; Sieber, D. *J. Am. Chem. Soc.* **2011**, *133*, 20611–20622.

[9] Zhang, J.; Holmes, A. E.; Sharma, A.; Brooks, N. L.; Rarig, R. S.; Zubieta, J.; Canary, J. W. *Chirality* **2003**, *15*, 180–189 and references therein.

[10] Bernar, I.; Fiser, B.; Blanco-Ania, D.; Gómez-Bengoa, E.; Rutjes, F. P. J. T. *Org. Lett.* **2017**, *19*, 4211–4214.

[11] Hydridopalladium complexes as key intermediates in the process: (a) Leoni, P.; Sommovigo, M.; Pasqall, M.; Midollini, S.; Braga, D.; Sabatino, P. *Organometallics* **1991**, *10*, 1038–1044; (b) Grushin, V. V. *Chem. Rev.* **1996**, *96*, 2011–2034; (c) Amatore, C.; Jutand, A.; Meyer, G.; Carelli, I.; Chiarotto, I. *Eur. J. Inorg. Chem.* **2000**, 1855–1859.

[12] Zimmer, R.; Reissig, H.-U. *Chem. Soc. Rev.* **2014**, *43*, 2888–2903.

[13] Different computational levels show consistent activation energy values for **30**: M06/6-311+G**(SDD): 19.7 kcal/mol; M06/def2TZVPP: 19.0 kcal/mol; B3LYP-D3/6-31G** (LANL2DZ): 17.8 kcal/mol. CPCM-MeCN solvent model was used in all cases.

[14] The exact nature of structure **31**, which could be a local minimum computational artifact along the reaction trajectory, does not compromise the low activation energy from **23** to **32**. At some point during the formation of **32**, the allene–palladium system should reorganize as in **31**.

[15] Zhao, Y.; Truhlar, D. G. *Theor. Chem. Acc.* **2008**, *120*, 215–241.

[16] Barone, V.; Cossi, M. *J. Phys. Chem. A* **1998**, *102*, 1995–2001.

[17] Cossi, M.; Rega, N.; Scalmani, G.; Barone, V. *J. Comp. Chem.* **2003**, *24*, 669–681.

[18] Weigend, F.; Ahlrichs, R. *Phys. Chem. Chem. Phys.* **2005**, *7*, 3297–3305.

[19] Weigend, F.; *Phys. Chem. Chem. Phys.* **2006**, *8*, 1057–1065.

[20] Grimme, S.; Antony, J.; Ehrlich, S.; Krieg, H. *J. Chem. Phys.* **2010**, *132*, 154104.

[21] Hay, P. J.; Wadt, W. R. *J. Chem. Phys.* **1985**, *82*, 270–283.

[22] Achard, T.; Lepronier, A.; Gimbert, Y.; Clavier, H.; Giordano, L.; Tenaglia, A.; Buono, G. *Angew. Chem. Int. Ed.* **2011**, *15*, 3552–3556.

[23] Efe, C.; Lykakis, I. N.; Stratakis, M. *Chem. Commun.* **2011**, *47*, 803–805.

[24] Ishikawa, T.; Mizuta, T.; Hagiwara, K.; Aikawa, T.; Kudo, T.; Saito, S. *J. Org. Chem.* **2003**, *68*, 3702–3705.

[25] Lee, J. W.; Kim, J. H.; Kim, B.-K.; Shin, W. S.; Jin, S.-H. *Tetrahedron* **2006**, *62*, 894–900.

[26] Helms, M.; Schade, W.; Pulz, R.; Watanabe, T.; Al-Harrasi, A.; Fisera, L.; Hlobilova, I.; Zahn, G.; Reissig, H.-U. *Eur. J. Org. Chem.* **2005**, *6*, 1003–1009.

[27] Ocello, R.; De Nisi, A.; Jia, M.; Yang, Q.-Q.; Monari, M.; Giacinto, P.; Bottoni, A.; Miscione, G. P.; Bandini, M. *Chem. Eur. J.* **2015**, *21*, 18445–18453.

[28] Nagarjuna Reddy, M.; Kumara Swamy, K. C. *Synthesis* **2014**, *46*, 1091–1099.

[29] Moghaddam, F. M.; Emami, R. *Synth. Comm.* **1997**, *27*, 4073–4077.

[30] Cui, D.-M.; Zheng, Z.-L.; Zhang, C. *J. Org. Chem.* **2009**, *74*, 1426–1427.

CHAPTER 4

Application of Allylic *N*,*O*-Acetals in the Synthesis of *N*-Heterocycles

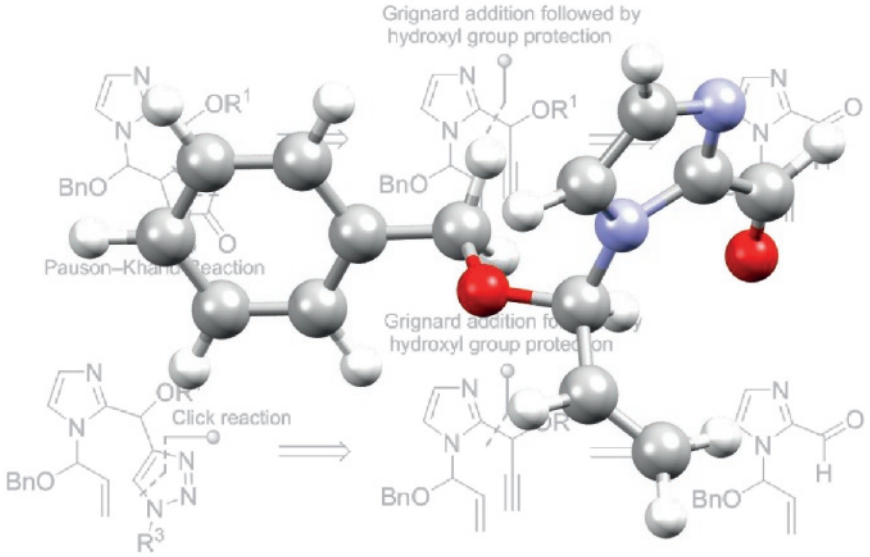

ABSTRACT

This chapter addresses the synthetic concept for derivatization of previously described heteroaromatic allylic *N,O*-acetals. Our efforts aimed to incorporate allylic and propargylic groups into the heteroaromatic ring of the allylic *N,O*-acetals and apply the obtained derivatives in the synthesis of biologically active structures valuable for pharmaceutical and agrochemical industries.

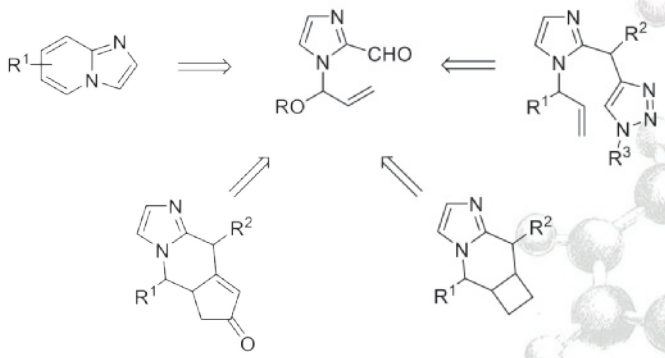

Chapter cover: "Synthetic Targets Utilizing Allylic *N,O*-Acetal **15** as a Building Block"

4.1 Introduction

Allylic *N,O*-acetals offer unique and multiple opportunities for the inclusion of nitrogen-based functionalities into organic molecules.[1] Recent breakthroughs in the preparation of these substrates by palladium-catalyzed hydroamination of alkoxy allenes have revitalized them as highly valuable synthetic precursors. As shown in Chapter 3, this procedure represents an efficient and atom economical entry to elaborate substrates derivatized with complex groups, including *N*-heterocycles. Inspired by these results, we envisaged that heteroaromatic allylic *N,O*-acetals **1** could be of great value in target-orientated syntheses of complex heterocycles, such as fused *N*-heterocyles **2** and **3**, conformationally restricted or strained structures **4** and azolyl triazoles **5** (Scheme 4.1). A variety of biologically active compounds contain these structural features and therefore their fast and easy preparation is relevant for pharmaceutical and agrochemical research.[2–6]

Scheme 4.1 *Synthetic Targets with Allylic N,O-Acetal* ***1*** *as Precursor.*

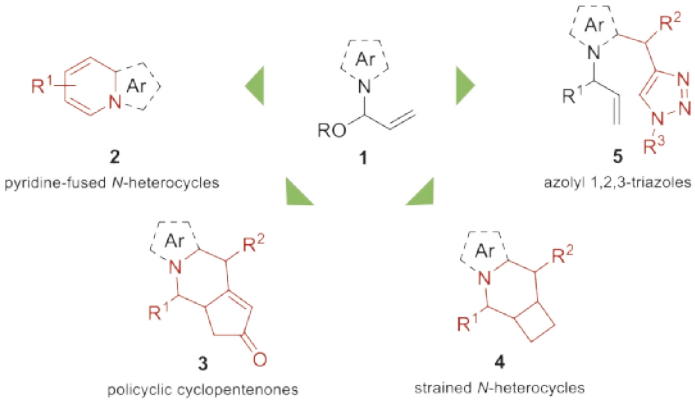

In particular, the imidazo[1,2-*a*]pyridine subunit is widely found in pharmacologically important drugs, including several anxyolytics, such as alpidem (**9**), zolimidine (**10**), and zolpidem (**11**) (Scheme 4.2).[2] Furthermore, imidazo[1,2-*a*]pyridines are promising lead compounds in fungicide research and therefore are of potential value for the ECHONET program.[3] Interest in these structures led us to investigate new methodologes for their preparation starting from the previously synthetized allylic *N,O*-acetal **8** (Chapter 3). Key challenges in this synthetic route are C-2 functionalization at the heteroaromatic part of the molecule, ring-closing metathesis (RCM)[4] of precursor **7** and further functionalization by elimination of a leaving group.

Scheme 4.2 *Proposed Retrosynthesis of Imidazo[1,2-a]pyridine Framework* **6** *(Top) and Drugs Containing this Structure (Bottom).*

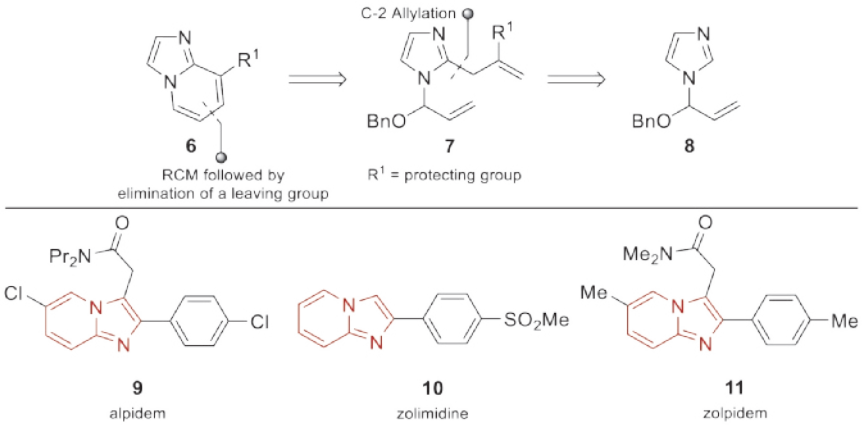

Diene **7** could additionally serve as a possible reactant for photocycloaddition reactions. Our group has already established the synthesis of conformationally restricted three-dimensional scaffolds through [2+2] photocycloaddition of allyl-substituted enamines.[5] Encouraged by these results we decided to apply this approach for the synthesis of strained *N*-heterocyclic scaffold **12** utilizing the same photochemical process (Scheme 4.3).

Scheme 4.3 *Proposed Retrosynthesis of Strained N-Heterocyclic Scaffold* **12**.

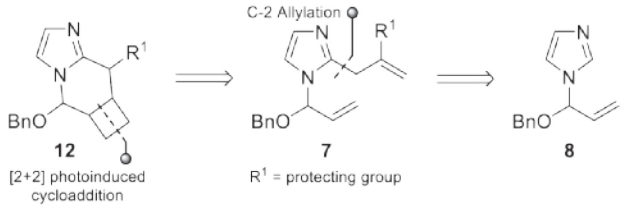

Apart from scaffolds **6** and **12**, we were also interested in the preparation of heterocyclic scaffold **13** (Scheme 4.4). Various cyclopent-2-enone derivatives display a wide range of applications in the fields of pharmacy, agriculture, and industry.[6] Therefore, extending these examples with scaffold **13** would contribute to the lead search of potential bioactive molecules for the agrochemical industry within the ECHONET program. The key step in this approach is the palladium-catalyzed hydroamination of imidazole-4-carbaldehyde to benzyloxyallene forming allylic *N,O*-acetal **15**, as described in Chapter 3. Addition of ethynylmagnesium bromide

to the aldehyde followed by protection of the formed alcohol would lead to enyne **14**. Upon [2+2+1] cycloaddition of enyne **14** with carbon monoxide, the so-called Pauson–Khand (PK) reaction,[7] the new *N*-heterocyclic scaffold **13** could be formed.

Scheme 4.4 *Proposed Retrosynthesis of N-Heterocyclic Scaffold* ***13***.

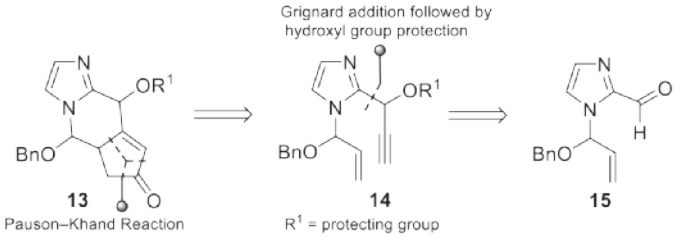

Moreover, we present attempts to utilize enyne **14** for the synthesis of azolyl 1,2,3-triazoles **16** via azide–alkyne 1,3-dipolar cycloaddition ("click chemistry"; Scheme 4.5).[8] These structures could be tested for their biological activity or further used in more elaborated synthetic transformations.[9]

Scheme 4.5 *Proposed Retrosynthesis of Azolyl 1,2,3-Triazoles* ***16***.

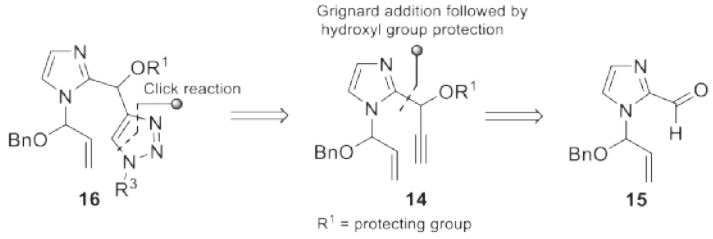

Our final attempts were focused on the incorporation of fluorine into these *N*-heterocyclic scaffolds. The electronegativity, size, and lipophilicity of fluorine can dramatically influence the chemical reactivity and pharmacological behavior of organic molecules in a positive sense.[10] Hence, the number of fluorine-containing compounds is increasing among pharmaceutical drugs and agrochemicals because of these favorable properties. Thus, we were interested in establishing a fluorination strategy to modify the physical and chemical properties of the studied compounds with the intention to examine their biological activity against pests.

With the aforementioned general goals in mind the stage was now set for developing the synthetic methodologies for preparation of scaffolds **6**, **12**, **13**, and **16**.

4.2 Results and Discussion

4.2.1 Introduction of Allyl and Propargyl Groups at the 2-Position of the Imidazole Ring

We began our study with the derivatization of heterocyclic *N,O*-acetal **8** at the C-2 position of the imidazole ring by introducing a second allyl group (Table 4.1).

Table 4.1 *Derivatization of Allylic N,O-Acetal 8 by a Deprotonation/Alkylation Approach.*

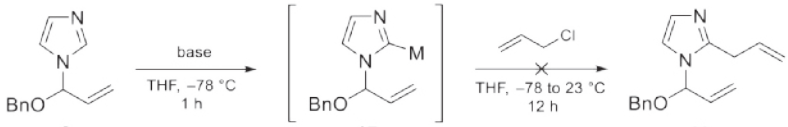

Entry	Base	Additive	*t* (°C)	Yield (%)[a]
1	^{n}BuLi	–	–78	–
2	LDA	–	–78	–
3	LTMP	–	–78	–
4	^{n}BuLi	TMEDA[a]	–78	–
5	[^{i}PrMgCl·LiCl]	–	0	–
6	[TMPMgCl·LiCl]	–	0	–
7	[TMPZnCl·LiCl]	–	0	–
8	[TMPZnCl·LiCl]	–	23	–
9	[TMPZnCl·LiCl]	[CuCN·2LiCl][a]	0	decomposition
10	[TMPZnCl·LiCl]	$Pd(OAc)_2$[a]	0	–

[a]Additive (10 mol %) was used in each experiment.

Two consecutive steps constituted the basis of this approach: (a) deprotonation of the C-2 position with an organolithium reagent or other base and (b) reaction of the formed anion with allyl chloride. Generation of the C-2 anion was initially carried out with ^{n}BuLi (1.05 equiv) at –78 °C in THF (entry 1). Upon treatment with the base, the corresponding lithiated intermediate **17** was formed. Its formation was confirmed through hydrogen–deuterium (H–D) exchange in an ^{1}H NMR experiment.[11] However, after addition of allyl chloride the ^{1}H NMR experiment of the reaction mixture showed no conversion to the desired product **18**. In fact, only the signals of the

starting materials were observed. Using other organolithium bases [lithium diisopropylamide (LDA) and lithium 2,2,6,6-tetramethylpiperidinide (LTMP)] or addition of *N,N,N′,N′*-tetramethylethane-1,2-diamine (TMEDA)[12] to the lithiated intermediate **17** was likewise unproductive (entries 2–4). A possible explanation for the observed lack of reactivity might be that the lone pair of the reacting carbon in the formed organolithium reagent **17** is too sterically hindered for the substitution reaction to occur.

Other methods were pursued because of the unwillingness of these lithium organic species to react with allyl chloride under the standard conditions. Inspired by the work done in the group of Knochel on the preparation of magnesium- and zinc-based reagents for selective metalation,[13a] the deprotonation of heterocyclic *N,O*-acetal **8** was carried out with [^{i}PrMgCl·LiCl], [TMPMgCl·LiCl] and [TMPZnCl·LiCl] in amounts ranging from equimolar up to a slight excess (entries 5, 6, and 7). In all these cases, fast deprotonation was observed and the corresponding Mg and Zn salts were even stable at 0 °C for several hours. Unluckily, neither of these organometallic intermediates reacted with allyl chloride at 0 °C or at elevated temperatures (up to 23 °C, entry 8). The same group reported an interesting improvement of the original procedure by transmetallation of the formed Mg or Zn organic species with Cu(I) salts.[13b,c] Following this procedure, subsequent transmetalation of the resulting organozinc intermediate to the corresponding organocopper salt of *N,O*-acetal **8** was performed by pretreating the reaction mixture with an equimolar amount of [CuCN·2LiCl] before adding allyl chloride (entry 9). However, instead of allylation, cleavage of *N,O*-acetal **8** to imidazole and unidentified side products was observed. In order to prevent this unwanted process, we thought of a palladium-catalyzed transmetalation as a possible alternative (entry 10), but with an unsuccessful result.

Next, we tested the reactivity of different substituted allyl chlorides towards the formed organometallic salt **17** upon deprotonation with two strong bases. In all cases the standard conditions (allyl chloride **19** or **20** [1.5 equiv], THF, –78 to 23 °C, 12 h) were applied (Table 4.2). As in the previous experiments with allyl chloride, alkylation with 2-chloroallyl chloride **19** and 2-fluoroallyl chloride **20** did not result in any reaction after 12 h, according to TLC (entries 1 and 2 for **19** and 3 and 4 for **20**). In case of adding an equimolar ammount of [CuCN·2LiCl], however, the ^{1}H NMR spectrum of the crude products showed a complex mixture in which imidazole and partially degraded benzyloxyallene were the major compounds (entry 3 for **19** and 6 for **20**).

Table 4.2 *Alkylation of Allylic N,O-Acetal 7 with Allyl Chlorides 19 and 20.*

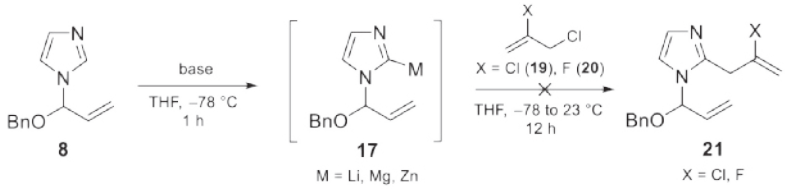

Entry	Base	Additive	Allyl chloride	Yield (%)
1	^{n}BuLi	–	**19**	–
2	[TMPZnCl·LiCl]	–	**19**	–
3	[TMPZnCl·LiCl]	[CuCN·2LiCl][a]	**19**	decomposition
4	^{n}BuLi	–	**20**	–
5	[TMPZnCl·LiCl]	–	**20**	–
6	[TMPZnCl·LiCl]	[CuCN·2LiCl][a]	**20**	decomposition

[a][CuCN·2LiCl] (10 mol %) was used in each experiment.

Despite that our pioneering attempts were fruitless and far from satisfactory, we realized that alkylation can be favored with other allylic halides. Generally, replacing chlorine with bromine or iodine can dramatically increase the reactivity of the allyl halide. Therefore, we tested the reactivity of allyl bromide **22** and allyl iodide **23** towards organozinc intermediate **17**, formed by deprotonation (Scheme 4.6). We found that treatment of intermediate **17** with tested halides at temperatures ranging from –78 °C up to 23 °C did not result in any conversion neither for allyl bromide **22**, nor for allyl iodide **23**.

Scheme 4.6 *Alkylation of Allylic N,O-Acetal 8 with Allyl Bromide 22 and Allyl Iodide 23.*

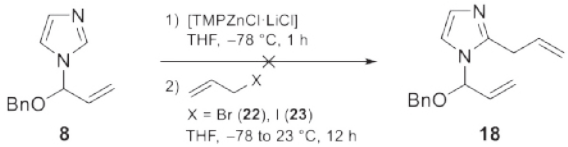

Because the lithiation/nucleophilic substitution of allylic *N,O*-acetal **8** with allyl halides was unsuccessful, an alternative method to introduce the second allylic group was proposed (Scheme 4.7). Metalation of allylic *N,O*-acetal **8** with ^{n}BuLi at –78 °C resulted in formation of organolithium intermediate **17**, which upon 1,2-addition onto acrolein led to the desired product **24** as a 50:50 mixture of diastereoisomers in 61% yield after purification by column chromatography. The likely

explanation for the success of this reaction is the higher reactivity of acrolein compared to the previously used allyl halides **21**–**23** (sp^2- vs sp^3-bonded carbon centers and a more electrophilic carbon atom). Additionally, the coordination of a lithium atom of intermediate **17** with the carbonyl group in acrolein makes it more reactive towards the nucleophilic attack.[14] The lithium alcoholate intermediate formed in this manner could be stabilized by an additional coordination with the nitrogen atom of the imidazole, driving the reaction towards the formation of the final product after the work up.

Scheme 4.7 *Synthesis of Diene* ***24*** *Starting from Allylic N,O-Acetal* ***8****.*

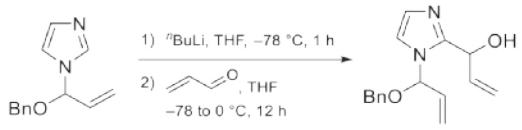

8 **24**
61%, dr 50:50

Product **24** was also formed via Grignard addition of organomagnesium reagents to heterocyclic *N,O*-acetal **15** (Scheme 4.8). This *N,O*-acetal was readily available through the earlier described palladium-catalyzed addition of imidazole-2-carbaldehyde **25** to alkoxy allene **26** yielding product **15** in 92% yield (Chapter 3). Subsequent addition of vinylmagnesium bromide to allylic *N,O*-acetal **15** afforded the corresponding diene **27** as a 65:35 mixture of diastereoisomers in 72% yield. This sequence was then further optimized and scaled up to gram scale in a one-pot process. Furthermore, the Grignard addition of ethynylmagnesium bromide to *N,O*-acetal **15** resulted in the formation of enyne **28** as a 55:45 mixture of diastereoisomers in 76% yield.

Scheme 4.8 *Synthesis of Diene* ***27*** *and Enyne* ***28****.*

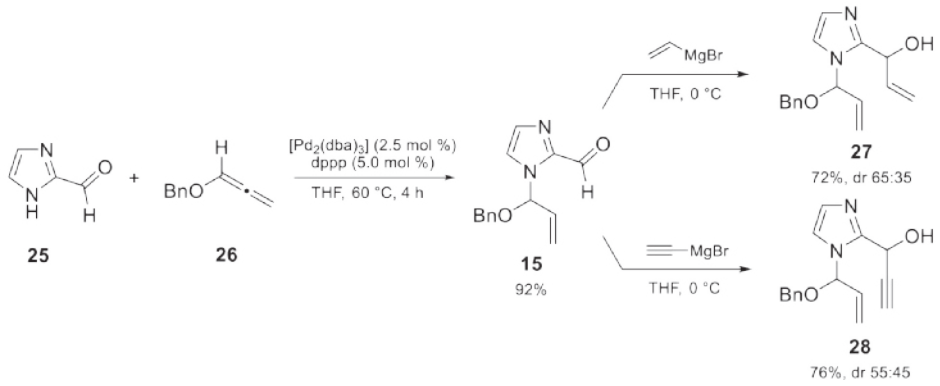

25 **26** **15** 92% **27** 72%, dr 65:35 **28** 76%, dr 55:45

4.2.2 Investigation of RCM of Diene 27 and Its Derivatives

With diene **27** in hand, the ring-closing metathesis experiments were carried out using the ruthenium catalysts **G1**, **G2**, and **G3** (Table 4.3 and Figure 4.1). The metathesis experiments were performed at high dilution (0.01 M) to prevent dimer formation. Besides, the mildest possible conditions were used to avoid decomposition of the *N*,*O*-acetal moiety of diene **27**.

Table 4.3 *Ring-Closing Metathesis of Diene* **27**.

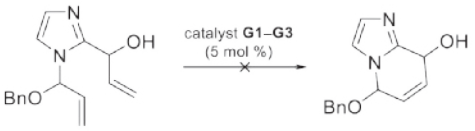

27
dr 50:50

29

Entry	Solvent	Catalyst	*t* (°C)	Time (h)	Yield (%)
1	PhMe	**G1**	23	24	–
2	PhMe	**G1**	70	6	–
3	PhMe	**G2**	23	24	–
4	PhMe	**G2**	70	6	–
5	PhMe	**G3**	23	24	–
6	HOAc	**G2**	23	24	–

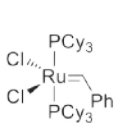

G1
Grubbs catalyst
1st generation

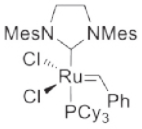

G2
Grubbs catalyst
2nd generation

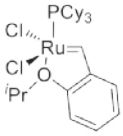

G3
Hoveyda–Grubbs catalyst
1st generation

Figure 4.1 *Ruthenium Catalysts Used in the Study.*

Subjection of compound **27** to the first generation Grubbs catalyst **G1** at either 23 °C or 70 °C in toluene resulted in no reaction (entries 1 and 2, Table 4.3). Use of the ruthenium–imidazolidine catalyst **G2** showed no reactivity either (entries 3 and 4). Unfortunately, attempts to improve the metathesis reaction by increasing the temperature, changing the solvent or using other catalysts did not lead to successful results (entries 4–6). The likely explanation for these observations might be that the ruthenium–alkylidene complex coordinates to the nitrogen at the 3-position of imidazole

27 rendering the catalyst inactive, similar to that observed by Grubbs's group in some early work on ruthenium–alkylidene complexes.[15] Moreover the hydroxy group could interact with the ruthenium alkylidene complex, thereby negatively influencing its reactivity. Several attempts were performed to circumvent these issues. First, we decided to convert the allylic alcohol in **27** into the corresponding allyl acetate **30** (Table 4.4). The protection with acetic anhydride (1.5 equiv) in pyridine at 23 °C yielded acetate **30** in 95% yield. This acetate was then further treated with Brønsted or Lewis acids prior to the addition of catalysts **G1–G3**. This treatment should result in the formation of the imidazolium ion, preventing the lone pair of the nitrogen of imidazole from inactivating the Grubbs catalyst.

Table 4.4 *Synthesis of Diene 30 and its Following RCM.*

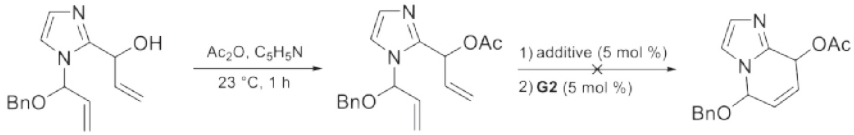

27 dr 50:50 — **30** 95%, dr 50:50 — **31**

Entry	Solvent	Additive	t (°C)	Yield (%)
1	CH_2Cl_2	HOAc	23	–
2	PhMe	HOAc	70	decomposition
3	CH_2Cl_2	$Ti(O^iPr)_4$	23	decomposition
4	PhMe	$Ti(O^iPr)_4$	70	decomposition

Using the modified procedure for RCM, acetate **30** was first premixed with HOAc or $Ti(O^iPr)_4$ and then Grubbs catalyst **G2** was added. Subjection of compound **30** to the second generation Grubbs catalyst **G2** in CH_2Cl_2 at 23 °C showed only starting material after 24 h (entry 1, Table 4.4). In contrast, heating the reaction mixture in toluene only produced cleavage of the *N,O*-acetal moiety (entry 2). Carrying out the reaction in the presence of $Ti(O^iPr)_4$ (2 equiv), a known method for circumventing intramolecular chelation of ruthenium–alkylidene complexes,[16] merely decomposition of the starting material was observed (entries 3 and 4).

Because of the inertness of dienes **27** and **30** towards the ruthenium catalysts, extension of the RCM reaction to diene **32** was attempted (Scheme 4.9). With the aim to obtain the desired heterocycle **33**, a two-step synthetic route was proposed: oxidation of the secondary alcohol of **27** with Dess–Martin periodinane (DMP) to ketone **30** and consecutive ring-closing metathesis

to form the new six-membered ring. In a preliminary study, the hydroxy group showed very good conversion rates at 23 °C, so that after 1 h of reaction, an isolated yield of 88% of the corresponding ketone was obtained. Despite this promising result, all our attempts to cyclize diene precursor **32** failed. Thus, compound **32** was subjected to ruthenium catalyst **G2** and **G3** at 70 °C in toluene, but in both cases no cyclic product could be observed and solely starting material was recovered. Considering all our efforts to perform RCM on compounds **27**, **30**, and **32** we realized that this process would require an entirely different type of reaction optimization. Therefore, this line of research was abandoned for future investigations.

Scheme 4.9 *Synthesis of Diene 32 and Attempts of RCM.*

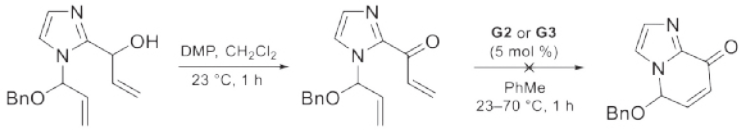

27 dr 50:50 — **32** 88% — **33**

4.2.3 [2+2] Photocycloaddition of Dienes 27 and 32

While performing the ring-closing metathesis studies of dienes **27** and **32**, we were also sidetracked into pursuing a [2+2] photocycloaddition of these products. This approach would lead to interesting strained carbocyclic structures, with structural features found in some natural products.[17] Initial explorative screenings of the reaction conditions were carried out in a quartz round-bottom flask (Table 4.5).

Table 4.5 *[2+2] Photocycloaddition of Dienes 27.*

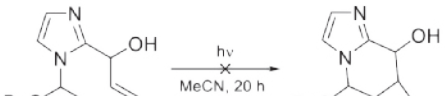

27 dr 50:50 — **34**

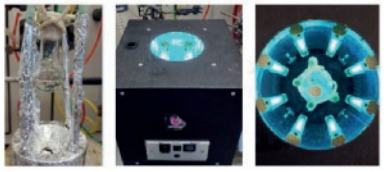

Entry	λ (nm)	*t* (°C)	Yield (%)
1	254	23	-
2	254	50	-
3	300	23	-
4[a]	254	23	-
5[b]	300	23	decomposition
6[b]	254	23	decomposition

[a]Acetone was used as a solvent. [b][$(CuOTf)_2$·PhH] (10 mol %).

The reaction mixture was irradiated in a Rayonet RMR-600 photochemical reactor, using eight lamps with a wavelength of 254 nm. However, photocycloadduct **30** was not formed under the reaction conditions and in all cases starting material was recovered. Thus, diene **25** did not react at 23 °C (entry 1) nor at 50 °C (entry 2). Utilizing lamps of different wavelength (300 nm) or changing the solvent (which at the same time acts as a sensitizer) did not yield any product either (entries 3 and 4). To shed more light on the process, we recorded the UV-vis absorption spectra of **27** and a UV absorption maximum at 210–230 nm was observed. This suggests that higher energy light for the excitation might be required, thereby explaining the non-reactivity of diene **27** in the reaction. Therefore, we decided to use a catalytic amount of $[(CuOTf)_2 \cdot PhH]$ to promote the reaction. As shown by Solomon et al., non-conjugated alkenes with a similar absorption maximum can be raised to the excited state in the present of this catalyst.[18] However, also in this case no product was formed either and partial degradation of the starting material was observed (entries 5 and 6).

Interestingly, the allylic *N,O*-acetal **32** underwent photoinduced isomerization to vinylic *N,O*-acetal **35** when using the same setup (Scheme 4.10). The reaction was complete after 4 h of irradiation with a wavelength of 300 nm yielding product **35** as a mixture of isomers with a nearly equimolar *Z*/*E*-ratio and in 94% yield.

Scheme 4.10 *Photoinduced Isomerization of Diene 32.*

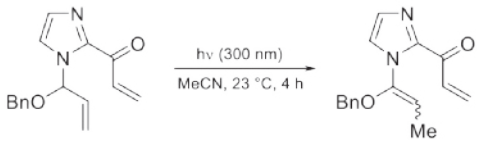

32 **35**

94%, *Z*/*E* 57:43

Despite the fact that [2+2] photocycloadditions of **27** and **32** were unsuccessful, these results accumulated the required knowledge for future investigations and establishing new collaborations.

4.2.4 Investigation of Pauson–Khand and Click Chemistry of Enyne 36

Enynes of type **14** may serve as suitable precursors for Pauson–Khand (PK) reactions and azide–alkyne 1,3-dipolar cycloadditions. Because propargylic alcohols tend to undergo isomerization to the corresponding α,β-unsaturated ketones in the presence of Lewis acids (including transition metals),[19] we decided first to protect the hydroxy group of enyne **28** as

acetate in a similar way as for diene **27**. The protection was achieved using an excess of acetic anhydride in pyridine at 23 °C yielding enyne **36** as a 55:45 mixture of diastereoisomers in 78% yield (Scheme 4.11).

Scheme 4.11 *Protection of Enyne **28** and Attempts of Pauson–Khand Reaction.*

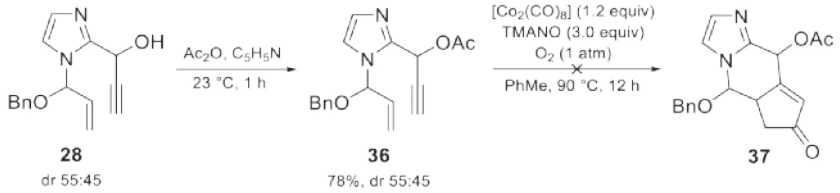

28
dr 55:45

36
78%, dr 55:45

37

We then submitted compound **36** to the most common reaction conditions to study the viability of the PK reaction for this type of substrates. First, it was stirred with $[Co_2(CO)_8]$ in toluene at 23 °C for 2 h and then the formed complex was treated with an excess of trimethylamine *N*-oxide (TMANO) under an oxygen atmosphere followed by heating at 90 °C. However, we did not observe the formation of the desired tricyclic product **37**. Conversely, decomposition of the starting material was observed leading to formation of unidentified side products.

Despite our first unsuccessful attempt, we further decided to screen different catalytic systems for the PK reaction (Table 4.6). In this regard, $[CpCo(CO)_2]$ drew our attention because it is a common catalyst used for a large variety of cycloadditions and cyclotrimerizations of alkynes.[20] Nonetheless, the reaction of enyne **36** with of $[CpCo(CO)_2]$ (0.6 equiv) in refluxing toluene under a CO atmosphere resulted only in decomposition of the starting material (entry 1).

Table 4.6 *Screening of the Catalyst for the PK reaction of Enyne **36**.*

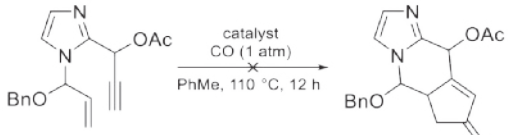

36
dr 55:45

37

Entry	Catalyst (equiv)	Additive (equiv)	Yield (%)
1	$[CpCo(CO)_2]$ (0.6)	–	decomposition
2	$[Rh(CO)_2Cl]_2$ (0.03)/(*R*)-BINAP (0.06)	AgOTf (0.06)	decomposition
3	$[Ir(cod)Cl]_2$ (0.1)/(*R*)-BINAP (0.2)	–	decomposition

In our quest for success of the reaction we thought of using complexes of other late transition metals, such as rhodium[21] or iridium,[22] which were proven to be effective in the PKR reaction. The corresponding active catalysts were prepared by premixing $[Rh(CO)_2Cl]_2$/AgOTf or $[Ir(cod)Cl]_2$ complexes with (*R*)-BINAP in toluene at 23 °C. After 30 min, substrate **36** was added to the reaction mixture and heated to refluxing toluene under a CO atmosphere (entries 2 and 3). However, no product formation was observed and additionally partial decomposition of the starting material was detected.

Furthermore, a preliminary study to examine the feasibility of the azide–alkyne cycloaddition was performed with propargylic acetate **36** and tosyl azide in the presence of various copper(I) catalysts, additives, solvents and temperatures (Table 4.7). An initial experiment was conducted with tosyl azide (1.1 equiv) and CuI (0.2 equiv) in acetonitrile at 23 °C. An overnight experiment (12 h) indicated that no reaction occurred and the starting material was fully recovered after filtration through a diatomaceous-earth pad (entry 1). We tried adding sodium ascorbate or 2-aminophenol to the reaction system to promote the "click reaction" (entries 2–4).[23] However, enyne **36** lacked the anticipated reactivity, even when heating the reaction mixture at 80 °C. Utilizing other copper catalysts like $[Cu(OTf)_2 \cdot PhH]$ or copper(I) thiophene-2-carboxylate [Cu(Tc)] had no influence on the reaction. In either case starting materials were fully or partially recovered with no indication of triazole formation.

Table 4.7 *Screening of the Reaction Conditions for the Azide–Alkyne Cycloaddition.*

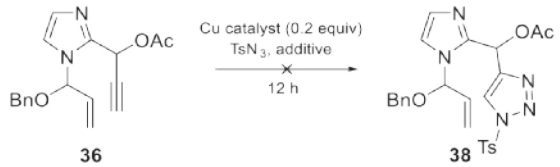

36
dr 55:45

38

Entry	Cu Catalyst	Additive	Solvent	*t* (°C)	Yield (%)
1	CuI	–	MeCN	24	–
2	$Cu(OAc)_2 \cdot H_2O$	sodium ascorbate	$^tBuOH/H_2O$ (2:1)	6	–
3	$Cu(OAc)_2 \cdot H_2O$	sodium ascorbate	$^tBuOH/H_2O$ (2:1)	24	–
4	$Cu(OAc)_2 \cdot H_2O$	2-aminophenol	MeCN	6	–
5	$[Cu(OTf)_2 \cdot PhH]$	–	PhH	24	–
6	[Cu(TC)]	–	PhH	24	–

4.2.5 Fluorination of Diene 27 and Enyne 28

Our final attempts to derivatize diene **27** and enyne **28** were focused on the nucleophilic fluorination with *N*,*N*-diethylaminosulfur trifluoride (DAST). We were pleased to find that all of the starting material **27** or **28** had disappeared after 6 h with 1.2 equiv of DAST at –30 °C in CH_2Cl_2 (Scheme 4.12). However, the outcome of the reaction was highly dependent on the substrate. Thus, fluorination of diene **27** proceeded through nucleophilic attack of the hydroxyl group on the sulfur atom of DAST to form intermediate **39**.[24] This unstable intermediate underwent further evolution to cationic species **40** and released fluoride, which then attacked at the allylic position and forming allyl fluoride **41** as a single *trans*-isomer. Compound **41** was the only observed product and obtained in 77% yield after purification. Conversely, fluorination of propargyl alcohol **28** proceeded at the saturated carbon in **43** leading to propargyl fluoride **44** as a 55:45 mixture of diastereoisomers in 83% yield after purification by column chromatography. The notable difference in reactivity for both substrates can be probably explained by the fact that allyl moiety in **40** is sterically more hindered compared to the propargyl moiety in **43**, making the nucleophilic substitution at the saturated carbon less favorable. Both compounds represent valuable lead structures for the screening of their biological activity.[25] Further studies on the mechanism of the fluorination reaction, as well as on the application of this methodology in target-orientated synthesis, are currently in progress in our laboratory.

Scheme 4.12 *Fluorination of Allylic Alcohol* ***27*** *and* ***28*** *with DAST Reagent.*

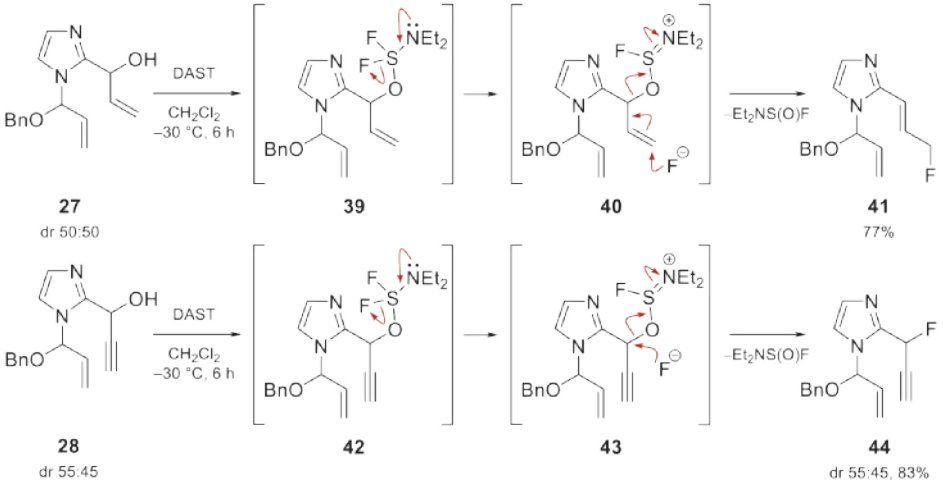

4.3 Conclusion

In summary, we have developed a general method for the synthesis of diene **27** and enyne **28** and derivatives in high yields starting from heteroaromatic allylic *N,O*-acetal **8**. Furthermore, attempts were made to establish approaches for the functionalization of these precursors based on ring-closing metathesis, [2+2] photocycloaddition, the Pauson–Khand reaction and azide-alkyne cycloaddition. Thus far, these investigations posed a significant challenge and were left for future studies. Finally, fluorination of diene and enyne derivatives with *N,N*-diethylaminosulfur trifluoride was examined. Thus, the reaction of diene **27** proceded by allylic rearrangement with fluoride attack at the alkene terminus. Conversely, fluorination of enyne **28** led exclusively to nucleophilic substitution at the sp^3 carbon of the propargyl group.

4.4 Acknowledgments

Dr. Dennis W. P. M. Löwik (Radboud University) is gratefully acknowledged for providing the practical knowledge necessary for recording the UV-vis absorption spectra.

4.5 Experimental Section

For general experimental details and the procedures for the preparation of the allylic *N,O*-acetals **8** and **15** see Section 3.5. Tosyl azide was prepared according to a literature procedure.[26] The [2+2] photocycloaddition was carried out in a Rayonet RMR-600 photochemical reactor, using eight RMR-2537Å (254 nm wavelength) or RMR-3000Å (300 nm wavelength) lamps. UV-vis absorption spectra were recorded on Varian Cary 50 UV-vis spectrophotometer.

Functionalization of Allylic *N,O*-Acetal 8 by a Deprotonation/Alkylation Approach

General procedure A: A solution of ^{n}BuLi (1.6 M in THF, 1.2 equiv) was added dropwise to solution of *N,O*-acetal **8** (0.1 M in THF, 1.0 equiv) in THF (5 mL) at –78 °C and stirred at the same temperature for 1 h. A solution of allyl halide (1.0 M in THF, 1.5 equiv) was added dropwise to the reaction mixture. The reaction mixture was further stirred at –78 °C for 1 h and then at 23 °C for 6 h. The reaction was quenched by addition of a saturated NH_4Cl solution (15 mL) while stirring at 23 °C for 15 min. The organic layer was dried over anhydrous $MgSO_4$, concentrated under reduced pressure, and the residue was analyzed with ^{1}H NMR.

General procedure B: Preparation of [TMPZnCl·LiCl]:[13b] A dry and argon-flushed 100 mL Schlenk flask, equipped with a magnetic stirring bar and a rubber septum was charged with

freshly distilled 2,2,6,6-tetramethylpiperidine (2.7 mL, 6 mmol, 1.0 equiv) dissolved in THF (20 mL). This solution was cooled to –40 °C and ^{n}BuLi (1.6 M in hexane, 10 mL, 16 mmol, 2.7 equiv) was added dropwise. After the addition was complete, the reaction mixture was allowed to warm slowly to –10 °C for 1 h. $ZnCl_2$ (1.0 M in THF, 17.6 mL, 17.6 mmol, 2.9 equiv) was added dropwise and the resulting solution was stirred at –10 °C for 30 min and then at 25 °C for 30 min. The solvents were then removed under vacuum affording a yellowish solid. Freshly distilled THF (16 mL) was then slowly added under vigorous stirring until the salts were completely dissolved affording 1 M solution of [TMPZnCl·LiCl] in THF.

Alkylation with allyl halide: A solution of [TMPZnCl·LiCl] (1.0 M in THF, 1.2 equiv) was added dropwise to a solution of *N,O*-acetal **8** (0.1 M in THF, 1.0 equiv) in THF (5 mL) at 0 °C and stirred at the same temperature for 1 h. A solution of allyl halide (1.0 M in THF, 1.5 equiv) was added dropwise to the reaction mixture. The reaction mixture was further stirred at 0 °C for 1 h and then at 23 °C for 24 h. The reaction was quenched by addition of a saturated NH_4Cl solution (15 mL) while stirring at 23 °C for 15 min. The organic layer was dried over anhydrous $MgSO_4$, concentrated under reduced pressure, and the residue was analyzed with ^{1}H NMR.

General procedure C:[13b] A solution of [TMPZnCl·LiCl] (1.0 M in THF, 1.2 equiv) was added dropwise to a solution of *N,O*-acetal **8** (0.1 M in THF, 1.0 equiv) in THF (5 mL) at 0 °C and stirred at that temperature for 1 h. The mixture was then cooled to –30 °C and [CuCN·2LiCl] (1 M solution in THF, 1.2 equiv) or $Pd(OAc)_2$ (0.05 equiv) was added. After 0.5 h of stirring at the same temperature, a solution of allyl halide (1.0 M in THF, 1.5 equiv) was added and the reaction mixture was stirred at –30 °C for 1 h and then at 23 °C for 24 h.

General procedure D: A solution of [^{i}PrMgCl·LiCl] (1 M in THF, 1.2 equiv) was added dropwise to a solution of *N,O*-acetal **8** (0.1 M in THF, 1.0 equiv) in THF (5 mL) at –30 °C and stirred at the same temperature for 1 h. A solution of allyl halide (1.0 M in THF, 1.5 equiv) was added dropwise to the reaction mixture. The reaction mixture was further stirred at –30 °C for 1 h and then at 23 °C for 6 h. The reaction was quenched by addition of saturated NH_4Cl solution (15 mL) while stirring at 23 °C for 15 min. The organic layer was dried over anhydrous $MgSO_4$, concentrated under reduced pressure, and the residue was analyzed with ^{1}H NMR.

Synthesis of Diene 27

***rac*-(*R*)-1-{1-[(*R*)-1-(Benzyloxy)allyl]-1*H*-imidazol-2-yl}prop-2-en-1-ol 27aa and *rac*-(*R*)-1-{1-[(*S*)-1-(benzyloxy)allyl]-1*H*-imidazol-2-yl}prop-2-en-1-ol 27ab.**

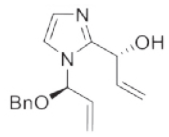

(±)-**27aa**

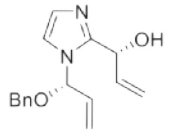

(±)-**27ab**

Vinylmagnesium bromide (1.0 M in THF, 5 mL, 5.0 mmol, 1.2 equiv) was added to a solution of allylic *N*,*O*-acetal **15** (1.0 g, 4.2 mmol, 1.0 equiv) in THF (100 mL) at 0 °C. The reaction was allowed to warm to 23 °C after 15 min and stirred for additional 3 h. The reaction mixture was quenched by addition of 0.1 M aqueous solution of HCl (200 mL) and extracted with Et_2O (3 × 50 mL). The organic phase was washed with brine, dried over $MgSO_4$, filtered and concentrated under reduced pressure. The crude material was purified by flash chromatography on silica gel (heptane/AcOEt 20:1→0:1) to afford a 1.9:1 mixture of diastereoisomers of product **27** as a light yellow oil (817 mg, 72%). R_F (silica gel, heptane/AcOEt 1:1): 0.09–0.34 (UV, $KMnO_4$ solution). The signals of the main isomer are indicated with an asterisk (*). **^{1}H NMR** [400 MHz, δ (ppm), $CDCl_3$]: 4.41 (d, J = 11.9 Hz, 1 H)*, 4.43 (d, J = 11.8 Hz, 1 H), 4.48 (d, J = 11.7 Hz, 1 H), 4.49 (d, J = 11.7 Hz, 1 H), 5.21–5.42 (m, 10 H)*, 6.09 (ddd, J = 17.1, 10.3, 4.6 Hz, 2 H)*, 6.14 (ddd, J = 17.2, 10.4, 5.3 Hz, 2 H)*, 6.35 (dt, J = 4.3, 1.5 Hz, 2 H)*, 6.82 (d, J = 1.3 Hz, 2 H)*, 7.06 (d, J = 1.4 Hz, 2 H)*, 7.26–7.39 (m, 10 H)*. **^{13}C NMR** [101 MHz, δ (ppm), $CDCl_3$]: 68.1, 68.2, 70.2, 70.3, 83.6, 83.7, 115.6, 117.6, 118.4, 118.5, 127.1, 127.72, 127.74, 127.87, 127.89, 128.0, 128.1, 128.4, 128.5, 134.6, 134.8, 134.9, 137.1, 137.8, 137.9, 148.6, 148.7. **FTIR** [$\tilde{\nu}$ (cm^{-1})]: 712, 734, 841, 1061, 1220, 1491, 2869, 3036, 3370. **HRMS** (ESI$^+$) calcd. for $(C_{16}H_{18}N_2O_2 + H)^+$ 271.1447, found 271.1441. By comparing the signal intensity of the benzylic protons a diastereomeric ratio of 65:35 was calculated. The diastereoisomers were not separated from each other.

Acetate Protection of Diene 27

***rac*-(*R*)-1-{1-[(*R*)-1-(Benzyloxy)allyl]-1*H*-imidazol-2-yl}allyl acetate 30aa and *rac*-(*R*)-1-{1-[(*S*)-1-(benzyloxy)allyl]-1*H*-imidazol-2-yl}allyl acetate 30ab.**

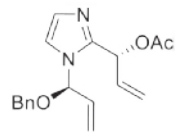

(±)-**30aa**

Acetic anhydride (0.16 mL, 1.65 mmol, 1.5 equiv) was added dropwise to a solution of diene **27** (300 mg, 1.1 mmol, 1.0 equiv) in pyridine (30 mL) which was cooled before to 0 °C. The reaction mixture was further stirred at 0 °C for 1 h and then at 23 °C for 1 h. The reaction was quenched by addition of saturated NH_4Cl solution (30 mL) and extracted with Et_2O

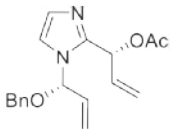

(±)-**30ab**

(3 × 10mL). The organic layer was dried over anhydrous $MgSO_4$ and concentrated under reduced pressure. The crude material was purified by flash chromatography on silica gel (heptane/AcOEt 20:1→4:1) to afford a 1:1 mixture of diastereoisomers of product **30** as a light yellow oil (326 mg, 95%). R_F (silica gel, heptane/ AcOEt 1:1): 0.21–0.42 (UV, $KMnO_4$ solution). **^{1}H NMR** [400 MHz, δ (ppm), $CDCl_3$]: 2.06 (s, 3 H), 2.11 (s, 3 H), 4.47 (s, 2 H), 4.52 (s, 2 H), 5.23–5.27 (m, 2 H), 5.31–5.34 (m, 2 H), 5.35–5.40 (m, 6 H), 5.92 (ddd, J = 17.6, 10.2, 4.2 Hz, 1 H), 5.96 (ddd, J = 17.6, 10.2, 4.3 Hz, 1 H), 6.07–6.16 (m, 1 H), 6.17–6.25 (m, 1 H), 7.01 (d, J = 1.3 Hz, 1 H), 7.03 (d, J = 1.3 Hz, 1 H), 7.10 (d, J = 1.4 Hz, 1 H), 7.13 (d, J = 1.4 Hz, 1 H), 7.27–7.37 (m, 10 H). **^{13}C NMR** [101 MHz, δ (ppm), $CDCl_3$]: 21.5, 22.1, 67.7, 68.2, 70.3, 70.6, 83.0, 83.9, 116.5, 117.7, 118.21, 118.23, 119.0, 119.3, 126.6, 127.9, 128.15, 128.19, 128.5, 128.65, 128.68, 128.8, 128.9, 134.1, 134.5, 136.5, 136.6, 137.1, 147.2, 148.4, 176.1, 176.3. **FTIR** [$\tilde{\nu}$ (cm^{-1})]: 756, 768, 913, 1063, 1211, 1497, 1743, 2830, 2869, 3016. **HRMS** (ESI^+) calcd. for $(C_{18}H_{20}N_2O_3 + H)^+$ 313.1552, found 313.1573. By comparing the signal intensity of the benzylic protons a diastereomeric ratio of 50:50 was calculated. The diastereoisomers were not separated from each other.

Synthesis of Enyne 28

***rac*-(*R*)-1-{1-[(*R*)-1-(Benzyloxy)allyl]-1*H*-imidazol-2-yl}prop-2-yn-1-ol 28aa and *rac*-(*R*)-1-{1-[(*S*)- 1-(benzyloxy)allyl]-1*H*-imidazol-2-yl}prop-2-yn-1-ol 28ab.**

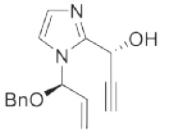

(±)-**28aa**

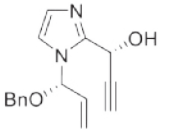

(±)-**28ab**

Ethynylmagnesium bromide (0.5 M in THF, 10 mL, 5.0 mmol, 1.2 equiv) was added to a solution of allylic *N*,*O*-acetal **15** (1.0 g, 4.2 mmol, 1.0 equiv) in THF (100 mL) which was cooled before to 0 °C. After 15 min, the reaction was allowed to warm to 23 °C and stirred for additional 6 h. The reaction mixture was quenched by addition of 0.1 M aqueous solution of HCl (200 mL) and extracted with Et_2O (3 × 50mL). The organic phase was washed with brine, dried over $MgSO_4$, filtered and concentrated under reduced pressure. The crude material was purified by flash chromatography on silica gel (heptane/AcOEt 40:1→1:1) to afford a 1.2:1 mixture of diastereoisomers of enyne **26** as a light yellow oil (856 mg, 76%). R_F (silica gel, heptane/AcOEt 1:1): 0.11–0.29 (UV, $KMnO_4$ solution). The signals of the main isomer are indicated with an asterisk (*). **^{1}H NMR** [400 MHz, δ (ppm), $CDCl_3$]: 2.55 (d, J = 2.4, Hz, 1 H)*, 2.61 (d, J = 2.4, Hz, 1 H), 4.44 (d, J = 11.6 Hz, 1 H), 4.52 (d, J = 11.6 Hz, 1 H)*, 4.58 (d, J = 11.6 Hz, 1 H)*,

4.59 (d, *J* = 11.6 Hz, 1 H), 5.34 (ddd, *J* = 10.5, 1.3, 0.9 Hz, 1 H)*, 5.35 (ddd, *J* = 10.6, 1.1, 0.8 Hz, 1 H), 5.41 (ddd, *J* = 17.2, 1.3, 0.8 Hz, 1 H)*, 5.42 (ddd, *J* = 17.2, 1.1, 0.8 Hz, 1 H), 5.66 (d, *J* = 2.4 Hz, 1 H)*, 5.67 (d, *J* = 2.4 Hz, 1 H), 6.02 (ddd, *J* = 17.2, 10.5, 4.3 Hz, 1 H), 6.03 (ddd, *J* = 17.2, 10.5, 4.2 Hz, 1 H)*, 6.37 (dt, *J* = 4.3, 1.4 Hz, 1 H)*, 6.45 (dt, *J* = 4.2, 1.5 Hz, 1 H), 6.88 (d, *J* = 1.3 Hz, 1 H), 6.91 (d, *J* = 1.3 Hz, 1 H)*, 7.04 (d, *J* = 1.4 Hz, 1 H), 7.08 (d, *J* = 1.4 Hz, 1 H)*, 7.26–7.39 (m, 10 H)*. **^{13}C NMR** [101 MHz, δ (ppm), $CDCl_3$]: 57.59, 57.64, 70.4, 70.5, 75.0, 75.3, 81.2, 81.4, 84.1, 84.3, 118.2, 118.3, 118.7, 118.8, 127.5, 127.6, 127.8, 128.0, 128.06, 128.11, 128.5, 128.6, 134.1, 134.4, 136.7, 136.8, 145.8, 146.1. **FTIR** [$\tilde{\nu}$ (cm^{-1})]: 682, 731, 841, 1112, 1301, 1454, 2172, 2917, 3106, 3320. **HRMS** (ESI^+) calcd. for ($C_{16}H_{16}N_2O_2$ + H)$^+$ 269.1290, found 269.1279. By comparing the signal intensity of the propargylic protons a diastereomeric ratio of 55:45 was calculated. The diastereoisomers were not separated from each other.

Acetate Protection of Enyne 28

***rac*-(*R*)-1-{1-[(*R*)-1-(Benzyloxy)allyl]-1*H*-imidazol-2-yl}prop-2-yn-1-yl acetate 36aa and *rac*-(*R*)-1-{1-[(*S*)-1-(benzyloxy)allyl]-1*H*-imidazol-2-yl}prop-2-yn-1-yl acetate 36ab.**

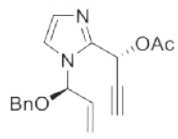

(±)-**36aa**

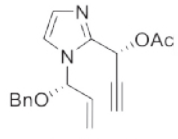

(±)-**36ab**

Acetic anhydride (81 µL, 0.84 mmol, 1.5 equiv) was added dropwise at 0 °C to a solution of enyne **28** (150 mg, 0.56 mmol, 1.0 equiv) in pyridine (15 mL) which was cooled before to 0 °C. The reaction mixture was further stirred at 0 °C for 1 h and then at 23 °C for 1 h. The reaction was quenched by addition of a saturated NH_4Cl solution (15 mL) and extracted with Et_2O (3 × 10mL). The organic layer was dried over anhydrous $MgSO_4$ and concentrated under reduced pressure. The crude material was purified by flash chromatography on silica gel (heptane/ AcOEt 20:1→4:1) to afford a 1.2:1 mixture of diastereoisomers of acetate **36** as a light yellow oil (132 mg, 76%). The signals of the main isomer are indicated with an asterisk (*). R_F (silica gel, heptane/AcOEt 1:1): 0.22–0.37 (UV, $KMnO_4$ solution). **^{1}H NMR** [400 MHz, δ (ppm), $CDCl_3$]: 2.11 (s, 3 H)*, 2.13 (s, 3 H), 2.39 (d, *J* = 2.1 Hz, 1 H)*, 2.41(d, *J* = 2.1 Hz, 1 H), 4.42 (d, *J* = 11.5 Hz, 1 H), 4.48 (d, *J* = 11.5 Hz, 1 H)*, 4.55 (d, *J* = 11.5 Hz, 1 H)*, 4.57 (d, *J* = 11.5 Hz, 1 H), 5.25 (ddd, *J* = 10.6, 1.3, 0.8 Hz, 1 H)*, 5.32 (ddd, *J* = 10.6, 1.3, 0.8 Hz, 1 H), 5.33 (ddd, *J* = 17.2, 1.3, 0.8 Hz, 1 H)*, 5.37 (ddd, *J* = 17.2, 1.3, 0.8 Hz, 1 H), 5.79 (d, *J* = 2.4 Hz, 1 H)*, 5.81 (d, *J* = 2.4 Hz, 1 H), 6.11 (ddd, *J* = 17.2, 10.6, 4.1 Hz, 1 H), 6.13 (ddd, *J* = 17.2, 10.5, 4.2 Hz, 1 H)*, 6.35 (dt, *J* = 4.1, 1.3 Hz, 1 H)*, 6.46 (dt, *J* = 4.1, 1.5 Hz, 1 H), 6.91 (d, *J* = 1.3

Hz, 1 H), 6.93 (d, *J* = 1.3 Hz, 1 H)*, 7.03 (d, *J* = 1.4 Hz, 1 H), 7.10 (d, *J* = 1.4 Hz, 1 H)*, 7.27–7.42 (m, 10 H)*. **^{13}C NMR** [101 MHz, δ (ppm), $CDCl_3$]: 21.1, 21.3, 65.1, 65.2, 75.2, 75.4, 80.4, 80.5, 113.1, 117.1, 117.3, 118.2, 118.3, 119.20, 119.23, 125.3, 128.21, 128.23, 128.7, 128.8, 129.2, 134.1, 134.3, 137.1, 137.3, 138.0, 143.9, 144.1, 169.8, 170.2. **FTIR** [$\tilde{\nu}$ (cm^{-1})]: 692, 814, 903, 1144, 1223, 1427, 1762, 2842, 3126. **HRMS** (ESI^+) calcd. for ($C_{18}H_{18}N_2O_3$ + $H)^+$ 311.1396, found 311.1381. By comparing the signal intensity of the propargylic protons a diastereomeric ratio of 55:45 was calculated. The diastereoisomers were not separated from each other.

Synthesis of Enyne 32

1-{1-[1-(Benzyloxy)allyl]-1*H*-imidazol-2-yl}prop-2-en-1-one 32.

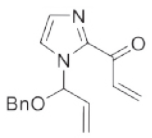

32

Dess–Martin periodinane (63 mg, 0.15 mmol, 1.2 equiv) was added portionwise to a solution of **27** (30 mg, 0.12 mmol, 1.0 equiv) in dry CH_2Cl_2 (2 mL) which was cooled before to 0 °C. The reaction was allowed to warm to 23 °C after 15 min and stirred for an additional 1 h. The reaction was quenched by addition of a saturated NH_4Cl solution (15 mL) while stirring at 23 °C for 15 min. The organic layer was dried over anhydrous $MgSO_4$ and concentrated under reduced pressure. The crude material was purified by flash chromatography on silica gel (heptane/AcOEt 20:1→4:1) to afford product **32** as a light yellow oil (28.0 mg, 88%). R_F (silica gel, heptane/AcOEt 1:1): 0.52 (UV, $KMnO_4$ solution). **^{1}H NMR** [400 MHz, δ (ppm), $CDCl_3$]: 4.49 (d, *J* = 11.5 Hz, 1 H), 4.55 (d, *J* = 11.5 Hz, 1 H), 5.32 (ddd, *J* = 10.5, 1.4, 1.0 Hz, 1 H), 5.39 (ddd, *J* = 17.1, 1.4, 1.0 Hz, 1 H), 5.90 (dd, *J* = 10.4, 1.8 Hz, 1 H), 6.00 (ddd, *J* = 17.1, 10.5, 4.4 Hz, 1 H), 6.53 (dd, *J* = 17.4, 1.8 Hz, 1 H), 7.17 (dt, *J* = 4.4, 1.4 Hz, 1 H), 7.25–7.37 (m, 6 H), 7.46 (d, *J* = 1.1 Hz, 1 H), 7.70 (dd, *J* = 17.4, 10.4 Hz, 1 H). **^{13}C NMR** [101 MHz, δ (ppm), $CDCl_3$]: 71.1, 85.6, 118.5, 122.4, 127.8, 128.1, 128.5, 129.4, 130.5, 132.8, 134.5, 136.4, 143.3, 180.8. **FTIR** [$\tilde{\nu}$ (cm^{-1})]: 688, 721, 809, 1084, 1201, 1500, 1721, 2842, 3015. **HRMS** (ESI^+) calcd. for ($C_{16}H_{16}N_2O_2$ + $H)^+$ 269.1290, found 269.1278.

Ring-Closing Metathesis of Dienes 27, 30 and 32

General procedure: Diene **27**, **30** or **32** (0.05 mmol, 1.0 equiv) and Grubbs catalyst **G1**, **G2** or **G3** (2.5 μmol, 0.05 equiv) were dissolved in a dry solvent (5 mL) and stirred at 23 °C or heated at 70 °C for 6–24 h under a nitrogen atmosphere. If stated, an additive (0.5 μmol, 0.1 equiv) was added. After cooling the reaction mixture to 23 °C, the mixture was filtered, the solvent was removed in vacuo, and the crude was purified by column chromatography (heptane/AcOEt 40:1→2:1).

[2+2] Photocycloaddition of Dienes 27 and 32

General procedure: A solution of **27** or **32** (0.1 mmol, 1.0 equiv) in 10 mL of deoxygenated MeCN in a 25 mL quartz flask was stirred and irradiated in a Rayonet RMR-600 photochemical reactor (using eight lamps of 254 or 300 nm of wavelength) for 4–20 h. If stated, [$(CuOTf)_2$·PhH] (0.01 mmol, 0.1 equiv) was added. After cooling to 23 °C, the solvent was removed in vacuo and the crude residue was purified by column chromatography as indicated.

(*Z*)-1-{1-[1-(Benzyloxy)prop-1-en-1-yl]-1*H*-imidazol-2-yl}prop-2-en-1-one 35a and (*E*)-1-{1-[1-(benzyloxy)prop-1-en-1-yl]-1*H*-imidazol-2-yl}prop-2-en-1-one 35b.

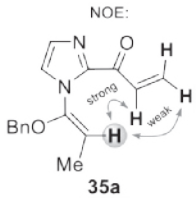

35a

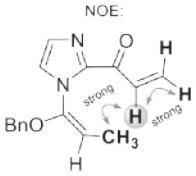

35b

Enyne **32** (27.0 mg, 0.1 mmol) was irradiated at 300 nm for 4 h according to the general procedure and then concentrated to leave an orange gum. The crude material was purified by flash chromatography on silica gel (heptane/AcOEt 10:1→1:1) to afford a 1.3:1 mixture of stereoisomers of the product **35** as a light yellow oil (25 mg, 94%). R_F (silica gel, heptane/AcOEt 1:1): 0.56 (UV, $KMnO_4$ solution). The signals of main isomer are indicated with an asterisk (*). **^{1}H NMR** [400 MHz, δ (ppm), $CDCl_3$]: 1.33 (d, *J* = 6.8 Hz, 3 H), 1.69 (d, *J* = 6.9 Hz, 3 H)*, 4.54 (s, 2 H)*, 4.78–4.83 (m, 2 H)*, 4.90 (s, 2 H), 5.82 (d, *J* = 10.5 Hz, 2 H), 6.48 (d, *J* = 17.4 Hz, 2 H), 6.97 (d, *J* = 0.9 Hz, 1 H)*, 7.06 (d, *J* = 0.9 Hz, 1 H), 7.12 (d, *J* = 0.9 Hz, 1 H), 7.17 (d, *J* = 0.9 Hz, 1 H)*, 7.18–7.31 (m, 10 H), 7.51 (dd, *J* = 17.4, 10.5 Hz, 1 H)*, 7.54 (dd, *J* = 17.3, 10.6 Hz, 1 H). **^{13}C NMR** [101 MHz, δ (ppm), $CDCl_3$]: 9.6, 10.0, 70.5, 70.6, 93.0, 104.0, 109.0, 124.9, 126.0, 126.9, 127.0, 127.19, 127.21, 127.4, 127.5, 128.3, 128.5, 128.66, 128.68, 131.2, 131.3, 135.0, 135.2, 142.5, 142.9, 145.2, 177.9, 178.1. **FTIR** [$\bar{\nu}$ (cm^{-1})]: 701, 744, 812, 1113, 1251, 1482, 1704, 2823, 3078. **HRMS** (ESI^+) calcd. for $(C_{16}H_{16}N_2O_2 + H)^+$ 269.1290, found 269.1282. By comparing the signal intensity of the benzylic protons a ratio of *Z*/*E* stereoisomers 57:43 was calculated. The stereoisomers were not separated from each other.

Pauson–Khand Reaction of Enyne 36

General procedure A: Enyne **36** (31.0 mg, 0.1 mmol, 1.0 equiv) was dissolved in 10 mL of dry toluene at 23 °C under a nitrogen atmosphere. Complex $[Co_2(CO)_8]$ (41.0 mg, 0.12 mmol, 1.2 equiv) was added to this solution and the resulting mixture was stirred for 2 h until complete conversion to the alkyne–cobalt complex. The reaction was then cooled to 0 °C and a suspension

of TMANO (22.5 mg, 0.3 mmol, 3.0 equiv) in 5 mL of dry toluene was added dropwise. Stirring was continued at 90 °C for 12 h under an oxygen atmosphere (balloon). After cooling to 23 °C, the mixture was filtered, the solvent was removed in vacuo, and the crude was purified by column chromatography (heptane/AcOEt 10:1→1:2).

General procedure B: Enyne **36** (31.0 mg, 0.1 mmol, 1.0 equiv) was dissolved in 10 mL of dry toluene at 23 °C under a nitrogen atmosphere. The metal complex ($[CpCo(CO)_2]$, $[Rh(CO)_2Cl]_2$, AgOTf or $[Ir(cod)Cl]_2$, (0.03–0.60 equiv), and (*R*)-BINAP (0.06–0.20 equiv) were added to this solution and the resulting mixture was submitted to three vacuum–N_2 cycles and three vacuum–CO cycles. The reaction was carried out at 110 °C for 12 h, under a CO atmosphere (balloon). After cooling to 23 °C, the mixture was filtered, the solvent was removed in vacuo, and the crude was purified by column chromatography (heptane/AcOEt 10:1→1:2).

Intramolecular Azide–Alkyne Cycloaddition of Enyne 36

General procedure: Enyne **36** (31.0 mg, 0.1 mmol, 1.0 equiv) and tosyl azide (21.7 mg, 0.11 mmol, 1.1 equiv) were dissolved in a dry solvent (10 mL) and the resulting mixture was stirred at 23 °C or heated at 80 °C for 12 h under a nitrogen atmosphere. If stated, additive (0.04 mmol, 0.4 equiv) was added. After cooling to 23 °C, the mixture was filtered, the solvent was removed in vacuo, and the crude was purified by column chromatography (heptane/AcOEt 20:1→1:1).

Fluorination of Diene 27 and Enyne 28 with DAST

General procedure: A solution of DAST (16 µL, 0.12 mmol, 1.2 equiv) in CH_2Cl_2 (5 mL) was added dropwise at −78 °C to a solution of **27** or **28** (0.1 mmol, 1.0 equiv) in dry CH_2Cl_2 (10 mL). After 15 min, the reaction was allowed to warm to −30 °C and stirred for additional 6 h. The reaction was quenched by addition of a saturated NH_4Cl solution (20 mL) while stirring at 23 °C for 15 min. The organic layer was dried over anhydrous $MgSO_4$, the solvent was removed in vacuo, and the crude residue was purified by column chromatography as indicated.

(*E*)-1-[1-(Benzyloxy)allyl]-2-(3-fluoroprop-1-en-1-yl)-1*H*-imidazole 41.

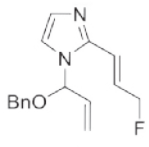

41

Diene **27** (27 mg, 0.1 mmol, 1.0 equiv) was treated with DAST according to the general procedure. The crude material was purified by flash chromatography on silica gel (heptane/AcOEt 20:1→2:1) to afford product **41** as a light yellow oil (21 mg, 77%). R_F (silica gel, heptane/AcOEt 1:1): 0.34 (UV, $KMnO_4$ solution). **^{1}H NMR** [400 MHz, δ (ppm), $CDCl_3$]: 4.33

(d, *J* = 11.9 Hz, 1 H), 4.54 (d, *J* = 11.9 Hz, 1 H), 5.02 (ddd, *J* = 46.4, 5.0, 1.7 Hz, 2 H), 5.33 (ddd, *J* = 17.1, 1.6, 0.7 Hz, 1 H), 5.37 (ddd, *J* = 10.6, 1.5, 0.7 Hz, 1 H), 5.78 (dt, *J* = 4.0, 1.4 Hz, 1 H), 6.00 (ddd, *J* = 17.2, 10.6, 4.0 Hz, 1 H), 6.53 (ddt, *J* = 15.6, 12.0, 5.0 Hz, 1 H), 6.80 (dd, *J* = 15.6, 5.0 Hz, 1 H), 7.04 (d, *J* = 1.1 Hz, 1 H), 7.12 (d, *J* = 1.1 Hz, 1 H), 7.28–7.37 (m, 5 H). **^{13}C NMR** [101 MHz, δ (ppm), $CDCl_3$]: 69.9, 82.5 (d, *J* = 166.8 Hz), 83.5, 118.3, 119.0, 127.1 (d, *J* = 2.1 Hz), 128.1, 128.4, 128.7, 129.4, 134.5 (d, *J* = 12.2 Hz), 136.1, 141.1, 144.2. **^{19}F NMR** [377 MHz, δ (ppm), $CDCl_3$]: –211.0 (tdd, *J* = 46.4, 12.0, 5.0 Hz). **FTIR** [$\tilde{\nu}$ (cm^{-1})]: 721, 827, 1032, 1103, 1261, 1486, 2914, 3098. **HRMS** (ESI^+) calcd. for $(C_{16}H_{17}FN_2O + H)^+$ 273.1403, found 273.1418.

***rac*-1-[(*R*)-1-(Benzyloxy)allyl]-2-[(*R*)-1-fluoroprop-2-yn-1-yl]-1*H*-imidazole 44aa and *rac*-1-[(*S*)-1-(benzyloxy)allyl]-2-[(*R*)-1-fluoroprop-2-yn-1-yl]-1*H*-imidazole 44ab.**

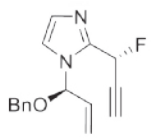

(±)-**44aa**

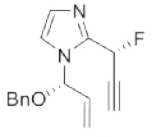

(±)-**44ab**

Enyne **28** (27 mg, 0.1 mmol, 1.0 equiv) was treated with DAST according to the general procedure. The crude material was purified by flash chromatography on silica gel (heptane/AcOEt 20:1→2:1) to afford a 1.2:1 mixture of diastereoisomers of product **44** as a light yellow oil (22.0 mg, 83%). R_F (silica gel, heptane/AcOEt 1:1): 0.25–0.41 (UV, $KMnO_4$ solution). The signals of main isomer are indicated with an asterisk (*). **^{1}H NMR** [400 MHz, δ (ppm), $CDCl_3$]: 2.87 (dd, *J* = 5.2, 2.4 Hz 1 H), 2.95 (dd, *J* = 5.2, 2.4 Hz, 1 H)*, 4.42 (d, *J* = 11.6 Hz, 1 H)*, 4.47 (d, *J* = 11.6 Hz, 1 H)*, 4.55 (d, *J* = 11.7 Hz, 1 H), 4.59 (d, *J* = 11.7 Hz, 1 H), 5.31–5.36 (m, 2 H), 5.38 (ddd, *J* = 10.6, 1.6, 1.0 Hz, 1 H)*, 5.44 (ddd, *J* = 17.2, 1.6, 0.9 Hz, 1 H)*, 6.00 (ddd, *J* = 17.2, 10.6, 4.1 Hz, 1 H), 6.04 (ddd, *J* = 17.2, 10.5, 4.1 Hz, 1 H)*, 6.24 (dt, *J* = 4.1, 1.6 Hz, 1 H), 6.26 (dd, *J* = 46.5, 2.4 Hz, 1 H)*, 6.28 (dt, *J* = 4.1, 1.6 Hz, 1 H)*, 6.31 (dd, *J* = 46.4, 2.4 Hz, 1 H), 7.12 (d, *J* = 0.9 Hz, 1 H)*, 7.13 (d, *J* = 1.4 Hz, 1 H), 7.18 (d, *J* = 0.9 Hz, 1 H)*, 7.21 (d, *J* = 0.9 Hz, 1 H), 7.27–7.39 (m, 10 H)*. **^{13}C NMR** [101 MHz, δ (ppm), $CDCl_3$]: 67.6, 68.1, 70.5 (d, *J* = 10.2 Hz), 71.2 (d, *J* = 10.2 Hz), 78.1 (d, *J* = 26.3 Hz), 78.7 (d, *J* = 26.3 Hz), 87.2 (d, *J* = 168.3 Hz), 90.2 (d, *J* = 168.6 Hz), 118.5, 118.7, 122.4, 123.1, 126.9, 127.8, 128.3, 128.4, 128.52, 128.55, 130.2, 130.5, 133.3, 133.7, 134.6, 134.8, 135.8, 136.0, 142.6, 142.9. **^{19}F NMR** [377 MHz, δ (ppm), $CDCl_3$]: –192.4 (dd, *J* = 46.4, 5.0 Hz). **FTIR** [$\tilde{\nu}$ (cm^{-1})]: 688, 802, 841, 1095, 1437, 1497, 2142, 2948, 3002, 3204. **HRMS** (ESI^+) calcd. for $(C_{16}H_{15}FN_2O + H)^+$ 271.1247, found 271.1263. By comparing the signal intensity of the propargylic protons a diastereomeric ratio of 55:45 was calculated. The diastereisomers were not separated from each other.

4.6 References and Notes

[1] Examples from our group and others can be found in Section 2.2 of this thesis.

[2] For imidazo[1,2-*a*]pyridine-based drugs, see: (a) Hieke, M.; Rödl, C. B.; Wisniewska, J. M.; la Buscató, E.; Stark, H.; Schubert-Zsilavecz, M.; Steinhilber, D.; Hofmann, B.; Proschak, E. *Bioorg. Med. Chem. Lett.* **2012**, *22*, 1969–1975; (b) Bagdi, A. K.; Santra, S.; Monir, K.; Hajra, A. *Chem. Commun.* **2015**, *51*, 1555–1575.

[3] Rival, Y.; Grassy, G.; Taudon, A.; Ecalle, R. *Eur. J. Med. Chem.* **1991**, *26*, 13–18.

[4] For extensive reviews on ring-closing metathesis, see: (a) Nicolaou, K. C.; Bulger, P. G.; Sarlah, D. *Angew. Chem. Int. Ed.* **2005**, *44*, 4490–4527; (b) Donohoe, T. J.; Orr, A. J.; Bingham, M. *Angew. Chem. Int. Ed.* **2006**, *45*, 2664–2670; (c) Monfette, S.; Fogg, D. E. *Chem. Rev.* **2009**, *109*, 3783–3816; (d) *Olefin Metathesis: Theory and Practice;* Grela, K., Ed.; John Wiley & Sons: Hoboken, NJ, 2014; (e) Sinclair, F.; Alkattan, M.; Prunet, J.; Shaver, M. P. *Polym. Chem.* **2017**, *8*, 3385–3398 and references therein.

[5] Blanco-Ania, D.; Gawade, S. A.; Zwinkels, L. J. L.; Maartense, L.; Bolster, M. G.; Benningshof, J. C. J.; Rutjes, F. P. J. T. *Org. Process Res. Dev.* **2016**, *20*, 409–413.

[6] Aitken, D. J.; Eijsberg, H.; Frongia, A.; Ollivier, J.; Piras, P. P. *Synthesis* **2014**, *46*, 1–24.

[7] For extensive reviews on the Pauson–Khand reaction, see: (a) Brummond, K. M.; Kent, J. L. *Tetrahedron* **2000**, *56*, 3263–3283; (b) Blanco-Urgoiti, J.; Añorbe, L.; Pérez-Serrano, L.; Domínguez, G.; Pérez-Castells, J. *Chem. Soc. Rev.* **2004**, *33*, 32–42; (c) Gibson, S. E.; Mainolfi, N. *Angew. Chem. Int. Ed.* **2005**, *44*, 3022–3037; (d) Shibata, T. *Adv. Synth. Catal.* **2006**, *348*, 2328–2336; (e) *The Pauson–Khand Reaction: Scope, Variations and Applications;* Rios, R., Ed.; John Wiley & Sons: Hoboken, NJ, 2012; (f) Ricker, J. D.; Geary, L. M. *Top. Catal.* **2017**, *60*, 609–619 and references therein.

[8] For extensive reviews on click reactions, see: (a) Hein, J. E.; Fokin, V. V. *Chem. Soc. Rev.* **2010**, *39*, 1302–1315; (b) Tanga, W.; Becker, M. L. *Chem. Soc. Rev.* **2014**, *43*, 7013–7039; (c) Haldón, E.; Nicasio, M. C.; Pérez, P. J. *Org. Biomol. Chem.* **2015**, *13*, 9528–9550; (d) Tiwari, V. K.; Mishra, B. B.; Mishra, K. B.; Mishra, N.; Singh, A. S.; Chen, X. *Chem. Rev.* **2016**, *116*, 3086–3240; (e) Singh, M. S.; Chowdhury, S.; Koley, S. *Tetrahedron* **2016**, *72*, 5257–5283 and references therein.

[9] For 1,2,3-triazoles as pharmacophores, see: Agalave, S. G.; Maujan, S. R.; Pore, V. S. *Chem. Asian J.* **2011**, *6*, 2696–2718 and references therein.

[10] Himo, F.; Lovell, T.; Hilgraf, R.; Rostovtsev, V. V.; Noodleman, L.; Sharpless, K. B.; Fokin, V. V. *J. Am. Chem. Soc.* **2005**, *127*, 210–216.

[11] Typical procedure: after stirring at –78 °C for 1 h, an aliquot of the reaction mixture was taken under a nitrogen atmosphere and dissolved in nearly the same volume of CD_3OD. The solvent mixture was evaporated and the crude product was analyzed with ^1H NMR.

[12] For the activation of organolithium reagents with TMEDA, see: Chadwick, S. T.; Ramirez, A.; Gupta, L.; Collum, D. B. *J. Am. Chem. Soc.* **2007**, *129*, 2259–2268.

[13] For the selective magnesiation or zincation using TMP bases, see: (a) Krasovskiy, A.; Malakhov, V.; Gavryushin, A.; Knochel, P. *Angew. Chem. Int. Ed.* **2006**, *45*, 6040–6044; (b) Piller, F. M.; Appukkuttan, P.; Gavryushin, A.; Helm, M.; Knochel, P. *Angew. Chem. Int. Ed.* **2008**, *47*, 6802–6806; (c) Bresser, T.; Knochel, P. *Angew. Chem. Int. Ed.* **2011**, *50*, 1914–1917.

[14] (a) *Modern Carbonyl Chemistry;* Otera, J., Ed.; Wiley-VCH: Weinheim, Germany, 2000; (b) *Lithium Compounds in Organic Synthesis. From Fundamentals to Applications;* Luisi, R., Capriati, V., Ed.; Wiley-VCH: Weinheim, Germany, 2014.

[15] (a) Fu, G. C.; Grubbs, R. H. *J. Am. Chem. Soc.* **1992**, *114*, 5426–5427; b) Fu, G. C.; Nguyen, S. T.; Grubbs, R. H. *J. Am. Chem. Soc.* **1993**, *115*, 9856–9857.

[16] Fürstner, A.; Langemann, K. *Synthesis* **1997**, 792–803.

[17] An overview of [2+2] cycloaddition reactions in natural product synthesis: Bach, T.; Hehn, J. P. *Angew. Chem. Int. Ed.* **2011**, *50*, 1000–1045.

[18] Solomon, R. G.; Kochi, J. K. *J. Chem. Soc., Chem. Commun.* **1972**, 559–560.

[19] Complete conversion to α,β-ketone **30** was observed on the ^1H NMR spectrum when the described reaction was performed on allylic alcohol **25** (Scheme 4.13). This process likely undergoes via activation of alkyne with cobalt(0)-complex followed by a 1,2-hydrogen shift. For similar results with ruthenium and rhodium complexes, see: (a) Haak, E. *Eur. J. Org. Chem.* **2007**, 2815–2824; (b) Casey, C. P.; Jiao, X.; Guzei, I. A. *Organometallics* **2010**, *29*, 4829–4836.

Scheme 4.13 *Cobalt-Catalyzed Isomerization of Propargyl Alcohol* ***26*** *to α,β-Unsaturated Ketone* ***30****.*

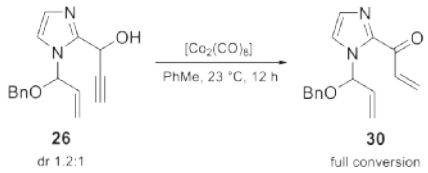

26
dr 1.2:1

30
full conversion

[20] Boñaga, L. V. R.; Zhang, H.-C.; Maryanoff, B. E. *Chem. Commun.* **2004**, 2394–2395; (b) Gray, B. L.; Wang, X.; Brown, W. C.; Kuai, L.; Schreiber, S. L. *Org. Lett.* **2008**, *10*, 2621–2624; (c) Young, D. D.; Teske, J. A.; Deiters, A. *Synthesis* **2009**, *22*, 3785–3790 and references therein.

[21] For Pauson–Khand-type reactions mediated by rhodium(I)-catalysts, see: (a) Jeong, N.; Sung, B. K.; Kim, J. S.; Park, S. B.; Seo, S. D.; Shin, J. Y.; In, K. Y.; Choi, Y. K. *Pure Appl. Chem.* **2002**, *74*, 85–91; (b) Kim, D. E.; Kim, I. S.; Ratovelomanana-Vidal, V.; Genêt, J.-P.; Jeong, N. *J. Org. Chem.* **2008**, 73, 7985–7989 and references therein.

[22] For Pauson–Khand-type reactions mediated by iridium(I)-catalysts, see: (a) Shibata, T.; Takagi, K. *J. Am. Chem. Soc.* **2000**, *122*, 9852–9853; (b) Shibata, T.; Toshida, N.; Yamasaki, M.; Maekawa, S.; Takagi, K. *Tetrahedron* **2005**, *61*, 9974–9979 and references therein.

[23] Wang, J.; Sánchez-Roselló, M.; Aceña, J. L.; del Pozo, C.; Sorochinsky, A. E.; Fustero, S.; Soloshonok, V. A.; Liu, H. *Chem. Rev.* **2014**, *114*, 2432–2506 and references therein.

[24] Sutherland, A.; Vederas, J. C. *Chem. Commun.* **1999**, 1739–1740.

[25] Due to a confidentiality agreement the results of the biological testing of the compounds will not be presented in the thesis.

[26] De Nanteuil, F.; Waser, J. *Angew. Chem. Int. Ed.* **2011**, *50*, 12075–12079.

CHAPTER 5

Alkyne-Directed Hydroarylation of Arenesulfonyl Ynamines

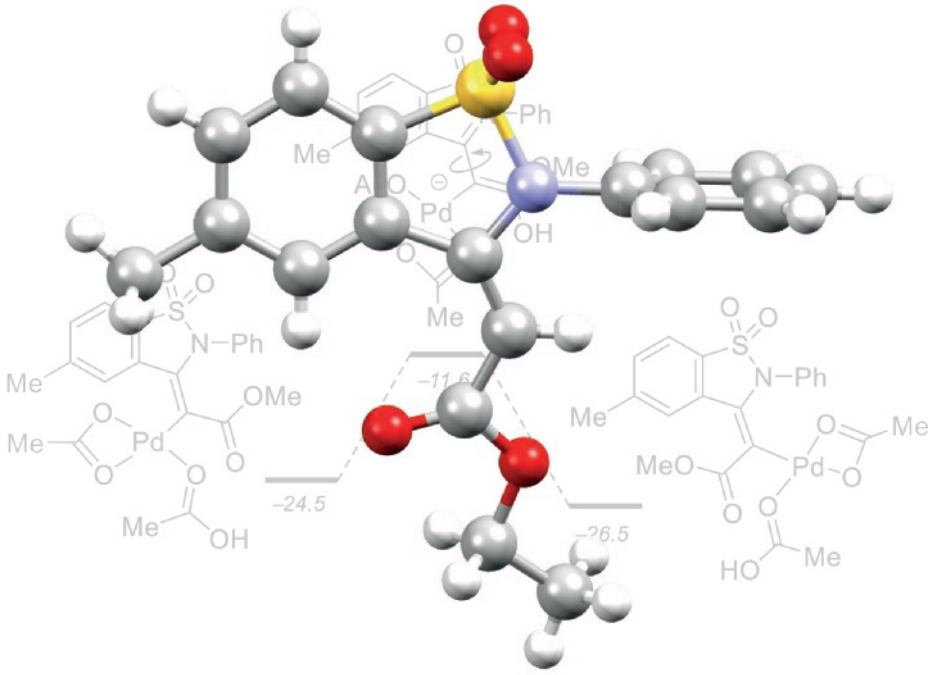

ABSTRACT

In this chapter we present the first example of completely regio- and highly stereoselective palladium-catalyzed intramolecular hydroarylation of arenesulfonyl ynamines. The presence of an electron-withdrawing group on the triple bond of the sulfonyl ynamine was crucial for the success of the reaction. Our mechanistic studies suggest an alkyne-directed 5-*exo*-dig cyclization pathway proceeding via a concerted deprotonation-metalation sequence. The obtained products, 1,2-benzothiazole-1,1-diones, are key elements of diverse biologically active compounds and useful reagents in organic synthesis.

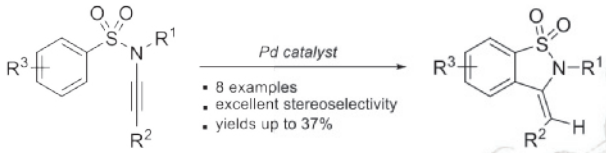

Part of this chapter was published in:

Bernar, I.; Blanco-Ania, D.; Sophie J. Stok; Sotorríos, L.; Gómez-Bengoa, E.; Rutjes, F. P. J. T. *Eur. J. Org. Chem.* **2018**, 5435–5444.

Chapter cover: "Crystal structure of (*E*)-1,2-benzothiazole-1,1-dione **2a**"

5.1 Introduction

Sulfonyl ynamines have recently emerged as a privileged class of ynamides.[1] They are stable compounds, readily prepared,[2] and easy to handle. The polarized alkyne system of sulfonyl ynamines shows excellent reactivity in a wide variety of reactions featuring π-acid catalysis,[3] metal-catalyzed cyclizations,[4] cycloadditions,[5] and rearrangements[6]. Among all of these transformations the palladium-catalyzed cyclizations of sulfonyl ynamines have been widely used for the synthesis of complex nitrogen-containing heterocycles (Chapter 2). With the idea of extending the chemistry of sulfonyl ynamines, we envisioned that arenesulfonyl ynamines **1** could be used as simple precursors for a single-step, atom-efficient synthesis of 1,2-benzothiazole-1,1-diones **2**, key elements of diverse biologically active compounds and useful reagents in organic synthesis (e.g., compounds **3**–**5**, Scheme 5.1).[7–11]

Scheme 5.1 *Retrosynthesis and Applications of 1,2-Benzothiazole-1,1-diones 2.*

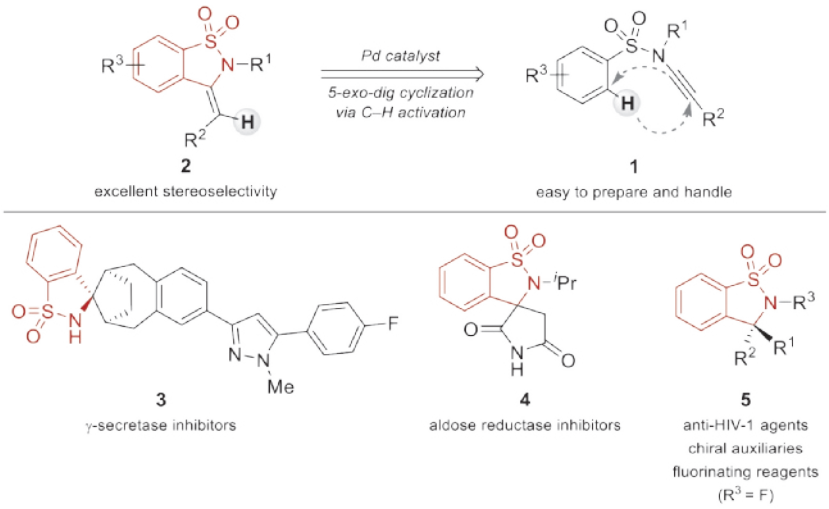

Considering that arenesulfonyl ynamines react in the presence of alkynophilic transition metals usually through π-activation of the triple bond, we anticipated that initial alkyne coordination might direct aromatic *ortho*-C–H activation followed by stereocontrolled intramolecular hydroarylation, similar to that of *N*-alkynyl indoles **6** developed by the group of Park[12] or the related alkynyl aryl ethers **8** developed by the group of Hiyama (Scheme 5.2).[13] To the best of our knowledge, alkyne-directed 5-*exo*-dig cyclizations of arenesulfonyl ynamines have not been yet explored. Therefore, we herein present our pioneering research within this topic.

Scheme 5.2 *Alkyne-Directed ortho-C–H Activation of N-Alkynyl Indoles* **6** *and Alkynyl Aryl Ethers* **8**.

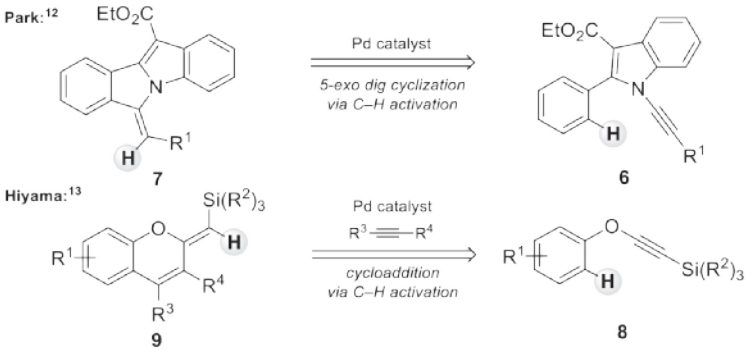

5.2 Results and Discussion

5.2.1 Synthesis of the Sulfonyl Ynamines

Sulfonyl ynamines **1** were prepared from sulfonamides **10** and trichloroethene (TCE) in the presence of a base (Scheme 5.3).[14] Generally, the anticipated α,β-dichloroenamines **11** were obtained in modest to excellent yields (64–91%) with the (*E*)-stereoisomer being the major product of the reaction.[15]

Scheme 5.3 *Synthesis of Sulfonyl Ynamines* ***1a, 1d, 1e, 1g–k***.

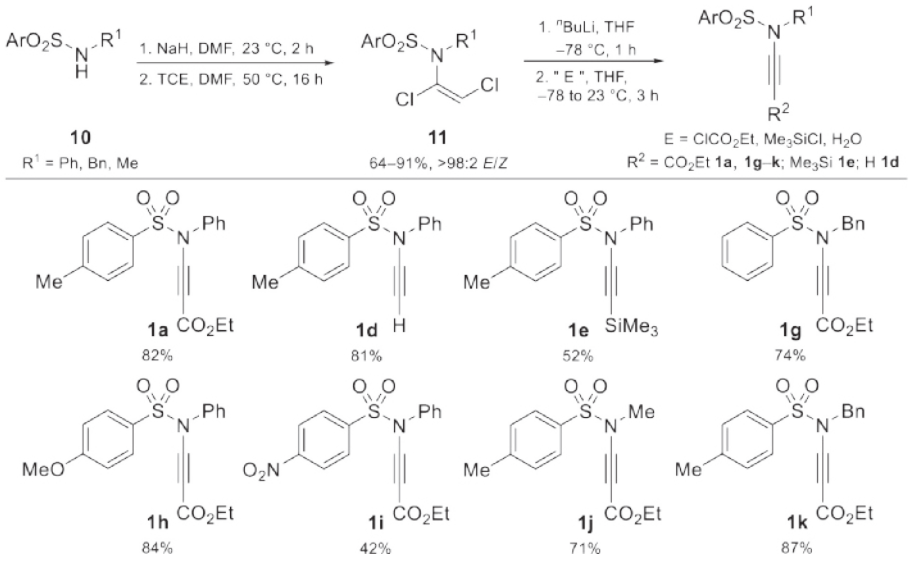

With α,β-dichloroenamines **11** in hand we continued the synthesis of sulfonyl ynamines **1**. This step requires strong bases such as ^{n}BuLi or PhLi to perform the dehydrochlorination of intermediate **12** to form chloroethyne **13** (Scheme 5.4).[16] The second equivalent of organolithium reagent triggers the chloro–lithium exchange in **13** leading to lithiated alkynide **14**. Consequently, intermediate **11** reacts with the electrophile and delivers sulfonyl ynamines **1a**, **1g–k** (ethyl chloroformate as electrophile) and **1e** (Me_3SiCl as electrophile) or sulfonyl ynamine **1d** (water as electrophile). Following this procedure and utilizing ^{n}BuLi (2.2 equiv) as a base, compounds **1a**, **1d**, **1e**, and **1g–k** were obtained in modest to very good yields (42–87%) over two steps and were subsequently used for the palladium-catalyzed intramolecular hydroarylation reaction.

Scheme 5.4 *Mechanism of Formation of the Sulfonyl Ynamines.*

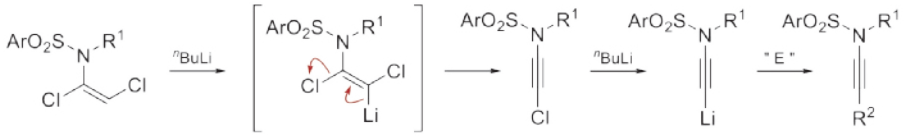

Additionally, we examined the possible functionalization of the already prepared sulfonyl ynamine **1d** using the following two approaches: copper(I)-catalyzed nucleophilic addition of **1d** to acyl chlorides[17] and Sonogashira cross-coupling of **1d** with iodobenzene (Scheme 5.5).[18] Thus, the addition of sulfonyl ynamine **1d** to pivaloyl or benzoyl chloride in the presence of DIPEA (2.0 equiv) and a catalytic amount of CuI (10 mol %) in chloroform at 30 °C resulted in the smooth formation of the corresponding sulfonyl ynamines **1b** and **1c** in very good yields (79 and 86%, respectively).

Scheme 5.5 *Synthesis of Sulfonyl Ynamines **1b** and **1c**.*

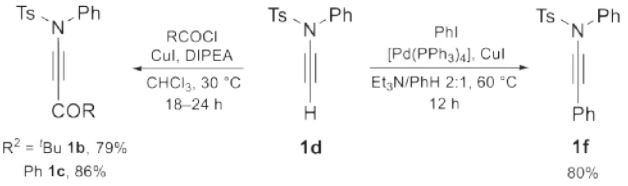

Furthermore, the Sonogashira coupling of sulfonyl ynamine **1d** with iodobenzene under optimized reaction conditions {[$Pd(PPh_3)_4$] (5.0 mol %), CuI (1.5 mol %), in Et_3N/PhH (2:1)} went to completion at 60 °C in 12 h, yielding the desired phenyl-substituted sulfonyl ynamine **1f** in 80% yield.

5.2.2 Optimization Studies for Intramolecular Hydroarylation of Sulfonyl Ynamine 1a

Our pioneering attempts to investigate the intramolecular hydroarylation of sulfonyl ynamine **1a** were designed in analogy to the palladium-catalyzed intramolecular hydroarylation of *N*-alkynyl indoles developed by Park et al.[12] and alkynyl aryl ethers developed by Hiyama et al.[13] Modifying their procedure, sulfonyl ynamine **1a** was converted to products **2a**, **10a**, **15**, and **16** in the presence of $Pd(OAc)_2$ (5 mol %) in toluene at 100 °C for 18 h (Table 5.1, entry 1).

Table 5.1 *Optimization of the Reaction Conditions.*

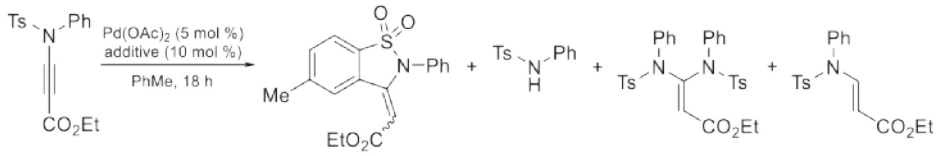

1a **2a** **10a** **15** **16**

			Ratio of products (%)[a]						Yield (%)[b]
Entry	*t* (°C)	Additive	**1a**	**2a**	**10a**	**15**	**16**	*E*/*Z*[a]	(*E*)-**2a**
1	100	–	27	35	33	3	2	82:18	21
2[c]	100	–	8	42	46	2	2	83:17	23
3	80	–	62	12	26	0	0	n.d.	<5
4	120	–	6	20	63	11	0	82:18	9
5	150	–	6	18	59	17	0	n.d.	<5
6	100	NaOAc[d]	28	14	58	0	0	85:15	8
7	100	Ac_2O	21	22	54	0	3	63:37	11
8	100	Tf_2NH	3	9	88	0	0	n.d.	<5
9	100	Zn	23	37	38	2	0	85:15	20

[a]Based on the ^1H NMR spectrum of the crude mixture. [b]Isolated yield. [c]$Pd(OAc)_2$ (10 mol %) was used. [d]NaOAc (2.0 equiv).

The (*E*)-exocyclic alkylidene product **2a** was isolated in 21% yield after purification of the crude mixture by neutral silica-gel column chromatography. Increasing the amount of $Pd(OAc)_2$ from 5 to 10 mol % improved somewhat the conversion of the starting material **1a** into the product mixture (entry 2). Nevertheless, the desired product **2a** was obtained in nearly the same yield as in the previous experiment after purification of the crude mixture by column chromatography. The structure of 1,2-benzothiazole-1,1-dione (*E*)-**2a** was unambiguously

determined by NMR spectroscopy and X-ray crystallography (Figure 5.1a). Interestingly, the crystal structure showed an extremely close proximity of the carbonyl group to the hydrogen at the 4-position in the cyclic sulfonamide group (with an O–H distance of only 2.133 Å). As a consequence, in the ^{1}H NMR experiment this proton experiences a higher external magnetic field because of the deshielding effect of the π-system of the carbonyl group (shielding /deshielding cone; Figure 5.1b). This deshielding increases the chemical shift of the studied proton of the (*E*)-isomer compared to the (*Z*)-isomer (9.23 vs 7.62 ppm for (*E*)-**2a** and (*Z*)-**2a**, respectively).

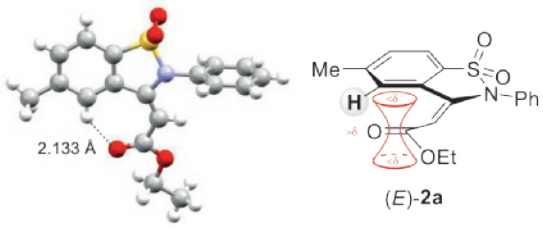

Figure 5.1 (a) *Crystal Structure of (E)-**2a** and (b) Deshielding of a Proton in Shielding/Deshielding Cone of Carbonyl Group.*

This reaction also showed degradation of sulfonyl ynamine **1a** under the reaction conditions forming *N*-phenyl sulfonamide **10a**, which was the main side product of the sulfonyl ynamine cyclization. Compound **10a** reacted further with **1a** to form the Michael adduct **15**, which was successfully isolated after purification. Furthermore, sulfonyl ynamine **1a** underwent partial hydrogenation of the triple bond to yield sulfonyl enamine **16** in a trace ammount.[19]

The intramolecular hydroarylation of sulfonyl ynamine **1a** was strongly dependent on the reaction temperature. Thus, starting material **1a** showed very low conversion rates at 80 °C (entry 3) with more than 53% of the starting material being recovered after purification. Increasing the temperature to 120 or 150 °C only led to decomposition of the starting material (entries 4 and 5). In all cases, 1,2-benzothiazole-1,1-dione **2a** was obtained in trace amounts in 5–9% yield. Our studies showed that addition of a base or Brønsted acid significantly decreased the amount of product **2a**, presumably because of the fast decomposition of the starting material under these reaction conditions (entries 6–8). *N*-Phenyl sulfonamide **10a** was the main product of the reaction with 58–88% conversion determined by ^{1}H NMR, whereas 1,2-benzothiazole-1,1-dione **2a** was formed only in minor amount in <11% yield after additional purification by silica-gel column chromatography. The use of $Pd(OAc)_2$ and Zn, a catalytic system developed by Hiyama et al., had no significant influence on the yield of **2a** (entry 9).[13]

Consequently, we studied the influence of the phosphine ligands on the palladium-catalyzed intramolecular hydroarylation of **1a** (Table 5.2). In general terms, addition of phosphine ligands increased the ratio of product **2a**. Thus, in the presence of PPh_3 as ligand the reaction afforded **2a** in 20% yield with excellent stereoselectivity (*E*/*Z*-ratio 92:8, entry 1). Addition of AcOH caused a significant drop in product yield and stereoselectivity (entry 2). The phosphine ligands dppp and PCy_3 showed very good stereoselectivity, but nonetheless poor reactivity (entries 3–6). To our delight, the highest yields of product **2a** (26–37%) together with excellent stereoselectivities (*E*/*Z*-ratio >90:10) were obtained employing the ligands P(*o*-Tol)$_3$ and P(*p*-Tol)$_3$ (entries 7–10). Thus, the reaction yielded 1,2-benzothiazole-1,1-dione **2a** in 37% yield and excellent stereoselectivity (*E*/*Z*-ratio 92:8) in the presence of P(*p*-Tol)$_3$ (entry 9).

Table 5.2 *Ligand Screening.*

			Ratio of products (%)[a]						Yield (%)[b]
Entry	Ligand	Additive	**1a**	**2a**	**10a**	**15**	**16**	*E*/*Z*[a]	(*E*)-**2a**
1	PPh_3	Zn	15	38	38	9	0	92:8	20
2	PPh_3	AcOH	34	23	39	0	4	74:26	13
3	dppp	Zn	12	30	53	3	2	86:14	16
4	PCy_3	–	13	48	36	0	3	90:10	27
6	PCy_3	Zn	16	48	36	0	0	89:11	23
7	P(*o*-Tol)$_3$	–	12	48	35	0	5	90:10	32
8	P(*o*-Tol)$_3$	Zn	16	43	41	0	0	90:10	26
9	P(*p*-Tol)$_3$	–	10	51	35	0	4	98:2	37
10	P(*p*-Tol)$_3$	Zn	15	53	31	0	1	95:5	34

[a]Based on the ^{1}H NMR spectrum of the crude mixture. [b]Isolated yield.

Additionally, we investigated the behavior of sulfonyl ynamine **1a** in the absence of $Pd(OAc)_2$ and in the presence of other possible catalysts (Table 5.3). No reaction was observed without $Pd(OAc)_2$ and starting material **1a** was recovered (entry 1). In the presence of palladium(0) the reaction took also place, albeit in a much lower conversion compared to $Pd(OAc)_2$ (entries 2 and 3). However, the cyclization of **1a** to **2a** took place only with palladium as catalyst. Thus, sulfonyl ynamine **1a** underwent partial decomposition to the side product **15** with AgOTf (10 mol %) when stirred in toluene at 23 °C for 18 h (entry 4). Likewise, the reaction of sulfonyl ynamine **1a** catalyzed by [ClAu(PPh_3)] (10 mol %) resulted in full decomposition of the starting material

(entry 5). Lastly, no reaction occurred when using Tf_2NH (10 mol %) as a potential catalyst for cyclization (entry 6).[20]

Table 5.3 *Cayalyst Screening.*

			Ratio of products (%)[a]						Yield (%)[b]
Entry	Catalyst	*t* (°C)	**1a**	**2a**	**10a**	**15**	**16**	*E*/*Z*[a]	(*E*)-**2a**
1	–	100	100	–	–	–	–	n.d.	n.d.
2	$Pd(PPh_3)_4$	100	30	10	58	2	0	90:10	7
3[c]	$Pd(PPh_3)_4$	100	43	23	17	3	14	92:8	14
4	AgOTf	23	10	0	0	48	0	n.d.	n.d.
5	$[ClAu(PPh_3)]$	100	unidentified products					n.d.	n.d.
6	Tf_2NH	23	100	0	0	0	0	n.d.	n.d.

[a]Based on the ^1H NMR spectrum of the crude mixture. [b]Isolated yield. [c]AcOH (10 mol %) was used.

5.2.3 Palladium-Catalyzed Intramolecular Hydroarylation of Sulfonyl Ynamines 1a–k

With these results in hand, we focused our attention on the scope and limitations of the reaction varying the substituents on the alkyne terminus, on the aromatic ring of the sulfonamide group and on the nitrogen for the hydroarylation of sulfonyl ynamines **1a–k** (Scheme 5.6). Notably, the presence of an electron-withdrawing group on the triple bond, e.g., ester or ketone, was essential for the success of the hydroarylation. Thus, sulfonyl ynamines with a ketone showed similar reactivity to sulfonyl ynamine **1a** proceeding with exclusive regioselectivity and excellent stereoselectivity (**2b** and **2c**). In stark contrast, when the reaction was performed with sulfonyl ynamines **1d–1f** (R^2 = H, Me_3Si, Ph) no cyclization was detected and only decomposition to **10a** was observed. Changing the conditions (solvent, temperature, palladium catalyst, addition of base) did not lead to products **2d–2f** either. Next, a series of electronically different sulfonyl ynamines were employed for this transformation. To our delight, we observed no significant difference in the reaction efficiency when changing the substituents at the aryl group of the sulfonamide. 1,2-Benzothiazole-1,1-diones (**2g–i**) were obtained in comparable yields and also with complete regioselectivity and excellent stereoselectivity. Finally, sulfonyl ynamines **1j** and **1k** were subjected to the reaction conditions to compare the reactivity of compounds with different substituents on the nitrogen. Compound **1j** formed product **2j** in 31% yield and compound **1k** resulted in the formation of a mixture of **2k** (*E*/*Z* >99:1) and **17** in 26 and 10% yield respectively.[21]

Scheme 5.6 *Scope of Sulfonyl Ynamines **1a–k** for the Intramolecular Hydroarylation.*

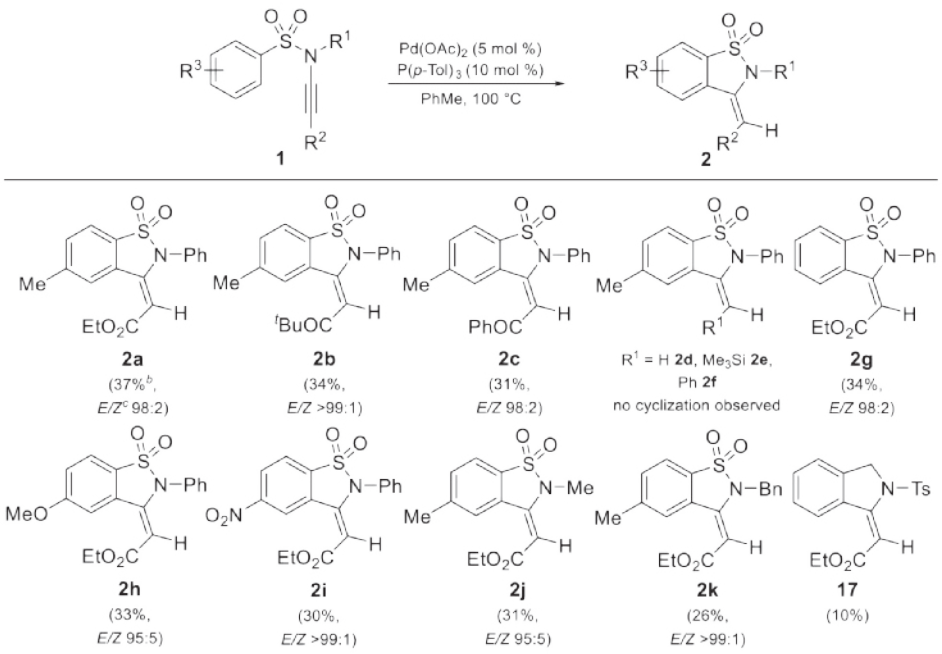

5.2.4 DFT Studies of the Reaction Mechanism

We investigated the reaction pathway with DFT calculations to gain a better understanding of the reaction mechanism. The most logical mechanistic scenario for the reaction of sulfonyl ynamine **1l** and $Pd(OAc)_2$ would involve coordination of the palladium(II) species to the substrate, as in **18**, followed by an alkyne-directed concerted deprotonation–metalation (CMD) sequence to form **19** (Figure 5.2).[22] Our attempts to compute this pathway indicated the six-membered transition state **TS1** in which one of the acetate groups is acting both as a κ^2 ligand and as a base. Our studies revealed a week intramolecular coordination of aromatic C–H bond to palladium center, which corresponds to agostic interactions.[23] Furthermore, the proton abstraction presents the highest activation barrier within the catalytic cycle (22.6 kcal/mol), and therefore should be considered as the rate-determining step of the reaction. Additionally, *ortho*-C–H activation in **TS1** proceeds much slower for the alkyne–H and alkyne–$SiMe_3$ substructures (24.5 and 24.6 kcal/mol, for **1d** and **1e**, respectively) compared to the corresponding alkyne–CO_2Me substructure **1l** (Table 5.4). The difference between these barrier values is >2.5 kcal/mol corresponding to a reaction rate more than 100 times slower, which is in agreement with the experimental results.

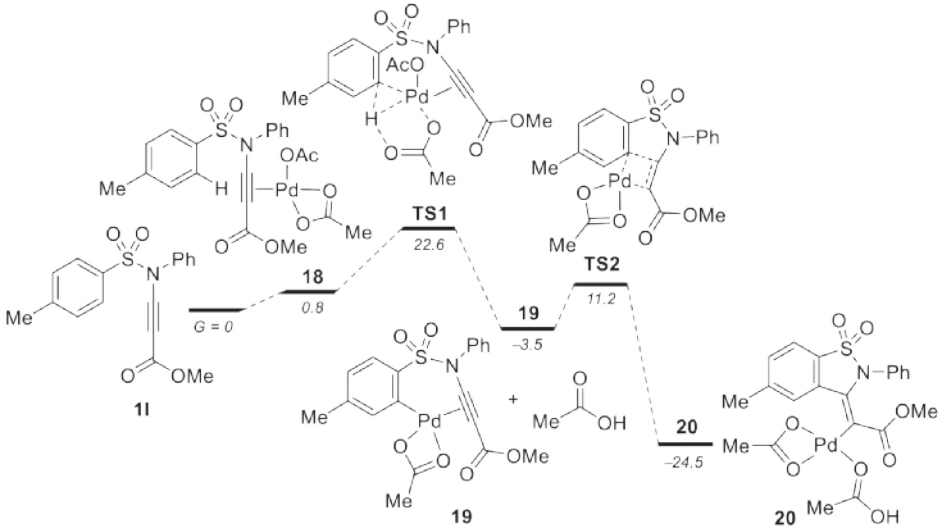

Figure 5.2 *Reaction Sequence Involving Alkyne-Directed C–H Activation Followed by Carbopalladation to Form* ***20****. Free Energies (298 K) with Respect to the Starting Materials Are Shown in kcal/mol.*

Table 5.4 *Energy Values for the C–H Activation Transition State* ***TS1*** *for Different Substituents at Alkyne Terminus. Free Energies (298 K) with Respect to Starting Materials Are Shown in kcal/mol.*

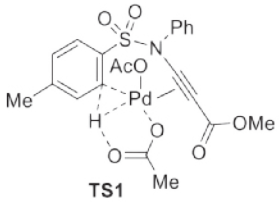

R	ΔG
CO_2Me	22.6
H	25.3
Me_3Si	25.4

Consequently, intermediate **19** performs a carbopalladation to the CC triple bond through **TS2**, leading to intermediate **20**. This step was also predicted to be a few kcal/mol higher for sulfonyl ynamines **1d** and **1e** (16.0 and 14.2 kcal/mol for **1d** and **1e**, respectively; Table 5.4) than for sulfonyl ynamine **1l** (11.2 kcal/mol). Further protonation of the "push-pull" alkenyl–palladium(II) species **20** with acetic acid forms an enol intermediate **21**, with almost free rotation around the exocyclic CC bond (Figure 5.3). We found that the enol structure **21** lies 12.9 kcal/mol higher in energy than palladium species **20**, confirming the feasibility of this or related

isomerization processes. The final protodemetalation with acetic acid via **TS3** renders the major product (*E*)-**2l** and recovers the palladium acetate catalyst.

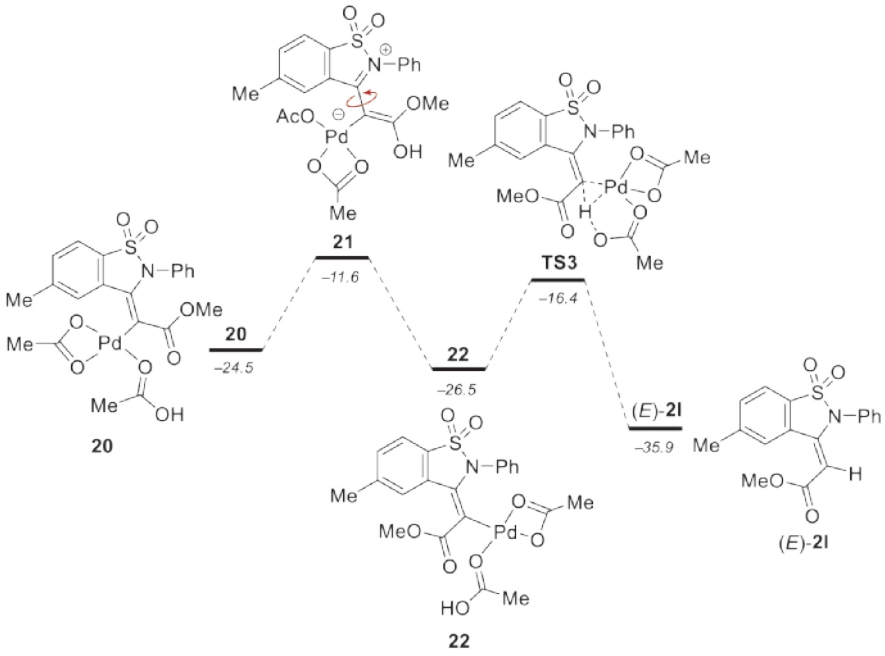

Figure 5.3 *Isomerization of* ***20*** *to* ***22*** *Followed by Protodemetalation to Form the Final Product (E)-****2l****. Free Energies (298 K) with Respect to Starting Materials Are Shown in kcal/mol.*

Our DFT calculations further revealed that the (*E*)-isomer is the most stable isomer (2.5 kcal/mol lower in energy than the (*Z*)-isomer, Scheme 5.7). To validate this result, (*E*)-**2a** and (*Z*)-**2a** were subjected independently to the same experimental conditions [$Pd(OAc)_2$ (5 mol %), $P(p\text{-Tol})_3$ (10 mol %) in toluene at 100 °C for 18 h]. We observed the formation of an 85:15 mixture of *E*/*Z* isomers after 18 h of reaction time. These results suggest that the cyclization of **1a** might proceed in a complete stereoselective manner, however, the major product might further undergo partial isomerization under the reaction conditions.

Summarizing all the studied reaction steps, the complete mechanistic profile for the hydroarylation of sulfonyl ynamine **1l** is presented in Figure 5.4.

Scheme 5.7 *Equilibration of (E)- to (Z)-Isomer of 1,2-Benzothiazole-1,1-dione* ***2a****.*

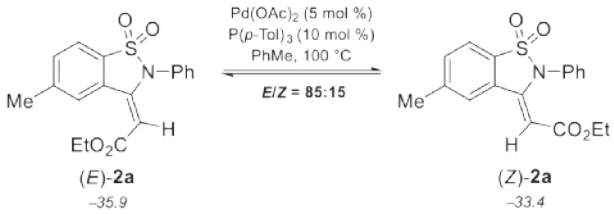

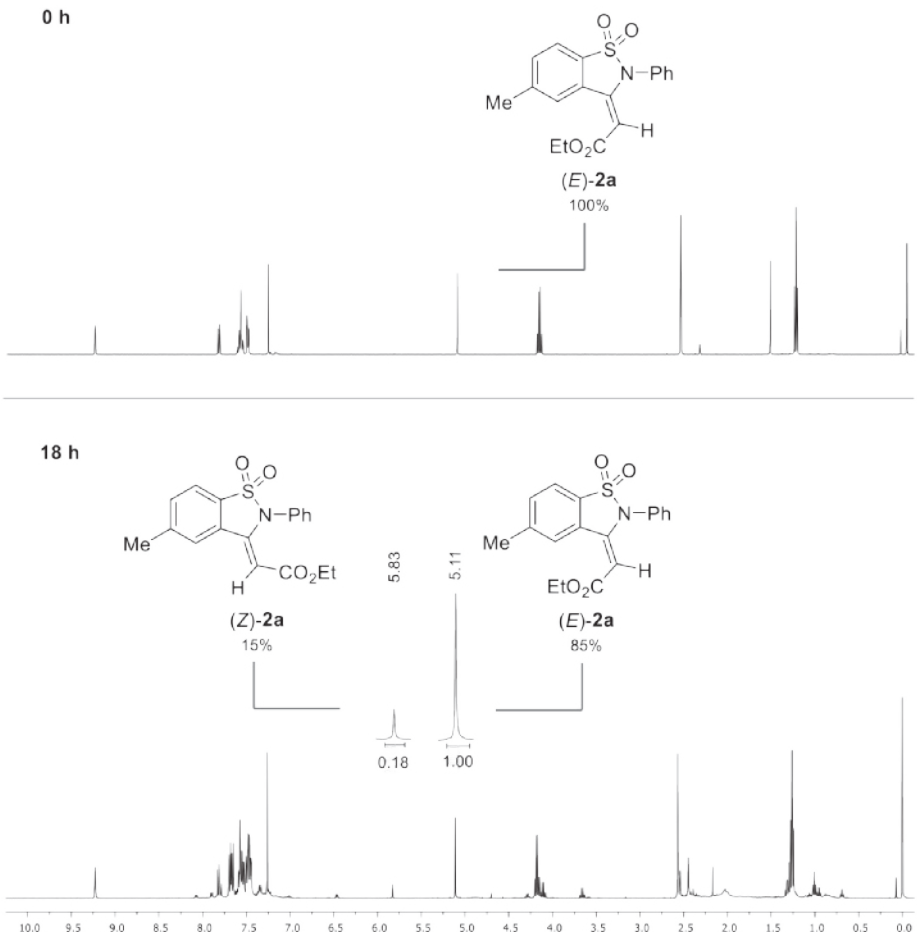

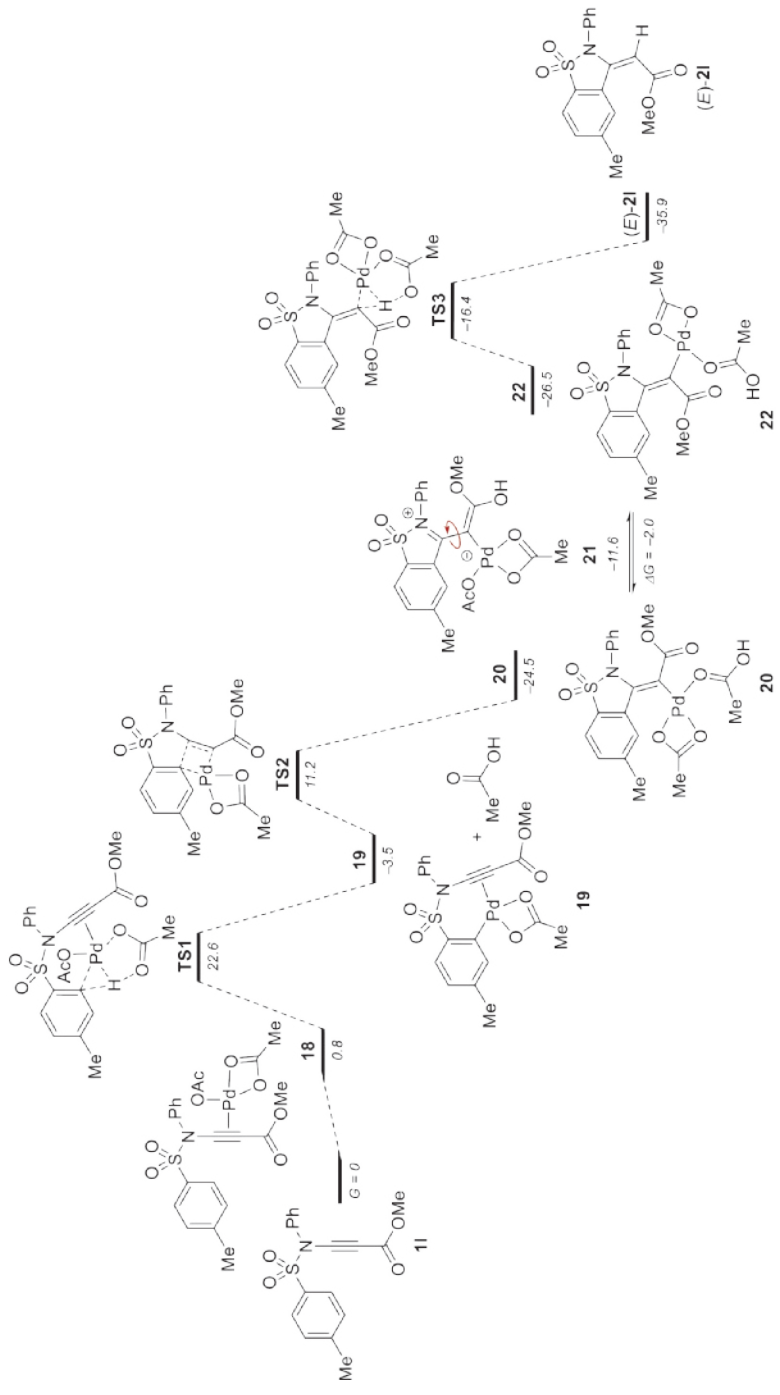

Figure 5.4 *Complete Computed Pathway for Cyclization of 1l. Free energies (298 K) with respect to starting materials are shown in kcal/mol.*

Moreover, the experimental case where the palladium atom binds one phosphine ligand was also computationally analyzed, and a similar mechanism was found (modeled with one PPh_3; Figure 5.5). In the presence of phosphine, the proposed transition state for CMD involves the decoordination of palladium from the alkyne during C–H abstraction, binding to three oxygens of the two acetate ligands (**TS4**). The activation energies of the CMD step are almost equal for this and the previous mechanism (23.7 kcal/mol for **TS4**, Figure 5.5 and 22.6 kcal/mol for **TS1**, Figure 5.4). Additionally, calculations showed that the addition to the triple bond is slightly more facile for this mechanism compared to the previous one (9.7 kcal/mol, from **24** to **TS5** kcal/mol). Surprisingly, the presence of the phosphine disfavors the final protodemetalation to a large extent, increasing its activation energy (15.3 kcal/mol, from **25** to **TS6**). Nonetheless, this effect does not alter the overall mechanism, since C–H activation in **TS4** is still the rate-limiting step.

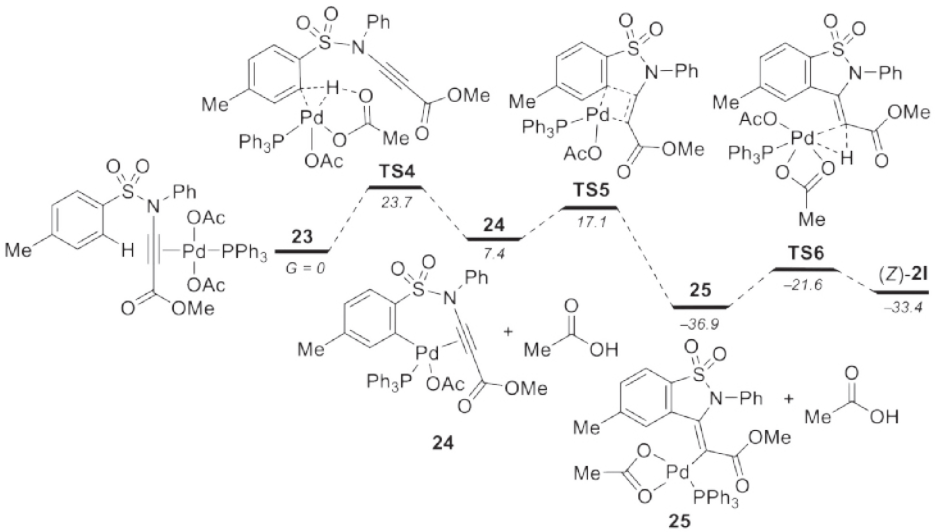

Figure 5.5 *Computed Pathway for Cyclization of* ***23****. Free Energies (298 K) with Respect to Starting Materials Are Shown in kcal/mol.*

Above this, we examined the possibility for the palladium atom to remain bound to the alkyne during the mechanism. In this case, the acetate ligand must leave the coordination sphere of the metal, giving rise to cationic species **TS7** (Scheme 5.8). This situation was proven to be highly disfavored, with the activation energy rising to an unaffordable value of 51.5 kcal/mol. Thus, **TS7** cannot compete with the neutral version **TS4** examined in Figure 5.5.

Scheme 5.8 *Computed Pathway for Cyclization of* ***26****. Free Energies (298 K) with Respect to Starting Materials Are Shown in kcal/mol.*

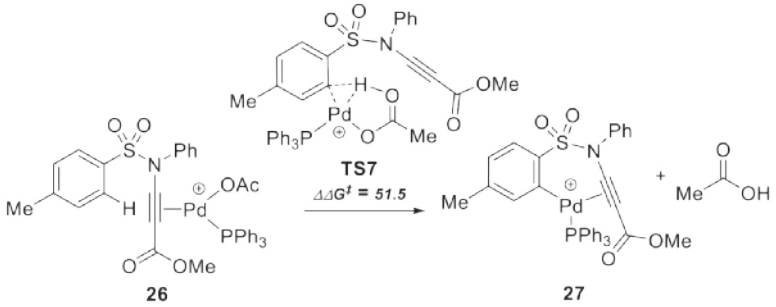

Finally, the most intriguing experimental data is the fact that palladium(0) species are also able to catalyze the process, to a similar extent as the palladium(II) species, although with the formation of significant amounts of side products **10a**, **15**, and **16**. It is well known that the CMD processes are usually catalyzed by palladium(II) or palladium(IV) species, but not palladium(0), and also that they need the presence of an internal or external basic ligand, such as acetate in the case of $Pd(OAc)_2$.[24] The fact that in the palladium(0)-promoted reaction some of the side products are derived from the cleavage of the C–N bond of the starting material (like **10a** and **15**), led us to hypothesize that the first step of this process could be the oxidative addition of palladium(0) to the alkyne–sulfonamide bond, as in **TS8** (Scheme 5.9). The computed activation energy of this step is moderate to high, but affordable at the reflux temperatures required for this process. The formation of palladium species **29** might explain the presence of active palladium(II) species in the reaction medium and the appearance of adducts lacking the alkyne–sulfonamide bond.

Scheme 5.9 *Insertion of Palladium(0) into the C–N Bond. Free Energies (298 K) with Respect to Starting Materials Are Shown in kcal/mol.*

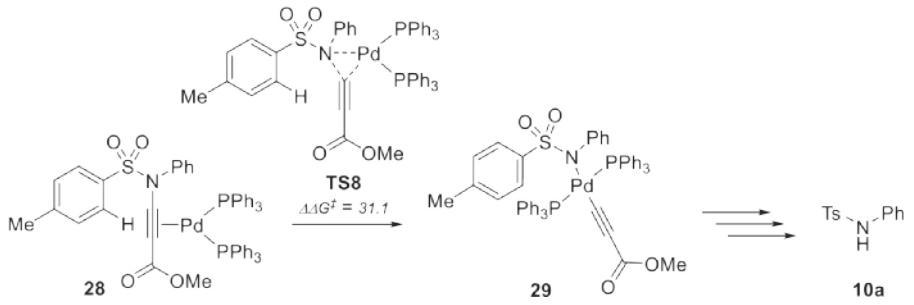

5.3 Conclusion

In a nutshell, we have demonstrated the first example of intramolecular hydroarylation of arenesulfonyl ynamines. Although the yields are relatively low, this unprecedented cyclization is completely regioselective and highly stereoselective: (*E*)-exocyclic 1,2-benzothiazole-1,1-diones **2** are the major isomers with an *E*/*Z*-ratio of up to 99:1. This method opens an easy access to benzothiazole heterocycles, which are valuable scaffolds in medicinal and organic synthesis. Our mechanistic studies suggest an alkyne-directed 5-*exo*-dig cyclization pathway, where the presence of an electron-withdrawing group at the triple bond was key for the success of the reaction. Optimization studies that broaden the synthetic scope and applications of the reaction are currently under investigation.

5.4 Acknowledgments

This research work was conducted with a strong support from Prof. Dr. E. Gómez-Bengoa (University of the Basque Country). Dr. P. T. Tinnemans (Radboud University) is kindly acknowledged for the crystal structure determination of compound (*E*)-**2a**. Huub van Amerongen is gratefully acknowledged for the preparation of some starting materials and optimization of the reaction conditions.

5.5 Experimental Section

Experimental studies: for general experimental details see Section 3.5. If stated, reactions were performed in a Biotage Initiator+ Microwave Synthesizer under a nitrogen atmosphere.

Computational studies: all structures were initially optimized using density functional theory (DFT) by using the B3LYP functional as implemented in Gaussian 09. Optimizations were carried out in a solvent model (IEFPCM, solvent = toluene) by using the 6-31G** basis set for non-metallic atoms and Stuttgart/Dresden (SDD) effective core potential for palladium. The calculation of the reaction species involves a correction to the free energy, that takes into account the change in degrees of freedom, e.g., association/dissociation steps. The critical stationary points were characterized by frequency calculations in order to verify that they have the right number of imaginary frequencies, and the intrinsic reaction coordinates (IRC) were followed to verify the energy profiles connecting the key transition structures to the correct associated local minima. The energies showed in this chapter have been refined by single-point calculations with the M06 functional and def2tzvpp basis set on the previously optimized structures. The values

correspond to free Gibbs energies and are given in kcal/mol. These energies are relative to the initial mixtures of starting material and corresponding palladium complexes, marked as G = 0.0 kcal/mol in each figure. Cartesian coordinates of the structures involved in the computational study can be found here.[25]

Synthesis of Sulfonamides 10a–f

General procedure:[26] The sulfonyl chloride (11 mmol, 1.1 equiv) was added portionwise to a solution of the amine (10 mmol, 1 equiv) and pyridine (950 mg, 12 mmol, 1.2 equiv) in CH_2Cl_2 (30 mL) with stirring. The reaction mixture was then stirred at 23 °C for 12 h before evaporation of CH_2Cl_2 and quenching the dry crude product with an aqueous NaOH solution (2 N, 100 mL). The aqueous solution was rinsed with diethyl ether (2 × 50 mL), then acidified with concentrated HCl and extracted with CH_2Cl_2 (3 × 50 mL). The combined organic washings were dried over sodium sulfate and concentrated in vacuo. The obtained crude product was used directly in the next step without further purification.

4-Methyl-*N*-phenylbenzenesulfonamide 10a.

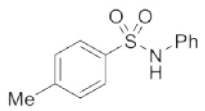

10a

Sulfonamide **10a** was prepared from aniline (0.9 g, 10 mmol) and 4-methylbenzenesulfonyl chloride (2.1 g, 11 mmol) according to the general procedure and obtained as a white solid (2.3 g, 92%). **^{1}H NMR** [400 MHz, δ (ppm), $CDCl_3$]: 2.35 (s, 3 H), 6.61 (bs, 1 H), 7.02–7.10 (m, 2 H), 7.12–7.25 (m, 5 H), 7.62–7.68 (m, 2 H). **^{13}C NMR** [101 MHz, δ (ppm), $CDCl_3$]: 21.6, 121.5, 125.1, 127.5, 129.2, 129.6, 136.0, 136.4, 143.9. These data were in accordance to those reported in the literature.[27]

***N*-Phenylbenzenesulfonamide 10b.**

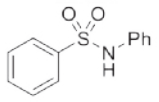

10b

Sulfonamide **10b** was prepared from aniline (0.9 g, 10 mmol) and benzenesulfonyl chloride (1.9 g, 11 mmol) according to the general procedure and obtained as a white solid (2.1 g, 90%). **^{1}H NMR** [400 MHz, δ (ppm), $CDCl_3$]: 6.58 (bs, 1 H), 7.02–7.09 (m, 2 H), 7.09–7.18 (m, 1 H), 7.20–7.29 (m, 2 H), 7.40–7.48 (m, 2 H), 7.50–7.58 (m, 1 H), 7.72–7.79 (m, 2 H). **^{13}C NMR** [101 MHz, δ (ppm), $CDCl_3$]: 121.6, 125.4, 127.3, 129.3, 129.7, 133.0, 136.5, 139.0. These data were in accordance to those reported in the literature.[27]

4-Methoxy-*N*-phenylbenzenesulfonamide 10c.

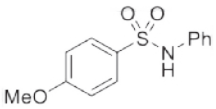

10c

Sulfonamide **10c** was prepared from aniline (0.9 g, 10 mmol) and 4-methoxybenzenesulfonyl chloride (2.3 g, 11 mmol) according to the general procedure and obtained as a white solid (2.1 g, 81%). **^{1}H NMR** [400 MHz, δ (ppm), $CDCl_3$]: 3.82 (s, 3 H), 6.70 (bs, 1 H), 6.81–6.96 (m, 2 H), 7.03–7.15 (m, 3 H), 7.18–7.31 (m, 2 H), 7.59–7.78 (m, 2 H). **^{13}C NMR** [101 MHz, δ (ppm), $CDCl_3$]: 55.7, 114.3, 121.6, 125.2, 129.4, 129.5, 130.7, 136.9, 163.2. These data were in accordance to those reported in the literature.[27]

4-Nitro-*N*-phenylbenzenesulfonamide 10d.

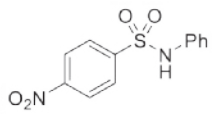

10d

Sulfonamide **10d** was prepared from aniline (0.9 g, 10 mmol) and 4-nitrobenzenesulfonyl chloride (2.4 g, 11 mmol) according to the general procedure and obtained as a light yellow solid (2.6 g, 94%). **^{1}H NMR** [400 MHz, δ (ppm), $CDCl_3$]: 6.02 (bs, 1 H), 7.07–7.32 (m, 5 H), 7.89–7.93 (m, 2 H), 8.22–8.30 (m, 2 H). **^{13}C NMR** [101 MHz, δ (ppm), $CDCl_3$]: 122.4, 124.3, 126.6, 128.7, 129.9, 135.2, 144.5, 150.3. These data were in accordance to those reported in the literature.[28]

***N*-Benzyl-4-methylbenzenesulfonamide 10e.**

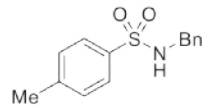

10e

Sulfonamide **10e** was prepared from benzylamine (1.1 g, 10 mmol) and 4-methylbenzenesulfonyl chloride (2.1 g, 11 mmol) according to the general procedure and obtained as a white solid (2.4 g, 91%). **^{1}H NMR** [400 MHz, δ (ppm), $CDCl_3$]: 2.32 (s, 3 H), 4.02 (d, J = 6.5 Hz, 2 H), 6.74 (t, J = 6.5 Hz, 1 H), 7.05–7.21 (m, 5 H), 7.27–7.31 (m, 2 H), 7.64–7.71 (m, 2 H). **^{13}C NMR** [101 MHz, δ (ppm), $CDCl_3$]: 21.7, 48.3, 128.3, 128.4, 129.1, 129.5, 130.9, 139.1, 139.2, 144.3. These data were in accordance to those reported in the literature.[29]

***N*,4-Dimethylbenzenesulfonamide 10f.**

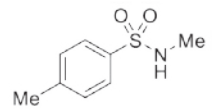

10f

Sulfonamide **10f** was prepared from methylamine hydrochloride (0.68 g, 10 mmol) and 4-methylbenzenesulfonyl chloride (2.1 g, 11 mmol) according to the general procedure and obtained as brown oil (1.7 g, 89%). **^{1}H NMR** [400 MHz, δ (ppm), $CDCl_3$]: 2.42 (s, 3 H), 2.62 (d, J = 5.5 Hz, 3 H), 4.45 (bs, 1 H), 7.29–7.33 (m, 2 H), 7.70–7.76 (m, 2 H). **^{13}C NMR** [101 MHz, δ (ppm), $CDCl_3$]: 21.2, 29.5, 127.3, 129.8, 135.7, 143.3. These data were in accordance to those reported in the literature.[30]

Synthesis of *N*-(1,2-Dichlorovinyl) Sulfonamides 11a–f

General procedure: The sulfonamide (8 mmol, 1.0 equiv) was added dropwise at 0 °C to a suspension of sodium hydride (60% dispersion in mineral oil, 670 mg, 16.8 mmol, 2.1 equiv) in DMF (30 mL) and the reaction mixture was allowed to warm to 23 °C during 2 h. Trichloroethene (800 µL, 8.8 mmol, 1.1 equiv) was slowly added to this solution and the resulting reaction mixture was then stirred at 50 °C for 16 h. After cooling to 23 °C, the reaction mixture was quenched with water (300 mL) and extracted with AcOEt (3 × 50 mL). The combined organic extracts were dried over sodium sulfate, concentrated in vacuo and the crude residue was purified by column chromatography as indicated. The *E*-configuration of the obtained products including the new compounds was assigned based on the ^{1}H NMR spectra and X-ray crystallography data known in the literature.[15]

***N*-[(*E*)-1,2-Dichlorovinyl]-4-methyl-*N*-phenylbenzenesulfonamide 11a.**

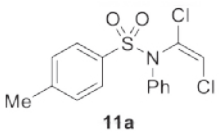

11a

Column chromatography (heptane/AcOEt 40:1→10:1) afforded product **11a** as a white solid (2.5 g, 91%). R_F (silica gel, heptane/AcOEt 1:1): 0.70 (UV, $KMnO_4$ solution). **^{1}H NMR** [400 MHz, δ (ppm), $CDCl_3$]: 2.41 (s, 3 H), 6.46 (s, 1 H), 7.19–7.27 (m, 2 H), 7.30–7.39 (m, 5 H), 7.61–7.69 (m, 2 H). **^{13}C NMR** [101 MHz, δ (ppm), $CDCl_3$]: 21.7, 120.5, 128.6, 128.8, 129.1, 129.3, 129.4, 130.7, 135.6, 137.7, 144.6. These data were in accordance to those reported in the literature.[31]

***N*-[(*E*)-1,2-Dichlorovinyl]-*N*-phenylbenzenesulfonamide 11b.**

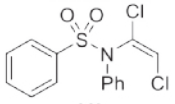

11b

Column chromatography (heptane/AcOEt 40:1→10:1) afforded product **11b** as a yellow oil (1.9 g, 72%). R_F (silica gel, heptane/AcOEt 10:1): 0.34 (UV, $KMnO_4$ solution). **^{1}H NMR** [400 MHz, δ (ppm), $CDCl_3$]: 6.46 (s, 1 H), 7.30–7.39 (m, 5 H), 7.43–7.50 (m, 2 H), 7.58–7.63 (m, 1 H), 7.75–7.80 (m, 2 H). **^{13}C NMR** [101 MHz, δ (ppm), $CDCl_3$]: 120.7, 128.6, 128.75, 128.79, 129.2, 129.4, 130.6, 133.6, 137.6, 138.5. **FTIR** [$\tilde{\nu}$ (cm^{-1})]: 811, 1089, 1169, 1363, 1489, 2934, 3086. **HRMS** (ESI^+) calcd. for $(C_{14}H_{11}Cl_2NO_2S + H)^+$ 327.9966, found 327.9954.

N-[(E)-1,2-Dichlorovinyl]-4-methoxy-N-phenylbenzenesulfonamide 11c.

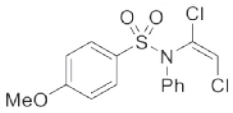

11c

Column chromatography (heptane/AcOEt 40:1→10:1) afforded product **11c** as a yellow oil (2.5 g, 87%). R_F (silica gel, heptane/AcOEt 7:1): 0.23 (UV, $KMnO_4$ solution). **^{1}H NMR** [400 MHz, δ (ppm), $CDCl_3$]: 3.86 (s, 3 H), 6.45 (s, 1 H), 6.86–6.98 (m, 2 H), 7.29–7.41 (m, 5 H), 7.65–7.73 (m, 2 H). **^{13}C NMR** [101 MHz, δ (ppm), $CDCl_3$]: 55.6, 113.9, 120.4, 128.7, 129.0, 129.3, 130.0, 130.7, 130.9, 137.8, 163.6. **FTIR** [$\bar{\nu}$ (cm^{-1})]: 809, 1089, 1160, 1261, 1361, 1489, 1594, 2945, 3085. **HRMS** (ESI$^+$) calcd. for $(C_{15}H_{13}Cl_2NO_3S + H)^+$ 358.0071, found 358.0092.

N-[(E)-1,2-Dichlorovinyl]-4-nitro-N-phenylbenzenesulfonamide 11d.

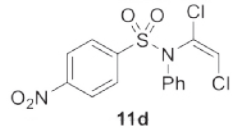

11d

Column chromatography (heptane/AcOEt 20:1→2:1) afforded product **11d** as a white solid (2.5 g, 82%). R_F (silica gel, heptane/AcOEt 10:1): 0.11 (UV, $KMnO_4$ solution). **^{1}H NMR** [400 MHz, δ (ppm), $CDCl_3$]: 6.51 (s, 1 H), 7.31–7.49 (m, 5 H), 7.81–7.99 (m, 2 H), 8.21–8.40 (m, 2 H). **^{13}C NMR** [101 MHz, δ (ppm), $CDCl_3$]: 121.3, 124.0, 128.7, 129.72, 129.77, 129.83, 129.84, 137.0, 144.1, 150.6. **FTIR** [$\bar{\nu}$ (cm^{-1})]: 685, 738, 1094, 1171, 1348, 1530, 3082, 3102. **HRMS** (ESI$^+$) calcd. for $(C_{14}H_{10}Cl_2N_2O_4S + H)^+$ 372.9817, found 372.9834.

N-Benzyl-N-[(E)-1,2-dichlorovinyl]-4-methylbenzenesulfonamide 11e.

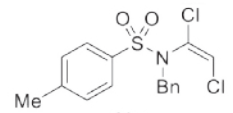

11e

Column chromatography (heptane/AcOEt 40:1→4:1) afforded product **11e** as a white solid (2.1 g, 73%). R_F (silica gel, heptane/AcOEt 10:1): 0.23 (UV, $KMnO_4$ solution). **^{1}H NMR** [400 MHz, δ (ppm), $CDCl_3$]: 2.47 (s, 3 H), 3.72–4.81 (bs, 2 H), 6.27 (s, 1 H), 7.28–7.34 (m, 5 H), 7.32–7.37 (m, 2 H), 7.80–7.86 (m, 2 H). **^{13}C NMR** [101 MHz, δ (ppm), $CDCl_3$]: 21.7, 52.0, 121.7, 128.2, 128.3, 129.3, 129.4, 129.8, 133.5, 135.3, 144.7. These data were in accordance to those reported in the literature.[15] Peak spanning 3.72–4.81 ppm was unresolved due to rotameric forms of this molecule.

N-[(E)-1,2-Dichlorovinyl]-N,4-dimethylbenzenesulfonamide 11f.

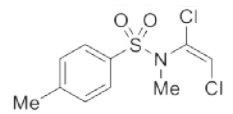

11f

Column chromatography (heptane/AcOEt 40:1→10:1) afforded the product **11f** as brown oil (1.4 g, 64%). R_F (silica gel, heptane/AcOEt 10:1): 0.13 (UV, $KMnO_4$ solution). **^{1}H NMR** [400 MHz, δ (ppm),

$CDCl_3$]: 2.45 (s, 3 H), 2.94 (s, 3 H), 6.39 (s, 1 H), 7.31–7.37 (m, 2 H), 7.79–7.85 (m, 2 H). **^{13}C NMR** [101 MHz, δ (ppm), $CDCl_3$]: 21.7, 37.9, 121.4, 127.8, 129.2, 129.5, 132.4, 143.2. **FTIR** [$\bar{\nu}$ (cm^{-1})]: 693, 722, 1084, 1160, 1333, 1498, 2986, 3012. **HRMS** (ESI^+) calcd. for $(C_{10}H_{11}Cl_2NO_2S + H)^+$ 372.9817, found 372.9834.

Synthesis of Sulfonyl Ynamines 1a–k

Sulfonyl ynamines **1a**, **1d**, **1e**, **1g**, **1h**, **1i**, **1j**, and **1k** were prepared according to the general procedure A, **1b** and **1c** were prepared from **1d** according to the general procedure B, and **1f** was prepared from **1d** according to the general procedure C.

General procedure A:[31] *n*Butyllithium (1.6 M in THF, 3.8 mL, 6 mmol, 2.1 equiv) was slowly added to a stirred solution of 1,2-dichlorovinyl sulfonamide (5 mmol, 1.0 equiv) in THF (30 mL) under an argon atmosphere at –78 °C. After stirring for 1 h, the lithium acetylide was treated with the corresponding electrophile and stirred for 1 h at –78 °C. The mixture was allowed to warm to 23 °C and stirred for 2–3 h. The reaction mixture was quenched with brine (100 mL) and extracted with Et_2O (2 × 50 mL). The combined organic extracts were dried over sodium sulfate, concentrated in vacuo, and the crude residue was purified by column chromatography as indicated.

General procedure B:[17] Sulfonyl ynamine **1d** (1.0 g, 3.7 mmol, 1.0 equiv), CuI (70 mg, 0.37 mmol, 0.1 equiv) and *N*,*N*-diisopropylethylamine (1.5 mL, 7.4 mmol, 2.0 equiv) were dissolved in chloroform (20 mL) under a nitrogen atmosphere. After 30 min, the acyl chloride (5.6 mmol, 1.5 equiv) was added and the mixture was stirred until completion as determined by TLC. Solvent was removed in vacuo and the crude residue was purified by column chromatography as indicated.

General procedure C:[18] Sulfonyl ynamine **1d** (1.0 g, 3.7 mmol, 1.0 equiv), iodobenzene (830 mg, 4.1 mmol, 1.1 equiv), and $[Pd(PPh_3)_4]$ (214 mg, 0.185 mmol, 0.05 equiv) were dissolved in a Et_3N/toluene mixture (2:1, 36 mL) under a nitrogen atmosphere. The solution was stirred at 23 °C for 10 min and CuI (11 mg, 0.06 mmol, 0.015 equiv) was then added. After heating the reaction mixture at 60 °C for 12 h, the mixture was diluted with AcOEt, filtered through a diatomaceous earth pad, and concentrated in vacuo. The resulting crude residue was purified by silica gel flash column chromatography as indicated.

Ethyl 3-(4-methyl-*N*-phenylbenzenesulfonamido)propanoate 1a.

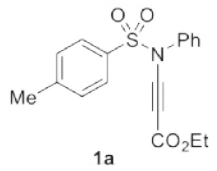

1a

Sulfonyl ynamine **1a** was prepared according to the general procedure A using 1,2-dichlorovinyl sulfonamide **11a** (1.7 g, 5.0 mmol). The resulting lithium acetylide was treated with freshly distilled ethyl chloroformate (714 µL, 7.5 mmol) at –78 °C for 15 min and at 23 °C for 2 h. Column chromatography (heptane/AcOEt 40:1→10:1; silica gel was washed with 1% Et_3N in heptane before being used for column chromatography) afforded product **1a** as a white solid (1.4 g, 82%). R_F (silica gel, heptane/AcOEt 10:1): 0.11 (UV, $KMnO_4$ solution). **^{1}H NMR** [400 MHz, δ (ppm), $CDCl_3$]: 1.31 (t, J = 7.1 Hz, 3 H), 2.46 (s, 3 H), 4.24 (q, J = 7.1 Hz, 2 H), 7.16–7.23 (m, 2 H), 7.29–7.34 (m, 2 H), 7.34–7.38 (m, 3 H), 7.58–7.67 (m, 2 H). **^{13}C NMR** [101 MHz, δ (ppm), $CDCl_3$]: 14.2, 21.8, 61.7, 66.6, 82.2, 126.5, 128.4, 129.3, 129.6, 130.0, 133.1, 137.5, 145.9, 154.8. These data were in accordance to those reported in the literature.[32]

***N*-(4,4-Dimethyl-3-oxopent-1-yn-1-yl)-4-methyl-*N*-phenylbenzenesulfonamide 1b.**

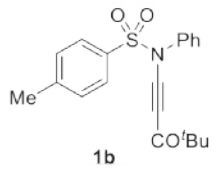

1b

Sulfonyl ynamine **1b** was prepared according to the general procedure B. The reaction with pivaloyl chloride (690 µL, 6.6 mmol) was performed at 30 °C for 18 h. Column chromatography (toluene; silica gel was washed with 1% Et_3N in heptane before being used for column chromatography) afforded product **1b** as a light yellow oil (1.1 g, 79%). R_F (silica gel, toluene): 0.32 (UV, $KMnO_4$ solution). **^{1}H NMR** [400 MHz, δ (ppm), $CDCl_3$]: 1.20 (s, 9 H), 2.40 (s, 3 H), 7.16–7.20 (m, 2 H), 7.24–7.28 (m, 2 H), 7.30–7.34 (m, 3 H), 7.53–7.59 (m, 2 H). **^{13}C NMR** [101 MHz, δ (ppm), $CDCl_3$]: 21.6, 26.3, 44.5, 73.6, 89.1, 126.3, 127.4, 128.3, 129.1, 129.3, 129.7, 133.2, 145.6, 193.2. These data were in accordance to those reported in the literature.[17]

4-Methyl-*N*-(3-oxo-3-phenylprop-1-yn-1-yl)-*N*-phenylbenzenesulfonamide 1c.

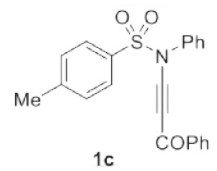

1c

Sulfonyl ynamine **1c** was prepared according to the general procedure B. The reaction with benzoyl chloride (767 µL, 6.6 mmol) was performed at 30 °C for 24 h. Column chromatography (heptane/AcOEt 20:1→10:1; silica gel was washed with 1% Et_3N in heptane before being used for column chromatography) afforded product **1c** as a light yellow oil (1.2 g, 86%). R_F (silica gel, heptane/AcOEt 10:1): 0.33 (UV, $KMnO_4$ solution). **^{1}H NMR** [400 MHz, δ (ppm), $CDCl_3$]: 2.42 (s, 3 H), 7.25–7.29 (m, 4 H), 7.36–7.41 (m, 3 H),

7.47–7.55 (m, 2 H), 7.60–7.65 (m, 3 H), 8.14–8.26 (m, 2 H). **^{13}C NMR** [101 MHz, δ (ppm), $CDCl_3$]: 21.7, 74.9, 90.2, 126.4, 128.2, 128.7, 129.2, 129.5, 129.9, 132.9, 133.5, 136.9, 137.1, 145.9, 176.8. These data were in accordance to those reported in the literature.[17]

_N_-Ethynyl-4-methyl-_N_-phenylbenzenesulfonamide 1d.

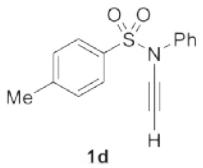

1d

Sulfonyl ynamine **1d** was prepared according to the general procedure A using 1,2-dichlorovinyl sulfonamide **11a** (1.7 g, 5.0 mmol). The resulting lithium acetylide was treated with water (10 mL) and the resulting mixture was stirred at 23 °C for 2 h. Column chromatography (heptane/AcOEt 20:1→10:1; silica gel was washed with 1% Et_3N in heptane before being used for column chromatography) afforded product **1d** as a light yellow oil (1.1 g, 81%). R_F (silica gel, heptane/AcOEt 10:1): 0.18 (UV, $KMnO_4$ solution). **^{1}H NMR** [400 MHz, δ (ppm), $CDCl_3$]: 2.44 (s, 3 H), 2.83 (s, 1 H), 7.23–7.34 (m, 7 H), 7.56–7.61 (m, 2 H). **^{13}C NMR** [101 MHz, δ (ppm), $CDCl_3$]: 21.7, 59.1, 75.8, 126.2, 128.2, 128.3, 129.0, 129.4, 132.7, 138.4, 145.0. These data were in accordance to those reported in the literature.[16]

4-Methyl-_N_-phenyl-_N_-[(trimethylsilyl)ethynyl]benzenesulfonamide 1e.

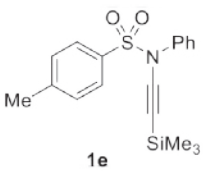

1e

Sulfonyl ynamine **1e** was prepared according to the general procedure A using 1,2-dichlorovinyl sulfonamide **11a** (1.7 g, 5.0 mmol). The resulting lithium acetylide was treated with trimethylsilyl chloride (952 µL, 7.5 mmol) at –78 °C for 15 min and at 23 °C for 2 h. Column chromatography (heptane/AcOEt 20:1; silica gel was washed with 1% Et_3N in heptane before being used for column chromatography) afforded product **1e** as a white solid (0.9 g, 52%). R_F (silica gel, heptane/AcOEt 10:1): 0.27 (UV, $KMnO_4$ solution). **^{1}H NMR** [400 MHz, δ (ppm), $CDCl_3$]: 0.17 (s, 9 H), 2.45 (s, 3 H), 7.21–7.25 (m, 2 H), 7.26–7.30 (m, 2 H), 7.30–7.36 (m, 3 H), 7.54–7.60 (m, 2 H). **^{13}C NMR** [101 MHz, δ (ppm), $CDCl_3$]: 0.16, 21.9, 73.4, 93.2, 126.3, 128.3, 128.6, 129.2, 129.5, 133.0, 138.7, 145.1. **FTIR** [$\tilde{\nu}$ (cm^{-1})]: 752, 834, 902, 1056, 1168, 1372, 1476, 1592, 2137, 2161, 2887, 3034. **HRMS** (ESI$^+$) calcd. for $(C_{18}H_{21}NO_2SSi + H)^+$ 344.1141, found 344.1134.

4-Methyl-*N*-phenyl-*N*-(phenylethynyl)benzenesulfonamide 1f.

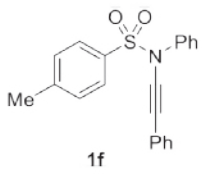

1f

Sulfonyl ynamine **1f** was prepared according to the general procedure C. Column chromatography (heptane/AcOEt 20:1→10:1; silica gel was washed with 1% Et_3N in heptane before being used for column chromatography) afforded product **1f** as a light yellow solid (1.0 g, 80%). R_F (silica gel, heptane/AcOEt 10:1): 0.27 (UV, $KMnO_4$ solution). **^{1}H NMR** [400 MHz, δ (ppm), $CDCl_3$]: 2.45 (s, 3 H), 7.27–7.36 (m, 9 H), 7.36–7.42 (m, 3 H), 7.61–7.65 (m, 2 H). **^{13}C NMR** [101 MHz, δ (ppm), $CDCl_3$]: 21.7, 70.6, 83.2, 122.7, 126.3, 126.5, 128.1, 128.32, 128.34, 129.0, 129.5, 131.4, 132.9, 139.0, 145.1. These data were in accordance to those reported in the literature.[33]

Ethyl 3-(*N*-phenylbenzenesulfonamido)propanoate 1g.

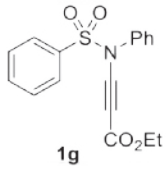

1g

Sulfonyl ynamine **1g** was prepared according to the general procedure A using 1,2-dichlorovinyl sulfonamide **11b** (1.6 g, 5.0 mmol). The resulting lithium acetylide was treated with freshly distilled ethyl chloroformate (714 μL, 7.5 mmol) at -78 °C for 15 min and at 23 °C for 2 h. Column chromatography (toluene; silica gel was washed with 1% Et_3N in heptane before being used for column chromatography) afforded product **1g** as a white solid (1.2 g, 74%). R_F (silica gel, toluene): 0.35 (UV, $KMnO_4$ solution). **^{1}H NMR** [400 MHz, δ (ppm), $CDCl_3$]: 1.31 (t, J = 7.1 Hz, 3 H), 4.24 (q, J = 7.1 Hz, 2 H), 7.14–7.22 (m, 2 H), 7.30–7.41 (m, 3 H), 7.49–7.58 (m, 2 H), 7.64–7.73 (m, 1 H), 7.74–7.80 (m, 2 H). **^{13}C NMR** [101 MHz, δ (ppm), $CDCl_3$]: 14.2, 61.8, 66.5, 81.9, 126.6, 128.3, 129.27, 129.29, 129.5, 134.6, 135.8, 137.0, 154.0. **FTIR** [$\tilde{\nu}$ (cm^{-1})]: 685, 726, 1088, 1123, 1204, 1372, 1702, 2218, 2982. **HRMS** (ESI$^+$) calcd. for $(C_{17}H_{15}NO_4S + H)^+$ 330.0800, found 330.0812.

Ethyl 3-(4-methoxy-*N*-phenylbenzenesulfonamido)propanoate 1h.

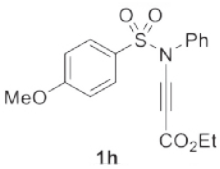

1h

Sulfonyl ynamine **1h** was prepared according to the general procedure A using 1,2-dichlorovinyl sulfonamide **11c** (1.8 g, 5.0 mmol). The resulting lithium acetylide was treated with freshly distilled ethyl chloroformate (714 μL, 7.5 mmol) at -78 °C for 15 min and at 23 °C for 2 h. Column chromatography (toluene; silica gel was washed with 1% Et_3N in heptane before being used for column chromatography) afforded product **1h** as colorless oil (1.5 g, 84%). R_F (silica gel, toluene): 0.25 (UV, $KMnO_4$ solution). **^{1}H NMR** [400 MHz, δ (ppm), $CDCl_3$]: 1.30 (t, J = 7.1 Hz, 3 H), 3.88 (s, 3 H), 4.23 (q, J = 7.1 Hz, 2 H), 6.91–

7.03 (m, 2 H), 7.15–7.24 (m, 2 H), 7.30–7.40 (m, 3 H), 7.64–7.73 (m, 2 H). **^{13}C NMR** [101 MHz, δ (ppm), $CDCl_3$]: 14.2, 55.8, 61.7, 66.6, 82.5, 114.4, 126.4, 127.2, 129.2, 129.5, 130.6, 137.2, 154.1, 164.4. **FTIR** [$\bar{\nu}$ (cm^{-1})]: 689, 1087, 1123, 1371, 1496, 1593, 1702, 2216, 2981. **HRMS** (ESI^+) calcd. for $(C_{18}H_{17}NO_5S + H)^+$ 360.0906, found 360.0922.

Ethyl 3-(4-nitro-*N*-phenylbenzenesulfonamido)propanoate 1i and ethyl 3,3-bis(4-nitro-*N*-phenyl-benzenesulfonamido)acrylate 30.

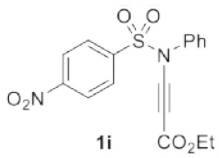

1i

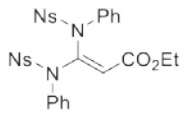

30

Sulfonyl ynamine **1i** and compound **30** were prepared according to the general procedure A using 1,2-dichlorovinyl sulfonamide **11d** (1.9 g, 5.0 mmol). The resulting lithium acetylide was treated with freshly distilled ethyl chloroformate (714 µL, 7.5 mmol) at –78 °C for 15 min and at 23 °C for 3 h. Column chromatography (toluene; silica gel was washed with 1% Et_3N in heptane before being used for column chromatography) afforded products **1i** (0.8 g, 42%) and **30** (1.3 g, 41%) as white solids. Product **30** was a common side product during the course of this reaction.[34] Compound **1i**: R_F (silica gel, toluene): 0.33 (UV, $KMnO_4$ solution). **^{1}H NMR** [400 MHz, δ (ppm), $CDCl_3$]: 1.32 (t, J = 7.1 Hz, 3 H), 4.25 (q, J = 7.1 Hz, 2 H), 7.17–7.23 (m, 2 H), 7.36–7.46 (m, 3 H), 7.92–8.00 (m, 2 H), 8.33–8.42 (m, 2 H). **^{13}C NMR** [101 MHz, δ (ppm), $CDCl_3$]: 14.1, 62.0, 66.5, 83.7, 124.5, 126.5, 129.7, 129.81, 129.84, 136.5, 140.9, 150.7, 153.6. **FTIR** [$\bar{\nu}$ (cm^{-1})]: 690, 740, 854, 1086, 1126, 1184, 1206, 1348, 1533, 1593, 1706, 2223, 2925, 3107. **HRMS** (ESI^+) calcd. for $(C_{17}H_{14}N_2O_6S + H)^+$ 375.0651, found 375.0659. Compound **30**: R_F (silica gel, toluene): 0.07 (UV, $KMnO_4$ solution). **^{1}H NMR** [400 MHz, δ (ppm), $CDCl_3$]: 1.41 (t, J = 7.1 Hz, 3 H), 4.33 (q, J = 7.1 Hz, 2 H), 6.14 (s, 1 H), 7.11–7.16 (m, 2 H), 7.20–7.23 (m, 2 H), 7.24–7.27 (m, 2 H), 7.33–7.38 (m, 2 H), 7.40–7.45 (m, 2 H), 7.45–7.50 (m, 3 H), 7.52–7.57 (m, 1 H), 7.93–8.00 (m, 2 H), 8.09–8.18 (m, 2 H). **^{13}C NMR** [101 MHz, δ (ppm), $CDCl_3$]: 14.1, 61.6, 110.0, 117.5, 123.4, 124.1, 129.4, 129.6, 129.7, 129.93, 129.97, 129.99, 130.0, 136.0, 136.3, 139.9, 143.4, 144.2, 149.9, 150.4, 163.9. **FTIR** [$\bar{\nu}$ (cm^{-1})]: 694, 740, 855, 1086, 1139, 1172, 1202, 1350, 1531, 1720, 3106. **HRMS** (ESI^+) calcd. for $(C_{29}H_{24}N_4O_{10}S_2 + H)^+$ 653.1012, found 653.1034.

Ethyl 3-(*N*,4-dimethylbenzenesulfonamido)propanoate 1j.

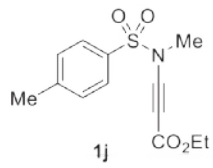

1j

Sulfonyl ynamine **1j** was prepared according to the general procedure A using 1,2-dichlorovinyl sulfonamide **11f** (1.4 g, 5.0 mmol). The resulting lithium acetylide was treated with freshly distilled ethyl chloroformate (714 µL, 7.5 mmol) at –78 °C for 15 min and at 23 °C for 2 h. Column chromatography (heptane/AcOEt 20:1→10:1; silica gel was washed with 1% Et_3N in heptane before being used for column chromatography) afforded product **1j** as a white solid (1.0 g, 71%). R_F (silica gel, heptane/AcOEt 1:1): 0.6 (UV, $KMnO_4$ solution). **^{1}H NMR** [400 MHz, δ (ppm), $CDCl_3$]: 1.31 (t, J = 7.1 Hz, 3 H), 2.47 (s, 3 H), 3.17 (s, 3 H), 4.23 (q, J = 7.1 Hz, 2 H), 7.35–7.44 (m, 2 H), 7.78–7.92 (m, 2 H). **^{13}C NMR** [101 MHz, δ (ppm), $CDCl_3$]: 14.2, 21.8, 38.5, 61.6, 66.0, 83.5, 128.0, 130.2, 133.0, 145.8, 154.1. These data were in accordance to those reported in the literature.[35]

Ethyl 3-(*N*-benzyl-4-methylbenzenesulfonamido)propanoate 1k.

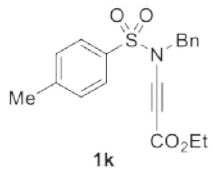

1k

Sulfonyl ynamine **1k** was prepared according to the general procedure A using 1,2-dichlorovinyl sulfonamide **11e** (1.8 g, 5.0 mmol). The resulting lithium acetylide was treated with freshly distilled ethyl chloroformate (714 µL, 7.5 mmol) at –78 °C for 15 min and at 23 °C for 2 h. Column chromatography (heptane/AcOEt 40:1→10:1; silica gel was washed with 1% Et_3N in heptane before being used for column chromatography) afforded product **1k** as a white solid (1.6 g, 87%). R_F (silica gel, heptane/AcOEt 10:1): 0.17 (UV, $KMnO_4$ solution). **^{1}H NMR** [400 MHz, δ (ppm), $CDCl_3$]: 1.28 (t, J = 7.1 Hz, 3 H), 2.44 (s, 3 H), 4.18 (q, J = 7.1 Hz, 2 H), 4.62 (s, 2 H), 7.24–7.33 (m, 7 H), 7.68–7.75 (m, 2 H). **^{13}C NMR** [101 MHz, δ (ppm), $CDCl_3$]: 14.2, 21.6, 55.3, 61.4, 68.1, 82.5, 127.6, 128.5, 128.6, 129.3, 129.7, 133.5, 134.1, 145.4, 153.9. These data were in accordance to those reported in the literature.[15]

Products of Palladium-Catalyzed Intramolecular Hydroarylation of Sulfonyl Ynamine 1a

General procedure: Sulfonyl ynamine **1** (343 mg, 1.0 mmol, 1.0 equiv) was dissolved in toluene (10 mL) under a nitrogen atmosphere in a Biotage microwave vial (10.0–20.0 mL) equipped with a magnetic stirring bar. $Pd(OAc)_2$ (11 mg, 0.05 mmol, 0.05 equiv) and tri(*p*-tolyl)phosphine (30 mg, 0.1 mmol, 0.1 equiv) were added at 23 °C. The vial was covered with a Teflon septum and secured via a crimped aluminum cap. The reaction was irradiated in a microwave at 100 °C for 18 h (30 second pre-stir, fixed hold time on, low absorbance level). The

reaction mixture was quenched with brine (50 mL) and extracted with AcOEt (2 × 20 mL). The resulting organic extracts were dried over sodium sulfate, concentrated in vacuo, and the crude residue was purified by column chromatography (toluene; silica gel was washed with 1% Et_3N in toluene before being used for column chromatography).

Ethyl (*E*)-2-(5-methyl-1,1-dioxo-2-phenyl-1,2-benzothiazol-3(2*H*)-ylidene)acetate (*E*)-2a.

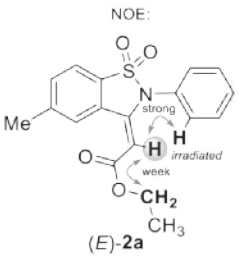

(*E*)-**2a**

Column chromatography afforded product (*E*)-**2a** as a white solid (127 mg, 37%). R_F (silica gel, toluene): 0.33 (UV, $KMnO_4$ solution). **^{1}H NMR** [400 MHz, δ (ppm), $CDCl_3$]: 1.26 (t, J = 7.1 Hz, 3 H), 2.57 (s, 3 H), 4.18 (q, J = 7.1 Hz, 2 H), 5.11 (s, 1 H), 7.47–7.51 (m, 2 H), 7.54–7.62 (m, 4 H), 7.82 (d, J = 7.9 Hz, 1 H), 9.23 (quint, J = 0.8 Hz, 1 H). **^{13}C NMR** [101 MHz, δ (ppm), $CDCl_3$]: 14.2, 22.2, 60.5, 97.0, 120.9, 127.4, 129.8, 130.36, 130.39, 130.43, 130.5, 131.0, 133.1, 144.8, 146.2, 166.1. **FTIR** [$\bar{\nu}$ (cm^{-1})]: 714, 902, 1089, 1174, 1302, 1512, 1635, 1737, 2992. **HRMS** (ESI$^+$) calcd. for $(C_{18}H_{17}NO_4S + H)^+$ 344.0957, found 344.0966.

Ethyl (*Z*)-2-(5-methyl-1,1-dioxo-2-phenyl-1,2-benzothiazol-3(2*H*)-ylidene)acetate (*Z*)-2a.

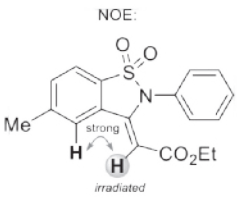

(*Z*)-**2a**

Column chromatography afforded product (*Z*)-**2a** as a white solid (7 mg, 2%). R_F (silica gel, toluene): 0.27 (UV, $KMnO_4$ solution). **^{1}H NMR** [400 MHz, δ (ppm), $CDCl_3$]: 1.01 (t, J = 7.1 Hz, 3 H), 2.54 (s, 3 H), 3.66 (q, J = 7.1 Hz, 2 H), 5.83 (s, 1 H), 7.36–7.49 (m, 5 H), 7.55 (m, J = 8.0, 1.2, 0.6 Hz, 1 H), 7.62 (quint, J = 0.6 Hz, 1 H), 7.79 (d, J = 8.0 Hz, 1 H). **^{13}C NMR** [101 MHz, δ (ppm), $CDCl_3$]: 13.9, 22.0, 60.4, 93.0, 121.5, 122.0, 126.9, 128.6, 128.9, 129.5, 130.2, 133.1, 134.9, 140.2, 144.9, 164.0. **FTIR** [$\bar{\nu}$ (cm^{-1})]: 693, 907, 1082, 1145, 1266, 1327, 1494, 1635, 1708, 3029. **HRMS** (ESI$^+$) calcd. for $(C_{18}H_{17}NO_4S + H)^+$ 344.0957, found 344.0943.

4-Methyl-*N*-phenylbenzenesulfonamide 10a.

Column chromatography afforded product **10a** as colorless oil (52 mg, 21%). The spectroscopic data are identical to those reported above.

Ethyl 3,3-bis(4-methyl-*N*-phenylbenzenesulfonamido)acrylate 15.

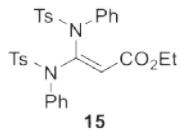

15

Column chromatography afforded product **15** as a colorless oil (6 mg, 1%). R_F (silica gel, toluene): 0.06 (UV, $KMnO_4$ solution). **^{1}H NMR** [400 MHz, δ (ppm), $CDCl_3$]: 1.39 (t, J = 7.1 Hz, 3 H), 2.30 (s, 3 H), 2.38 (s, 3 H), 4.33 (q, J = 7.1 Hz, 2 H), 6.09 (s, 1 H), 6.86–6.94 (m, 4 H), 7.06–7.12 (m, 2 H), 7.12–7.19 (m, 6 H), 7.26–7.33 (m, 2 H), 7.33–7.40 (m, 3 H), 7.42–7.48 (m, 1 H). **^{13}C NMR** [101 MHz, δ (ppm), $CDCl_3$]: 14.1, 21.5, 21.6, 61.1, 115.5, 127.3, 128.18, 128.23, 128.93, 128.97, 129.1, 129.4, 129.5, 130.0, 130.2, 135.1, 136.0, 136.8, 137.1, 140.6, 143.5, 144.3, 164.7. **FTIR** [$\bar{\nu}$ (cm^{-1})]: 695, 814, 1087, 1139, 1167, 1362, 1489, 1531, 1719, 2981. **HRMS** (ESI^+) calcd. for $(C_{31}H_{30}N_2O_6S_2 + H)^+$ 591.1624, found 591.1638.

Ethyl (*E*)-3-(4-methyl-*N*-phenylbenzenesulfonamido)acrylate 16.

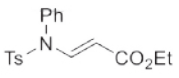

16

Column chromatography afforded product **16** as a colorless oil (21 mg, 6%). R_F (silica gel, toluene): 0.12 (UV, $KMnO_4$ solution). **^{1}H NMR** [400 MHz, δ (ppm), $CDCl_3$]: 1.24 (t, J = 7.1 Hz, 3 H), 2.44 (s, 3 H), 4.14 (q, J = 7.1 Hz, 2 H), 4.62 (d, J = 13.8 Hz, 1 H), 6.88–6.97 (m, 2 H), 7.27–7.32 (m, 2 H), 7.35–7.45 (m, 3 H), 7.53–7.60 (m, 2 H), 8.37 (d, J = 13.7 Hz, 1 H). **^{13}C NMR** [101 MHz, δ (ppm), $CDCl_3$]: 14.3, 21.7, 60.1, 100.0, 121.7, 127.8, 129.7, 129.86, 129.89, 134.8, 135.1, 143.9, 144.9, 167.1. **FTIR** [$\bar{\nu}$ (cm^{-1})]: 727, 906, 1089, 1170, 1368, 1624, 1737, 2245, 2981. **HRMS** (ESI^+) calcd. for $(C_{18}H_{19}NO_4S + H)^+$ 346.1113, found 346.1131.

Palladium-Catalyzed Intramolecular Hydroarylation of Sulfonyl Ynamines 1a–k

General procedure: Sulfonyl ynamine **1** (1.0 mmol, 1.0 equiv) was dissolved in toluene (10 mL) under a nitrogen atmosphere in a Biotage microwave vial (10.0–20.0 mL) equipped with a magnetic stirring bar. $Pd(OAc)_2$ (11 mg, 0.05 mmol, 0.05 equiv) and tri(*p*-tolyl)phosphine (30 mg, 0.1 mmol, 0.1 equiv) were added at 23 °C. The vial was covered with a Teflon septum and secured via a crimped aluminum cap. The reaction was irradiated in a microwave at 100 °C for 18 h (30 second pre-stir, Fixed Hold Time On, Low absorbance level). The reaction mixture was quenched with brine (50 mL) and extracted with AcOEt (2 × 20 mL). The resulting organic extracts were dried over sodium sulfate, concentrated in vacuo, and the crude residue was purified by column chromatography as indicated.

Ethyl (*E*)-2-(5-methyl-1,1-dioxo-2-phenyl-1,2-benzothiazol-3(2*H*)-ylidene)acetate (*E*)-2a

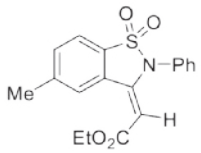

(*E*)-**2a**

(*E*)-1,2-Benzothiazole-1,1-dione **2a** was prepared according to general procedure using sulfonyl ynamine **1a** (343 mg, 1.0 mmol). *E*/*Z*-Ratio = 98:2 was determined by ^{1}H NMR spectroscopy. Column chromatography (toluene; silica gel was washed with 1% Et_3N in heptane before being used for column chromatography) afforded product (*E*)-**2a** as a white solid (127 mg, 37%). The spectroscopic data are identical to those reported above (see subsection "Products of Palladium-Catalyzed Intramolecular Hydroarylation of Sulfonyl Ynamine **1a**").

(*E*)-3,3-Dimethyl-1-(5-methyl-1,1-dioxo-2-phenyl-1,2-benzothiazol-3(2*H*)-ylidene)butan-2-one (*E*)-2b.

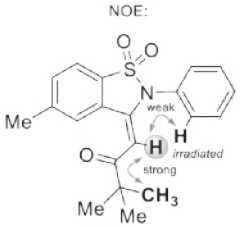

(*E*)-**2b**

(*E*)-1,2-Benzothiazole-1,1-dione **2b** was prepared according to the general procedure using sulfonyl ynamine **1b** (355 mg, 1.0 mmol). *E*/*Z*-Ratio > 99:1 was determined by ^{1}H NMR spectroscopy. Column chromatography (toluene; silica gel was washed with 1% Et_3N in heptane before being used for column chromatography) afforded product (*E*)-**2b** as a white solid (121 mg, 34%). R_F (silica gel, toluene): 0.28 (UV, $KMnO_4$ solution). **^{1}H NMR** [400 MHz, δ (ppm), $CDCl_3$]: 1.05 (s, 9 H), 2.57 (s, 3 H), 5.71 (s, 1 H), 7.48–7.53 (m, 2 H), 7.54–7.65 (m, 4 H), 7.82 (d, J = 7.9 Hz, 1 H), 9.10 (quint, J = 0.6 Hz, 1 H). **^{13}C NMR** [101 MHz, δ (ppm), $CDCl_3$]: 22.3, 26.8, 44.7, 101.5, 121.0, 127.8, 129.4, 130.4, 130.5, 130.6, 130.8, 130.9, 133.4, 145.1, 145.6, 204.3. **FTIR** [$\tilde{\nu}$ (cm^{-1})]: 695, 966, 1078, 1183, 1322, 1566, 1673, 2965. **HRMS** (ESI^+) calcd. for $(C_{20}H_{21}NO_3S + H)^+$ 356.1320, found 356.1343.

(*E*)-2-(5-methyl-1,1-dioxo-2-phenyl-1,2-benzothiazol-3(2*H*)-ylidene)-1-phenylethan-1-one (*E*)-2c.

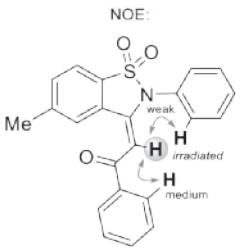

(*E*)-**2c**

(*E*)-1,2-Benzothiazole-1,1-dione **2c** was prepared according to the general procedure using sulfonyl ynamine **1c** (375 mg, 1.0 mmol). *E*/*Z*-Ratio = 98:2 was determined by ^{1}H NMR spectroscopy. Column chromatography (toluene; silica gel was washed with 1% Et_3N in heptane before being used for column chromatography) afforded product (*E*)-**2c** as a white solid (116 mg, 31%). R_F (silica gel, toluene): 0.31 (UV, $KMnO_4$ solution). **^{1}H NMR** [400 MHz, δ (ppm), $CDCl_3$]: 2.57 (s, 3 H), 6.09

(s, 1 H), 7.37–7.45 (m, 2 H), 7.48–7.55 (m, 1 H), 7.56–7.66 (m, 6 H), 7.72–7.79 (m, 2 H), 7.85 (d, J = 8.0 Hz, 1 H), 9.00 (quint, J = 0.5 Hz, 1 H). **^{13}C NMR** [101 MHz, δ (ppm), $CDCl_3$]: 22.2, 102.4, 121.1, 127.4, 127.7, 128.2, 128.6, 129.1, 130.5, 130.6, 130.7, 130.9, 132.8, 133.6, 139.4, 145.1, 146.4, 189.7. **FTIR** [$\tilde{\nu}$ (cm^{-1})]: 696, 959, 1185, 1323, 1565, 1653, 1724, 2922, 3064. **HRMS** (ESI^+) calcd. for $(C_{22}H_{17}NO_3S + H)^+$ 376.1007, found 376.1015.

Intramolecular Hydroarylation of 1d, 1e and 1f.

Sulfonyl ynamines **1d, 1e** or **1f** were submitted to the reaction conditions according to general procedure. ^{1}H NMR spectroscopy of the crude product indicated partial degradation of the starting material to 4-methyl-*N*-phenylbenzenesulfonamide **10a** and additional unidentified products. The formation of products **2d, 2e,** or **2f** was not observed.

Ethyl (*E*)-2-(1,1-dioxo-2-phenyl-1,2-benzothiazol-3(2*H*)-ylidene)acetate (*E*)-2g.

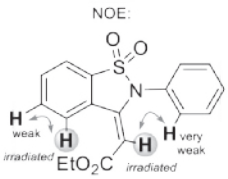

(*E*)-**2g**

(*E*)-1,2-Benzothiazole-1,1-dione **2g** was prepared according to the general procedure using sulfonyl ynamine **1g** (330 mg, 1.0 mmol). *E*/*Z*-Ratio = 98:2 was determined by ^{1}H NMR spectroscopy. Column chromatography (toluene; silica gel was washed with 1% Et_3N in heptane before being used for column chromatography) afforded product (*E*)-**2g** as a white solid (112 mg, 34%). R_F (silica gel, toluene): 0.31 (UV, $KMnO_4$ solution). **^{1}H NMR** [400 MHz, δ (ppm), $CDCl_3$]: 1.28 (t, J = 7.1 Hz, 3 H), 4.20 (q, J = 7.1 Hz, 2 H), 5.16 (s, 1 H), 7.46–7.56 (m, 2 H), 7.57–7.67 (m, 3 H), 7.76–7.85 (m, 2 H), 7.92–8.02 (m, 1 H), 9.44 (m, 1 H). **^{13}C NMR** [101 MHz, δ (ppm), $CDCl_3$]: 14.4, 60.7, 97.6, 121.3, 127.4, 129.9, 130.5, 130.6, 130.7, 131.2, 132.5, 133.3, 133.9, 146.2, 166.3. **FTIR** [$\tilde{\nu}$ (cm^{-1})]: 692, 910, 1045, 1099, 1157, 1186, 1324, 1619, 1708, 2925. **HRMS** (ESI^+) calcd. for $(C_{17}H_{15}NO_4S + H)^+$ 330.0800, found 330.0827.

Ethyl (*E*)-2-(5-methoxy-1,1-dioxo-2-phenyl-1,2-benzothiazol-3(2*H*)-ylidene)acetate (*E*)-2h.

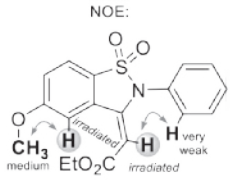

(*E*)-**2h**

(*E*)-1,2-Benzothiazole-1,1-dione **2h** was prepared according to the general procedure using sulfonyl ynamine **1h** (360 mg, 1.0 mmol). *E*/*Z*-Ratio = 95:5 was determined by ^{1}H NMR spectroscopy. Column chromatography (toluene; silica gel was washed with 1% Et_3N in heptane before being used for column chromatography) afforded product (*E*)-**2h** as a white solid (119 mg, 33%). R_F (silica gel, toluene): 0.17 (UV, $KMnO_4$ solution). **^{1}H NMR** [400 MHz, δ (ppm), $CDCl_3$]: 1.25 (t, J = 7.1 Hz, 3 H),

3.98 (s, 3 H), 4.16 (q, *J* = 7.1 Hz, 2 H), 5.12 (s, 1 H), 7.25 (dd, *J* = 8.7, 2.2 Hz, 1 H), 7.47–7.52 (m, 2 H), 7.53–7.64 (m, 3 H), 7.83 (d, *J* = 8.6 Hz, 1 H), 9.14 (d, *J* = 2.3 Hz, 1 H). **^{13}C NMR** [101 MHz, δ (ppm), $CDCl_3$]: 14.3, 56.1, 60.5, 97.2, 113.4, 119.7, 122.4, 125.1, 129.6, 130.43, 130.49, 130.53, 131.0, 146.3, 164.0, 166.2. **FTIR** [$\bar{\nu}$ (cm^{-1})]: 1103, 1183, 1252, 1307, 1473, 1583, 1621, 1707, 2988, 3118. **HRMS** (ESI^+) calcd. for $(C_{18}H_{17}NO_5S + H)^+$ 360.0906, found 360.0919.

Ethyl (*E*)-2-(5-nitro-1,1-dioxo-2-phenyl-1,2-benzothiazol-3(2*H*)-ylidene)acetate (*E*)-2i.

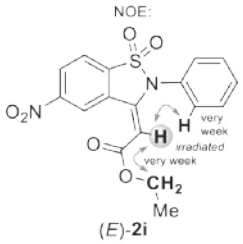

(*E*)-**2i**

(*E*)-1,2-Benzothiazole-1,1-dione **2i** was prepared according to the general procedure using sulfonyl ynamine **1i** (375 mg, 1.0 mmol). *E*/*Z*-Ratio > 99:1 was determined by ^{1}H NMR spectroscopy. Column chromatography (toluene; silica gel was washed with 1% Et_3N in heptane before being used for column chromatography) afforded product (*E*)-**2i** as a white solid (113 mg, 30%). R_F (silica gel, toluene): 0.28 (UV, $KMnO_4$ solution). **^{1}H NMR** [400 MHz, δ (ppm), $CDCl_3$]: 1.28 (t, *J* = 7.1 Hz, 3 H), 4.24 (q, *J* = 7.1 Hz, 2 H), 5.27 (s, 1 H), 7.46–7.56 (m, 2 H), 7.58–7.69 (m, 3 H), 8.12 (d, *J* = 8.5 Hz, 1 H), 8.61 (dd, *J* = 8.5, 1.9 Hz, 1 H), 10.43 (d, *J* = 1.9 Hz, 1 H). **^{13}C NMR** [101 MHz, δ (ppm), $CDCl_3$]: 14.2, 61.2, 99.9, 122.5, 125.6, 127.3, 129.1, 129.6, 130.7, 130.9, 131.1, 137.6, 143.8, 151.2, 165.6. **FTIR** [$\bar{\nu}$ (cm^{-1})]: 694, 740, 1095, 1113, 1186, 1341, 1537, 1706, 2926, 3111. **HRMS** (ESI^+) calcd. for $(C_{17}H_{14}N_2O_6S + H)^+$ 375.0651, found 375.0667.

Ethyl (*E*)-2-(2,5-dimethyl-1,1-dioxo-1,2-benzothiazol-3(2*H*)-ylidene)acetate (*E*)-2j.

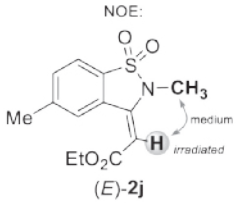

(*E*)-**2j**

(*E*)-1,2-Benzothiazole-1,1-dione **2j** was prepared according to the general procedure using sulfonyl ynamine **1j** (281 mg, 1.0 mmol). *E*/*Z*-Ratio = 95:5 was determined by ^{1}H NMR spectroscopy. Column chromatography (toluene; silica gel was washed with 1% Et_3N in heptane before being used for column chromatography) afforded product (*E*)-**2j** as colorless oil (87 mg, 31%). R_F (silica gel, toluene): 0.23 (UV, $KMnO_4$ solution). **^{1}H NMR** [400 MHz, δ (ppm), $CDCl_3$]: 1.35 (t, *J* = 7.1 Hz, 3 H), 2.54 (s, 3 H), 3.15 (s, 3 H), 4.25 (q, *J* = 7.1 Hz, 2 H), 5.33 (s, 1 H), 7.50 (d, *J* = 7.9 Hz, 1 H), 7.76 (d, *J* = 7.9 Hz, 1 H), 9.17 (s, 1 H). **^{13}C NMR** [101 MHz, δ (ppm), $CDCl_3$]: 14.3, 22.2, 26.5, 60.5, 95.0, 120.8, 127.9, 129.8, 130.5, 132.7, 144.8, 144.9, 166.0. **FTIR** [$\bar{\nu}$ (cm^{-1})]: 701, 823, 1039, 1137, 1159, 1315, 1619, 1708, 2982. **HRMS** (ESI^+) calcd. for $(C_{13}H_{15}NO_4S + H)^+$ 282.0800, found 282.0819.

Ethyl (*E*)-2-(2-benzyl-5-methyl-1,1-dioxo-1,2-benzothiazol-3(2*H*)-ylidene)acetate (*E*)-2k and ethyl (*E*)-2-[2-(4-methylbenzenesulfonyl)isoindolin-1-ylidene]acetate 17.

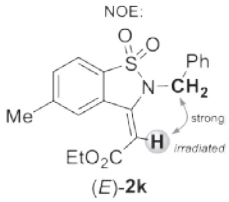

(*E*)-**2k**

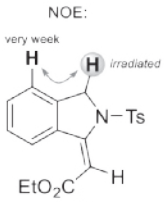

17

(*E*)-1,2-Benzothiazole-1,1-dione **2k** and compound **17** were prepared according to the general procedure using sulfonyl ynamine **1k** (357 mg, 1.0 mmol). *E*/*Z*-Ratio > 99:1 was determined by ^{1}H NMR spectroscopy. Column chromatography (toluene; silica gel was washed with 1% Et_3N in heptane before being used for column chromatography) afforded product (*E*)-**2k** as a white solid (93 mg, 26%) and product **17** as a colorless oil (36 mg, 10%). Compound (*E*)-**2k**: R_F (silica gel, toluene): 0.30 (UV, $KMnO_4$ solution). **^{1}H NMR** [400 MHz, δ (ppm), $CDCl_3$]: 1.26 (t, *J* = 7.1 Hz, 3 H), 2.53 (s, 3 H), 4.15 (q, *J* = 7.1 Hz, 2 H), 4.84 (s, 2 H), 5.28 (s, 1 H), 7.27–7.33 (m, 1 H), 7.34–7.40 (m, 2 H), 7.40–7.44 (m, 2 H), 7.52 (dd, *J* = 7.9, 0.6 Hz, 1 H), 7.81 (d, *J* = 7.9 Hz, 1 H), 9.13 (quint, *J* = 0.6 Hz, 1 H). **^{13}C NMR** [101 MHz, δ (ppm), $CDCl_3$]: 14.4, 22.4, 44.5, 60.6, 96.5, 121.0, 127.2, 127.8, 128.1, 129.1, 130.1, 130.4, 132.9, 134.1, 143.7, 145.1, 166.0. **FTIR** [$\bar{\nu}$ (cm^{-1})]: 670, 732, 831, 1136, 1168, 1311, 1626, 1706, 2986, 3098. **HRMS** (ESI^+) calcd. for $(C_{19}H_{19}NO_4S + H)^+$ 358.1113, found 358.1118. Compound **17**: R_F (silica gel, toluene): 0.21 (UV, $KMnO_4$ solution). **^{1}H NMR** [400 MHz, δ (ppm), $CDCl_3$]: 1.32 (t, *J* = 7.1 Hz, 3 H), 2.40 (s, 3 H), 4.19 (q, *J* = 7.1 Hz, 2 H), 5.02 (s, 2 H), 6.43 (s, 1 H), 7.28–7.39 (m, 4 H), 7.41–7.47 (m, 1 H), 7.76–7.83 (m, 2 H), 9.13 (d, *J* = 8.1 Hz, 1 H). **^{13}C NMR** [101 MHz, δ (ppm), $CDCl_3$]: 14.6, 21.8, 55.4, 60.1, 96.7, 121.9, 127.7, 128.4, 128.9, 130.1, 131.3, 133.0, 134.6, 138.1, 145.1, 152.0, 167.0. **FTIR** [$\bar{\nu}$ (cm^{-1})]: 667, 800, 1089, 1165, 1344, 1620, 1705, 2922. **HRMS** (ESI^+) calcd. for $(C_{19}H_{19}NO_4S + H)^+$ 358.1113, found 358.1132.

X-ray Crystallography of (*E*)-2a

General procedure: A high quality single crystal of (*E*)-**2a** was obtained by slow evaporation of the solvent. A saturated solution of (*E*)-**2a** in toluene was prepared and filtered over an Acrodisc HPLC syringe filter to ensure the absence of crystallites. The resulting filtrate was transferred to a scintillation flask that was sealed and equipped with a hollow needle to allow slow evaporation of the solvent. The acquired single crystal was subjected to single X-ray diffraction. Mercury software (Version 3.9; Cambridge Crystallographic Data Centre) was used to visualize the structure.

5.6 References and Notes

[1] (a) Dekorver, K. A.; Li, H.; Lohse, A. G.; Hayashi, R.; Lu, Z.; Zhang, Y.; Hsung, R. P. *Chem. Rev.* **2010**, *110*, 5064–5106; (b) Evano, G.; Coste, A.; Jouvin, K. *Angew. Chem. Int. Ed.* **2010**, *49*, 2840–2859; (c) Lu, T.; Hsung, R. P. *ARKIVOC* **2014**, *i*, 127–141; (d) Wang, X.-N.; Yeom, H.-S.; Fang, L.-C.; He, S.; Ma Z.-X.; Kedrowski, B. L.; Hsung, R. P. *Acc. Chem. Res.* **2014**, *47*, 560–578; (e) Cook A., M.; Wolf, C. *Tetrahedron Lett.* **2015**, *56*, 2377–2392.

[2] Zhang, Y.; Hsung, R. P.; Tracey, M. R.; Kurtz, K. C. M.; Vera, E. L. *Org. Lett.* **2004**, 6, 1151–1154.

[3] (a) Wezeman, T.; Zhong, S.; Nieger, M.; Bräse, S. *Angew. Chem. Int. Ed.* **2016**, *55*, 3823–3827; (b) Evano, G.; Lecomte, M.; Thilmany, P.; Theunissen, C. *Synthesis* **2017**, *49*, 3183–3214.

[4] (a) Greenaway, R. L.; Campbell, C. D.; Holton, O. T.; Russell, C. A.; Anderson, E. A. *Chem. Eur. J.* **2011**, *17*, 14366–14370; (b) García, P.; Harrak, Y.; Diab, L.; Cordier, P.; Ollivier, C.; Gandon, V.; Malacria, M.; Fensterbank, L.; Aubert, C. *Org. Lett.* **2011**, *13*, 2952–2955; (c) Rettenmeier, E.; Schuster, A. M.; Rudolph, M.; Rominger, F.; Gade, C. A.; Hashmi, A. S. K. *Angew. Chem. Int. Ed.* **2013**, *52*, 5880–5884; (d) Siva Reddy, A.; Leela Siva Kumari, A.; Saha, S.; Kumara Swamya, K. C. *Adv. Synth. Catal.* **2016**, *358*, 1625–1638.

[5] (a) Dateer, R. B.; Shaibu, B. S.; Liu, R.-S. *Angew. Chem. Int. Ed.* **2012**, *51*, 113–117; (b) Karad, S. N.; Bhunia, S.; Liu, R.-S. *Angew. Chem. Int. Ed.* **2012**, 51, 8722–8726; (c) Karad, S. N.; Liu, R. S. *Angew. Chem. Int. Ed.* **2014**, *53*, 9072–9076; (d) Shu, C.; Wang, Y.-H.; Zhou, B.; Li, X.-L.; Ping, Y.-F.; Lu, X.; Ye, L.-W. *J. Am. Chem. Soc.* **2015**, *137*, 9567–9570.

[6] (a) Bendikov, M.; Duong, H. M.; Bolanos, E.; Wudl, F. *Org. Lett.* **2005**, *7*, 783–786; (b) Gomes, F.; Fadel, A.; Rabasso, N. *J. Org. Chem.* **2012**, *77*, 5439–5444; (c) Brioche, J.; Meyer, C.; Cossy, J. *Org. Lett.* **2013**, *15*, 1626–1629; (d) Li, D.-Y.; Wei, Y.; Shi, M. *Eur. J. Org. Chem.* **2015**, 4108–4113.

[7] For 1,2-benzothiazole-1,1-diones **2** as inhibitors of γ-secretase, see: Castro Pineiro, J. L.; Hannam, J. C.; Harrison, T.; Madin, A.; Ridgill, M. P. Alkenyl-Substituted Spirocyclic Sulfamides as Inhibitors of Gamma-Secretase. U.S. Patent 7,371,771, May 13, 2008.

[8] For 1,2-benzothiazole-1,1-diones **2** as inhibitors of aldose reductase, see: Wrobel, J.; Dietrich, A.; Woolson, S. A.; Millen, J.; McCaleb, M.; Harrison, M. C.; Hohman, T. C.; Sredy, J.; Sullivan, D. *J. Med. Chem.* **1992**, *35*, 4613–4627.

[9] For 1,2-benzothiazole-1,1-diones **2** as anti-HIV-1 agents, see: (a) Baker, D. C.; Jiang, B. Sultams: Solid Phase and Other Synthesis of Anti-HIV Compounds and Compositions. U.S. Patent 6,353,112, March 5, 2002; (b) Mao, J.; Baker, D. C. Sultams: Catalyst Systems for Asymmetric

Reduction of a C=N Intermediate. Biological Compositions and Methods for Making the Sultams. U.S. Patent 6,458,962, October 1, 2002; (c) Zhang, S.; Li, L.; Hu, Y.; Zha, Z.; Wang, Z.; Loh, T. P. *Org. Lett.* **2015**, *17*, 1050–1053.

[10] (a) Oppolzer, W.; Wills, M.; Kelly, M. J.; Signer, M.; Blagg, J. *Tetrahedron Lett.* **1990**, *31*, 5015–5018; (b) Oppolzer, W.; Rodriguez, I.; Starkemann, C.; Walther, E. *Tetrahedron Lett.* **1990**, *31*, 5019–5022; (c) Oppolzer, W.; Kingma, A. J.; Pillai, S. K. *Tetrahedron Lett.* **1991**, *32*, 4893–4896; (d) Ahn, K. H.; Kim, S.; Ham, C. *Tetrahedron Lett.* **1998**, *39*, 6321–6322.

[11] (a) Differding, E.; Bersier, P. M. *Tetrahedron* **1992**, *48*, 1595–1604; (b) Lal, G. S.; Pez, G. P.; Syvret, R. G. *Chem. Rev.* **1996**, *96*, 1737–1755; (c) Takeuchi, Y.; Suzuki, T.; Satoh, A.; Shiragami, T.; Shibata, N. *J. Org. Chem.* **1999**, *64*, 5708–5711.

[12] Alam, K.; Hong, S. W.; Oh, K. H.; Park, J. K. *Angew. Chem. Int. Ed.* **2017**, *56*, 13387–13391.

[13] (a) Minami, Y.; Shiraishi, Y.; Yamada, K.; Hiyama, T. *J. Am. Chem. Soc.* **2012**, *134*, 6124–6127; (b) Minami, Y.; Yamada, K.; Hiyama, T. *Angew. Chem. Int. Ed.* **2013**, *52*, 10611–10615; (c) Minami, Y.; Kanda, M.; Sakai, M.; Hiyama, T. *Chem. Lett.* **2014**, *43*, 181–183; (d) Minami, Y.; Kanda, M.; Sakai, M.; Hiyama, T. *Tetrahedron* **2015**, *71*, 4522–4534; (e) Minami, Y.; Kodama, T.; Hiyama, T. *Angew. Chem. Int. Ed.* **2015**, *54*, 11813–11816; (f) Minami, Y.; Noguchi, Y.; Yamada, K.; Hiyama, T. *Chem. Lett.* **2016**, *45*, 1210–1212; (g) Minami, Y.; Sakai, M.; Anami, T.; Hiyama, T. *Angew. Chem. Int. Ed.* **2016**, *55*, 8701–8705; (h) Minami, Y.; Hiyama, T. *Acc. Chem. Res.* **2016**, *49*, 67–77.

[14] (a) Viehe, H. G. *Angew. Chem. Int. Ed.* **1967**, *6*, 767–778; (b) van der Heiden, R.; Brandsma, L. *Synthesis* **1987**, *1*, 76–77; (c) Moyano, A.; Charbonnier, F.; Greene, A. E. *J. Org. Chem.* **1987**, *52*, 2919–2922.

[15] The *E*-configuration was assigned based on the ^{1}H NMR spectra and X-ray crystallography data known from the literature. For more details see: Mansfield, S. J.; Campbell, C. D.; Jones, M. W.; Anderson, E. A. *Chem. Commun.* **2015**, *51*, 3316–3319.

[16] Brückner, D. *Tetrahedron* **2006**, 62, 3809–3814.

[17] Zhang, P.; Cook, A. M.; Liu, Y.; Wolf, C. *J. Org. Chem.* **2014**, *79*, 4167–4173.

[18] Tracey, M. R.; Zhang, Y.; Frederick, M. O.; Mulder, J. A.; Hsung, R. P. *Org. Lett.* **2004**, *6*, 2209–2212.

[19] Siva Reddy, A.; Kumara Swamya, K. C. *Angew. Chem. Int. Ed.* **2017**, *56*, 6984–6988.

[20] This result excludes the reaction mechanism involving electrophilic aromatic substitution of keteniminium ion formed upon protonation with $NHTf_2$. For cyclization of keteniminium ions

catalyzed by Brønsted acids, see: (a) ref. 3; (b) Yamaoka, Y.; Yoshida, T.; Shinozaki, M.; Yamada, K.-I.; Takasu, K. *J. Org. Chem.* **2015**, *80*, 957–964.

[21] Product **17** is presumably formed by aromatic *ortho*-C–H activation of the benzyl group followed by the intramolecular hydroarylation.

[22] For an overview on concerted deprotonation-metalation sequences, see: Lapointe, D.; Fagnou, K. *Chem. Lett.* **2010**, *39*, 1118–1126 and references therein.

[23] Brookhart, M.; Green, M. L. H.; Parkin, G. *Proc. Natl. Acad. Sci. USA* **2007**, *104*, 6908–6914

[24] For cyclometalations with $Pd(OAc)_2$, see: (a) Lafrance, M.; Rowley, C. N.; Woo, T. K.; Fagnou, K. *J. Am. Chem. Soc.* **2006**, 128, 8754–8756; (b) García-Cuadrado, D.; Braga, A. A. C.; Maseras, F.; Echavarren, A. M. *J. Am. Chem. Soc.* **2006**, *128*, 1066–1067; (c) García-Cuadrado, D.; de Mendoza, P.; Braga, A. A. C.; Maseras, F.; Echavarren, A. M. *J. Am. Chem. Soc.* **2007**, *129*, 6880–6886; (d) Gorelsky, S. I.; Lapointe, D.; Fagnou, K. *J. Am. Chem. Soc.* **2008**, *130*, 10848–10849, and references therein.

[25] Bernar, I.; Blanco-Ania, D.; Stok, S. J.; Sotorríos, L.; Gómez-Bengoa, E.; Rutjes, F. P. J. T. *Eur. J. Org. Chem.* **2018**, 5435–5444.

[26] O'Sullivan, S.; Doni, E.; Tuttle, T.; Murphy, J. A. *Angew. Chem. Int. Ed.* **2014**, *53*, 474–478.

[27] Zhang, W.; Xie, J.; Rao, B.; Luo, M. *J. Org. Chem.* **2015**, *80*, 3504–3511.

[28] Laha, J. K.; Jethava, K. P.; Dayal, N. *J. Org. Chem.* **2014**, *79*, 8010–8019.

[29] Heffernan, S. J.; Beddoes, J. M.; Mahon, M. F.; Hennessy, A. J.; Carbery, D. R. *Chem. Commun.* **2013**, *49*, 2314–2316.

[30] Li, F.; Xie, J.; Shan, H.; Sun, C.; Chen, L. *RSC Adv.* **2012**, *2*, 8645–8652.

[31] Geary, L. M.; Hultin, P. G. *Org. Lett.* **2009**, *11*, 5478–5481.

[32] Gillie, A. D.; Jannapu Reddy, R.; Davies, P. W. *Adv. Synth. Catal.* **2016**, *358*, 226–239.

[33] Davies, P. W.; Cremonesi, A.; Martin, N. *Chem. Commun.* **2011**, *47*, 379–381.

[34] This side product is a result of addition of 4-nitro-*N*-phenylbenzenesulfonamide (**8d**) to **1i** formed during the reaction.

[35] Chen, P.; Song, C.-X.; Wang, W.-S.; Yua, X.-L.; Tang, Y. *RSC Adv.* **2016**, *6*, 80055–80058.

CHAPTER 6

Synthesis of Potential Crop-Protecting Agents via Photoinduced Rearrangement of 1,2-Benzothiazole-1,1-diones

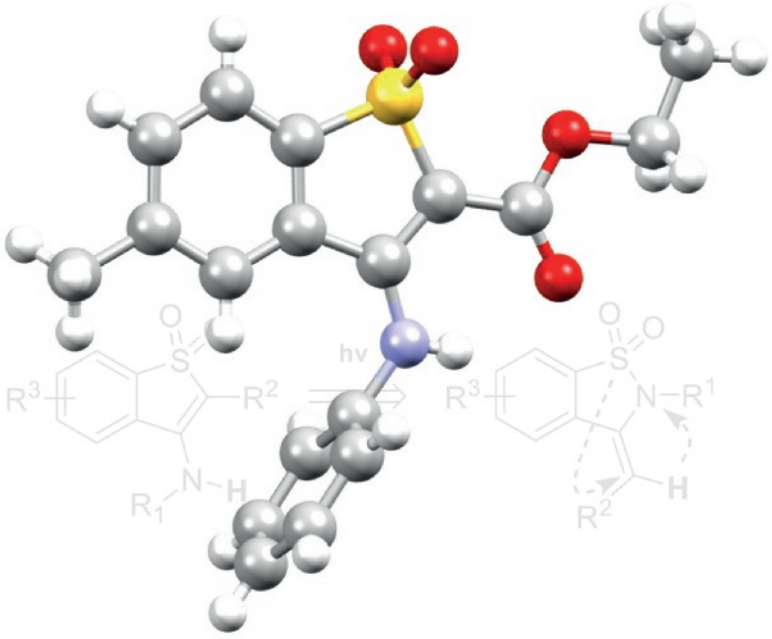

ABSTRACT

3-Amino-1-benzothiophene-1,1-diones are highly potent bioactive molecules valuable for medicinal and agrochemistry. However, the number of methods for their preparation is limited. The aim of this chapter was therefore to develop novel methodology that provided fast and easy access to these compounds. In an attempt to reach this goal, we have designed a highly efficient photoinduced rearrangement of 1,2-benzothiazole-1,1-diones that yields the desired products in excellent yields.

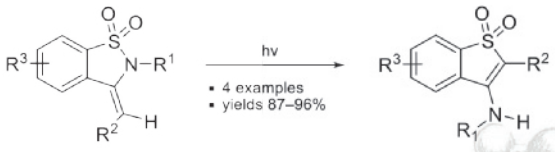

Part of this chapter was published in:

Bernar, I.; Blanco-Ania, D.; Sophie J. Stok; Sotorríos, L.; Gómez-Bengoa, E.; Rutjes, F. P. J. T. *Eur. J. Org. Chem.* **2018**, 5435–5444.

Chapter cover: "Crystal structure of 3-amino-1-benzothiophene-1,1-dione **1a**"

6.1 Introduction

Organosulfur compounds are widely present in a variety of natural products and drugs with important applications in the chemical community.[1] Among them, the 3-amino-1-benzothiophene-1,1-dione scaffold **1** has attracted particular attention in medicinal and agrochemistry (Figure 6.1).[2–4] Compounds containing this core structure are highly potent pharmacophores in medicinal chemistry, such as scaffold **2**.[2] Furthermore 3-amino-1-benzothiophene-1,1-diones **3** and **4** modulate the activity of a number of biological targets including protein kinases[3] and HIF-2a protein, inhibition of which could be useful in the treatment of several forms of cancer and iron overload disorders.[4] Another example is scaffold **5**, which exhibits antagonism activity towards TRPV1 receptor ligands, implicated in mediation of many types of pain.[5] In particular, our interest in these and related scaffolds was awakened because they are potential crop-protecting agents (e.g., fungicides, herbicides, and insecticides),[6] and therefore targets of the ECHONET program.

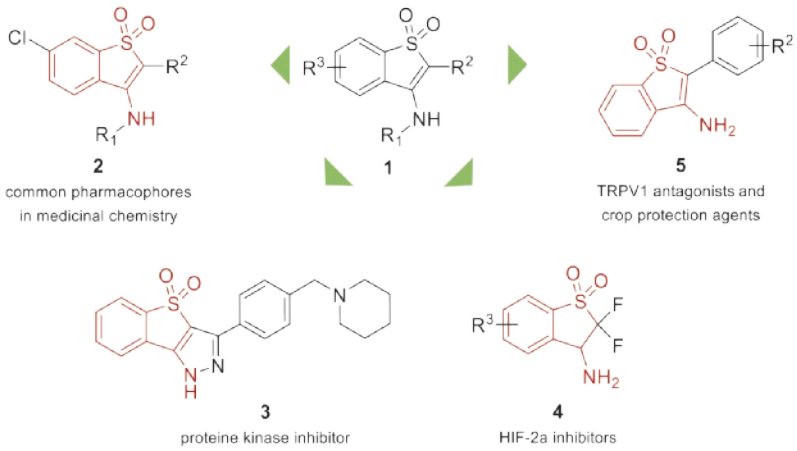

Figure 6.1 *Activity of 3-Amino-1-benzothiophene-1,1-dione Derivatives.*

Up till now, there are only a few approaches known toward the synthesis of 3-amino-1-benzothiophene-1,1-diones **1**.[7] Most of them consist of multiple steps with a poor to modest overall yield of the final products. We envisaged that 1,2-benzothiazole-1,1-diones (Chapter 5) could serve as simple precursors to form the desired scaffold **1**. Our approach was based on the photoinduced 1/N→3/C-sulfonyl group migration previously reported for vinylsulfonamides (Scheme 6.1).

Scheme 6.1 *Examples of Photoinduced [1,3]Sigmatropic Rearrangement of the Sulfonyl Group.*

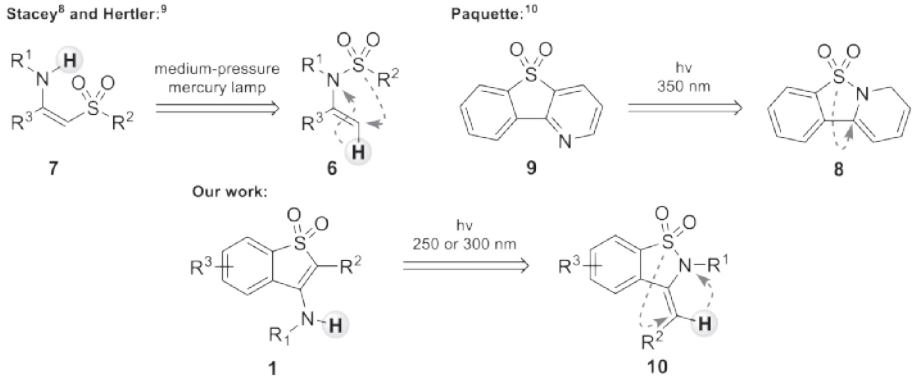

Thus, Stacey et al.[8] and Hertler[9] have independently described the rearrangement of *N*-alkyl-*N*-vinylsulfonamides **6** to β-sulfonylenamines **7** upon irradiation with a medium-pressure mercury lamp. The authors proposed a homolytic S–N bond cleavage followed by [1,3]sigmatropic rearrangement of the generated sulfinate radical as the reaction mechanism. Another example of photoinduced rearrangement was reported by Paquette et al., who observed the transformation of 1,2-benzothiazole-1,1-dione **8** into compound **9** upon photochemical activation.[10] Inspired by these literature findings, we wanted to adapt these processes to 1,2-benzothiazole-1,1-diones **10**. In this manner we aimed to develop a novel process to synthesize the highly valuable 3-amino-1-benzothiophene-1,1-dione scaffold **1**.

6.2 Results and Discussion

6.2.1 Optimization Studies for the Photoinduced Rearrangement of 1,2-Benzothiazole-1,1-diones

Our initial experiments to perform photoinduced sulfonyl migration in 1,2-benzothiazole-1,1-diones were conducted with the (*E*)-isomer of **10a** (Table 6.1). This compound underwent partial isomerization to its (*Z*)-isomer when irradiated with UV light at a wavelength of 254 or 300 nm in MeCN at 23 °C for 6 h (entries 1 and 2). These observations are in line with our previous results on isomerization studies of **10a**, in which we found that the (*E*)-isomer was the most stable isomer of **10a** (2.5 kcal/mol lower in energy than the (*Z*)-isomer, section 5.2.4). Careful examination of the ^{1}H NMR spectrum of the crude mixture showed, however, no formation of product **1a**.

Gratifyingly, after increasing the temperature to 50 °C (*E*)-1,2-benzothiazole-1,1-dione **10a** underwent photoinduced rearrangement to 3-amino-1-benzothiophene-1,1-dione **1a** in 34% yield after purification (entry 3). After several screening studies, the yield of the desired product was increased to 41% when irradiating with a wavelength of 300 nm (entry 4). Moreover, an irradiation time of more than 6 h was crucial for a high conversion to the rearranged product **1a** (entries 5 and 6). Thus, when either stereoisomer of **10a** or the mixture of both was irradiated at 50 °C for 24 h, a nearly complete photochemical conversion into 3-amino-1-benzothiophene-1,1-dione **1a** was observed. The final product was isolated in 92% yield after purification. Finally, our studies showed that the conversion rates and the yields of product **1a** were the highest in MeCN compared to acetone or benzene (entries 7 and 8, respectively).

Table 6.1 *Screening of the Reaction Conditions.*

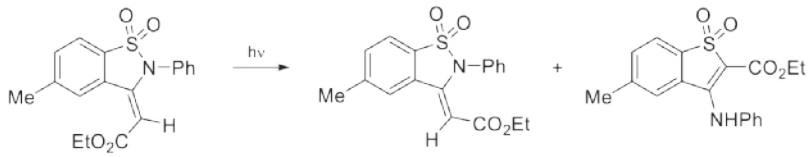

(*E*)-**10a** (*Z*)-**10a** **1a**

					Ratio of products (%)[a]			Yield (%)[b]
Entry	λ (nm)	*t* (°C)	Solvent	Time (h)	(*E*)-**10a**	(*Z*)-**10a**	**1a**	**1a**
1	254	23	MeCN	6	53	47	0	–
2	300	23	MeCN	6	58	42	0	–
3	254	50	MeCN	6	28	27	45	34
4	300	50	MeCN	6	34	19	47	41
5	300	50	MeCN	18	11	15	74	65
6	300	50	MeCN	24	5	2	93	92
7	300	50	Me_2CO	24	16	11	73	68
8	300	50	PhH	24	22	23	55	51

[a]Based on the ^{1}H NMR spectrum of the crude mixture. [b]Isolated yield.

6.2.2 Scope of the Photoinduced Rearrangement of 1,2-Benzothiazole-1,1-diones

Consequently, several 1,2-benzothiazole-1,1-dione derivatives were subjected to the same reaction conditions (300 nm, MeCN, 50 °C, 24 h) to study the scope of this transformation (Scheme 6.2). Interestingly, this photoinduced rearrangement showed no significant difference

in the reaction efficiency when changing the substituents at the aryl group of the sulfonamide (R^2 = Me, H, and OMe, substrates **10a–c**) or on the nitrogen (R^1 = Bn, substrate **10d**). The corresponding products were obtained in excellent yields in all cases. Additionally, we were able to grow high-quality single crystals of 3-amino-1-benzothiophene-1,1-diones **1a** and **1d** and confirm their structures by X-ray crystallography.

Scheme 6.2 *Scope of the Photoinduced Rearrangement of 1,2-Benzothiazole-1,1-diones **10a–d**.*

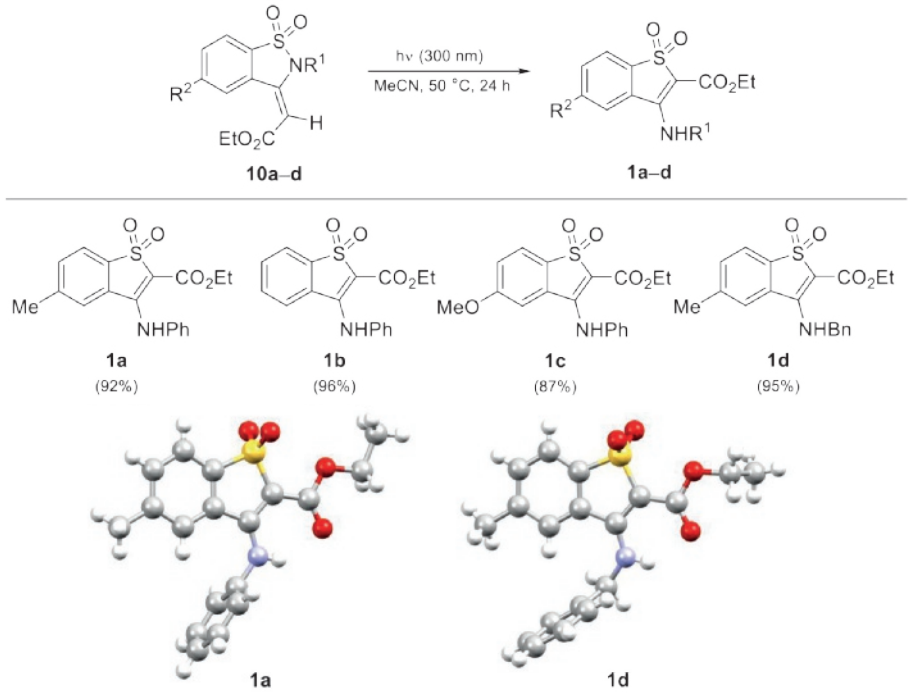

6.2.3 Mechanism of the Rearrangement

Herein we also propose a plausible mechanism on the basis of previously reported photoinduced cleavages of sulfonamides (Scheme 6.3).[8–11] This [1,3]sigmatropic rearrangement entails a homolytic cleavage of the sulfonamide S–N bond of 1,2-benzothiazole-1,1-dione **10**, followed by colligation of the resulting sulfinate radical with the C-terminus of the enaminyl radical **11**. Subsequent tautomerization of the formed imine **12** results in 3-amino-1-benzothiophene-1,1-dione **1a**.

Scheme 6.3 *Plausible Reaction Sequence.*

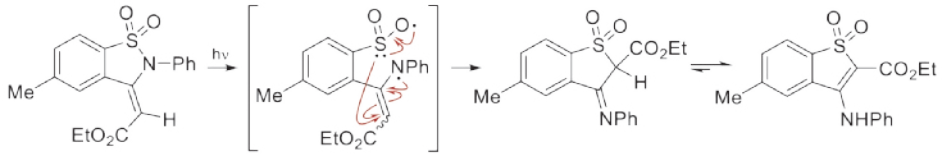

6.3 Conclusion

We have presented a highly efficient photoinduced rearrangement of 1,2-benzothiazole-1,1-diones **10** to 3-amino-1-benzothiophene-1,1-dione derivatives proceeding in excellent yields (4 examples, yields 87–96%). In addition, we propose a photoinduced [1,3]sigmatropic rearrangement of the sulfonyl group by S–N bond cleavage followed by colligation to form scaffold **1** as reaction mechanism. Further investigations to extend the scope of the reaction, and to better apprehend the mechanism are currently underway.

6.4 Acknowledgments

Dr. P. T. Tinnemans (Radboud University) is kindly acknowledged for the determination of the crystal structures.

6.5 Experimental Section

For general experimental details see Section 3.5. The photoinduced rearrangement was carried out in a Rayonet RMR-600 photochemical reactor using eight RMR-2537Å (254 nm wavelength) or RMR-3000Å (300 nm wavelength) lamps.

Photochemical Rearrangement of 1,2-Benzothiazole-1,1-diones

General procedure:[12] 1,2-Benzothiazole-1,1-dione **10** (0.1–1.0 mmol, 1.0 equiv) in 10 mL of deoxygenated MeCN was added to a 25 mL quartz flask with stirring. This flask was irradiated in a Rayonet RMR-600 photochemical reactor, using eight lamps of 300 nm of wavelength for 24 h with internal temperature of 50 °C. After cooling to 23 °C, the solvent was removed in vacuo and the crude residue was purified by column chromatography as indicated.

Ethyl 5-methyl-1,1-dioxo-3-(phenylamino)-1-benzothiophene-2-carboxylate 1a.

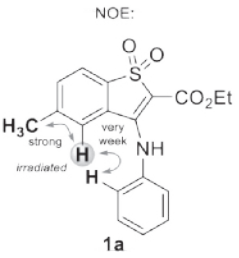

1a

3-Amino-1-benzothiophene-1,1-dione **1a** was prepared according to the general procedure using 1,2-benzothiazole-1,1-dione **10a** (343 mg, 1.0 mmol). Column chromatography (toluene; silica gel was washed with 1% Et_3N in heptane before being used for column chromatography) afforded product **1a** as a white solid (316 mg, 92%). R_F (silica gel, toluene): 0.22 (UV, $KMnO_4$ solution). **^{1}H NMR** [400 MHz, δ (ppm), $CDCl_3$]: 1.45 (t, J = 7.1 Hz, 3 H), 2.12 (s, 3 H), 4.43 (q, J = 7.1 Hz, 2 H), 6.40 (quint, J = 0.5 Hz, 1 H), 7.30–7.34 (m, 2 H), 7.37–7.41 (m, 1 H), 7.44–7.54 (m, 3 H), 7.71 (d, J = 7.8 Hz, 1 H), 10.43 (bs, 1 H). **^{13}C NMR** [101 MHz, δ (ppm), $CDCl_3$]: 14.4, 21.7, 61.1, 100.1, 121.2, 125.9, 126.5, 127.0, 128.6, 129.8, 133.6, 137.4, 138.2, 142.8, 155.0, 164.5. **FTIR** [$\bar{\nu}$ (cm^{-1})]: 704, 730, 1027, 1122, 1160, 1247, 1285, 1569, 1657, 2854, 2925. **HRMS** (ESI$^+$) calcd. for $(C_{18}H_{17}NO_4S + H)^+$ 344.0957, found 344.0963.

Ethyl 1,1-dioxo-3-(phenylamino)-1-benzothiophene-2-carboxylate 1b.

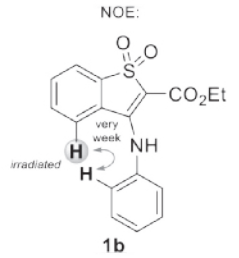

1b

3-Amino-1-benzothiophene-1,1-dione **1b** was prepared according to the general procedure using 1,2-benzothiazole-1,1-dione **10b** (33 mg, 0.1 mmol). Column chromatography (toluene; silica gel was washed with 1% Et_3N in heptane before being used for column chromatography) afforded the product **1b** as a white solid (31 mg, 96%). R_F (silica gel, toluene): 0.24 (UV, $KMnO_4$ solution). **^{1}H NMR** [400 MHz, δ (ppm), $CDCl_3$]: 1.45 (t, J = 7.1 Hz, 3 H), 4.44 (q, J = 7.1 Hz, 2 H), 6.66 (d, J = 8.0 Hz, 1 H), 7.23–7.28 (m, 1 H), 7.29–7.36 (m, 2 H), 7.43–7.54 (m, 3 H), 7.58–7.62 (m, 1 H), 7.83 (d, J = 7.6 Hz, 1 H), 10.44 (bs, 1 H). **^{13}C NMR** [101 MHz, δ (ppm), $CDCl_3$]: 14.4, 61.3, 99.9, 121.6, 125.7, 125.9, 126.9, 128.7, 130.0, 132.1, 133.2, 137.4, 141.0, 154.8, 164.6. **FTIR** [$\bar{\nu}$ (cm^{-1})]: 702, 763, 1161, 1246, 1284, 1434, 1561, 1610, 1657, 2854, 2925. **HRMS** (ESI$^+$) calcd. for $(C_{17}H_{15}NO_4S + H)^+$ 330.0800, found 330.0813.

Ethyl 5-methoxy-1,1-dioxo-3-(phenylamino)-1-benzothiophene-2-carboxylate 1c.

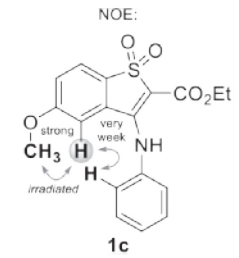

1c

3-Amino-1-benzothiophene-1,1-dione **1c** was prepared according to the general procedure using 1,2-benzothiazole-1,1-dione **10c** (36 mg, 0.1 mmol). Column chromatography (toluene; silica gel was washed with 1% Et_3N in heptane before being used for column chromatography) afforded the product **1c** as a white solid (31 mg, 87%). R_F (silica gel, toluene): 0.20 (UV, $KMnO_4$ solution). **^{1}H NMR** [400 MHz, δ (ppm), $CDCl_3$]: 1.45 (t, J = 7.1 Hz, 3 H), 3.48 (s, 3 H), 4.43 (q, J = 7.1 Hz, 2 H), 6.13 (d, J = 2.2 Hz, 1 H), 7.04 (dd, J = 8.5, 2.2 Hz, 1 H), 7.32–7.38 (m, 2 H), 7.44–7.53 (m, 3 H), 7.72 (d, J = 8.5 Hz, 1 H), 10.41 (bs, 1 H). **^{13}C NMR** [101 MHz, δ (ppm), $CDCl_3$]: 14.4, 55.4, 61.2, 100.7, 111.6, 118.3, 122.8, 127.2, 127.8, 128.8, 130.0, 132.7, 137.4, 154.4, 162.3, 164.5. **FTIR** [$\bar{\nu}$ (cm^{-1})]: 703, 729, 910, 1021, 1162, 1245, 1567, 1655, 2926. **HRMS** (ESI^+) calcd. for $(C_{18}H_{17}NO_5S + H)^+$ 360.0906, found 330.0927.

Ethyl 3-(benzylamino)-5-methyl-1,1-dioxo-1-benzothiophene-2-carboxylate 1d.

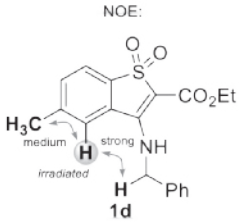

1d

3-Amino-1-benzothiophene-1,1-dione **1d** was prepared according to the general procedure using 1,2-benzothiazole-1,1-dione **10d** (36 mg, 0.1 mmol). Column chromatography (toluene; silica gel was washed with 1% Et_3N in heptane before being used for column chromatography) afforded the product **1d** as a white solid (34 mg, 95%). R_F (silica gel, toluene): 0.25 (UV, $KMnO_4$ solution). **^{1}H NMR** [400 MHz, δ (ppm), $CDCl_3$]: 1.40 (t, J = 7.1 Hz, 3 H), 2.40 (s, 3 H), 4.36 (q, J = 7.1 Hz, 2 H), 5.02 (d, J = 5.9 Hz, 2 H), 7.33–7.40 (m, 3 H), 7.40–7.46 (m, 2 H), 7.49 (d, J = 7.8 Hz, 1 H), 7.59 (s, 1 H), 7.77 (d, J = 7.8 Hz, 1 H), 9.44 (bs, 1 H). **^{13}C NMR** [101 MHz, δ (ppm), $CDCl_3$]: 14.5, 22.2, 50.0, 61.0, 100.1, 121.2, 125.9, 126.5, 127.0, 128.6, 129.8, 133.6, 137.4, 138.2, 142.8, 154.9, 164.5. **FTIR** [$\bar{\nu}$ (cm^{-1})]: 735, 786, 1141, 1216, 1268, 1577, 1659, 2925, 3254. **HRMS** (ESI^+) calcd. for $(C_{19}H_{19}NO_4S + H)^+$ 358.1113, found 358.1133.

X-Ray Crystallography of compounds 1a and 1d

General procedure: High quality single crystals of **1a** and **1d** was obtained by slow solvent evaporation. Saturated solutions of **1a** and **1d** in toluene were prepared and filtered over an Acrodisc HPLC syringe filter to ensure the absence of crystallites. The resulting filtrates were transferred to scintillation flasks that were sealed and equipped with hollow needle to allow slow

evaporation of the solvent. The acquired single crystals were subjected to single X-ray diffraction. Mercury software (Version 3.9; Cambridge Crystallographic Data Centre) was used to visualize the structures.

6.6 References and Notes

[1] (a) Cremlyn, R. G. *An Introduction to Organosulfur Chemistry;* John Wiley & Sons: Chichester, U.K., 1996; (b) *Organosulfur Chemistry in Asymmetric Synthesis*; Toru, T., Bolm, C., Eds.; Wiley-VCH: Weinheim, Germany, 2008.

[2] For the 3-amino-1-benzothiophene-1,1-dione scaffold as pharmacophore in medicinal chemistry, see: (a) Friebe, W.-G.; Reinholz, E.; Wilhelms, H. Bicyclic Sulfones, Processes for Their Production and Pharmaceutical Agents Containing Them. U.S. Patent 5,547,980, August 29, 1991; (b) Hrib, N. J.; Jurcak, J. G. Benzo[b]thiophen-3-yl Piperazines as Antipsychotic Agents. U.S. Patent 5,240,927, August 31, 1993; (c) Hrib, N. J.; Jurcak, J. G.; Mutlib, A. E. Substituted Benzothienylpiperazines and Their Use. U.S. Patent 5,801,176, September 1, 1998; (d) Salvati, M. E.; Mitt, T.; Patel, R. N.; Hanson, R. L.; Brzozowski, D.; Goswami, A.; Chu, L. N. H.; Li, W.-S.; Simpson, J. H.; Totleben, M. J.; He, W. Method For the Preparation of Fused Heterocyclic Succinimide Compounds and Analogs Thereof. U.S. Patent 6,953,679, October 11, 2005; (e) Salvati, M. E.; Balog, J. A.; Pickering, D. A.; Giese, S.; Fura, A.; Li, W.; Patel, R. N.; Hanson, R. L.; Mitt, T.; Roberge, J. Y.; Corte, J. R.; Spergel, S. H.; Rampulla R. A.; Misra, R. N.; Xiao, H.-Y. Fused Heterocyclic Succinimide Compounds and Analogs Thereof, Modulators of Nuclear Hormone Receptor Function. U.S. Patent 7,141,578, November 28, 2006.

[3] Doyle, K. J.; Rafferty, P.; Steele, R. W.; Wilkins, D. J.; Arnold, L. D.; Hockley, M.; Ericsson, A. M.; Iwasaki, N.; Ogawa, N. Tricyclic Pyrazole Derivatives. U.S. Patent 6,462,036, October 8, 2002.

[4] (a) Dixon, D. D.; Grina, J.; Josey, J. A.; Rizzi, J. P.; Schlachter, S. T.; Wallace, E. M.; Wang, B.; Wehn, P.; Xu, R.; Yang, H. Cyclic Sulfone and Sulfoximine Analogs and Uses Thereof. WO 2015095048, June 25, 2015; (b) Bruick, R. K.; Chen, Y.; Ruiz, J. C. F. HIF-2α Inhibitors for Treating Iron Overload Disorders. WO 2016057242, April 14, 2016.

[5] Kyle, D. J.; Tafesse, L. Heterocyclic TRPV1 Receptor Ligands. U.S. Patent 8,546,388, October 1, 2013.

[6] Fischer, R.; Kretschik, O.; Schenke, T.; Schenkel, R.-I.; Wiedemann, J.; Erdelen, C.; Losel, P.; Drewes, M. W.; Feucht, D.; Andersch, W. α-Phenyl-β-ketosulfone. U.S. Patent 6,670,385, December 30, 2003.

[7] For the synthesis of 3-amino-1-benzothiophene-1,1-diones, see: (a) Ried, W.; Oremek, G. *Liebigs Ann. Chem.* **1981**, 619–622; (b) Gajewski, R. P.; Jackson, J. L.; Jones, N. D.; Swartzendruber, J. K.; Deeter, J. B. *J. Org. Chem.* **1989**, *54*, 3311–3317; (c) Tauber, C.; Klade, M.; Sterk, H.; Junek, H. *Monatsh. Chem.* **1990**, *120*, 299–309; (d) Deady, L. W.; Kaye, A. J.; Finlay, G. J.; Baguley, B. C.; Denny, W. A. *J. Med. Chem.* **1997**, *40*, 2040–2046; (e) Baumgarth, M.; Beier, N.; Gericke, R. *J. Med. Chem.* **1998**, *41*, 3736–3747; (f) Cekavicus, B.; Liepinsh, E.; Vigante, B.; Sobolevs, A.; Ozols, J.; Duburs, G. *Tetrahedron Lett.* **2001**, *42*, 4239–4241; (g) Shefer, N.; Rozen, S. *J. Org. Chem.* **2011**, *76*, 4611–4616; (h) Blades, K.; Demeritt, J.; Fillery, S.; Foote, K. M.; Greenwood, R.; Gregson, C.; Hassall, L. A.; McGuire, T. M.; Pike, K. G.; Williams, E. *Tetrahedron Lett.* **2014**, *55*, 3851–3855; (i) Kalugin, V. E.; Shestopalov, A. M. *Russ. Chem. Bull.* **2015**, *64*, 878–882 and references 2–6 therein.

[8] Stacey, F. W.; Sauer, J. C.; Mckusic, B. C. *J. Am. Chem. Soc.* **1959**, *81*, 987–992.

[9] Hertler, W. Photoimaging Systems Based upon Photosensitized Rearrangement of *N*-Vinyl Sulfonamides to β-Sulfonylvinylamines. U.S. Patent 3,814,604, June 4, 1974.

[10] Paquette, L. A.; Dura, R. D; Modolo, I. *J. Org. Chem.* **2009**, *74*, 1982–1987.

[11] For examples of photoinduced cleavage of the sulfonamide group, see: (a) Weiss, B.; Dürr, H.; Haas, H. J. *Angew. Chem. Int. Ed.* **1980**, *19*, 648–650; (b) Kawamura, K.; Sasaki, F. *J. Photopolym. Sci. Technol.* **2001**, *14*, 265–272; (c) Park, K. K.; Lee, J. J.; Ryu, J. *Tetrahedron* **2003**, *59*, 7651–7659; (d) Kato, J.; Kakehata, H.; Maekawab, Y.; Yamashita, T. *Chem. Commun*. **2006**, 4498–4500.

[12] For more details on the reaction setup, see Sections 4.2.4 and 4.5 of this thesis.

CHAPTER 7

Conclusion and Future Perspectives

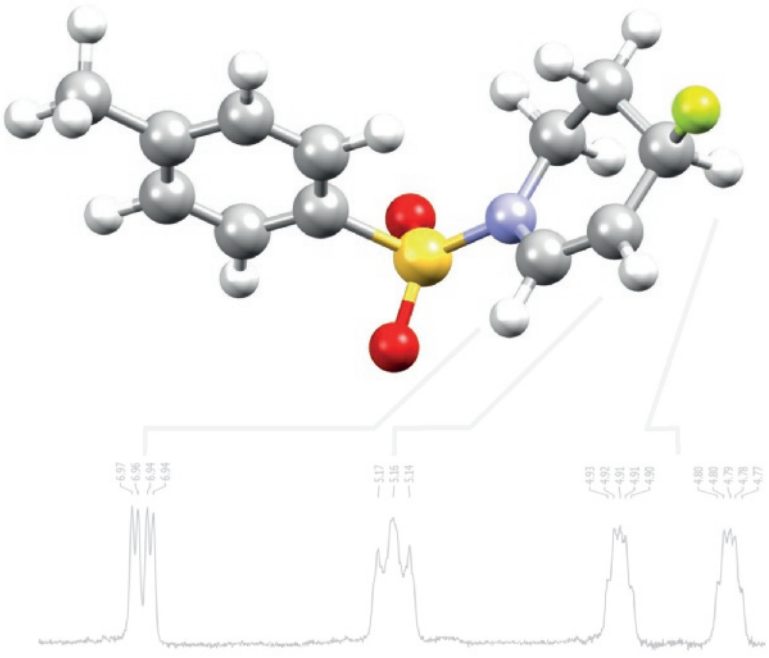

ABSTRACT

Palladium-catalyzed transformations are among the most attractive synthetic reactions for the preparation of chemical libraries of nitrogen-containing heterocycles. Our research on this topic resulted in straightforward and efficient procedures for the preparation of several privileged scaffolds that occur in biologically active compounds. In this chapter, we wish to highlight some additional studies. More specifically, the nucleophilic fluorination of cyclic *N,O*-acetals and the photoinduced sulfonyl rearrangement in sulfonyl enamines seemed promising and therefore may represent an excellent starting point for future research.

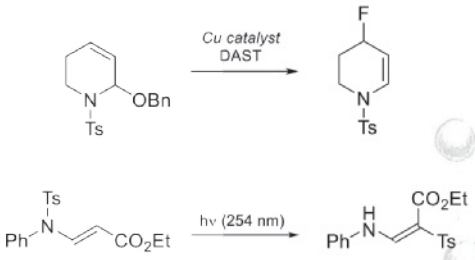

Chapter cover: "Characteristic ^{1}H NMR signals of allyl fluoride **10**"

7.1 Conclusion of the Work with an Introduction to Future Studies

Nitrogen heterocycles are the most significant structural components of agrochemicals.[1] Although an immense variety of efficient methodologies for the synthesis of bioactive *N*-heterocycles have been reported, the development of novel approaches is in continuous demand. The aim of the presented work was therefore to develop novel synthetic methods for the preparation and derivatization of *N*-heterocycles. In particular, we developed two approaches for the synthesis of *N*-heterocyclic scaffolds based on palladium-catalyzed intra- and intermolecular additions to CC multiple bonds. The first approach allowed us fast and easy access to heteroaromatic allylic *N,O*-acetals in a highly efficient and enantioselective manner. These useful building blocks were then further used in the target-oriented synthesis of complex heterocycles. The second approach was a two-step reaction sequence including a palladium-catalyzed intramolecular hydroarylation of sulfonyl ynamines followed by a photoinduced rearrangement to form the 3-amino-1-benzothiophene-1,1-dione scaffold. Compounds containing this functionality are considered potential crop-protecting agents in the agrochemical sector. Yet, these were not the only results obtained from this research. In the following sections, we would like to present several valuable findings gathered during the development of the aforementioned methods. We hope that these results will serve as a stimulus for future research towards the chemistry of *N*-heterocycles.

7.2 Study of Nucleophilic Fluorination of Cyclic *N,O*-Acetals

Incorporation of fluorine atoms into biologically active molecules often drastically improves their chemical, physical, and biological properties leading to the invention of novel materials,[2] drugs,[3] and agrochemicals.[4] In line with this behavior, fluorine-containing compounds represent 25% of all herbicides present on the market worlwide.[5] In general, there are three strategies for incorporating fluorine into molecules: electrophilic, nucleophilic, and radical fluorinations.[6] Each of these methods has possible benefits and drawbacks depending on the substrate involved. We envisioned that conjugated iminium ions are of particular interest as substrates for less common nucleophiles. These iminium ion intermediates can be easily generated from allylic *N,O*-acetals upon treatment with a Lewis acid as shown in multiple examples in Chapter 2. To extend these results, we studied the nucleophilic fluorination of conjugated iminium ions **2** generated from allylic *N,O*-acetals **1** (Scheme 7.1). In this manner we aimed to introduce the fluorine atom into the scaffold and synthesize more complex heterocyclic molecules.

Scheme 7.1 *Proposed Reaction Sequence for Fluorination of Allylic N,O-Acetals* ***1****.*

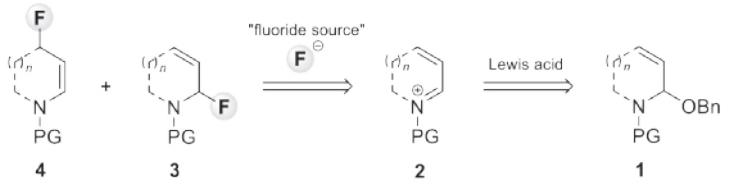

Some initial steps towards solving this research challenge were already undertaken. Particularly, we chose cyclic allylic *N,O*-acetal **8** as electrophiles for the fluorination process (Scheme 7.2). This substrate was successfully prepared in a two-step procedure via a palladium-catalyzed hydroamination of benzyloxyallene (**6**) with sulfonamide **5** followed by ring-closing metathesis of the obtained diolefin **7**.

Scheme 7.2 *Synthesis of Cyclic Allylic Acetal* ***8****.*

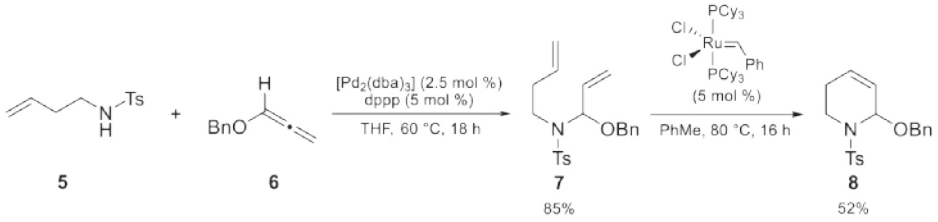

With cyclic allylic acetals **8** in hand, the fluorination experiments were carried out using different Lewis acids and fluoride sources (Table 7.1). Isomerized product **9** and allyl fluoride **10** were the main products of these optimization studies. Remarkably, the 1,2-addition of fluoride to the iminium ion, which could possibly lead to formation of the product **3**, was not observed.

Thus, cyclic allylic acetal **8** underwent predominantly isomerization to allyl ether **9** in the presence of $BF_3{\cdot}OEt_2$ (0.2 equiv) and DAST (1.2 equiv; entry 1). Additionally, 1-tosyl-1,2-dihydropyridine **11** was a common side product of the reaction. More importantly, allyl fluoride **10** was spotted among the minor products. Inspired by this finding, we tested alternative fluoride sources with the aim of increasing the conversion to allyl fluoride **10**. Contrary to our expectations, only a trace amount of the starting material reacted (7% conversion, entry 2) and only allyl ether **9** was formed using $BF_3{\cdot}OEt_2$ (0.2 equiv) in combination with $NEt_3{\cdot}3HF$ (1.2 equiv). Unfortunately, no signs of allyl fluoride **10** were observed.

Table 7.1 *Screening of Reaction Conditions.*

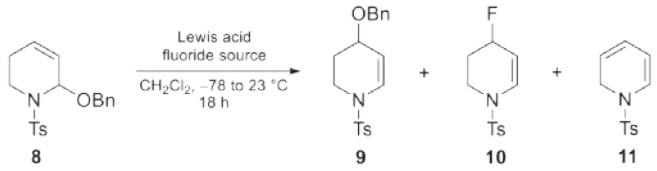

			Ratio of products (%)[a]			
Entry	Lewis Acid	Fluoride Source	**8**	**9**	**10**	**11**
1	$BF_3{\cdot}OEt_2$	DAST	15	70	11	4
2	$BF_3{\cdot}OEt_2$	$NEt_3{\cdot}3HF$	93	7	0	0
3[b]	$BF_3{\cdot}OEt_2$	CsF	11	89	0	0
4	$Sn(OTf)_2$	DAST	17	78	5	0
5	TiF_4	DAST	78	22	0	0
6	**12**	DAST	5	22	73	0
7	**13**	DAST	5	9	86	0
8	**14**[c]	DAST	7	18	75	0

[a]Based on the ^1H NMR spectrum of the crude mixture. [b]MeCN was used as the solvent. [c]Generated in situ by premixing **13** and DAST, and stirring at 23 °C for 0.5 h.

Treatment of the cyclic allyl acetal **8** with $BF_3{\cdot}OEt_2$ (0.2 equiv) and CsF (1.2 equiv) led to 89% conversion to isomerized product **9**, however, no evidence for product **10** was found again (entry 3). By changing the Lewis acid, we observed poor to modest conversion to allyl ether **9** and no formation of allyl fluoride **10** (entries 4 and 5). Inspired by the work of Dang et al.[7] and Cheng et al.[8] on catalytic nucleophilic fluorination with copper–*N*-heterocyclic carbene complexes, we decided to utilize catalysts **12**–**14** in our study (Figure 7.1). To our delight, the experimental investigations showed rather good conversions to allyl fluoride **10** with only a minor amount of allyl ether **9** being formed (entries 6–8, Table 7.1). Catalyst **13** (0.2 equiv) was most effective of all copper complexes used and gave the highest conversion to product **10** (up to 86%, entry 7).

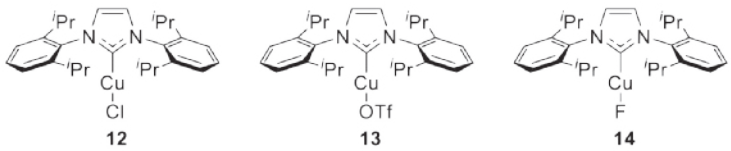

Figure 7.1 *Structure of Copper(I)-N-Heterocyclic Carbene Complexes used in the Study.*

Furthermore, the ^{1}H NMR spectrum of the crude reaction mixture evidenced the allyl fluoride type structure being present in the main product (Figure 7.2).

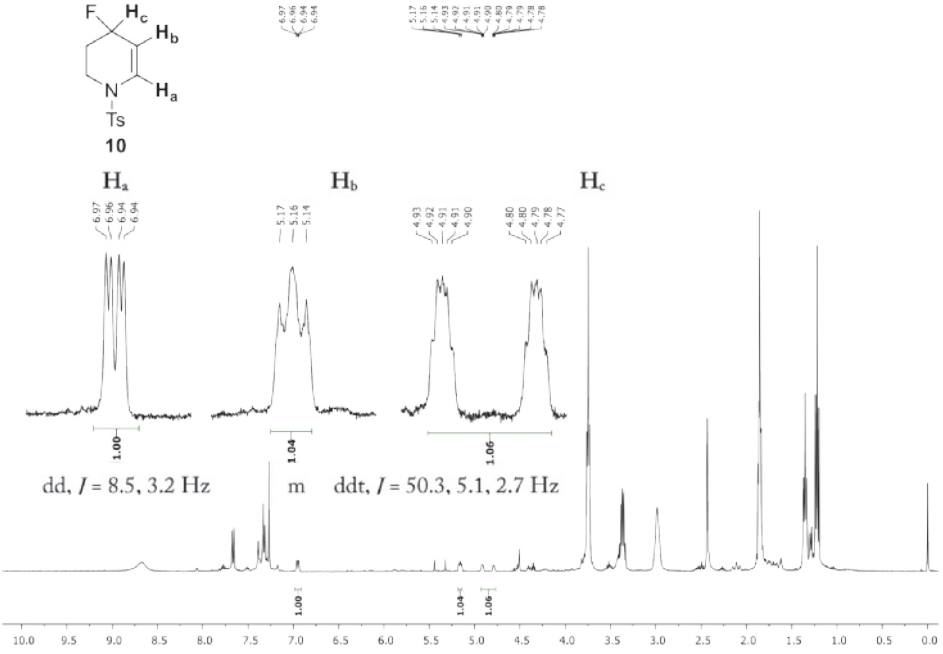

Figure 7.2 *^{1}H NMR of the Crude Mixture with Highlighted Main Signals of Compound **10**.*

Unfortunately, we were unable to isolate product **10** in pure form. This compound hydrolyzed remarkably easy to allyl alcohol **15** upon purification by silica-gel column chromatography (Scheme 7.3). Hence, this side product (**15**) was isolated in 36% overall yield. In addition, compound **15** further reacted with allyl fluoride **10** on the silica-gel column. In this manner diallyl ether **16** was formed in one of the fractions during chromatographic purification and obtained in 17% isolated yield.

Scheme 7.3 *Synthesis of Allyl Fluoride **10** and its Decomposition upon Purification.*

To sum up, these early findings provide a valuable framework for a new way of introducing the fluorine atom into *N*-heterocycles based on iminium ion chemistry. Further work needs to be carried out to isolate compound **10** as well as to broaden the successful examples of fluorination.

7.3 Photoinduced Sulfonyl Rearrangement of Sulfonyl Enamines

Our work on photoinduced [1,3]sigmatropic rearrangement of the sulfonyl group presented in Chapter 6 opened the door for the application of this process in agrochemical research. Developed by us, this procedure respresents a clear advance on current methods for the preparation of 3-amino-1-benzothiophene-1,1-diones, biologically active compounds used as crop-protection agents. Furthermore, we envision that the described photoinduced sulfonyl rearrangement could be further applied to linear and cyclic sulfonyl enamines **17** (Scheme 7.4). This system has the potential to undergo the 1/N→3/C-sulfonyl migration to form β-sulfonyl enamines **18** upon excitation with UV light, similar to the photochemical activation of 1,2-benzothiazole-1,1-diones.

Scheme 7.4 *Retrosynthesis and Applications of Amino Sulfonyl Scaffold **18**.*

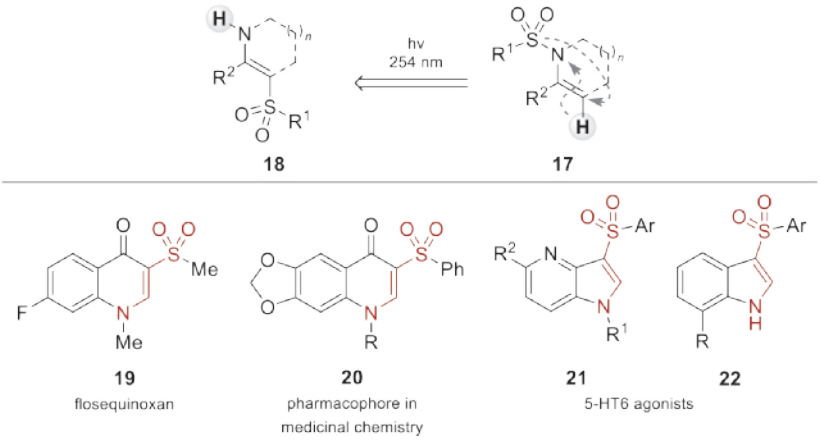

The proposed method could eventually become an initial step in the preparation of highly potential pharmacophores for medicinal chemistry based on the amino sulfonyl motif. Among them, 3-sulfonylquinolinone derivatives such as flosequinoxan **19**, used for the treatment of chronic heart failure,[9] and bioactive pharmacophore **20**, an attractive target for the discovery of new drugs for treatment of disorders of the autoimmune system or inflammatory diseases.[10]

Moreover, the amino sulfonyl motif constitutes the structure of many 5-HT6 receptor agonists such as 3-arenesulfonylpyrrolo[3,2-*b*]pyridines **21** and 3-arenesulfonylindoles **22**, which have proven useful in the treatment of central nervous system disorders.[11] Currently, a number of molecules from these compound classes are active in phase I and II clinical trials for cognitive impairment in Alzheimer's disease and schizophrenia.[12]

We are now in the process of investigating this type of rearrangement for acyclic arenesulfonyl enamines. In particular, tosyl-protected enamine **23** was selected as the model substrate for the examination of the reaction (Scheme 7.5). Our preliminary studies showed that irradiation of sulfonyl enamine **23** with 254 nm UV lamps in MeCN at 50 °C for 18 h resulted in a highly regio- and stereoselective formation of (*E*)-β-Ts enamine **24** in 78% yield and >98:2 *E*/*Z*-ratio of stereoisomers. Furthermore, the structure of (*E*)-**24** was unambiguously determined by NOE NMR spectroscopy.

Scheme 7.5 *Photoinduced Rearrangement of Sulfonyl Enamine 23.*

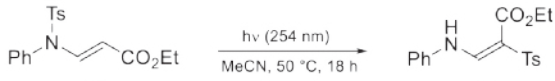

23 **24**

(78%, >98:2 *E*/*Z*)

A plausible mechanism based on the high regio- and stereoselectivity of the process as well as previous reports on radical additions to electron poor enamines,[13] is outlined in Scheme 7.6. Firstly, a sulfinate radical is generated via homolytic cleavage of the sulfonamide S–N bond upon photochemical activation. Subsequently, this electron-deficient radical selectively attacks the β-carbon of enaminyl intermediate **25** forming imine **26**. Subsequent tautomerization of imine **26** results in the formation of the thermodynamically more stable *E*-isomer of **24**, which contains an intramolecular hydrogen bond.

Scheme 7.6 *Plausible Reaction Mechanism.*

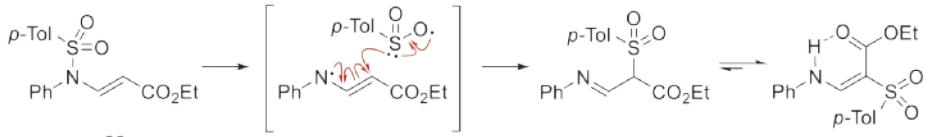

23 **25** **26** **24**

Future studies on the current topic will be aimed to verify this reaction mechanism and extend this process to a broader array of examples.

7.4 Acknowledgments

Guillem Loren, Jeroen Louwsma and Ulviye Öztas (Radboud University) are gratefully acknowledged for their work towards nucleophilic fluorination of cyclic *N,O*-acetals.

7.5 Experimental Section

For general experimental details see Section 3.5. Copper–*N*-heterocyclic carbene complex **12** was directly purchased from Sigma-Aldrich.

Synthesis of Copper(I)-*N*-Heterocyclic Carbene Complex 13

[1,3-Bis(2,6-diisopropylphenyl)imidazol-2-ylidene]copper(I) triflate 13.[14]

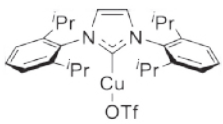

13

Copper–*N*-heterocyclic carbene complex **12** (244 mg, 0.5 mmol, 1.0 equiv) and AgOTf (128 mg, 0.5 mmol, 1.0 equiv) were disolved in dry THF (2.0 mL) and the flask was sealed. The reaction mixture was stirred at 23 °C for 3 h. The resulting white solids were then filtered off through a pad of diatomaceous earth and washed with dry CH_2Cl_2. The filtrate was concentrated under reduced pressure to afford complex **13** as a white solid (277 mg, 92%), which was used without further purification. **^{1}H NMR** [400 MHz, δ (ppm), $CDCl_3$]: 1.22 (d, J = 6.7 Hz, 12 H), 1.26 (d, J = 6.8 Hz, 12 H), 2.51 (sept, J = 6.7 Hz, 4 H), 7.19 (s, 2 H), 7.32 (d, J = 7.6 Hz, 4 H), 7.52 (t, J = 7.8 Hz, 2 H). **^{13}C NMR** [101 MHz, δ (ppm), $CDCl_3$]: 23.9, 24.5, 28.7, 119.2 (q, J = 316.3 Hz), 120.7, 123.5, 123.9, 124.3, 130.6, 133.8, 145.3, 177.3. **^{19}F NMR** [377 MHz, δ (ppm), $CDCl_3$]: –77.7. Th ese data were in accordance to those reported in the literature.[14]

Synthesis of Cyclic Allylic *N,O*-Acetal 8

***N*-(But-3-en-1-yl)-4-methylbenzenesulfonamide 5.**[15]

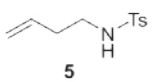

5

Tosyl chloride (3.2 g, 16.9 mmol, 1.2 equiv) was added slowly to a solution of 3-buten-1-amine (1.0 g, 14.1 mmol, 1 equiv), Et_3N (3.0 mL, 21.1 mmol, 1.5 equiv), and DMAP (517 mg, 4.2 mmol, 0.3 equiv) in CH_2Cl_2 (30 mL) at 0 °C. The reaction mixture was warmed to 23 °C, stirred for 3 h, and quenched with water. The aqueous layer was then extracted CH_2Cl_2 (3 × 50 mL). The combined organic phases were dried over Na_2SO_4, filtered, and the solvent was removed in vacuo. The crude mixture was purified by column chromatography (heptane/AcOEt 40:1→1:1) to afford product **5** as a light yellow oil (2.9 g, 92%). **^{1}H NMR** [400 MHz, δ (ppm), $CDCl_3$]: 2.19–2.24

(m, 2 H), 2.43 (s, 3 H), 3.02 (dt, J = 6.6, 6.2 Hz, 2 H), 4.35 (bt, J = 6.1 Hz, 1 H), 5.00–5.11 (m, 2 H), 5.62 (ddt, J = 17.1, 10.3, 6.9 Hz, 1 H), 7.29–7.35 (m, 2 H), 7.72–7.76 (m, 2 H). **^{13}C NMR** [101 MHz, δ (ppm), $CDCl_3$]: 21.6, 33.5, 42.4, 118.6, 127.1, 129.7, 134.3, 137.1, 143.5. These data were in accordance to those reported in the literature.[15]

***N*-[1-(Benzyloxy)allyl]-*N*-(but-3-en-1-yl)-4-methylbenzenesulfonamide 7.**[16]

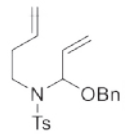

7

$[Pd_2(dba)_3]$ (85 mg, 0.09 mmol, 0.025 equiv) and 1,3-bis(diphenylphosphanyl)propane (76 mg, 0.19 mmol, 0.05 equiv) were dissolved in dry THF (50 mL). Sulfonamide **5** (1.0 g, 4.4 mmol, 1.2 equiv) and benzyloxyallene (540 mg, 3.7 mmol, 1.0 equiv) were added and the flask was sealed. The reaction mixture was stirred at 60 °C for 18 h. After cooling the reaction mixture to 23 °C, the mixture was filtered, the solvent was removed in vacuo, and the crude was purified by column chromatography (heptane/AcOEt 20:1→2:1) to afford product **7** as a light yellow oil (1.2 g, 85%). **^{1}H NMR** [400 MHz, δ (ppm), $CDCl_3$]: 2.38–2.47 (m, 2 H), 2.43 (s, 3 H), 3.09 (ddd, J = 14.6, 9.6, 6.4 Hz, 1 H), 3.26 (ddd, J = 14.7, 9.9, 6.4 Hz, 1 H), 4.55 (d, J = 12.0 Hz, 1 H), 4.71 (d, J = 12.0 Hz, 1 H), 4.96–5.05 (m, 2 H), 5.22–5.26 (m, 1 H), 5.43–5.49 (m, 2 H), 5.62–5.66 (m, 1 H), 5.66–5.76 (m, 1 H), 7.26–7.38 (m, 7 H), 7.68–7.73 (m, 2 H). **^{13}C NMR** [101 MHz, δ (ppm), $CDCl_3$]: 21.4, 34.9, 43.3, 69.3, 86.5, 116.5, 119.5, 126.7, 127.4, 127.5, 128.2, 129.7, 133.7, 135.1, 137.6, 137.9, 143.2. These data were in accordance to those reported in the literature.[16]

6-Benzyloxy-*N*-(4-methylbenzenesulfonyl)-1,2,3,6-tetrahydropyridine 8.[16]

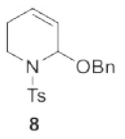

8

Allylic *N,O*-acetal **7** (1.1 g, 3.0 mmol, 1.0 equiv) and Grubbs catalyst 1st generation (123 mg, 0.15 mmol, 0.05 equiv) were dissolved in dry toluene (50 mL) and heated at 80 °C for 16 h under a nitrogen atmosphere. After cooling the reaction mixture to 23 °C, the mixture was filtered, the solvent was removed in vacuo, and the crude was purified by column chromatography (heptane/AcOEt 40:1→2:1) to afford product **8** as a colorless oil (536 mg, 52%). **^{1}H NMR** [400 MHz, δ (ppm), $CDCl_3$]: 1.74–1.77 (m, 2 H), 2.42 (s, 3 H), 3.39–3.44 (m, 1 H), 3.82–3.86 (m, 1 H), 4.63 (d, J = 11.9 Hz, 1 H), 4.81 (d, J = 11.8 Hz, 1 H), 5.47–5.49 (m, 1 H), 5.66–5.80 (m, 2 H), 7.19–7.42 (m, 7 H), 7.66–7.73 (m, 2 H). **^{13}C NMR** [101 MHz, δ (ppm), $CDCl_3$]: 21.3, 23.2, 37.6, 69.5, 79.5, 124.6, 126.6, 127.5, 128.0, 128.3, 129.1, 129.6, 137.5, 138.2, 143.8. These data were in accordance to those reported in the literature.[16]

Fluorination of Cyclic Allylic *N,O*-Acetal 8

General procedure: A solution of DAST (159 μL, 1.2 mmol, 1.2 equiv) in CH_2Cl_2 (10 mL) was added dropwise at –78 °C to a solution of **8** (343 mg, 1.0 mmol, 1.0 equiv) and **12** (120 mg, 0.2 mmol, 0.2 equiv) in dry CH_2Cl_2 (30 mL). After stirring for 1 h at –78 °C, the reaction was allowed to warm to 23 °C and stirred for additional 18 h. Finally, the solvent was removed in vacuo and the crude residue was purified by column chromatography (heptane/AcOEt 40:1→1:1).

4-(Benzyloxy)-*N*-(4-methylbenzenesulfonyl)-1,2,3,4-tetrahydropyridine 9.

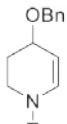

9

Column chromatography afforded product **9** as a colorless oil (31 mg, 9%). **^{1}H NMR** [400 MHz, δ (ppm), $CDCl_3$]: 1.61–1.75 (m, 1 H), 1.91–1.99 (m, 1 H), 2.42 (s, 3 H), 3.17 (dt, *J* = 11.9, 2.7 Hz, 1 H), 3.66 (dt, *J* = 11.9, 4.1 Hz, 1 H), 3.82 (dd, *J* = 6.5, 3.7 Hz, 1 H), 4.46 (d, *J* = 11.9 Hz, 1 H), 4.50 (d, *J* = 11.9 Hz, 1 H), 5.15 (ddd, *J* = 8.2, 4.5, 1.3 Hz, 1 H), 6.82 (d, *J* = 8.3 Hz, 1 H), 7.20–7.39 (m, 7 H), 7.63–7.72 (m, 2 H). **^{13}C NMR** [101 MHz, δ (ppm), $CDCl_3$]: 21.4, 23.6, 36.8, 63.5, 81.2, 124.3, 126.4, 127.8, 128.1, 128.2, 129.4, 129.7, 137.1, 138.6, 142.7. **FTIR** [$\bar{\nu}$ (cm^{-1})]: 701, 823, 1039, 1137, 1159, 1315, 1619, 1708, 2865, 2982. **HRMS** (ESI$^+$) calcd. for $(C_{19}H_{21}NO_3S + H)^+$ 344.1320, found 344.1339.

4-Fluoro-*N*-(4-methylbenzenesulfonyl)-1,2,3,4-tetrahydropyridine 10.

Upon purification by column chromatography allylic fluoride **10** decomposed to allylic alcohol **15** and allylic ether **16**.

***N*-(4-Methylbenzenesulfonyl)-1,2,3,4-tetrahydropyridin-4-ol 15.**

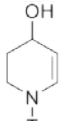

15

Column chromatography afforded product **15** as a colorless oil (91 mg, 36%). **^{1}H NMR** [400 MHz, δ (ppm), $CDCl_3$]: 1.70–1.76 (m, 1 H), 1.78–1.87 (m, 1 H), 2.43 (s, 3 H), 3.11 (dt, *J* = 12.0, 3.1 Hz, 1 H), 3.67 (dt, *J* = 12.0, 4.3 Hz, 1 H), 4.10 (dd, *J* = 6.9, 3.2 Hz, 1 H), 5.11 (ddd, *J* = 8.3, 4.8, 1.2 Hz, 1 H), 6.80 (d, *J* = 8.3 Hz, 1 H), 7.28–7.36 (m, 2 H), 7.62–7.72 (m, 2 H). **^{13}C NMR** [101 MHz, δ (ppm), $CDCl_3$]: 21.5, 30.0, 39.1, 59.9, 108.5, 127.0, 127.9, 129.9, 134.8, 144.0. These data were in accordance to those reported in the literature.[17]

4,4'-Oxybis[(4-methylbenzenesulfonyl)-1,2,3,4-tetrahydropyridine] 16.

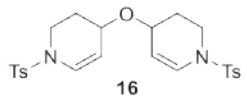

16

Column chromatography afforded product **16** as a colorless oil (83 mg, 17%) as a mixture of diastereoisomers. **^{1}H NMR** [400 MHz, δ (ppm), $CDCl_3$]: 1.60–1.67 (m, 2 H), 1.71–1.80 (m, 2 H), 2.42 (s, 6 H), 3.05 (dt, J = 11.9, 3.0 Hz, 1 H), 3.11 (dt, J = 11.9, 3.0 Hz, 1 H), 3.52–3.63 (m, 2 H), 3.78–3.81 (m, 1 H), 3.82–3.86 (m, 1 H), 4.94 (ddd, J = 8.4, 4.5, 1.0 Hz, 1 H), 4.98 (ddd, J = 8.3, 4.7, 1.2 Hz, 1 H), 6.74 (d, J = 5.5 Hz, 1 H), 6.76 (d, J = 5.4 Hz, 1 H), 7.27–7.32 (m, 4 H), 7.59–7.66 (m, 4 H). **^{13}C NMR** [101 MHz, δ (ppm), $CDCl_3$]: 21.5, 27.7, 28.0, 39.5, 39.6, 64.0, 64.3, 106.8, 106.9, 126.8, 126.9, 127.8, 128.0, 129.6, 129.8, 135.0, 135.1, 143.9. **FTIR** [$\bar{\nu}$ (cm^{-1})]: 695, 942, 1054, 1167, 1269, 1352, 1641, 2873, 2928. **HRMS** (ESI$^+$) calcd. for ($C_{24}H_{28}N_2O_5S_2$ + H)$^+$ 489.1518, found 489.1536. At this stage of the research we were unable to identify the stereochemistry of the obtained allyl ether **16**. Additionally, we didn't find another diastereomers of compound **16** after the purification on the column chromatography.

Photochemical Rearrangement of Sulfonyl Enamine 23

General procedure: Sulfonyl enamine **23** (50 mg, 0.15 mmol, 1.0 equiv) in deoxygenated MeCN (10 mL) was added to a 25 mL quartz flask with stirring. This flask was irradiated in a Rayonet RMR-600 photochemical reactor, using eight lamps of 254 nm of wavelength for 24 h with an internal temperature of 50 °C. After cooling to 23 °C, the solvent was removed in vacuo and the crude residue was purified by column chromatography. Column chromatography (heptane/AcOEt 40:1→10:1) afforded product **24** as a yellow oil (39 mg, 78%).

Ethyl (*Z*)-3-(phenylamino)-2-(4-methylbenzenesulfonyl)acrylate 24.

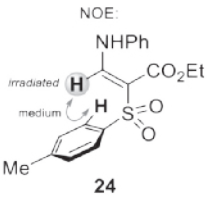

24

***R*$_F$** (silica gel, heptane/AcOEt 1:1): 0.56 (UV, $KMnO_4$ solution). **^{1}H NMR** [400 MHz, δ (ppm), $CDCl_3$]: 1.29 (t, J = 7.2 Hz, 3 H), 2.45 (s, 3 H), 4.26–4.35 (m, 2 H), 4.90 (s, 1 H), 7.12–7.20 (m, 1 H), 7.30–7.39 (m, 4 H), 7.45–7.56 (m, 2 H), 7.74–7.85 (m, 2 H), 8.98 (bs, 1 H). **^{13}C NMR** [101 MHz, δ (ppm), $CDCl_3$]: 13.9, 21.8, 63.7, 120.2, 125.3, 129.1, 129.3, 130.1, 133.8, 136.8, 146.5, 156.5, 163.2. **FTIR** [$\bar{\nu}$ (cm^{-1})]: 669, 756, 815, 1082, 1147, 1332, 1696, 1743, 2926, 3339. **HRMS** (ESI$^+$) calcd. for ($C_{18}H_{19}NO_4S$ + H)$^+$ 346.1113, found 346.1125.

7.6 References and Notes

[1] *Bioactive Heterocyclic Compound Classes – Agrochemicals*; Lamberth, C., Dinges, J., Eds.; Wiley-VCH: Weinheim, Germany, 2012.

[2] (a) Berger, R.; Resnati, G.; Metrangolo, P.; Weber, E.; Hulliger, J. *Chem. Soc. Rev.* **2011**, *40*, 3496–3508; (b) Kirsch, P. *Modern Fluoroorganic Chemistry: Synthesis, Reactivity, Applications*; Wiley-VCH: Weinheim, Germany, 2013; (c) Tirotta, I.; Dichiarante, V.; Pigliacelli, C.; Cavallo, G.; Terraneo, G.; Bombelli, F. B.; Metrangolo, P.; Resnati, G. *Chem. Rev.* **2015**, *115*, 1106–1129; (d) Preshlock, S.; Tredwell, M.; Gouverneur, V. *Chem. Rev.* **2016**, *116*, 719–766.

[3] (a) Mueller, K.; Faeh, C.; Diederich, F. *Science* **2007**, *317*, 1881–1886; (b) Purser, S.; Moore, P. R.; Swallow, S.; Gouverneur, V. *Chem. Soc. Rev.* **2008**, *37*, 320–330; (c) Wang, J.; Sánchez-Roselló, M.; Aceña, J. L.; del Pozo, C.; Sorochinsky, A. E.; Fustero, S.; Soloshonok, V. A.; Liu, H. *Chem. Rev.* **2014**, *114*, 2432–2506; (d) Zhou, Y.; Wang, J.; Gu, Z.; Wang, S.; Zhu, W.; Aceña, J. L.; Soloshonok, V. A.; Izawa, K.; Liu, H. *Chem. Rev.* **2016**, *116*, 422–518.

[4] (a) Jeschke, P. *ChemBioChem* **2004**, *5*, 570–589; (b) Jeschke, P. *Pest Manage. Sci.* **2010**, *66*, 10–27.

[5] Fujiwara, T.; O'Hagan, D. *J. Fluorine Chem.* **2014**, *167*, 16–29 and references therein.

[6] For general reviews, see: (a) Ma, J.-A.; Cahard, D. *Chem. Rev.* **2004**, *104*, 6119–6146; (b) Furuya, T.; Kamlet, A. S.; Ritter, T. *Nature* **2011**, *473*, 470–477; (c) Xu, X. H.; Matsuzaki, K.; Shibata, N. *Chem. Rev.* **2015**, *115*, 731–764; (d) Neumann, C. N.; Ritter, T. *Angew. Chem. Int. Ed.* **2015**, *54*, 3216–3221; (e) Ni, C.; Hu, M.; Hu, J. *Chem. Rev.* **2015**, *115*, 765–825; (f) Yang, X.; Wu, T.; Phipps, R. J.; Toste, F. D. *Chem. Rev.* **2015**, *115*, 826–870; (g) Champagne, P. A.; Desroches, J.; Hamel, J.-D.; Vandamme, M.; Paquin, J.-F. *Chem. Rev.* **2015**, *115*, 9073–9174; (h) Campbell, M. G.; Ritter, T. *Chem. Rev.* **2015**, *115*, 612–633.

[7] Dang, H.; Mailig, M.; Lalic, G. *Angew. Chem. Int. Ed.* **2014**, *53*, 6473–6476.

[8] Cheng, L.-J.; Cordier, C. J. *Angew. Chem. Int. Ed.* **2015**, *54*, 13734–13738.

[9] (a) Sim, M. F.; Yates, D. B. Method of Treating Heart Disease. U.S. Patent 4,552,884, Nov 12, 1985; (b) Maclean, L.; Roberts, D. L.; Barron, K.; Nichol, K. J.; Harrison, A. E. Process for the Synthesis of 3-Thio-4-quinolone Derivatives and Intermediate Compounds for Use Therein, and Their Use as Medicaments. EP 0317149, May 24, 1989; (c) Maclean, L.; Roberts, D. L.; Barron, K.; Nichol, K. J.; Harrison, A. E. Process for the Preparation of 1-Methyl-3-methylthio-4-quinolone and the Sulfinyl, and Sulfonyl Analogs Thereof. U.S. Patent 5,011,931, April 30, 1991; (d) Weishaar, R. E.; Kirker, M. L.; Wallace, A. M.; Ferraris, V. A.; Britton, L. W.; Sim, M. F. *Eur. J. Pharmacol.*

1993, *236*, 363–366; (e) Hinson, J. L.; Hind, I. D.; Weidler, D. J. *J. Pharm. Sci.* **1994**, *83*, 382–385; (f) Birch, A. M.; Davies, R. V.; Maclean, L.; Robinson, K. *J. Chem. Soc., Perkin Trans. 1* **1994**, 387–392; (g) Kashiyama, E.; Yokoi, T.; Odomi, M.; Kamataki, T. *Xenobiotica* **1999**, *29*, 815–826.

[10] Wallner, K. F.; Olofsson, J. P.; Hultqvist, M. K.; Pelcman, B. H. Quinolinone Derivatives for Use in the Treatment of an Autoimmune Disease and/or an Inflammatory Disease. WO 2012127214, Sept 27, 2012.

[11] (a) Bertonas, R. C.; Lenicek, S. E.; Antane, S. A. 1-(Aminoalkyl)-3-sulfonylazaindoles as 5 Hydroxy-tryptamine-6 Ligands. U.S. Patent 7,585,873, Sept 8, 2009; (b) Schechter, L. E.; Pong, K.; Zaleska, M. M. Use of 5-HT6 Agonist for the Treatment and Prevention of Neurodegenerative Disorders. U.S. Patent 6,128,744, June 15, 2006; (c) Dupuis, D. S.; Mannoury la Cour, C.; Chaput, C.; Verrièle, L.; Lavielle, G.; Millan, M. J. *Eur. J. Pharmacol.* **2008**, *588*, 170–177; (d) Bernotas, R. C.; Antane, S. A.; Lenicek, S. E.; Haydar, S. N.; Robichaud, A. J.; Harrison, B. L.; Zhang, G. M.; Smith, D.; Coupet, J.; Schechter, L. E. *Bioorg. Med. Chem. Lett.* **2009**, *19*, 6935–6938.

[12] (a) Bernotas, R. C.; Lenicek, S.; Antane, S.; Cole, D. C.; Harrison, B. L.; Robichaud, A. J.; Zhang, J. M.; Smith, D.; Platt, B.; Lin, Q.; Li, P.; Coupet, J.; Rosenzweig-Lipson, S.; Beyer, C. E.; Schechter, L. E. *Bioorg. Med. Chem.* **2009**, *17*, 5153–5163; (b) Benhamú, B.; Martín-Fontecha, M.; Vázquez-Villa, H.; Pardo, L.; López-Rodríguez, M. L. *J. Med. Chem.* **2014**, *57*, 7160–7181, and references therein.

[13] Jiang, H.; Huang, W.; Yu, Y.; Yi, S.; Li, J.; Wu, W. *Chem. Commun.* **2017**, *53*, 7473–7476.

[14] Cheng, L.-J.; Cordier, C. J. *Angew. Chem. Int. Ed.* **2015**, *54*, 13734–13738.

[15] Durel, V.; Lalli, C.; Roisnel, T.; van de Weghe, P. *J. Org. Chem.* **2016**, *81*, 849–859.

[16] (a) Kinderman, S. S.; Doodeman, R.; van Beijma, J. W.; Russcher, J. C.; Tjen, K. C. M. F.; Kooistra, T. M.; Mohaselzadeh, H.; van Maarseveen, J. H.; Hiemstra, H.; Schoemaker, H. E.; Rutjes, F. P. J. T. *Adv. Synth. Catal.* **2002**, *344*, 736–748; (b) Kinderman, S. S. Transition Metal Catalyzed Formation and Transformations of Allylic *N,O*-Acetals with a Focus on Olefinic-Amino Acids. Ph.D. Thesis, University of Amsterdam, the Netherlands, 2003.

[17] Berti, F.; Favero, L.; Pineschi, M. *Synthesis* **2016**, 2645–2652.

SUMMARY

The use of agrochemicals is often considered a quick, easy, and inexpensive solution to pests and weed control, however the extensive rely on such agricultural practices can lead to considerable damage to the ecosystem. Therefore, the need in new pest management solutions continues unabated, especially in the perspective of a fast growth of human population worldwide. This thesis deals with the exploration of novel approaches for the preparation of chemical libraries, with a view to accessing products of value to the fine chemicals sector, such as agrochemicals. In particular, this dissertation is focused on the use of palladium-catalyzed reactions of alkoxy allenes and sulfonyl ynamines for the preparation of derivatized *N*-heterocycles.

The presented research is a single workpackage within a large ITN network, and Chapter 1 begins with an overview of this program. Chapter 2 provides a more technical introduction to the project. Specifically, palladium-catalyzed reactions of alkoxy allenes and sulfonyl ynamines were reviewed together with applications of these methods in the rapid assembly of complex *N*-heterocyclic structures (Figure 1). Multiple examples in this comprehensive and updated overview demonstrate that these transformations proceed in highly chemo-, regio- and stereoselective manner.

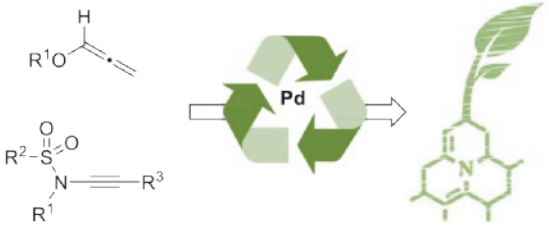

Figure 1 *Alkoxy Allenes and Sulfonyl Ynamines: Versatile Substrates for the Palladium Catalysis.*

Chapter 3 describes a general method for the preparation of heteroaromatic allylic *N,O*-acetals **1** (Scheme 1). This methodology resulted in a library of 22 novel compounds (yields up to 95%), 6 of which were prepared in a highly enantioselective manner (ee's up to 94%). Additionally, our *in silico* investigations of the reaction suggest a new palladium(0)-driven mechanistic pathway that proceeds through protonation of the palladium–allene complex to form a η^3-allylpalladium species.

Scheme 1 *Synthesis of Heteroaromatic Allylic N,O-Acetals* ***1****.*

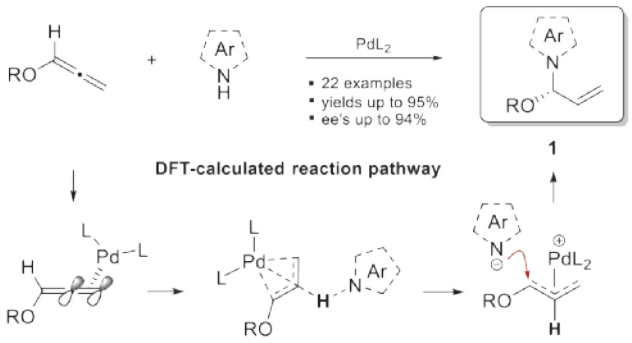

Such a process involves a reactive carbene-like local minimum **2**, which is a crucial link that connects both intermediates (Figure 2).

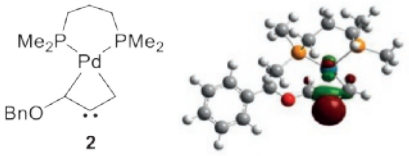

Figure 2 *3D Representation of the HOMOs of Palladium–Allene Complex* ***2****.*

Chapter 4 follows up on the work describing the synthetic concept for derivatization of previously described heteroaromatic allylic *N,O*-acetals **1**. Hence, allylic and propargylic groups were successfully incorporated into the previously prepared *N,O*-acetal scaffold **3** using Grignard addition of vinyl- or ethynylmagnesium bromides (Scheme 2).

Scheme 2 *Synthesis of an Allylic N,O-Acetal Scaffolds Ccontaining an Imidazole Bearing an Allyl/Propargyl Fragment at C-2 Position. These Structures Were Further Used in Several Ring Forming Processes.*

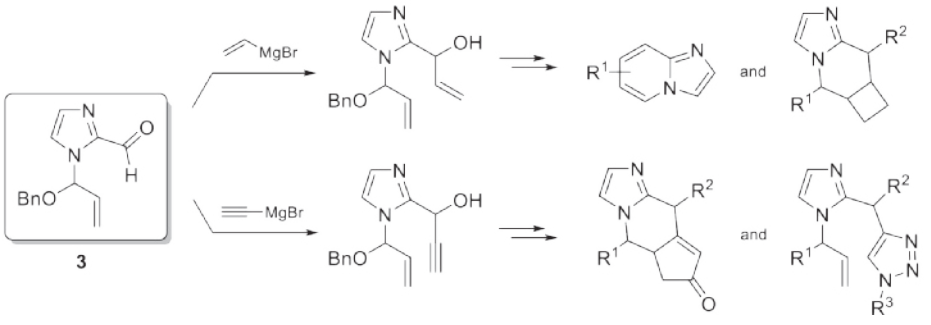

Moreover, participation of the obtained derivatives in the ring closing metathesis, photochemically promoted [2+2] cycloadditions, Pauson–Khand, and "click" reactions were investigated. Unfortunately, none of these methods delivered any of the desired polycyclic products, although the substrates do appear to participate in fluorination reaction with DAST reagent that has the potential to be further exploited.

In Chapter 5, a novel intramolecular hydroarylation of arenesulfonyl ynamines **4** was disclosed (Scheme 3). The presence of an electron-withdrawing group on the triple bond of the sulfonyl ynamine **4** was crucial for the success of the reaction (e.g., $R^2 = CO_2Et$). Despite the low yields, this unprecedented cyclization was completely regioselective and highly stereoselective: (*E*)-exocyclic 1,2-benzothiazole-1,1-diones **5** were the major isomers with an *E*/*Z*-ratio of up to 99:1. The reaction sequence was investigated using DFT methods. An alkyne-directed 5-*exo*-dig cyclization pathway was suggested, where C–H activation and isomerization of a "push-pull" alkenyl–palladium(II) species were found out to be key steps in the reaction mechanism.

Scheme 3 *Intramolecular Hydroarylation of Arenesulfonyl Ynamines 4.*

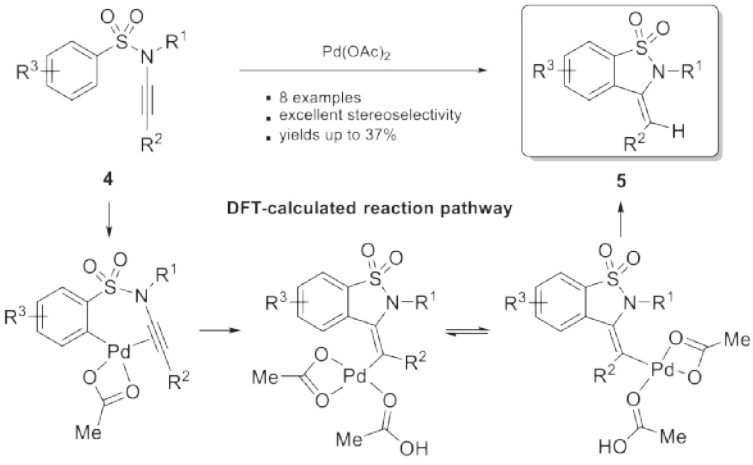

Chapter 6 seeks to exploit a photochemically promoted rearrangement of 1,2-benzothiazole-1,1-diones **5** (Scheme 4). Although discussed briefly, it is clear that this new method has significant potential for the efficient synthesis of 3-amino-1-benzothiophene-1,1-diones **6** (4 examples, yields 87–96%), highly potent bioactive molecules valuable for medicinal and agrochemistry.

Scheme 4 *Photoinduced Rearrangement of 1,2-Benzothiazole-1,1-diones* **5**.

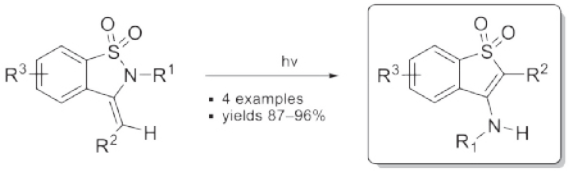

5 **6**

Chapter 7 is the final section of the thesis and provides an overview of the advances made during the research programme. Thus, the nucleophilic fluorination of cyclic *N,O*-acetal **7** and the photoinduced sulfonyl rearrangement in sulfonyl enamine **8** seemed promising and are likely to form the basis of the future work (Scheme 5).

Scheme 5 *Fluorination of Cyclic N,O-Acetal* **7** *and Photoinduced Rearrangement of Sulfonyl Enamine* **8**.

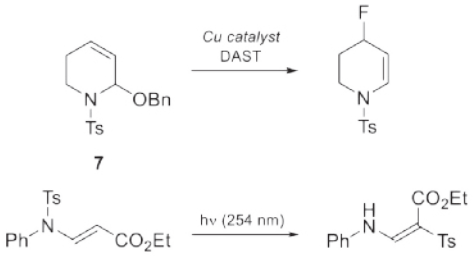

7

8

SAMENVATTING

Het gebruik van agrochemicaliën wordt vaak beschouwd als een snelle, makkelijke en goedkope methode voor gewasbescherming en plaagbestrijding. Echter, veelvuldig en overvloedig gebruik van deze middelen kan leiden tot aanzienlijke schade aan het ecosysteem. Het is daarom, zeker in het licht van de snelgroeidende wereldpopulatie, van groot belang dat er nieuwe geïntergreerde gewasbeschermingsmiddelen worden ontwikkeld. Dit proefschrift beschrijft de ontwikkeling van nieuwe chemische bibliotheken met als doel de ontwikkeling van nieuwe fijnchemicaliën, in het bijzonder agrochemicaliën, mogelijk te maken. Meer specifiek richt dit proefschrift zich op het gebruik van palladiumgekatalyseerde reacties van alkoxy-allenen en sulfonyl-ynamines voor het maken van gefunctionaliseerde *N*-heterocyclische systemen.

Dit werk is onderdeel van een groter ITN-netwerk en hoofdstuk 1 begint met een beschrijving van dit programma. Hoofdstuk 2 biedt een meer technische introductie van het project. In het bijzonder worden palladium gekatalyseerde reacties van alkoxy allenen en sulfonyl ynamines besproken en de toepassing van deze reactie in de snelle assemblage tot complexe *N*-heterocyclische structuren (Figuur 1). Verschillende voorbeelden in dit uitgebreide overzicht laten zien dat deze omzettingen zeer chemo-, regio- en stereoselectief verlopen.

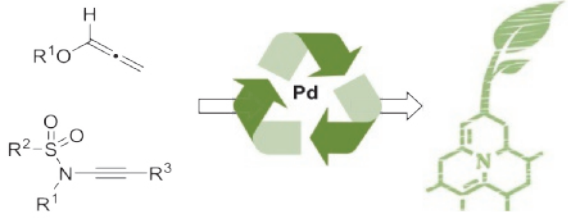

Figuur 1 *Alkoxy Allenen en Sulfonyl Ynamines: Veelzijdige Substraten voor Palladium Gekatalyseerde Reacties.*

Hoofdstuk 3 beschrijft een algemene methode voor de bereiding van heterocyclische allylische *N,O*-acetalen 1 (Schema 1). Deze methode resulteerde in een bibliotheek van 22 nieuwe verbindingen met opbrengsten tot 95%, waarbij 6 verbindingen zeer enantioselectief werden verkregen (met ee-waardes tot 94%). Verder suggereren *in silico* experimenten dat deze reacties via een palladium(0)-gedreven mechanisme verlopen door protonering van een palladium–alleen complex en de vorming van een η^3-allylpalladium-component.

Schema 1 *Synthese van Heteroaromatische Allylische N,O-Acetalen* ***1****.*

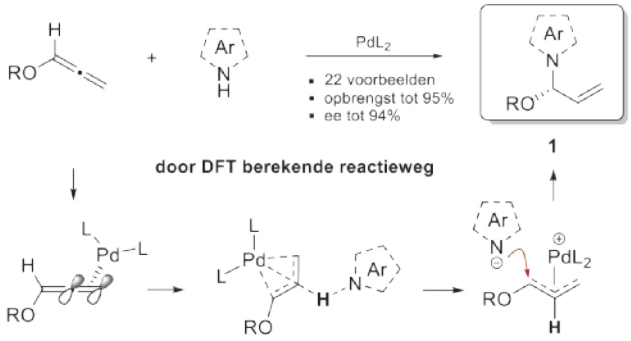

In dit proces vormt een reactief, carbeen-achtig lokaal minimum **2**, de cruciale link tussen beide intermediairen (Figuur 2).

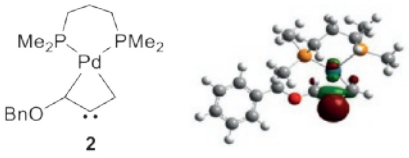

Figuur 2 3D W*eergave van de HOMO's van het Palladium–Alleen Complex.*

Hoofdstuk 4 vormt een uitbreiding op het synthetische concept voor de derivatisering van de eerder beschreven heteroaromatische allylische *N,O*-acetalen **1**. Hierin is beschreven dat allylische en propagylische groepen met succes zijn ingebouwd in het eerder gesynthetiseerde *N,O*-acetal-molecuul **3** door Gringard-additie met behulp van vinyl- en ethynyl-magenisumbromides (Schema 2).

Schema 2 *Synthese van Allylische N,O-acetal, Imidazool-Bevattende Kapstokmoleculen met een Allylische of Propagylgroep op de C-2 Positie. Deze Structuren Werden Verder Toegepast in Verschillende Ringvormingprocessen.*

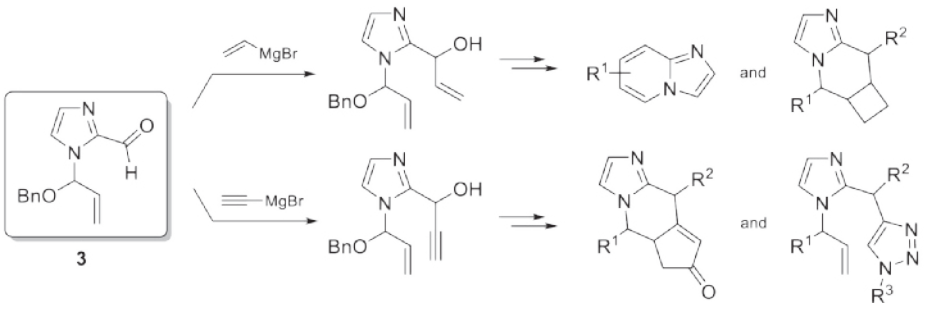

Verder werd participatie van de verkregen derivaten in ringsluitingsmetatheses, fotochemisch gepromote [2+2]-cycloaddities, Pauson–Khand-reacties en "click-reacties" onderzocht. Helaas leverde geen van de deze methodes de gewenste polycyclische producten op. Er werd wel gevonden dat de substraten participeerden in fluoridering-reacties met het DAST-reagens, wat het potentieel heeft om verder onderzocht te worden.

In hoofdstuk 5 is een nieuwe intramoleculaire hydroarylering van areensulfonyl ynamines **4** beschreven (Schema 3). Hier bleek dat de aanwezigheid van een elektronenzuigende groep op de driedubbele binding van de sulfonyl ynamine **4** cruciaal was voor het verlopen van de reactie (bijvoorbeeld, R^2 = CO_2Et). Ondanks de matige opbrengsten, bleek deze niet eerder vertoonde cyclisatie volledig regioselectief en zeer stereoselectief: (*E*)-exocyclische 1,2-benzothiazool-1,1-dionen **5** waren de meest gevonden isomeren met een *E*/*Z*-verhouding tot en met 99:1. Het reactiemechanisme werd verder onderzocht door middel van DFT-methodes. Hierin werd een alkyngerichte 5-*exo*-dig cyclisatie route gesuggereerd, terwijl C–H-activering en isomerisatie van "push-pull" alkenyl–palladium(II)-componenten de sleutelstappen bleken te zijn in het reactiemechanisme.

Schema 3 *Intramoleculaire Hydroarylering van Areensulfonyl Ynamines 4.*

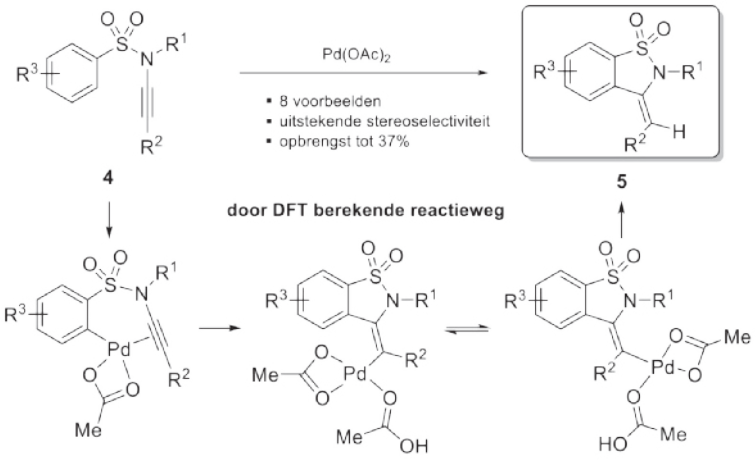

Hoofdstuk 6 beschrijft de verdere exploitatie van de fotochemisch gepromote omlegging van de in het vorige hoofdstuk beschreven 1,2-benzothiazool-1,1-dionen **5** (Schema 4). Hoewel slechts kort besproken is het overduidelijk dat deze nieuwe methode een geweldig potentieel heeft voor de efficiënte synthese van 3-amino-1-benzothiofeen-1,1-dionen **6** (4 voorbeelden, opbrengsten 87-96%), wat goedwerkende veelbelovende bioactieve moleculen zijn in het veld van de medicinale en agrochemie.

Schema 4 *Lichtgeinduceerde Omlegging van 1,2-Benzothiazool-1,1-dionen 5.*

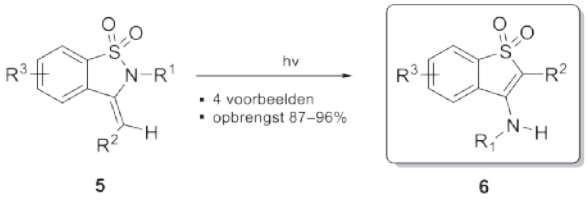

5 6

Hoofdstuk 7 is de laatste sectie van dit proefschrift en biedt een overzicht van alle vorderingen die gemaakt zijn in dit onderzoeksprogramma. In conclusie, de nucleofiele fluorinering van cyclische *N,O*-acetal **7** en de fotogeinduceerde sulfonyl-omlegging van sulfonyl enamin **8** bleken veelbelovend en zijn zeker een goede basis voor verder onderzoek (Schema 5).

Schema 5 *Fluorinering van Cyclische N,O-Acetal 7 en de Fotogeinduceerde Omlegging van Sulfonyl Enamin 8.*

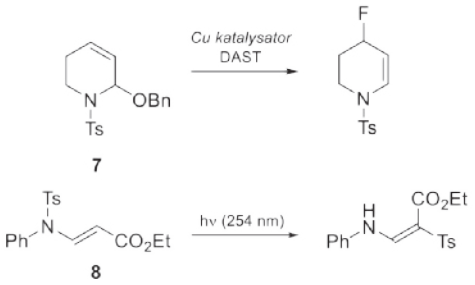

7 **8**

ACKNOWLEDGEMENTS

Starting my PhD studies was a serious step in my life. I like to think of it as of roller coaster ride. It's like you're going along and don't know what to expect in the next moment. I've had my ups. Moments of happiness when I felt extremely proud of who I am, what I'm doing and those who are my friends. I've had my downs. Moments when my life seemed to be upside down and inside out and every which way. If four years of this "amusement ride" have taught me anything, it is this: enjoy every moment of the life, hang on until the top will come again, and more important, appreciate **the people** with whom you're sharing this ride…

"*Dear Prof. Dr. Floris Rutjes, I hereby wish to apply for the Marie Curie PhD Scholarship provided by the Radboud University of Nijmegen...*" zo is ons eerste contact begonnen, **Floris.** Allereerst wil ik je bedanken dat je mijn solicitatie brief niet rechtstreeks naar je prullenbak hebt gestuurd. Na gesproken te hebben via de mail was het voor mij een groot genoegen om je voor het eerst te ontmoeten tijdens ons interview en een nog grotere eer dat ik hierna lid mocht worden van jou groep. Bedankt voor al je ideeën, vrijheid om te kiezen waar ik aan zou willen werken, en natuurlijk je geduld... vooral tijdens die momenten dat ik met je probeerde te praten in het Nederlands.

Dani, has sido (y seguirás siéndolo) un ejemplo a seguir! ¡Desde el día en que te conocí hasta este momento, admiro tu enorme entusiasmo por la vida! Fundaste la "Academia Blanco" para compartir su conocimiento ilimitado de química orgánica con todos los que tienen sed de ella. Creo que es hora de extenderlo a todos los aspectos de la vida, incluyendo las guías para viajes, restaurantes, películas o música. ¡El mundo necesita tu experiencia en este campo!

The life at the faculty can be compared with the "Lord of the Rings" saga (together with **Albert** we named it "LORD OF THE WINGS"): all of us are different, we may come from different places, and maybe sometimes there are some tension between different "*fractions*", but nonetheless we succeeded to make our faculty a place where everyone is welcome, especially during the "*borrels*". And for that, I thank you all!

Principal investigators of the faculty: **Daniela, Dennis, Evan, Jana, Jasmin, Hans, Kim, Martin, Paul, Peter, Roeland, Thomas,** and **Wilhelm.**

Staff members: **Ad**, **Désiréé**, **Jacky**, **Jan**, Helene, **Marieke**, **Paul Tinnemans** ("*next time skip the NMR and come straight to me*", *I will certainly do!*), **Paul White** (*thanks for your huge enthusiasm for NMR*), **Paula**, **Peter van Dijk** (*thanks for sharing your positive attitude and life wisdom with me*), **Peter van Galen**, **René** (*the man that can fix anything*), and **Theo**.

Wing 1 (Home Sweet Home): Alberto, **Alejandra** (*siempre* 5), Annika, Bastiaan, Britta, Bram, Claudia, **Edu** (*lo siento por todas la cicatrices que tienes por mi culpa*), Jorge, Dave, Ferdi, Freek, GATT team, Giuseppe, **Hidde**, Imke, Irfan, Joep, Johan, Jona, Luc, Luuk, **Lianne**, Lise, **Lorenzo** (*tu sei il prossimo*), **Marcel** (*dankje voor de samenvatting*), **Maria**, Mark, Matthijs, Nanda, Paloma, **Peter Spannring** (*the prodigal son*), René, **Rens** (*surfing, Rocket League, Grenoble, good times mate*), **Rosa**, Ruud, Sagar, **Sam** (*Mr. Tarantino*), Sebastian, Selma, Stefan, Ton, Tony, **Torben** (*wir sind endlich klar, mein Lieber!*), **Victor** (*Who you gonna call?*), Vlado, and Willem-Jan.

Wing 2 (My New Adventure): Agata, **Albert**, Alex, Alexandra, **Anne** (*how's life?*), Britta, Daan, **James** (*what is life?*), Jan Lauko, Jiangkun, Francesca, Kenny, Lena, **Lía** (*super good*), Mahesh, Marc, Max, Oliver, Pattama, Pieter, Sergey, Sjoerd, Wessel, Wesley, and Will.

Wing 4 and 8: **Abbas** (*Linsen soup. The Best!*), **Danny**, Guilherme, Jan Zelenka, Jordi, David, Emilia, Emilien, **Giordano** (*te ne stai andando troppo presto*), Marta, Miriam, Max, **Paola**, **Sjoerd**, and Vijay.

I am so thankful to my students! **Sophie**, **Huub** and **Guillem** a.k.a. **Will** (*make someone happy, then you'll be happy too*), thanks for the great contributions to parts of this book. **Sybren** (*the most gifted child*), **Jeroen**, **Freek** and **Ulviye** thank you for being part of my PhD life.

Thank you, ECHONET team for the great and fun moments we had in every meeting: a great thanks to our "*junior league*" (Ala, Béla, Caroline, Guilhem, Jennifer, Júlia, Jokin, Malcolm, Martina, Silvia, Sylvestre, and Tim) and "*champions league*" (Enrique, Ernesto, Dina, Joe, Josep, Matt, Pieter, Stefan, and Stephen). It was an honor to meet you all! **Enrique** and **Béla**, thank you for our fruitful collaboration (*palladium reactions are still a big mystery to me*). **Ernesto** and **Dina**, I'm so grateful to you for hosting me in Sesto Fiorentino (*it was probably one of the best summers I had*)!

I would like to extend my gratitude to **Roeland** and **Hans** for offering me the ENCOPOL postdoctoral position and wait for me while I was busy with this manuscript.

I want to thank to my paranymphs, two very special girls who were with me since the beginning of my PhD journey. **Alejandra**, te admiro como persona! Tú nunca te rindes, sin importar lo difíciles que sean los desafíos. También aprendes muy rápido y te conviertes en la mejor en esas cosas que te gustan. Quién sabe, quizás algún día te conviertas en **Dani Blanco 2**, versión mejorada. Te debo una disculpa por todos mis terribles chistes. No los tengas en cuenta, tú sabes que te aprecio en mi vida! **María**, gracias por los grandes momentos que compartimos durante estos cuatro años, especialmente las cenas que organizaste. Eres una anfitriona fantástica! ¡Sigue manteniendo tu gran actitud española que tanto necesita esta facultad!

Thanks to my international friends, **Dani Brasileño, Darío, Edu, Ester, Julio, Laura, Lía, Lavinia, Marc, Merce, María, Riccardo**, and **Roque**. You gave me total freedom to be myself.

Ich möchte mich auch ganz herzlich bei meinen "*Corpsbrüder*" bedanken. Lieber **Tommy** und **Ben**, danke für die gute Zeit die wir miteinander hatten! Bierjunge!

Especially i would like to thank to **Hanna** for her great patience whilst I was busy with this thesis and for her wholehearted support in every possible way. Дякую, що ти в мене є!

To my family, **Mum, Dad,** and **Sister**. Thank you for your unconditional support!

LIST OF PUBLICATIONS

Bernar, I.; Fiser, B.; Blanco-Ania, D.; Gómez-Bengoa, E.; Rutjes, F. P. J. T. Pd-Catalyzed Hydroamination of Alkoxyallenes with Azole Heterocycles: Examples and Mechanistic Proposal. *Org. Lett.* **2017**, *19*, 4211–4214.

Bernar, I.; Blanco-Ania, D.; Stok, S. J.; Sotorríos, L.; Gómez-Bengoa, E.; Rutjes, F. P. J. T. Synthesis of 3-Amino-1-benzothiophene-1,1-diones by Alkyne-Directed Hydroarylation and 1/N→3/C-Sulfonyl Migration. *Eur. J. Org. Chem.* **2018**, 5435–5444.

Bernar, I.; Blanco-Ania, D.; Ruliaman, R.; Rutjes, F. P. J. T. Palladium-Catalyzed Nucleophilic Additions to Alkoxy Allenes. *Manuscript in Preparation.*

LIST OF GIVEN TALKS

Bernar, I. How to Feed 10 Billion Dinner Guests? Presented at the Radboud Talks, Nijmegen, the Netherlands, March 30, 2016.

Bernar, I. Palladium-Catalyzed Hydroamination of Alkoxy Allenes with Azole Heterocycles: Examples and New Mechanistical Proposal. Presented at the Symposium on Advances in Heterocyclic Organic Chemistry (SAHOC), Sheffield, UK, September 1–2, 2016.

Bernar, I. Selective Functionalization of Aromatic Heterocycles through Hydroamination of Alkoxy Allenes. Presented at the Chemistry as Innovating Science (CHAINS), Veldhoven, the Netherlands, December 6–8, 2016.

CURRICULUM VITAE

Ivan Bernar was born on 11th of January 1989 in Khust, Ukraine, a charming town in Western Ukraine famous for its Narcissus Valley, castle ruins and green tomatoes (credits to *Hanna*). Whilst in high school, at Khust Gymnasia, he discovered his passion for "home-made" chemistry experiments. However, not all of them were successful. He once tried to prepare nitric acid in his family home, but something went terribly wrong, and he caught the floor of his room on fire (sorry mum). This was the moment Ivan realized - it is time to study Chemistry… properly!

His chemistry quest began at Taras Shevchenko National University of Kyiv, where he attended the Bachelor's program in Chemistry. In his final year, Ivan found his real bond for Organic Chemistry and decided to master it alongside gaining international experience abroad. After his graduation, he moved to Berlin where he started the Master's program in Organic Chemistry at Freie Universität Berlin. Since the beginning of his studies, Ivan has worked in highly multicultural environments and enjoyed meeting new people. He gained an outstanding opportunity to share his passion and develop his skills whilst collaborating with different research groups around the globe.

During his Master's program, Ivan conducted his first independent research project led by Prof. Hans-Ulrich Reißig in Berlin. Together with Dr. Léa Bouché, he worked on the synthesis of novel carbohydrate mimetics. After this internship, he won the DAAD-IAESTE fellowship for research work at Hong Kong Polytechnic University. Under the supervision of Prof. Michael Yu Wing-Yiu, he learned to perform his first palladium-catalyzed reactions. Following his return to Berlin, Ivan went on to do an internship at the Scripps Research Institute in La Jolla under the supervision of Dr. Brandon Rosen and Prof. Phil S. Baran. His project was devoted to the preparation of a synthetic library of (+)-Yahazunol. After this research project, he joined the team of Dr. Andreas Burgard at Sanofi in Höchst where he was involved in development of anti-malarial drug 'Artemisinin'.

Several years of intensive studies and practical training prepared Ivan for a PhD in Synthetic Organic Chemistry. In October 2013, he was selected for Marie Skłodowska-Curie scholarship (ECHONET ITN) under the supervision of Dr. Daniel Blanco Ania and Prof. Floris P. J. T. Rutjes. In his doctoral thesis, Ivan studied palladium-catalyzed synthesis of novel *N*-heterocycles. The results of this research are presented in this book. As part of his training, Ivan also moved to Florence for a three-month secondment in the research group of Prof. Ernesto G. Occhiato, where he worked on gold-catalyzed Nazarov reactions.

Since March 2018, Ivan has been working as a post-doctoral researcher in the group of Prof. Roeland J. M. Nolte at Radboud University. The project focuses on the development of manganese-catalyzed epoxidation reactions of olefins and polyenes.

Palladium catalysis has revolutionized synthetic organic chemistry: it has made possible the construction of complex organic molecules in a highly efficient manner. The present book highlights two palladium-catalyzed transformations: hydroamination of alkoxy allenes and intramolecular hydroarylation of sulfonyl ynamines. Broad scope of substrates, excellent regio- and stereocontrol of these reactions make them particularly valuable for the preparation and derivatization of N-heterocycles. The presented methods generate products of promising value as fine chemicals, such as agrochemicals. We hope that this in-depth study promotes the continued interest in palladium catalysis together with the chemistry of alkoxy allenes and sulfonyl ynamines.